Praxis-Kalibrierung der neuen mobilen Grossversuchsanlage MLS10 für beschleunigte Verkehrslastsimulation auf Strassenbelägen in der Schweiz

Performance-Calibration of the novel full-scale test machine MLS10 for accelerated traffic simulation on Swiss roads

Etalonnage sur site du nouvel appareil mobile à vraie grandeur MSL10 pour la simulation rapide de l'usure des routes en Suisse

Empa, Eidgenössische Materialprüfungs- und Forschungsanstalt
Martin Arraigada, Dr., dipl. Ing.
Manfred N. Partl, Prof. Dr., dipl. Ing. ETH
Hiroyuki Kato, dipl. Ing.
Andrés Pugliessi, dipl. Ing.
Andreas Treuholz, Msc.

October 2013 **1432**

Praxis-Kalibrierung der neuen mobilen Grossversuchsanlage MLS10 für beschleunigte Verkehrslastsimulation auf Strassenbelägen in der Schweiz

Performance-Calibration of the novel full-scale test machine MLS10 for accelerated traffic simulation on Swiss roads

Etalonnage sur site du nouvel appareil mobile à vraie grandeur MSL10 pour la simulation rapide de l'usure des routes en Suisse

Empa, Eidgenössische Materialprüfungs- und Forschungsanstalt
Martin Arraigada, Dr., dipl. Ing.
Manfred N. Partl, Prof. Dr., dipl. Ing. ETH
Hiroyuki Kato, dipl. Ing.
Andrés Pugliessi, dipl. Ing.
Andreas Treuholz, Msc.

October 2013   **1432**

Impressum

Forschungsstelle und Projektteam

Projektleitung
Manfred N. Partl, Prof. Dr., dipl. Ing. ETH

Mitglieder
Martin Arraigada, Dr., dipl. Ing.
Andrés Pugliessi, dipl. Ing.
Hiroyuki Kato., dipl. Ing.
Andreas Treuholz, MSc.

Begleitkommission

Präsident
Andreas Gantenbein   (ASTRA)

Mitglieder
Hans-Peter Beyeler   (ASTRA)
Luzia Seiler   (ASTRA)
Carlo Mariotta   (FOKO)
Rolf Meier   (KI)
Fridolin Vögeli   (AG)
Martin Horat   (VSS)
Thomas Arn   (VSS)
Jürg Siegenthaler   (Infra)
Manfred Partl   (Betreiber)
Markus Caprez   (Betreiber)
Peter Richner   (Betreiber)
Martin Arraigada   (Betreiber)

Antragsteller

Bundesamt für Strassen (ASTRA)

Bezugsquelle

Das Dokument kann kostenlos von http://www.mobilityplatform.ch heruntergeladen werden.

Index of contents

Zusammenfassung

Dieser Bericht enthält die Resultate der ersten drei beschleunigten Verkehrslastsimulationen der Empa im Rahmen der Kalibration der neuartigen Grossversuchsanlage MLS10, die durch die Universität Stellenbosch in Südafrika entwickelt und hergestellt wurde. Hierzu wurden verschiedene nach Schweizer Normen erstellte Belagsaufbauten mit der MLS10 belastet. Die dadurch gewonnenen Erkenntnisse sind hilfreich in Bezug auf eine Abschätzung der Anzahl Verkehrslasten bis zur Versagensgrenze bestimmter Belagsaufbauten. Da die MLS10 ein Prototyp ist, diente dieses Projekt auch als Möglichkeit, allfällige „Kinderkrankheiten" zu erkennen und die Leistungsfähigkeit der Maschine zu verbessern.

Die vorliegende Forschungsarbeit bestätigte, dass die MLS10 in Kombination mit geeigneten Sensoren und Techniken zur Belagsbeurteilung in reproduzierbarer Weise wertvolle Informationen zur Ermittlung der Dauerhaftigkeit realer Beläge liefert. Es konnte gezeigt werden, dass die MLS10 dank ihrer Mobilität und Flexibilität an verschiedenen Orten eingesetzt werden kann. Ein zentraler Punkt der durchgeführten Tests war zudem, die Verbesserung der Funktionalität der Maschine und die Erarbeitung der notwendigen Kenntnisse, wie die MLS10 am effizientesten zu betreiben ist. Ausserdem erlaubte dieses Projekt sowohl eine anwendungsorientierte Optimierung verschiedener Sensor- und Messsysteme, wie Thermoelemente, Dehnungsmessstreifen und Beschleunigungssensoren, als auch den periodischen Einsatz zerstörungsfreier Prüfmethoden, wie Querprofilmessung, Portable Seismic Pavement Analyzer (PSPA), Falling Weight Deflectometer (FWD), ETH Delta Verformungsmessungen und Georadar (GPR).

Das Kalibrierungsprojekt der MLS10 wurde Ende 2010 nach mehr als 2'400'000 Lastwechseln und 5 getesteten Belägen abgeschlossen. Die Tests in „Filderen" ergaben, dass die neue Belagsstruktur der Autobahn A1, wie auch eine schwächere Version derselben, eine hohe Steifigkeit und Tragfähigkeit aufweist und eine beträchtliche Zeit erfordert, um mit der MLS10 signifikante Veränderungen in den Belagsschichten herbeizuführen. Dies bestätigt, dass die Dimensionierung und die Konstruktion des Belags nach den geltenden Schweizer Normen von guter Qualität ist. Auch konnte festgestellt werden, dass das in „Filderen" mit der MLS10 auf neuen Belägen erzielte Verhalten vergleichbar war mit jenem eines 20 Jahre alten Belags auf dem "Rastplatz Suhr", der eine gute Langzeitperformance aufweist. Diese positiven Erkenntnisse wurden auch durch Resultate an der "Neuen Staffeleggstrasse" bestätigt, bei welcher es sich zudem gezeigt hat, dass die MLS10 auch auf Belägen mit einer Steigung von 5% eingesetzt werden kann. Dies unter der Voraussetzung, dass sie so positioniert werden kann, dass die Last auf den Maschinenrahmen gleichmässig verteilt wird. Allerdings sollte dies aus Sicherheitsgründen möglichst vermieden werden.

Die Resultate dieser Forschungsarbeit können als gute Referenz benutzt werden, um Beläge mit neu eingesetzte Materialien oder Einbautechniken zu vergleichen und zu beurteilen, da solche Beläge zumindest ähnlich positives Verhalten zeigen müssten als die in dieser Arbeit untersuchten Beläge.

Für zukünftige MLS10 Einsätze wird vorgeschlagen, sich auf schwächere Belagsaufbauten zu konzentrieren, um deren Tragfähigkeitsgrenze innerhalb einer vernünftigeren Zeitspanne zu erreichen und darauf basierend die Versagensmechanismen solcher Beläge analysieren zu können. Um solche Tragfähigkeitstests auch für neu entwickelte Beläge durchführen zu können, wird empfohlen, diese auf speziell für diesen Zweck hergestellten Testfeldern durchzuführen.

Résumé

Ce rapport contient les résultats des trois premiers essais accélérés de revêtements réalisés par l'Empa afin d'évaluer l'efficacité du simulateur de charge mobile MLS10, un prototype développé et construit par l'Université Stellenbosch en Afrique du Sud. Différents revêtements, structures et matériaux correspondant aux normes suisses ont été testés à l'aide du MLS10 afin de procéder au calibrage de cette machine. Les informations recueillies devaient permettre d'estimer la durée et le nombre de charges nécessaires pour induire des dommages évaluables sur un type de revêtement spécifique. Le MLS10 étant au stade de prototype, ces essais étaient aussi l'occasion d'identifier ses "défauts de jeunesse" et de continuer à l'améliorer.

Ce travail a confirmé que le MLS10, combiné avec le type de capteurs et les techniques d'évaluation de revêtements adéquats, fournissait des informations précieuses quant à l'évaluation de la réponse mécanique à la charge de vrais revêtements d'une manière reproductible. Il a pu être démontré que le MLS10 pouvait être déployé sur un grand nombre de sites du fait de son design, montrant sa grande flexibilité et sa grande mobilité. Une des conséquences les plus intéressantes parmi les tests effectués est la possibilité d'améliorer la fonctionnalité du MLS10, et d'apprendre à s'en servir efficacement. L'étude a également permis de comparer et d'évaluer différentes méthodes de mesures en optimisant leur application avec une approche plus holistique, comme par exemple l'application de capteurs de température, de jauges de déformation et d'accéléromètres et l'utilisation de capteurs non-destructifs appliqués périodiquement, en particulier des mesures du profil transversal, un analyseur sismique de chaussée portable (en anglais PSPA, Portable Seismic Pavement Analyzer), un déflectomètre à masse tombante (an anglais FWD, Falling Weight Deflectometer), un appareil ETH Delta ainsi qu'un géoradar (an anglais GPR, Ground Penetrating Radar).

Le projet de calibrage du MLS10 s'est achevé à la fin 2010 après plus de 2 400 000 applications de charges et 5 revêtements. Les résultats obtenus à "Filderen" (Canton d'Argovie) montrent que la nouvelle structure de l'autoroute A1, ainsi que des versions moins résistantes du revêtement, ont une bonne rigidité et une grande force portante et nécessitent un temps et des efforts considérables pour générer un changement significatif à la réponse de dommages induits par la charge. Cela confirme que le dimensionnement du revêtement et sa fabrication selon les standards actuels suisses est de bonne qualité. En effet, le comportement observé avec le MLS10 sur des revêtements neufs à Filderen était comparable au comportement d'un revêtement de vingt ans sur la "Rastplatz Suhr" avec des bonnes performances sur le long terme.

Ces résultats positifs ont également été confirmés par les résultats d'essais sur le nouveau revêtement à la "Neue Staffeleggstrasse", ce qui a pu montrer que le MLS10 pouvait être utilisé sur des revêtements avec des pentes à 5% indiquant qu'il peut être positionné de telle sorte que le chargement de la structure de la machine peut être réalisé en équilibre. Cependant, pour des raisons de sécurité, il est recommandé d'éviter des applications extrêmes.

Les résultats trouvés lors de cette étude fournissent un bon point de référence pour des tests de revêtements neufs où des techniques récentes de construction et de nouveaux types de matériaux sont utilisés, étant donné que ces revêtements neufs devraient montrer au moins un comportement positif similaire à ceux analysés dans cette étude.

Pour les prochaines utilisations du MLS10, il est recommandé de se focaliser sur des essais sur des revêtements moins résistants pour atteindre la limite de la force portante dans un temps raisonnable et donc pour connaître les mécanismes de fracture présents dans ce type de constructions. Afin de conduire également de tels essais de "torture" pour des développements de revêtements neufs, il est recommandé de réaliser ces tests sur des champs d'essais spécifiquement dédiés à cette étude.

Summary

This report contains the findings of the first three accelerated pavement testing (APT) experiments carried out by Empa as part of the calibration of full-scale Model Load Simulator MLS10, which is a prototype developed and constructed by University Stellenbosch from South Africa. Different structures designed with Swiss Standards, materials and constructions were trafficked with the MLS10 in order to perform a sort of calibration of the machine. This information would help estimating the duration and number of load applications to induce an assessable distress in a certain type of pavement. As the MLS10 is a prototype, this test would be also seen as an opportunity to identify start-up problems and continue improving the performance of the device.

This work confirmed that the MLS10, in combination with the right type of sensors and pavement evaluation techniques, provides valuable information for evaluating the mechanical service capability of real pavements in a reproducible way. It was demonstrated that the MLS10 can be deployed to many places thanks to its design, which showed high flexibility and mobility. One of the most valuables outcomes of these tests was the possibility to improve the functionality of the MLS10, and to learn how to operate the machine in an efficient way. The research also allowed to compare and evaluate different measurement methods optimizing their application in a holistic way, such as combined application of temperature sensors, strain gauges and accelerometers and the use of periodically applied non-destructive sensors, in particular transverse profilometers, portable seismic pavement analyzer (PSPA), falling weigh deflectometer (FWD), ETH Delta deflectometer and ground penetrating radar (GPR).

The calibration project of the MLS10 was concluded at the end of 2010 after more than 2'400'000 load applications and 5 trafficked pavements. The tests in "Filderen" revealed that the new structure of the A1 highway, as well as other weaker versions of this pavement, have high stiffness and bearing capacity and require a considerable amount of time and effort to generate significant changes in the response from load induced distress. This confirms that the dimensioning of the pavement and its construction according to actual Swiss Standards is of good quality. In fact, the behavior observed with the MLS10 on the new pavements in Filderen was comparable to the behavior of a 20 year old pavement on the "Rastplatz Suhr" with good long term performance.

These positive findings were also confirmed by the test results of the new pavement in "Neue Staffeleggstrasse", which also showed that the MLS10 can be used on pavements with a slope of 5% provided that it can be positioned such that the loading of the machine frame can be realized in a balanced way. However, it is recommended to avoid such extreme applications for safety reasons.

The results found in this research provide a good point of reference for testing new pavements where new construction techniques and new types of materials are used, since these new pavements would have to show at least similar positive behavior than the pavements investigated in this research.

For next uses of the MLS10 it is recommended to focus on testing weaker pavements in order to reach the bearing capacity limit within a reasonable period of time and therefore learn what are the most common distress mechanisms present for this types of constructions. In order to be able to conduct such torture tests also for new pavement developments it is recommended to perform those test on testing fields specifically devoted for that purpose.

1   Introduction

Assessment of pavements under real load and climatic conditions is essential for understanding their response and performance in order to design and construct cost effective structures. One way to obtain information is by studying a pavement over years under real traffic loads. Accelerated Pavement Testing (APT) is a technology that allows testing a pavement under realistic conditions but in a compressed period of time. This type of tests can help reducing the increasing costs for road construction and management, with a relative low investment. APT provides a mean of evaluating paving materials. It helps improving the structural design and features, among other possible applications.

Of primary concern is to simulate traffic volume in a reasonable short time and at acceptable cost by producing a measurable response or inducing significant deterioration of the structure. The acceleration of damage in testing can be achieved by an increased rate of load applications, increased load magnitudes (loads greater than the pavement design load), modification of loading characteristics, reduced pavement thicknesses, imposed adverse environmental conditions, or a combination of these factors. It is important that the APT conditions do not differ significantly from actual in-service conditions, such that the APT produces pavement distress types similar to those observed with in-service pavements. Therefore, application of traffic loads at an increased repetition rate, inducing more load applications in a short period of time, is the most desirable means of accelerating pavement damage.

In 2008, Switzerland purchased through Empa the MLS10, a prototype APT device to replace the dismantled Circular Test Track (in German called Rundlauf). The Circular Test Track was a stationary APT equipment that was located in Dübendorf and was in service successfully for about 15 years. The report containing the purchase evaluation process of the MLS10 as well as the results of the firsts tests carried out by the South African manufacturer in Switzerland can be found in [1]. The device represents a new APT technology which has the ability of producing as much as 6'000 unidirectional load applications in one hour. A description of the MLS10 can be found in the next chapter.

The MLS10 was first put into service in the region of Hinwil, Switzerland as part of the ASTRA Project 2004/07, with assistance of the South African designers from University of Stellenbosch. Objective of those tests was to evaluate the machine under Swiss climatic conditions and to learn the basic principles of operation. This exercise provided a good overview of the functioning of the MLS10 allowed identifying many of the start-up problems, typical of prototypes.

Following completion of important refurbishing work in the mechanic, electric and hydraulic system, the MLS10 was ready for deployment under operation of a local team. It was decided to carry out an experimental project for evaluating the performance of the machine when testing pavements made according to Swiss Standards with local materials and construction techniques. These pavements had to be tested in order to estimate how many load applications are necessary to produce measurable distress in the structure and provide information about the distress mechanisms as well as the amount of time and other resources necessary to evaluate a road in Switzerland.

After experiencing some deviations in the original plan, a dedicated testing site was constructed using the same material and design as for the A4 motorway Zürich Westring (called Zürich Westumfahrung). In total, four variations of the motorway's pavement were constructed close by the real motorway, in the region called "Filderen". On this test site, a total of 3'000'000 MLS10 load applications were planned. These tests were the first APT projected under supervision of Empa personnel. Due to the limited time window for the tests and some delays caused by repair and improvement work of the prototype, the final number of load applications applied in all the structures was about 1'600'000. This was not enough to reach the theoretical amount of load applications corresponding to the bearing capacity of the pavements. Moreover, the pavements proved to be very stiff and no significant sign of distress was observed after the applied MLS10 loading.

Consequently, two other APT campaigns with weaker pavements were planned in 2010. The first one was located in a rest area of the A1 motorway between Zürich and Bern, called "Rastplatz Suhr". The old pavement of this area, which was closed for the APT, was trafficked with the MLS10 for about one month. The other pavement was a new cantonal road in Aargau, the "Neue Staffeleggstrasse". This new construction was available for being trafficked with MLS10 during around two months previous to the opening of the road to normal traffic.

In parallel to the work related to the MLS10 calibration project, two master students carried out different research activities taking advantage of having access to APT. From their work, two master theses resulted: one in collaboration with University of Rosario, Argentina, and the other with KTI Karlsruhe Institute of Technology in Germany. Publications related to the results obtained from their work can be found elsewhere [2] [3] [4].

The present report contains the description and the results obtained from the APTs carried out at the three locations mentioned above. It is organized chronologically, with general information about the machine and the objectives of the project at the beginning of the report. The first two Appendixes contain information concerning the construction of one of the sites. The Appendix III presents some publications derived from the findings of this research work.

2   The Mobile Load Simulator MLS10

The MLS10 is a full scale mobile APT device developed by the University of Stellenbosch of South Africa, in collaboration with Empa and ETH/IGT. The machine loads the pavement with unidirectional tire passings in a length of about 4.2m, simulating the load of half an axle of a truck. The rolling speed of the tires can go up to 22km/h, reproducing the passing of up to 6'000 half axles per hour. A hydro-pneumatic suspension system allows setting the loads applied by the tires up to 65kN, corresponding to 130kN axle load. The MLS10 and can be equipped with single and dual tires.

The MLS10 has a total weight of 32t and basically consist of a steel frame made of two large iron plates connected through four robust tanks of about 2m long and 1m diameter, attributing a very stiff configuration to the whole system (Fig. 2.1). One of the tanks is used for water storage and the other three for diesel, each having 1300l capacity. This provides additional ballast and allows operating the machine for about 300h without refueling. Attached to the internal face of the frame plates are two pairs of guide rails that form a closed loop path, like a chain saw.
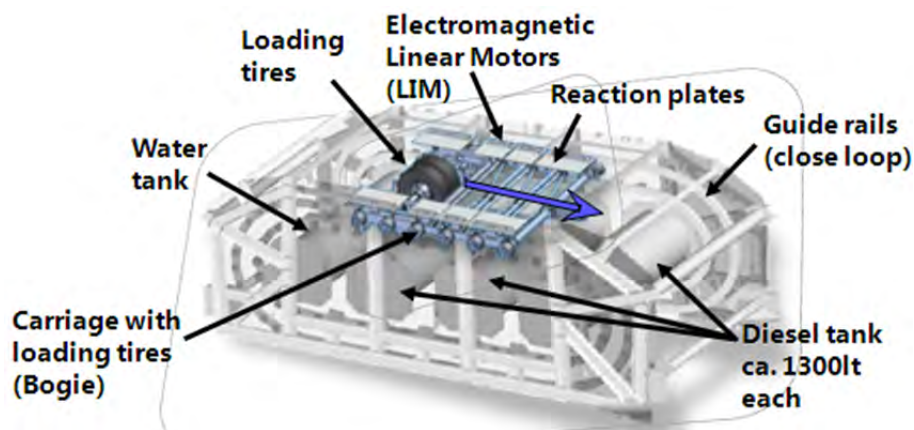
Fig. 2.1 3D view of the MLS10 frame and detail of one of the bogies

The tires for loading the pavement are mounted in bogies, which are strong steel framed carriages that are coupled to a kind of chain rolling along the guide rails. The 4 bogies of the MLS10 have steel wheels that fit within the rails. The bogies are pulled contactlessly by 24 linear induction motors (LIM). The rails are built in such a way that the freely revolving tires touch down smoothly to the surface before loading the pavement over the trafficked path length. A schema of the loading system is depicted in Fig. 2.2.
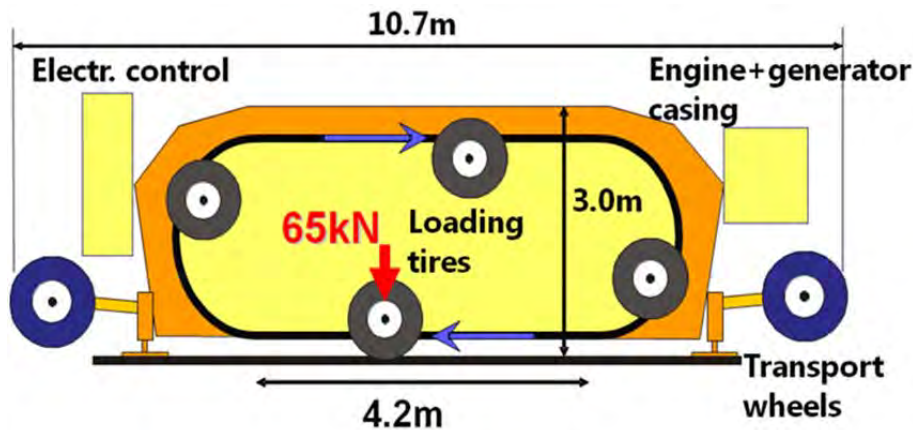
Fig. 2.2 Schema of the loading principle

The frame is enclosed by a noise reduction cover, confining all moving. In order to monitor the loading during trafficking, the dynamic movements of the suspension system are registered electronically and transferred via Bluetooth to a computer. The MLS10 is equipped with four transport wheels which can be raised and lowered hydraulically, thus lifting up the whole frame by about 1m and giving room for maintenance work, such as checking tire pressures and pavement sensors, as well as measurements of profiles, crack and damage inspection or measurements with more elaborated devices, such as the portable seismic pavement analyzer PSPA or ground penetrating radar GPR. The transport wheels allow the maneuvering of the machine around the test site and to drive it to or off low bed trucks for long distance transport. The possibility of easily driving the MLS10 on a flatbed truck makes it fully mobile. The MLS10 has a generator for fully autonomous powering of the machine. A bulk view of the MLS10 is presented in Fig. 2.3.

Fig. 2.3 View of the MLS10

3   Objectives

The present research project focuses on the performance oriented calibration and validation of the recently purchased Full Scale Mobile Load Simulator MLS10 for APT in Switzerland. The term "performance oriented calibration test" used for the title of the project, refers to the following goals of the work:

- Correlate the destructive effect of the MLS10 loading to different types of heavy traffic pavements designed and constructed using Swiss Standards under the influence of local weather conditions. The word "calibration" is used to account for the correlation between the numbers of load applications necessary to cause a certain distress in typical Swiss pavements.

- Acquire experience in operating the MLS10 and assess the required human and technical resources needed to conduct APT tests. Conduct invaluable practical optimization with respect to the operational crew to improve the organization of resources in a cost effective way.

- Evaluate the MLS10 itself, detect operational shortcomings and technical defects for improving the performance of the machine, which is a prototype and the first of this class in the world. The calibration was foreseen as an expensive and time consuming testing phase in which the machine has to be known and improved before testing under more extreme conditions.

- Propose and evaluate testing procedures as well as instrumentation and software to collect research data. Establish and formalize the data handling, cleansing, processing, storage and software.

These objectives were formulated considering the lack of previous practical experience in using a full-scale APT device of these characteristics in the country.

4   Location of the test sites

The selection of the test sites was done bearing in mind technical, logistical and environmental restrictions. One of the principal requirements had to do with the size and geometry of the area reserved for the tests. A testing site for MLS10 has to be compatible with the transportation and in-situ maneuverability of the machine. It should allow the implementation of the safety and environmental requirements such as noise level limitation during operation. It was recognized that these restrictions make the deployment of the MLS10 sometimes complicated. However, thanks to the active support of the members of the user's advisory board (called Nutzerbeirat) it was possible to deploy the machine to three different locations. The Nutzerbeirat is a board formed by representatives of different parties of interest that help managing the use of the MLS10 in the most effective way.

For Test Site 1, the new pavement of the A4 motorway Zürich Westumfahrung was chosen as the most suitable place for the initial phase of the calibration work. However due to the fact that the MLS10 can produce extensive damage to the pavement, it was decided not to carry out the tests on the motorway itself. Instead, an ad-hoc testing site (Test Site 1) with the same pavement structure as in the motorway was constructed in the "Filderen" area, in the Knonaueramt region from Canton Aargau (Fig. 4.1). Three other pavement sections were also built on the same site. The layout of the pavements will be discussed in the next chapter. The pavements were constructed between September and October 2008, using the same materials, layer geometry and same construction company involved in the construction of the motorway. Trafficking of the sections was done mostly during summer and autumn 2009.

Test Site 2 was located in a rest area of the A1 motorway, named "Rastplatz Suhr", between Rothrist and Lenzburg. The section was closed for vehicle drivers during a little more than one month between May and June 2010. In this period, the MLS10 was transported and set up. In addition, sensors were installed and trafficking was carried out.

Test Site 3 was located in the new cantonal road near Aarau called "Neue Staffeleggstrasse", where the machine was moved to in July 2010 for testing prior to the opening of the road in October 2010.
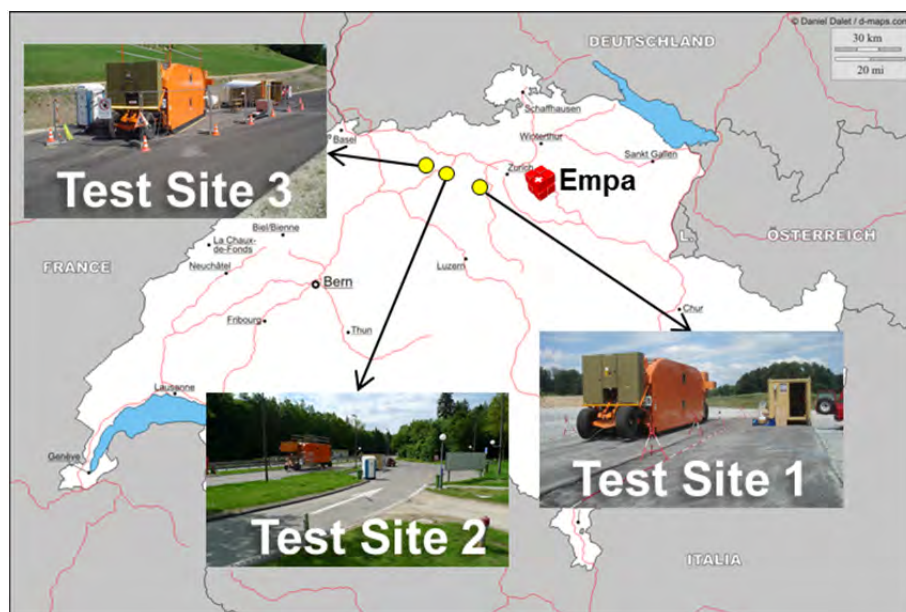

Fig. 4.1 Map showing the location of the tests sites

5 Test Site 1: Filderen

5.1 Experimental Setup

5.1.1 Layout and construction of the test sections

The test site comprised four different sections. Each section F1 to F4 was built in a rectangular area of 5m x 20m, totalizing a paved surface of 10m x 40m, as outlined in Fig. 5.1. The main difference between each of the four sections was the number of asphalt layers.

Section F4 was built following the exact design of the nearby real motorway pavement. It corresponds to the design of heavy duty full-depth asphalt pavements, described in the Swiss standards [4] [5]. This pavement is the thickest structure of the dimensioning catalogue, prepared for the highest traffic loading in Switzerland. It has 5 layers, 2 of them stabilized hydraulically with cement (called "Stabi 1" and "Stabi 2") and 3 layers with bituminous binder. The cement bounded layers were made of 65% recycled aggregate and 35% Gravel Sand II. The hydraulic binder used for the mix was "Georoc Doroport RB N", a special product of the cement producer Holcim, in a quantity of 86kg/m^3. The cement bounded layers were designed to 220mm and 180mm thickness, and the material was characterized with compression tests, that can be found in Appendix I.4. A Stress Absorbing Membrane Interlayer (SAMI) was laid separating the asphalt concrete layers from the hydraulic stabilized layers. On top of the SAMI, a base layer of 80mm was constructed using asphalt concrete material type AC T 22H according to the Swiss standard SN 640431-1b-NA [6]. The design of the 80mm binder layer type AC B 22 N and the 30mm rough asphalt AC MR 8 was carried out following the same standard. The design protocols of the asphalt mixes can be checked in Appendix 0. Due to the modest bearing capacity of the original subgrade made of an old clay containing embankment, the material was replaced by molasses with the addition of 25-30kg/m^3 "Georoc Dorosol C 30". The standard [7] sets a minimum ME value of 30'000MN/m^2 for the static plate bearing tests. The results of the static plate bearing tests after the subgrade reinforcement are presented in Appendix I.2.

The construction of section F3 was proposed as a structural variation of the pavements recommended in the Swiss standards. It had almost the same layer distribution and was built with the same materials as section F4, but with the only difference that it had no surface layer. The construction of both pavements was carried out at the same time, but in section F3 the rough asphalt concrete layer AC MR 8 was not laid. As a result, a pavement was obtained with a reduced bearing capacity that is weaker than the equivalent in the catalog pavement. In this way, the relative reduction of life expectancy according to the standards could be evaluated more accurately, since variables affecting the behavior of the pavement like material, construction practices, etc. would be the same for both sections.

Following the same concept, the structural composition of section F1 was considered based on section F4. In order to reduce the bearing capacity to a higher degree, the surface and the binder layers were not constructed. As a result, a 3 layer pavement composed by Stabi 2, Stabi 1 and AC T 22N was obtained.

Due to time restrictions and the exceptional performance of the other sections, section F2 was not trafficked and therefore its detailed description is not included in this report.
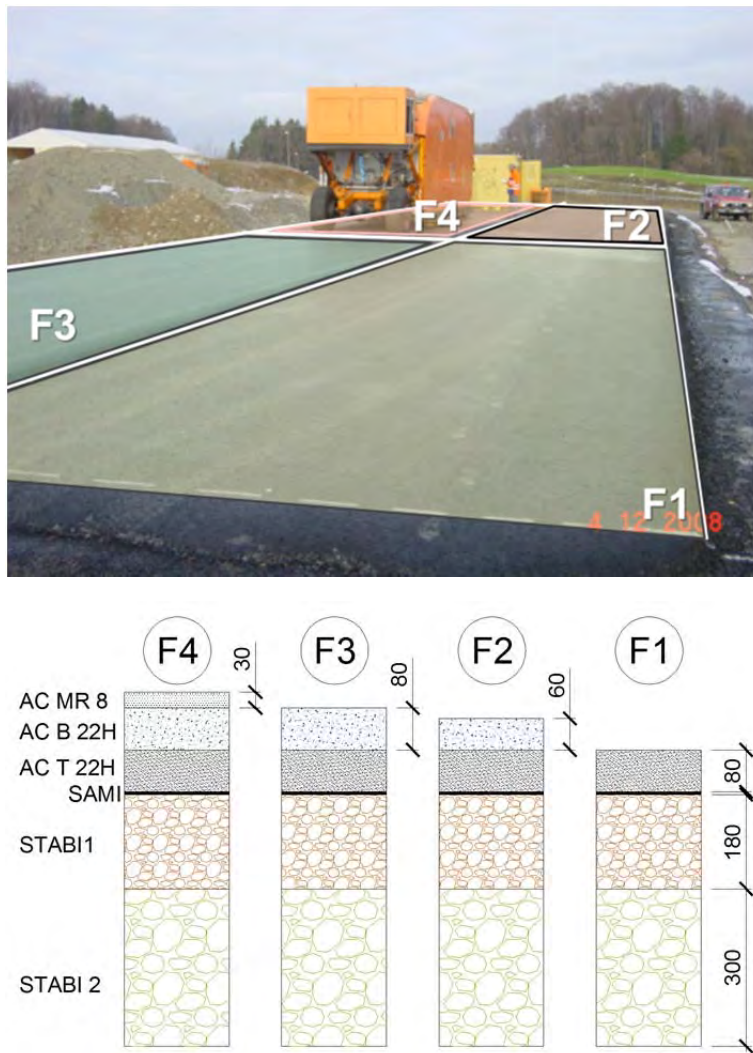
Fig. 5.1 Distribution of the test sections and pavement structures.

5.1.2   Load configuration

The MLS10 machine was setup to apply 65kN in each of the four bogies, using a twin tire configuration. This is the maximum load that the MLS10 is able to induce with this type of tire and it corresponds to a total axle load of 130kN. The loads were measured using static scales. The tire pressure was set to 7.5bar. The trafficking speed used for the tests was 22km/h. For these tests, the MLS10 was equipped with Goodyear 455/50 R22.5 twin tires.

5.1.3   Number of expected MLS10 load applications

According to the Swiss design standard SN 640324a [4], each of the pavements of section F1, F3 and F4 correspond to a certain type of pavement characterized by the Structural Number (SN). The SN is calculated with the thickness of each of the layers of the pavement and the coefficient of bearing capacity (a) of the materials. Following the standard, it is possible to make a classification of the structure in one of 6 types. Each type is designed to last a certain amount of 8.16t axle loading in 20 years' time. Since the MLS10 loading corresponds to a 13.3t axle, the destructive effect according to the Swiss standard SN 640320 [25] is 8.46 times higher. Fig. 5.2 summarizes the calculation of the number of expected MLS10 load applications to reach the bearing capacity of the pavements of each test section.

Fig. 5.2 Number of loads required to reach the bearing capacity of each section

Material	F1		F3		F4	
	Coef. bearing capacity a	Thickness [cm]	Coef. bearing capacity a	Thickness [cm]	Coef. bearing capacity a	Thickness [cm]
AC MR 8	-	-	-	-	4	3
AC B 22 H	-	-	4	8	4	8
AC T 22 H	4	8	4	8	4	8
Stabi	2.4	48	2.4	48	2.4	48
SN	147		179		191	
Pavem. type	T6-S1		T6-S1		T6-S1	
Loads appl.	8'628'900		8'628'900		8'628'900	

5.1.4 Evaluation of pavement performance

Deterioration of pavements is traditionally carried out by means of visual inspections, which provides a subjective appreciation of the cracking of road surface, or the development of rutting, among other types of distress. The need of a more accurate definition of pavement distress, lead to the development of devices which can be transported and used in different sections of a road without creating damage. These devices usually measure the deflection of the surface to obtain an indication of the condition of the structure. Most recently, different kinds of sensors are available for being installed in roads for monitoring the deterioration over time. Instrumented pavements using strain gauges and temperature sensors are not rare nowadays [8] [9]. However, installation and robustness of the sensors as well as data acquisition process and interpretation are still a complex issue. In this research project, the deterioration of the pavement was evaluated using different types of methods and sensors. In this report they are classified as permanent sensors embedded in the pavement or periodically applied non-destructive devices. The list of methods used in this project along with a short explanation about the installation is given below.

Stationary sensors embedded in the pavement

- Temperature sensors: Thermocouple wires type K, were placed between the layers during construction of the pavement. These wires are for general purpose temperature measurements in asphalt, concrete and ambient air. They have Teflon insulation and can be used successfully without further protection in the paving process, even at high temperatures.

- Strain gauges: For measuring the deformation of the pavement under load, gauges were embedded at different depths of the pavement. The installation of the sensors was carried out simultaneously with the construction of the different layers of the pavement. Three different types of installation were tried. In the first one, the sensors were laid without any protection on top of one layer. However, sensors installed this way didn't survive the construction. Therefore, another method was used in which the strain gauges were placed in an H shaped trench previously cut in that layer. For the last method, the H shaped trench was prepared by embedding wooden dummies in

the hot mix asphalt during compaction (see Fig. 5.3). After finishing the compaction of the layers, the dummies were taken out and the sensors were placed in the trench.
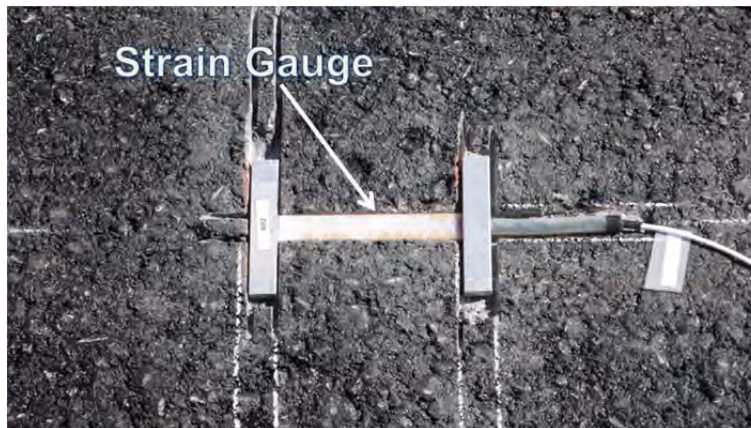
Fig. 5.3 Strain gauges, installation in the pavement

- Accelerometers: In order to obtain the dynamic deflection of the pavement under the MLS10, 3 accelerometers were installed in a line perpendicular to the trafficking direction. The mounting was done by drilling holes of 5cm diameter down to a depth of 3cm (see Fig. 5.4). The accelerometers were screwed to plates firmly attached to the bottom of the hole. The sensors selected for this work were the capacitive accelerometers model 3700 from PCB. These accelerometers are rugged and were specially prepared with integrated water proof cabling to withstand extreme climatic conditions. Data acquisition was done simultaneously with the strain gauges and stored for postprocessing analysis. More information about the data analysis and interpretation can be found elsewhere [13] [14].
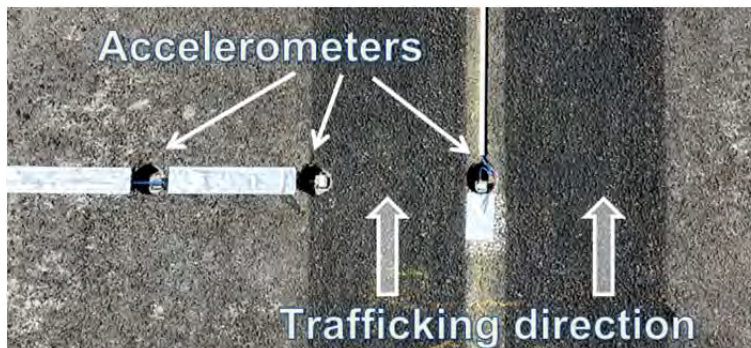
Fig. 5.4 Installation of the accelerometers

Periodically applied non-destructive sensors

- Transversal profiles: Permanent deformation of the pavement surface was calculated by analysing three profile measurements for each section, all perpendicular to the trafficking direction. Measurements were carried out with the MLS profiler. The profiler consists of a steel beam which has a wheel on the bottom side (see Fig. 5.5). For each measurement, the beam is fixed to two steel plates that are glued to the pavement surface, outside the trafficked area which serve as "reference points". The beam distance to pavement can be set with a pair of adjustable feet at each end of the beam. This setup provides a stable frame for the measurements. A moving wheel situated in the bottom part of the beam travels in contact to the surface of the pavement, following any unevenness up to 1mm. The combination of vertical and horizontal movement allows drawing the profile, which is expected to change throughout the tests due to permanent deformation. Consequently, measurements were taken recurrently after a regular number of load applications in order to follow the increase of rutting versus the accumulated number of loads.
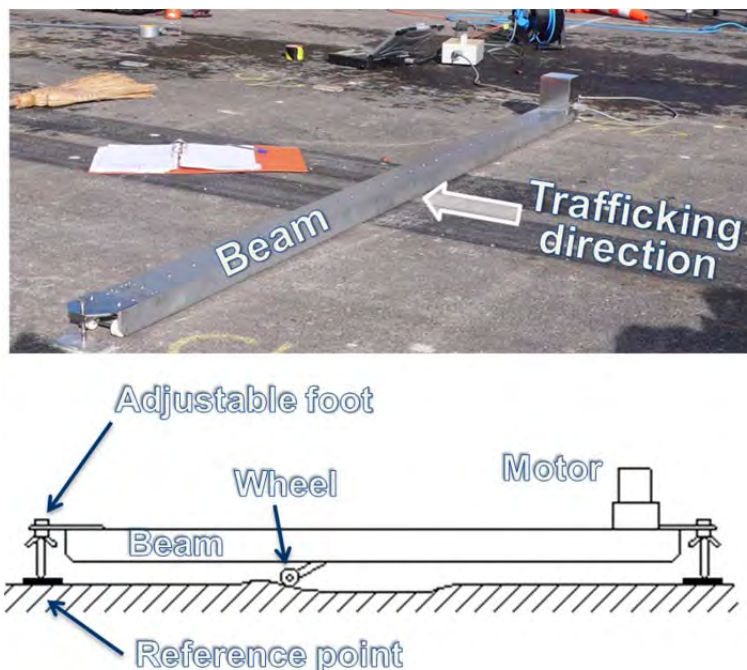
Fig. 5.5 View of the profiler used for rutting measurements

- Portable Seismic Pavement Analyser (PSPA): Monitoring of seismic stiffness of the pavement layers was conducted with the PSPA. The device uses the theory of wave propagation in continuous media to determine the seismic modulus of each layer. Literature describing the theory about PSPA stiffness calculations can be found in [10], [11] und [12]. The PSPA is composed of two ultrasonic receivers, one source and one spectral analyser that sample the analogous electric signal coming from the receivers into numerical data. The distance between the source and both receivers is fixed and defines the setup. The device is equipped with a thermometer in one foot, in direct contact with the pavement surface. Measured values are used later for temperature normalization. A picture of the device is presented in Fig. 5.6. For this APT three measurements per test section, two in each of the wheel paths and one outside the trafficking zone, were carried out.
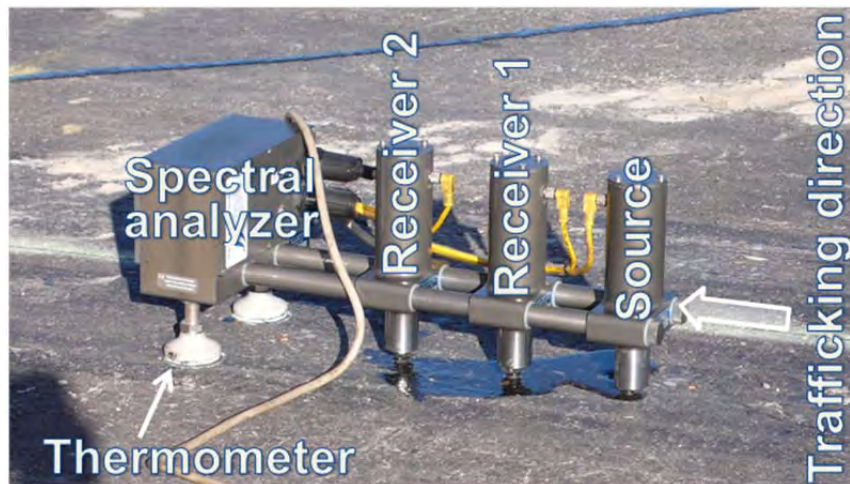
Fig. 5.6 View of the PSPA in measuring position

- Falling Weight Deflectometer (FWD): It is one of the most used devices for structural evaluation of pavements. It consists of a trailer containing a mass and a line of geophones to measure deflection as shown in Fig. 5.7. It can simulate the load of a passing truck by dropping a heavy weight on the pavement surface. The dynamic characteristics of the load are controlled with a spring element. The transient impulse load induces a deflection basin on the pavement surface, which is detected by a series of geophones in contact to the surface of the pavement. Surface velocities are recorded and converted to deflection. The amplitude and shape of the deflection obtained with this device are generally considered as an indicator of the structural condition of the pavement. Literature about the FWD and its application in pavement engineering can be found elsewhere [15] [16].
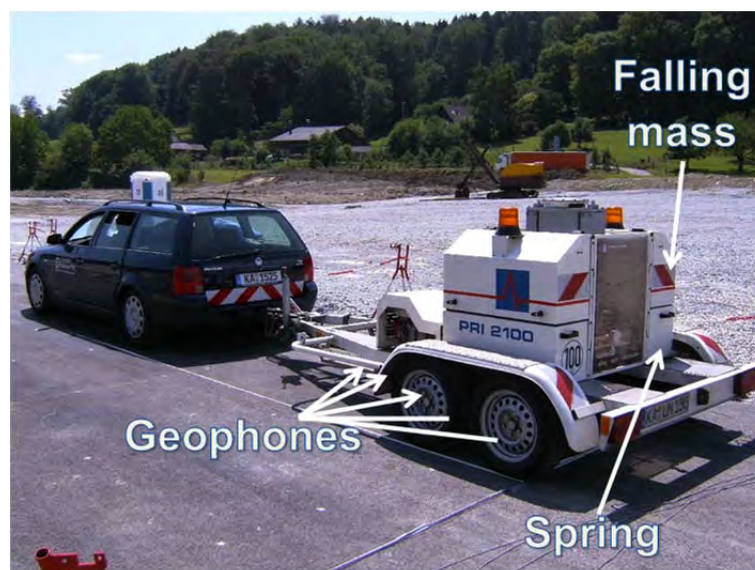
Fig. 5.7 View of the Falling Weight Deflectometer (FWD) in testing position

- ETH Delta: The road deflection measurement device "ETH Delta", allows measuring the static deflection bowl under an axle load [17]. The device consists of two main beams, 6m long and a transversal tube fixed on their front end (Fig. 5.8). Twelve fingers with highly precise laser measurement sensors mounted at their tips are connected to the transversal tube, providing a frame for the measurements. The two main beams are based at the ground about 4.5m away from the loading point. Since temperature changes during measurement can make the device slightly moving, two mirrors for optical laser sensors are placed on the tube ends and its movement are measured from two points at the rear (approx. 7m) end of the beam. For obtaining the pavement deflection bowl, the device is placed at the measurement location and a heavy vehicle with known axle load (can be a truck, a heavy construction equipment or even the MLS10) is moved longitudinally towards and away from the position of the ETH Delta. The set of lasers of the device record the deflection while the vehicle is moving. The combination of the deflection records with the distance of axle load distance allows creating 2D or 3D deflection maps of the pavement under the axle load. The measured deflections can be used to calculate the elastic modulus of the layers and compare them at different loadings. In addition, the deflection maps for different loadings can be compared in order to detect visible changes due to modifications in pavement stiffness.
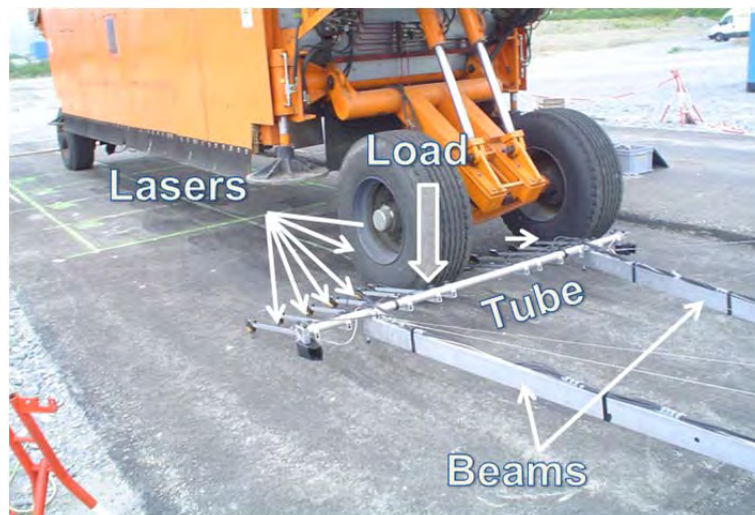
Fig. 5.8 Measurement of pavement deflection with ETH Delta

- Ground Penetrating Radar (GPR): This is a non-destructive testing device that uses electromagnetic waves to determine the geometry of a structure. The working principle is based on the measurement of the change of the dielectric permeability of the different materials. The device consists of an antenna that radiates an electromagnetic signal to the subsurface, which is reflected in every interface between layers. The same antenna collects the reflection of the signal, which is processed by the central unit and stored in a laptop for later post processing. Radar data is collected along parallel lines (see Fig. 5.9) as a series of single measurement tracks. When single track measurements are plotted next to each other, the result is an image that will show the properties of the subsurface. Such a representation is called radar profile and the resolution and depth depends on the size of antenna. Antennas that produce high frequency signals have higher resolution (can detect changes in dialectical permeability in small areas), but only near the surface, whereas lower frequency antennas go deeper in the inspection, but the resolution is poor, compared to the first ones.

Fig. 5.9 Inspection of the pavement with GPR.

Additional assessments

- Additionally to the measurements described above, visual inspection of the pavement surface to detect distress like cracking, bleeding, etc., were carried out periodically. Finally, forensic investigation of pavement deterioration, if any, was done by coring samples and taking slabs for later testing in the laboratory.

5.1.5   Location of the sensors and non-destructive testing

A scheme of the sensor postitions and a table with the depth of installation for each section is depicted in Fig. 5.10, Fig. 5.11 and Fig. 5.12 for sections F1, F3 and F4 respectively. The profiles to evaluate the permanent surface deformation were taken in the middle of the trafficking path and 1m to each side. PSPA measurements were carried out in each wheel path and outside the load application area. The set of three accelerometers, one in the middle of the trafficking path and the other two at 0.30m and 0.60m distance transversal to the trafficking axis are also shown in the figures. In section F1 no strain gauges were installed.
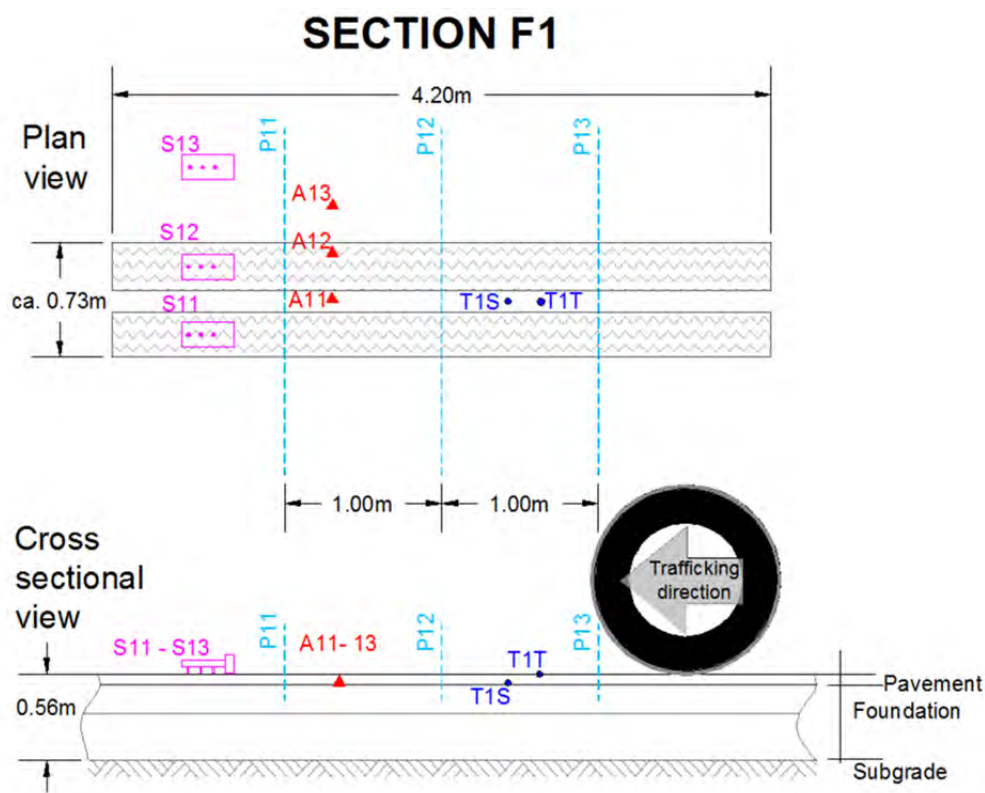
SECTION F1

Section	Thermocouple	Depth [cm]	Strain gauge	Depth [cm]	Direction
F1	T1T	0	-	-	-
	T1S	-8	-	-	-

Fig. 5.10 Schema with the position of the sensors embedded in the pavement and periodic measurements in section F1, showing the designation of the different sensors together with their position and direction
S: PSPA
A: Accelerometer
P: Transversal profile
T: Thermocouples
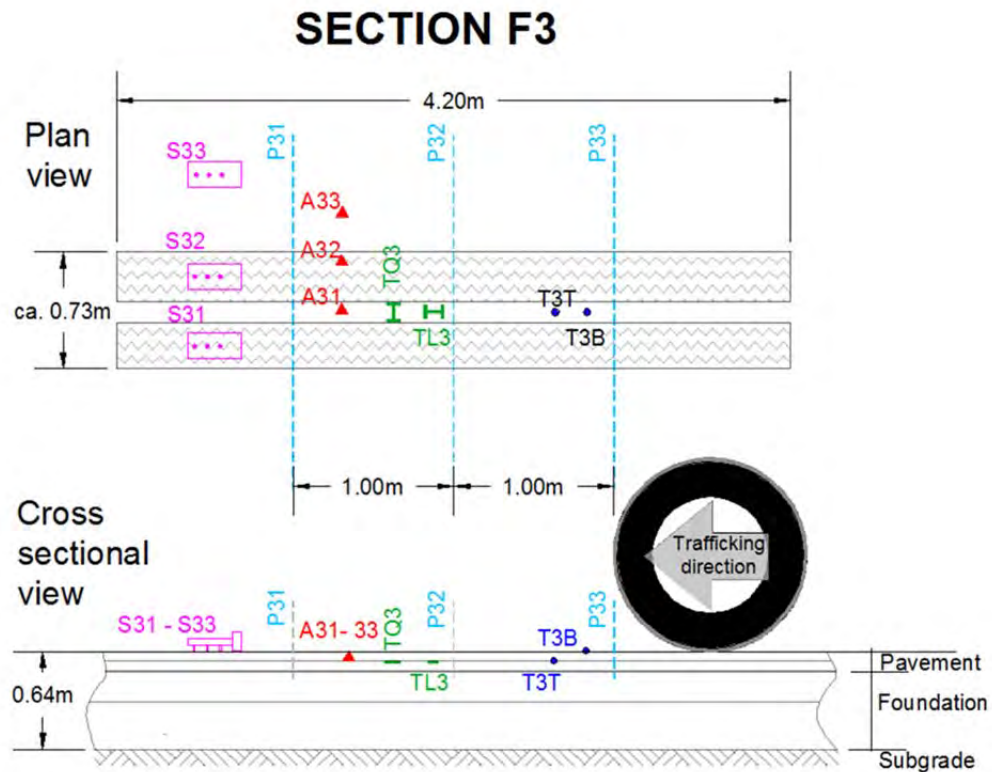
Section	Thermocouple	Depth [cm]	Strain gauge	Depth [cm]	Direction
	T3B	0	TQ3	-8	
F3					
	T3T	-8	TL3	-8	

Fig. 5.11 Schema with the position of the sensors embedded in the pavement and peri-odic measurements in section F3, showing the designation of the different sensors to-gether with their position and direction
S: PSPA
A: Accelerometer
P: Transversal profile
T: Thermocouples
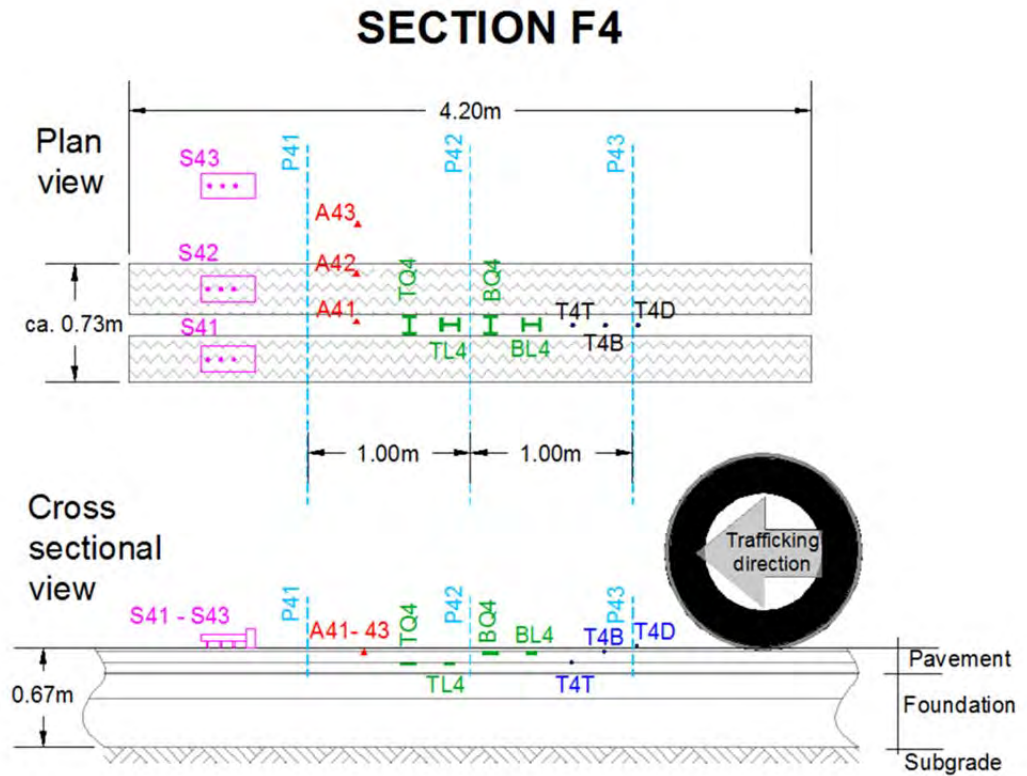
SECTION F4

Section	Thermocouple	Depth [cm]	Strain gauge	Depth [cm]	Direction
F4	T4D	0	BQ4	-3	
	T4B	-3	BL4	-3	
	T4T	-11	TQ4	-11	
	-	-	TL4	-11	

Fig. 5.12 Schema with the position of the sensors embedded in the pavement and periodic measurements in section F4, showing the designation of the different sensors together with their position and direction
S: PSPA
A: Accelerometer
P: Transversal profile
T: Thermocouples

For the FWD tests, a grid of points covering the trafficked and not-trafficked pavement was defined to carry out the measurements following a fixed arrangement (see Fig. 5.13, Fig. 5.14 and Fig. 5.15). The FWD was positioned in the regular pattern defined by lines and points comprising the load application area of the MLS10 and the zone outside this and the influence range of the MLS10. To that end, 5 lines from A to E with 9 measuring points per line were defined. In section F1 there were only 8 points per measurement line. For the tests, the FWD was placed so that the falling weight of the device coincides with the location of the points, having the FWD geophones aligned with the trafficking direction. The measuring grid, about 12m long and 3m wide had the MLS10 load application area in its center comprising the lines B and C (sections F3 and F4), more precisely the 13th, 14th, 15th, 22nd, 23rd and 24th measurement points. For section F1, the loading area comprised lines C and D and measuring points 20th, 21st, 22nd, 28th, 29th and 30th. Deflections were obtained for loading impacts of 65kN and 90kN. Measurements were carried out at different trafficking times, as described later in § 5.2.3.
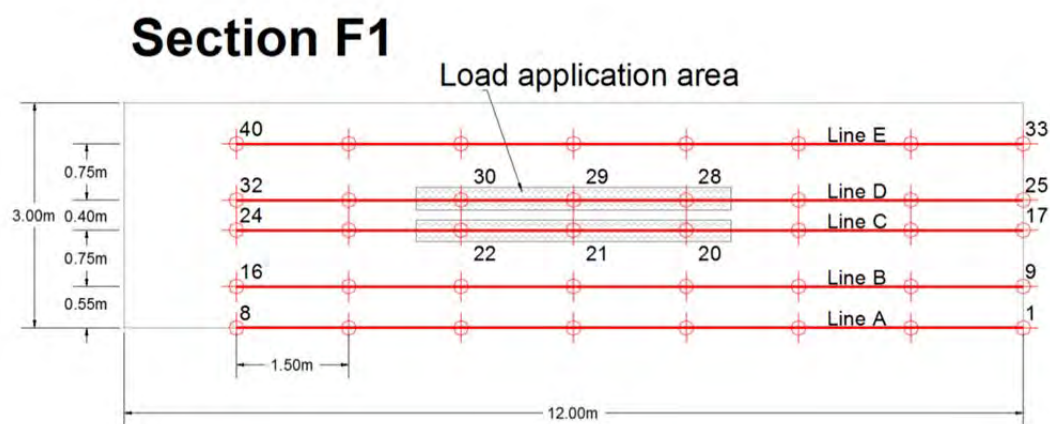
Fig. 5.13 FWD measurement grid in section F1
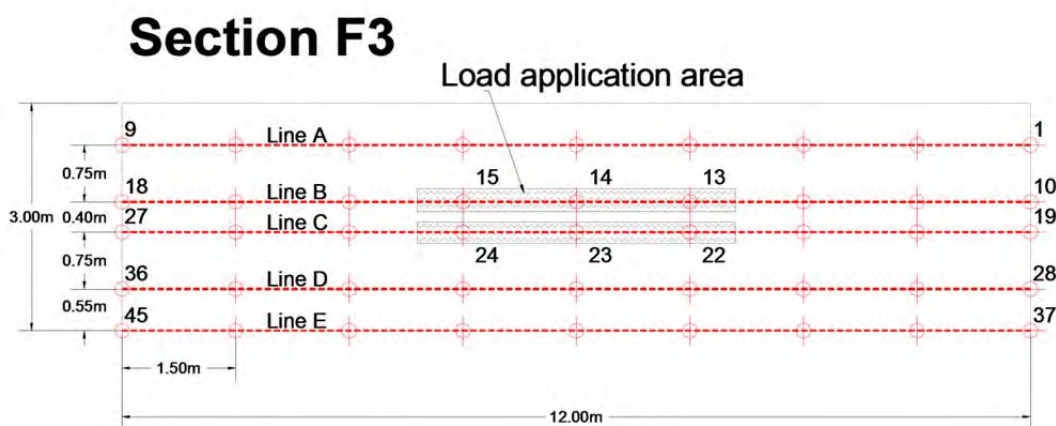
Fig. 5.14 FWD measurement grid in section F3.
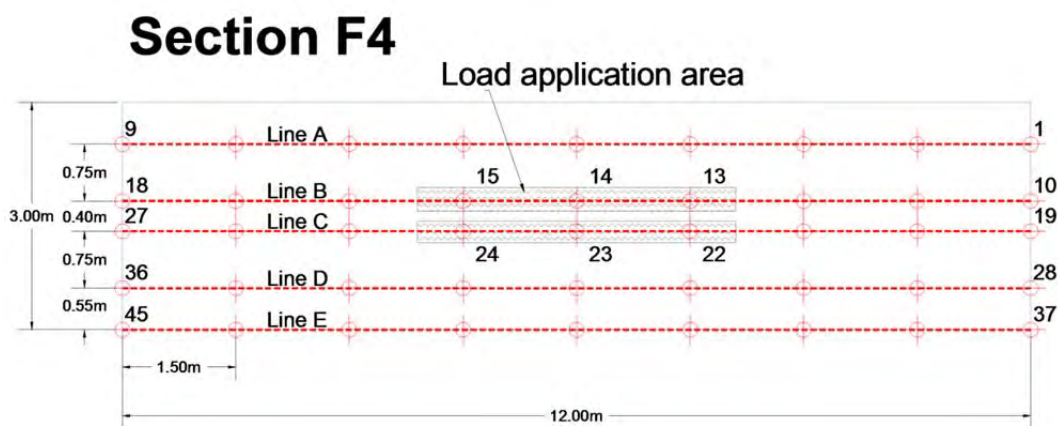
Fig. 5.15 FWD measurement grid in section F4

ETH Delta deflection measurements were carried out using the MLS10 as vehicle to load the pavement. The MLS10 was driven from a far position until the front transport wheels of the machine reached the measuring location. The front right wheel, which load is about 80kN, was fitted shortly between the lasers of the device. Then, the MLS10 was driven backwards to the starting position. In each section, two measuring positions A and B inside and outside the load application area respectively, were defined (see Fig. 5.16, Fig. 5.17 and Fig. 5.18). Measurements were carried out at different trafficking times, as described later in § 5.2.3. The outside position was planned to serve as measurement reference and to control the validity of the measurements, since it was expected that the results obtained in the not-trafficked pavement remain the same throughout the trafficking history.
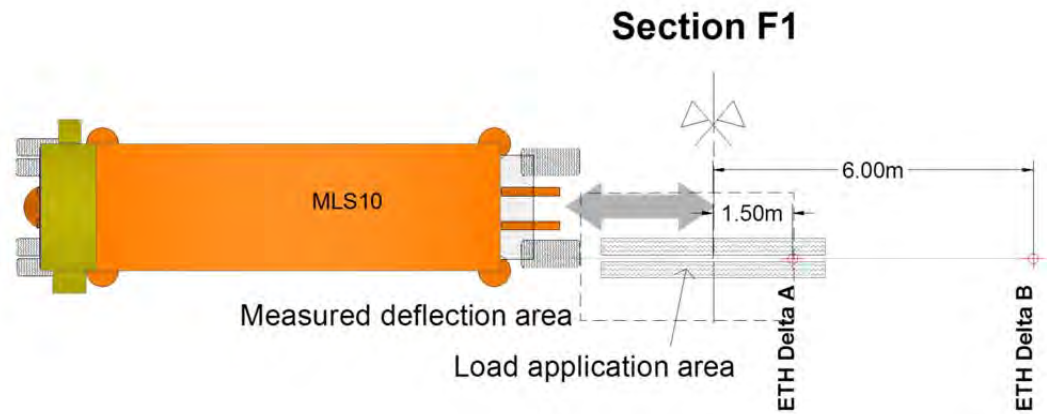
Section F1

Fig. 5.16 ETH Delta measuring positions in section F1
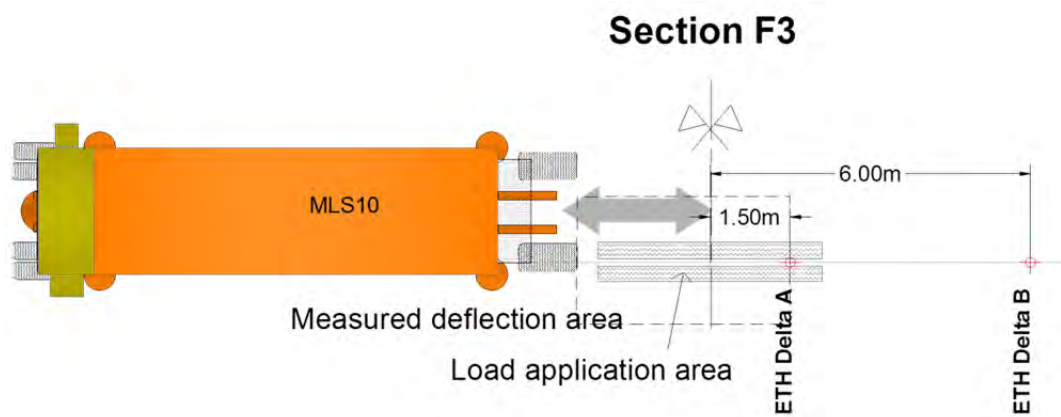
Section F3

Fig. 5.17 ETH Delta measuring positions in section F3
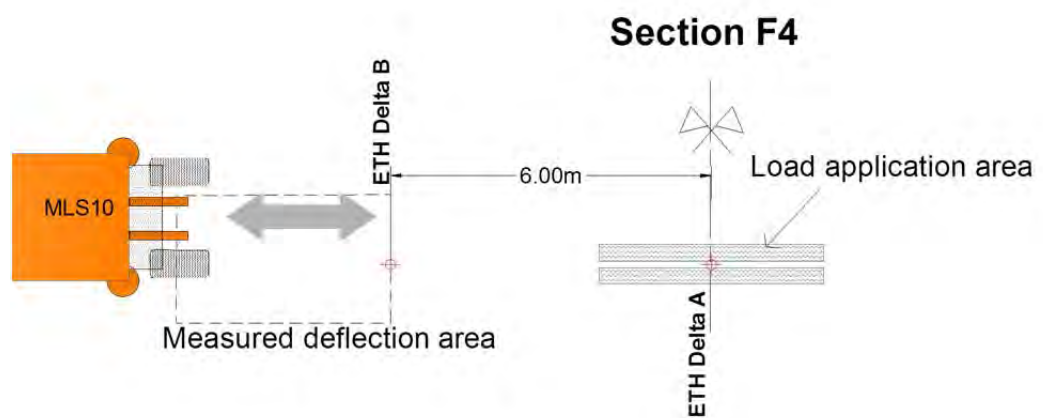
Section F4

Fig. 5.18 ETH Delta measuring positions in section F4

5.2   Operation

5.2.1   Loading history

The goal of the test program was to reach, in a first phase, 3'000'000 MLS10 load applications of 65kN. After reaching this amount of loads it would be decided if an extension of the test period was required to fulfill the main objective of the project.

The MLS10 was deployed to the testing site during two seasons. The first operation period started 12th of November 2008 and finished on 5th of November 2009. Due to a crack in one of the bogies the machine was sent back for refurbishing during winter break. Newly designed bogies were installed and the MLS10 was operational again shortly after winter. The 28th of May 2009 the tests were continued until 4th of November 2009. In total, 1'605'928 loads were applied to the three different pavements of Sections F1, F2 and F4 throughout a total of 161 days. The machine was regularly displaced on the testing site to have, on average, the same temperature profile in each section. The accumulated number of loads through the duration of the tests is presented as a line in Fig. 5.19. Horizontal segments in the line represent the days where the MLS10 was not operational due to holidays, weekends, breakdowns, measurements, installation of sensors, etc. The problems and actions done to improve the performance of the machine during this period are described in the next section. The line shows that, at the beginning of the tests, the performance of the machine was poor because of prolonged breakdowns and repairing times. In the second half of the testing period, the performance increased, due to a clear reduction of the breakdowns.
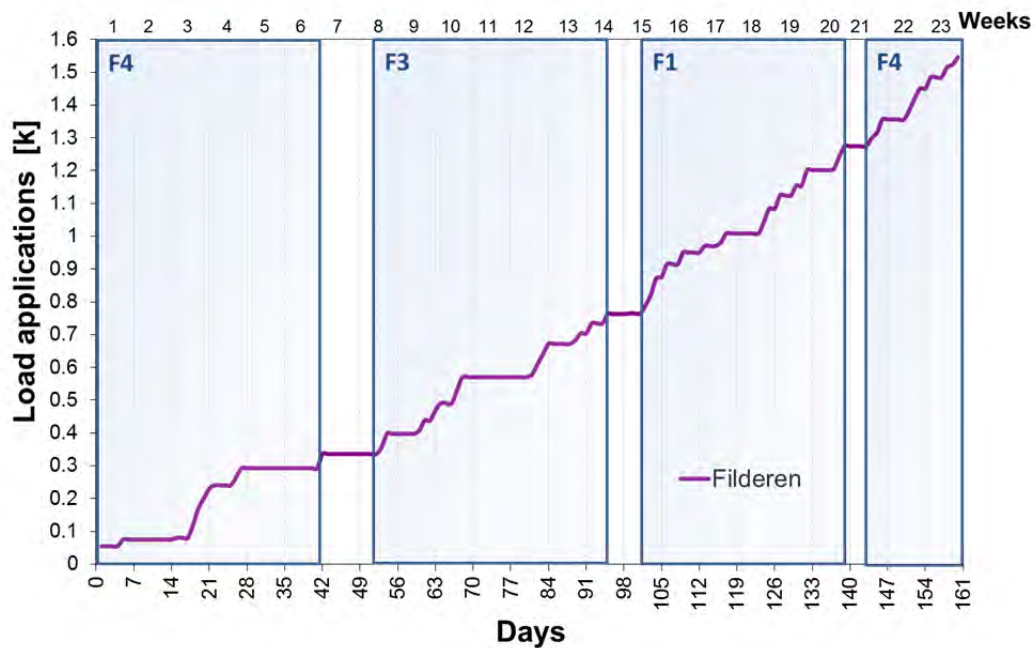
Fig. 5.19 Number of MLS10 accumulated load applications vs. time

At the end of the testing period, the amount of accumulated load applications in each section was:

Section F1:   439'000 MLS10 load applications

Section F3:   427'000 MLS10 load applications

Section F4:   765'000 MLS10 load applications

5.2.2 Interruptions due to machine malfunctioning

One of the objectives of this project had to do with the evaluation of the machine itself. It was expected that, as the MLS10 is a prototype, the occurrence of operational interruptions due to malfunctioning would be much higher than for a mass production device. The MLS10 was purchased with a guarantee agreement, implying that any breakdown occurring within one year after the acquisition had to be repaired and afforded by the South African developer with the agreement and support of Empa. In this section, a list of the main breakdowns and the actions carried out are briefly presented.

12.11.2008 Cracks in old bogies.

During routine control of the MLS10, an extended fatigue crack was discovered in the center of one of the bogies (Fig. 5.20). After discussion with University of Stellenbosch, new bogies were designed, constructed and installed in the machine. These work lasted several months and were carried out during winter 2008/2009.

Fig. 5.20 Crack in the old bogies (left) and replacement work carried out at Empa (right)

24.06.2009 Damage on wheel bearing

An inadequate installation of special bearings in the steel wheels of the new bogies caused breaking of one these bearings and extensive damage in one of the wheels. All bearings and a wheel had to be replaced (see Fig. 5.21). The work was carried out on site and caused a breakdown of more than 2 weeks.

Fig. 5.21 Damaged bearing (left) and replacement work carried out in Filderen (right).

22.07.2009 Defect in the fixation of the trafficking wheel

During a routine check, a problem in the fixation of the trafficking wheels was detected and the design was changed and improved (see Fig. 5.23). The repairing took several days.

Fig. 5.22 Picture showing the insecure fixation of the trafficking wheel

05.08.2009 Cracks in the new bogies

After a routine check, new fatigue cracks were discovered (see Fig. 5.23). It was decided to fix them by welding on site and to revise the design of the the bogies for later reinforcement. The problem caused a delay of more than 2 weeks.

Fig. 5.23 Crack (links) and welding (right)

Other problems, mostly due to broken screws and small pieces and leakage of cooling system, or hydraulic system, were solved relatively fast. In any case, they represented a sensible reduction in the efficiency of the work.

5.2.3 Non-destructive tests history

ETH Delta and FWD non-destructive tests were performed at different trafficking times. Fig. 5.24 gives detailed information about the history of the measurements.

Fig. 5.24 Date and number of MLS10 load applications for each non-destructive test.

Date	FWD tests			ETH Delta tests		
	Section F1	Section F3	Section F4	Section F1	Section F3	Section F4
29.06.09	0	0	353'000	-	-	-
15.09.09	188'000	427'000	396'000	-	-	-
16.09.09	-	-	-	188'000	427'000	396'000
22.10.09	439'000	-	550'000	-	-	-
10.11.09	-	-	-	439'000	-	740'000

The FWD measurements were carried out with a device and personnel from KTI Karlsruhe Institute of Technology in Germany, as part of a master thesis of Martin Umminger [18]. Testing with ETH Delta device was carried out by staff of the Institute for Geotechnical Engineering (IGT) of ETH.

5.3 Measurement results

In this chapter, the data obtained from the sensors embedded in the pavement as well as the non-destructive testing carried out in the test sections are presented and analyzed individually. The interpretation of the results is focused in the detection of distress in the pavement.

5.3.1   Temperature

Data Evaluation

For each sensor, temperature values are obtained every 5 seconds and the average of all readings over 5 minutes are stored in a table with the date and timestamp in the first column. The information is stored in the internal memory of the Squirel, the data acquisition system (DAQ) device for temperature recordings. The data is downloaded to a computer using a special software and stored as an ASCII file. The tables are used to display the temperature evolution in time, as shown in next section, or to estimate the temperature profile of the pavement when required.

Summary of the Temperature Records

Fig. 5.25, Fig. 5.26 and Fig. 5.27 show the temperature distribution of each section during the periods when the MLS10 was positioned for trafficking. The horizontal axis displays time and the vertical axis contains the temperature. The tracks in the figure show the records by each of the sensors, whose location was described in § 5.1.5. The lines show the temperature measured by each sensor and grey traces placed vertically over in the figure, reveal when the MLS10 was trafficking the section. The shapes of the curves show, as expected, an increase of temperature during the day and lower temperatures at night. Additionally, the sensors near the pavement surface are more sensitive to air temperature changes or to the sunshine rays than the ones that are installed deeper in the pavement.
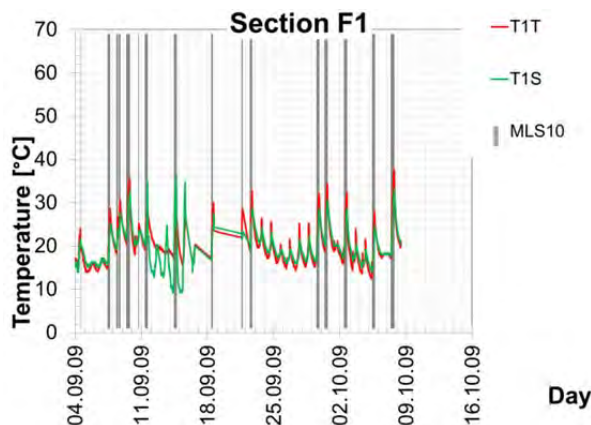
Fig. 5.25 Temperature distribution measured in section F1
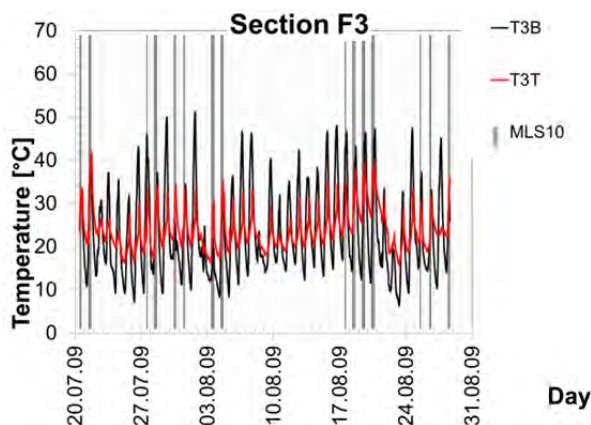
Fig. 5.26 Temperature distribution measured in section F3

a)

b)
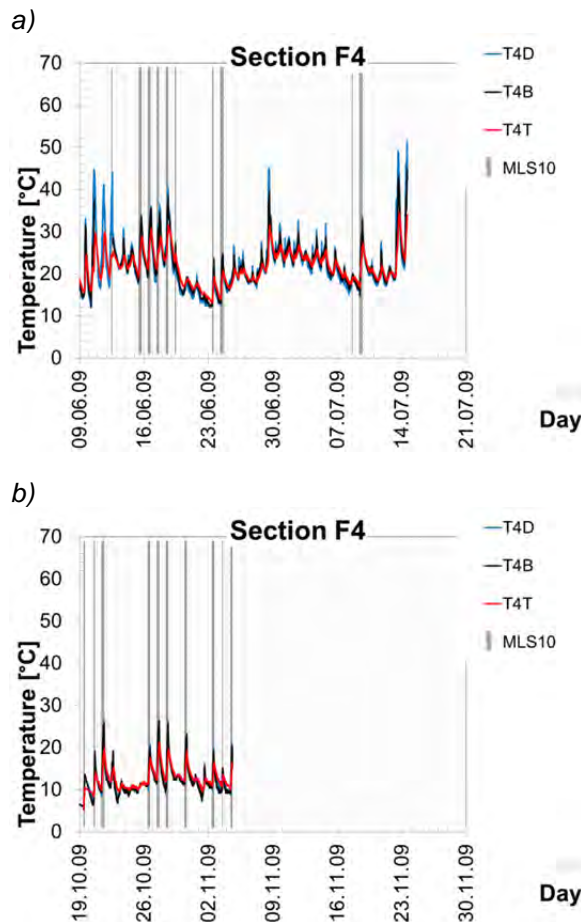
Fig. 5.27 Temperature distribution measured in section F4, for the two periods of MLS10 trafficking in a) June and July and b) October and November 2009

In some of the cases it can be noticed that the increase of temperature in the pavement is not only produced by the sun or the temperature of the air. There is also an increase of temperature that is partially caused by the transmition of the heat produced by the machine itself and the dissipation of the energy induced by the rolling of the tires over the pavement. This means that the pavement increases the temperature locally in the zone near the rolling tires. This can be explained as deformation energy produced by the rolling tires being transformed to heat due to internal friction in the pavement . Fig. 5.28 shows an example of this effect in section F1. The figure shows the temperature during 3 days in which the MLS10 was trafficking the section. The continuous lines show the temperature of each of the sensors in section F1 and how it grows in coincidence with the initiation of the trafficking (gray columns). As soon as the MLS10 stop trafficking the section, the temperature of the pavement decreases, even if it is during the daylight period. This means that the machine heats the pavement through the intense rolling intervals and the temperature will be always above the exterior air temperature.
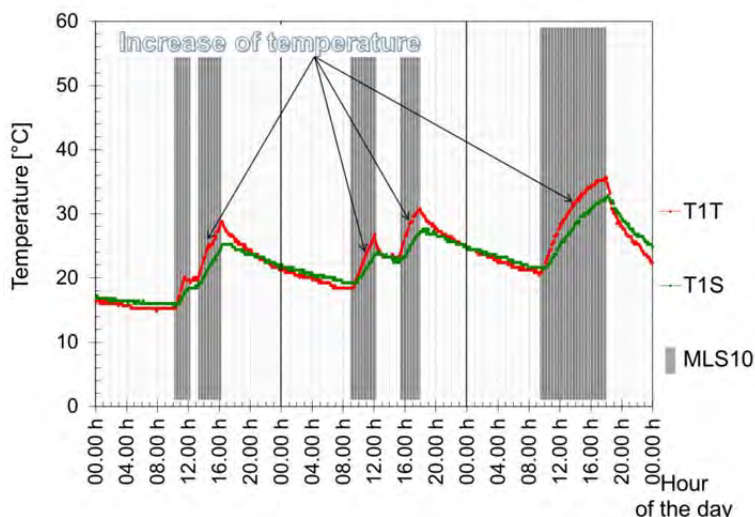
Fig. 5.28 Increase of temperature due to MLS10 loading

Fig. 5.27 summarizes the average temperatures over the testing period and the average temperature exclusively while the machine was running. These temperatures will be used for comparing the results of the different measurements in each of the test sectios, as they have a big influence on the pavement response. The table shows that, although the temperature over the testing period is quite similar for all the sections, during traffickingin they have a bigger variance. The highest temperature is of 29.6°C in section F3 and lowest of 18.7°C in section F4.

Fig. 5.29 Average temperatures

Thermocouple	Average temperature over testing period [°C]	Average temperature during trafficking [°C]
T1T	19.7	27.5
T1S	20.0	23.8
T3B	23.2	28.5
T3T	23.8	29.6
T4D	22.6	23.4
T4B	22.8	20.3
T4T	22.5	18.7

5.3.2 Transversal pavement profiles

Data Evaluation

Data is recorded in an ASCII file. The file contains a table with the position of the profiler's small wheel perpendicular to the traffic direction and the vertical position. In this case, the length of the profile was set to 1400mm, taking a measurement every 1mm. The data is first cleaned, taking away any outliers caused by small stones that could have been

situated along the small wheel path, and then averaged considering 5mm windows. Then, the first measurement is set as reference. Next, every profile taken in the same position is substracted from the reference, obtaining the permanent deformation relative to the original pavement surface.

Because of channelized trafficking, the tire treads produce clear longitudinal imprints on the pavement surface. The form of the rutting is therefore different from what is usually found in a road, where vehicles wander within the lane and tires have different shapes. Estimation of rutting outlined in the SN 640925b [26], as the maximum distance between a latch sitting perpendicular to the rut and the pavement below, is thus not used for MLS10 channelized trafficking. Fig. 5.30 shows a schema of the rut depth calculation methodology employed in this report, in the case of twin tires loading.
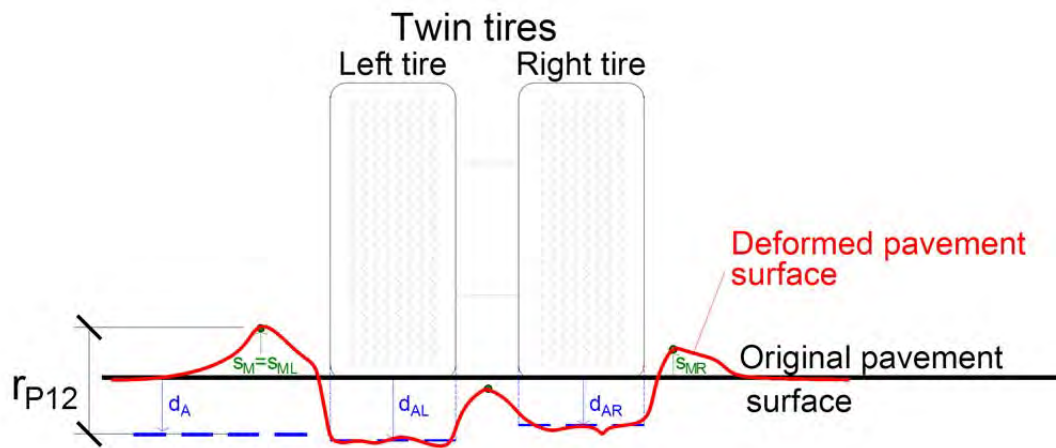
Fig. 5.30 Example for the calculation of the rut depth from a profile measurement, where
d_{AL}:   dipping average left tire
d_{AR}:   dipping average right tireA
d_A: dipping average
s_{ML}:   shoving maximum left tire
s_{MR}:   shoving maximum right tire
s_M: shoving maximum
r_{P12} rut depth for Profile 12

Deformation of the pavement surface is characterised by downwards dipping under the tires and, in some cases, by upward shoving along the wheelpath sides. The dipping average d_A is calculated as the mean of the dipping average under each tire (d_{AL} for left tire and d_{AR} for right tire).

$$d_A = \frac{1}{2}(d_{AL} + d_{AR})$$

In the case that the pavement presents upwards shoving, s_M is defined as the highest value between the shoving maximum on the left and right side of the wheel path (s_{ML} and s_{MR} respectively).

$$s_M = s_{ML} > s_{MR}$$

If there is no upwards shoving, s_M is equal to zero. The rut depth is then defined as the difference between the shoving s_M (positive value or zero) and the dipping average d_M (negative value). For the Profile 12 the rutting r_{P12}would be:

$$r_{P12} = s_M - d_A$$

After calculating the rut depth for every profile measurement, the values are plotted against the number of MLS10 loads applications, as presented in next chapters. The evo-

lution of the rut depth vs. the number load applications is modeled using potential functions.

Summary of the Results

Fig. 5.31, Fig. 5.32 and Fig. 5.33 show the progressive surface deformation of the pavement in the middle profile of each section. The colored lines are the relative total rutting at different trafficking times. The vertical axis in the figures is scaled to -20mm for later comparison with other pavement profiles. Inside each figure, a window subfigure presents the rutting progress of the pavement vs. the number of MLS10 load applications. It includes the approximation of the results with a potential function, the coefficient of determination R^2 and the average pavement temperature calculated in the previous chapter.
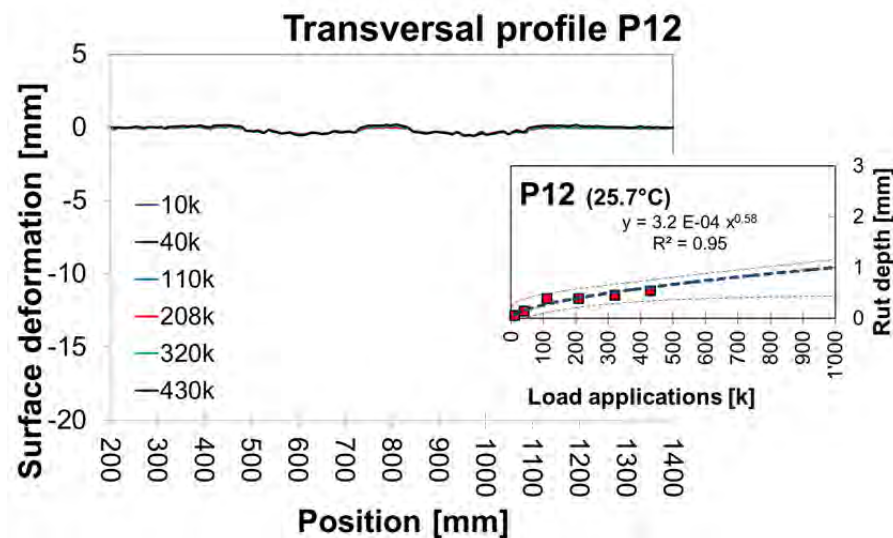
Fig. 5.31 Rutting profiles P12 measured in the middle section F1. The subfigure presents the progressive rut depth vs. number of MLS10 applications fitted with a power function, including 95% prediction bounds
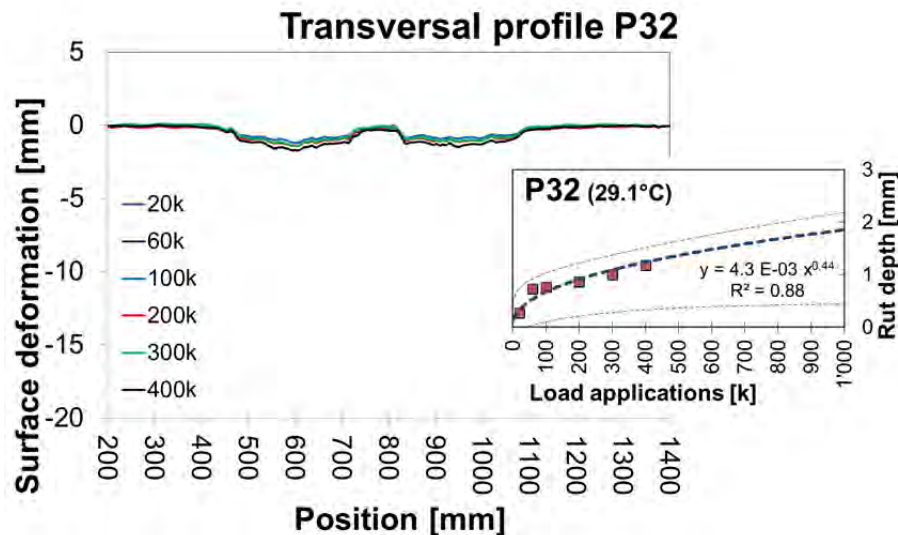
Fig. 5.32 Rutting profiles P32 measured in the middle section F3. The subfigure pre-
sents the progressive rut depth vs. number of MLS10 applications fitted with a power
function, including 95% prediction bounds
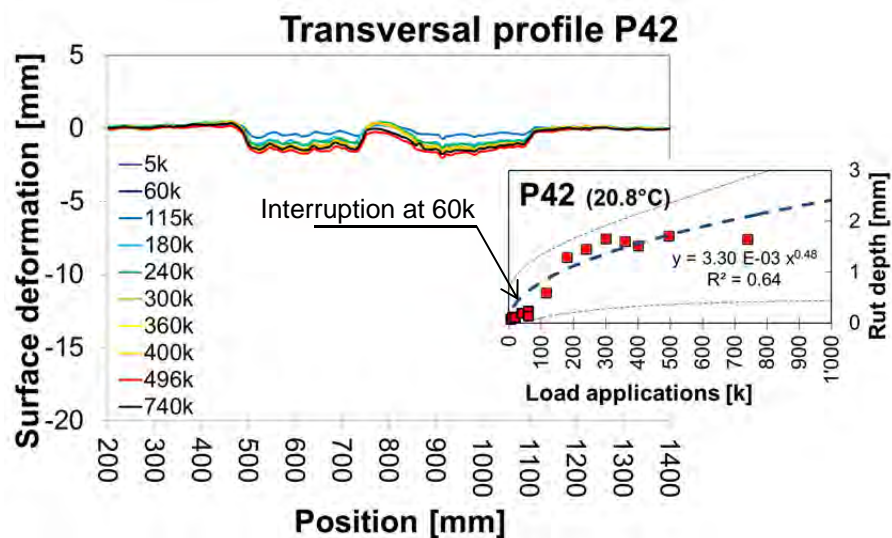
Fig. 5.33 Rutting profiles P42 measured in the middle section F4. The subfigure pre-
sents the progressive rut depth vs. number of MLS10 applications fitted with a power
function, including 95% prediction bounds

In section F4, the first 60'000 load applications were carried out in year 2008. Trafficking
was resumed after several months' interruption in 2009. During this break the testing field
was used for other purposes and the fix references for the profile measurements were
removed. Therefore, the results show a clear discontinuity in the progression trend
(Fig. 5.33). This is also observed in the poor coefficient of determination R^2 of the poten-
tial approximation.

Fig. 5.34 shows the rutting progression vs. the number of MLS10 load applications for
the three testing sections. The figure reveals that in all cases measured rut depth re-
mained below 2mm. This means that the pavement tested in Filderen are very stiff, as
expected. In some cases rutting showed a small reduction, probably due to errors pro-
duced by the deformation of the profiler from different temperatures. In or-der to model

the deformation, the points were approximated with a power function. Note that section F4 shows larger rutting in spite of the lower average temperature. Hence, this rutting behavior cannot be attributed to temperature but to the accumulated permanent deformation of the bituminous layers.
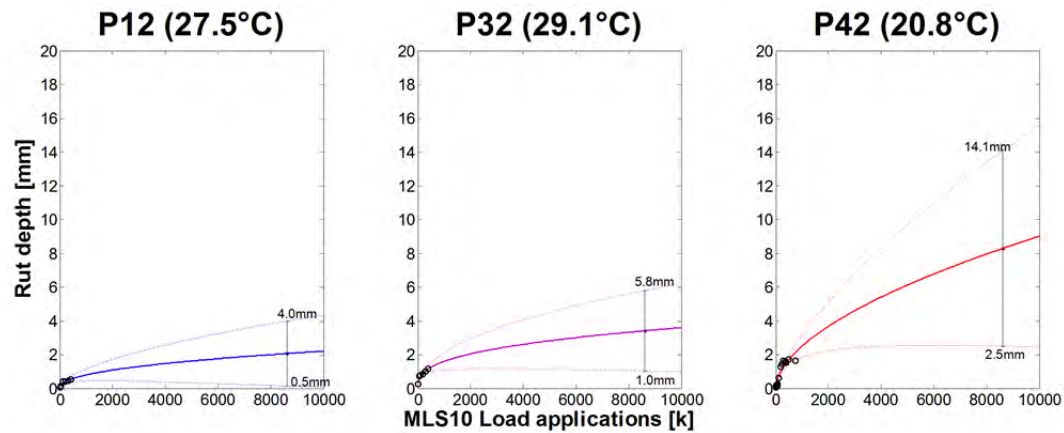
Fig. 5.34 Predicted rut depth vs. number of MSL10 load applications for each section, including 95% prediction bounds

The approximation functions to predict maximum rut depth in each section and the coefficients of determination R^2 are listed below:

Section F1, Profile12: $r_{P12} = 3.2 \, 10^{-4} \times N^{0.58}$ $R^2 = 0.95$

Section F3, Profile32: $r_{P32} = 4.3 \, 10^{-3} \times N^{0.44}$ $R^2 = 0.88$

Section F4, Profile42: $r_{P42} = 3.3 \, 10^{-3} \times N^{0.48}$ $R^2 = 0.66$

where N is the number of MLS10 load applications and r is the rut depth for one profile, in mm. As mentioned before, the coefficient of determination R^2 for the approximation function of profile 42 is quite poor, while the approximation of profile 12 is reasonably accurate. Nevertheless, a calculation of the expected rut depth by 8'628'900 MLS10 load applications, when it is expected to reach the bearing capacity of the pavements (see §5.1.3) and considering a prediction bound of 95%, would lead to the following rut values:

Section F1, Profile12: $r_{P12} = 0.5mm - 4.0mm$

Section F3, Profile32: $r_{P32} = 1.0mm - 5.8mm$

Section F4, Profile42: $r_{P42} = 2.5mm - 14.1mm$

According to these results, the expected failure due to rutting will happen far after the expected service of 20 years. The thickest structure (section F4) will have the biggest rutting whereas the weaker (section F1) will have the less rutting. Since pavement in section F4 was the only one with an MR 8 surface course, means that the permanent deformation of the pavement is mostly caused by the deformation of the top bituminous layers.

5.3.3 Strain gauges

Signals obtained with the strains gauges were recorded every 5 minutes. Each of the records comprised blocks of 30s measurements, saved as ASCII files and named with the measurement timestamp. The sampling rate was set to 1200Hz. The measurements were triggered and recorded automatically.

Fig. 5.35 shows a typical strain signal recorded with one of the strain gauges. In this example, only 2 s of the signal are displayed, showing the strains induced by the passing of 3 MLS10 loading axles. The figure contains also the timestamp of the file as well as the measured temperatures.
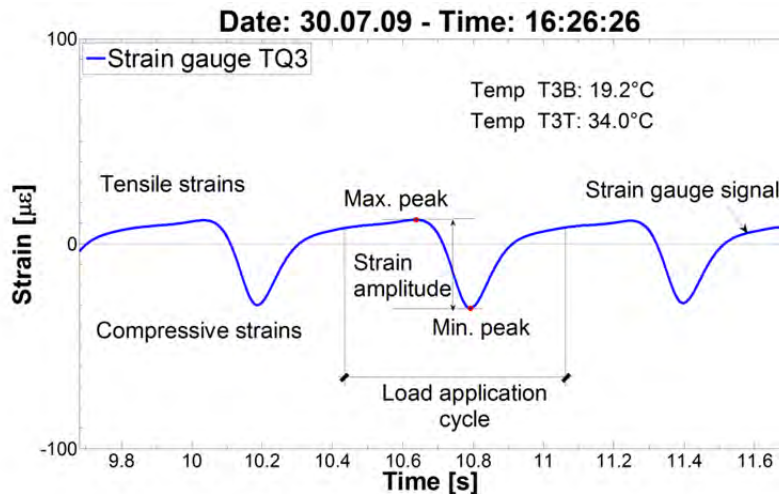

Fig. 5.35 Example of the strains recorded in the pavement.

Normally, positive values represent tensile and negative values compressive strains. However, due to normal baseline signal drift of the sensor and data acquisition system, or because of non-compensated temperature fluctuation, it is difficult to determine the zero-line. Consequently, all measurements were set to zero before start of recording.

Data Evaluation

With respect to strain data evaluation, the main assumption is that any change in measured strain amplitudes over time (or number of load applications) might show a change in the structural response from the development of distresses. For example, it is expected that formation and progress of cracks will increase the pavement deformation when loaded.

However, not only distress has an effect on the deformation of the structure. The change of temperature throughout the day changes the stiffness of the asphalt concrete. Normally, temperature, measured strains and pavement deformation increase from morning to evening while the modulus of asphalt concrete decrease. A similar effect is produced by slowly moving loads which produce larger strains, corresponding to lower modulus values. This means that the deformation of the pavement is affected not only by the loss of stiffness from traffic induced damage, which is the main focus of interest of these measurements, but also from temperature and load induced change of its viscoelastic mechanical response. In order to detach the strains from the influence of the loading speed, only measurements at MLS10 speed of 22km/h where taken in consideration.

With the purpose of characterizing the deformation by a strain value that is independent of temperature and loading speed, the following methodology and procedure was applied:

Measurements were analysed automatically with a post processing script using the software Matlab. The script worked with the files containing strains and temperature measurements and number of MLS10 cycles. As a result, it delivered a table summarizing the strains. Previously to the analysis, it was necessary to check the data and discard corrupted files and/or files with noise, outliers, etc. The valid files were stored in folders named with the date when the measurements were carried out. The script read each folder and went through each of the files taking the following steps:

1. Perform low pass filtering of the records with 20Hz cut-off frequency to clean for high frequency noise.

2. Calculate the absolute difference between the maximum and minimum strain peak of each load cycle, regardless where the zero-line is.

3. Determine average of all strain differences of each loading cycle, obtaining one single strain value (strain amplitude) for each file. This value is then assigned to the timestamp of the file.

4. Use of the timestamp, to obtain the temperature of the pavement from the temperature file and combined it with the strain amplitude in a table.

5. Assign the strain amplitudes of a single day to the number of accumulated load applications up to that date and store them in the same table.

The process is carried out through every day with measurements, giving as a result a table with four columns: in the first one the timestamp, in the second one the strain amplitude, in the third one the pavement temperature and the last one the number of load applications. The number of rows is equal to the number of valid measurements.

Then, the script uses this table and the temperature file, carrying out the following steps:

6. Calculate the average temperature throughout the tests

7. Use a sigmoidal function to approximate the strain amplitudes obtained during one measurement day.

8. The coefficients of the sigmoidal approximation employ for estimating a strain value for the average temperature (equivalent strain). Fig. 5.36 shows an example of how the equivalent strain is calculated.

9. Store the equivalent strains in a summary table that contains also the accumulated number of load applications of the day.

10. Finally, display the equivalent strains vs. the number of MLS10 load applications. Fig. 5.37 shows an example for the results of sensor TQ3. In the figure, the equivalent strains present a trend, which is fitted with a linear equation.
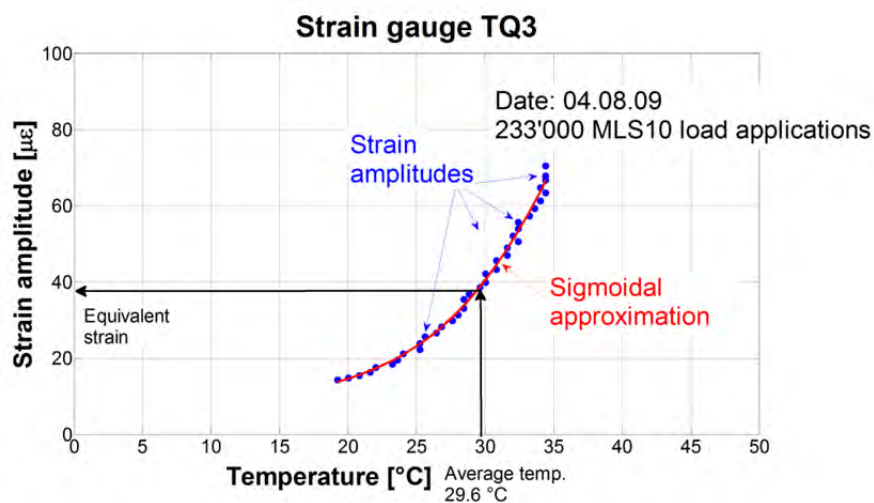
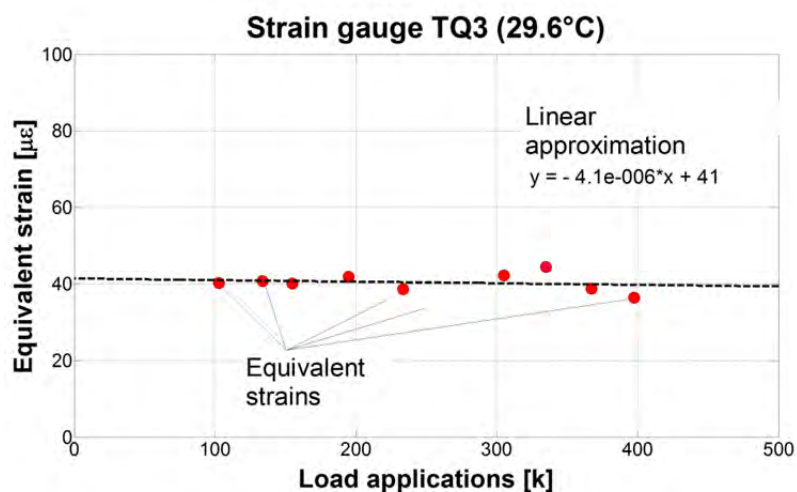*Fig. 5.36 Example of the script calculation methodology and definition of equivalent strain*

Fig. 5.37 Example of the script output for section F3, strain gauge TQ3.

Summary of the Results

<u>Section F3</u>

Strain under MLS10 loading, measured with sensors TQ3 and TL3 installed 3cm below the surface of section F3, are shown in Fig. 5.38. The strains recorded with the gauge installed in the trafficking direction (TL3) show that in this spot the pavement is "compressed" before the twin tires reach the position of the sensor. Then, when the tire is above the sensor there is a "tensile" peak that changes to "compressive" when the tires roll away from the gauge position. The gauge that is positioned perpendicular to the trafficking direction (TQ3) shows that the horizontal strains produced by the rolling tires in this location of the pavement are only of "compressive" nature. The form of the peaks is asymetric which means tha the pavement deformates differently before and after the tire passing. The strains return to the zero-value gradually, showing the viscoelastic nature of the bituminous materials which are part of the pavement. The results obtained are similar to those that can be found in the literature [19] [20].
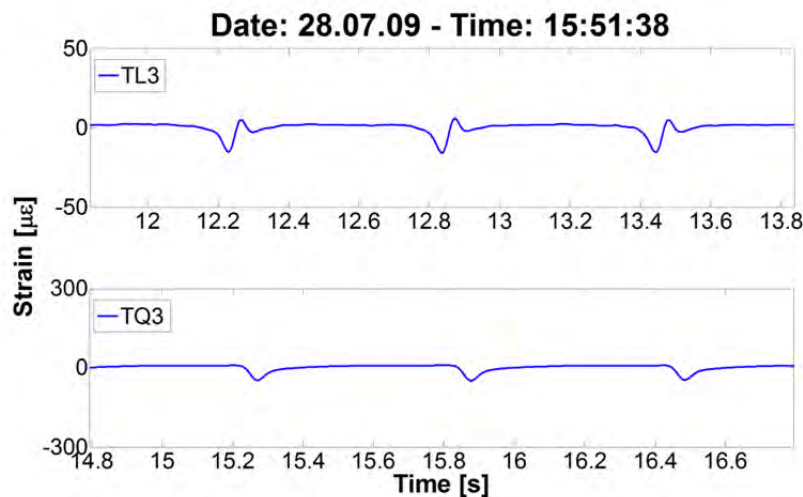
Fig. 5.38 Strains measured in Section F3, 8cm below the surface.

The analysis of the strains following the method described in the last chapter shows an increasing strain amplitude with increasing temperature. The shape of the equivalent strain values during the course of the tests also exhibits a good correlation with a sigmoidal curve. Fig. 5.39 presents the calculated equivalent strains in section F3.

a)
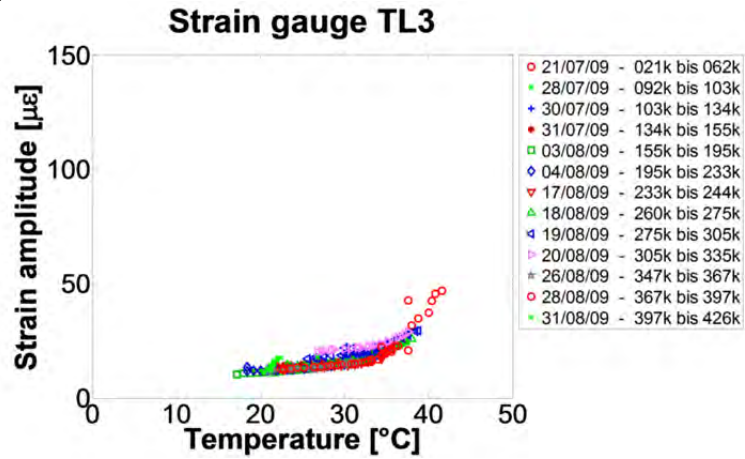
b)

Fig. 5.39 Evolution of strain amplitudes during the course of the tests in section F3, for strain gauges a) TL3 and b) TQ3

Fig. 5.40 presents the calculated equivalent strains for a temperature of 29.1°C vs. the number of MLS10 load applications. For TL3, the equivalent strains during the whole test remain constant at around 13$\mu\varepsilon$. Also BQ4 results present a constant strain level at 41$\mu\varepsilon$. This suggests that the pavement did not show any type of change in the mechanical properties cased by cracking or any other type of distress until the end of the tests.

a)

b)
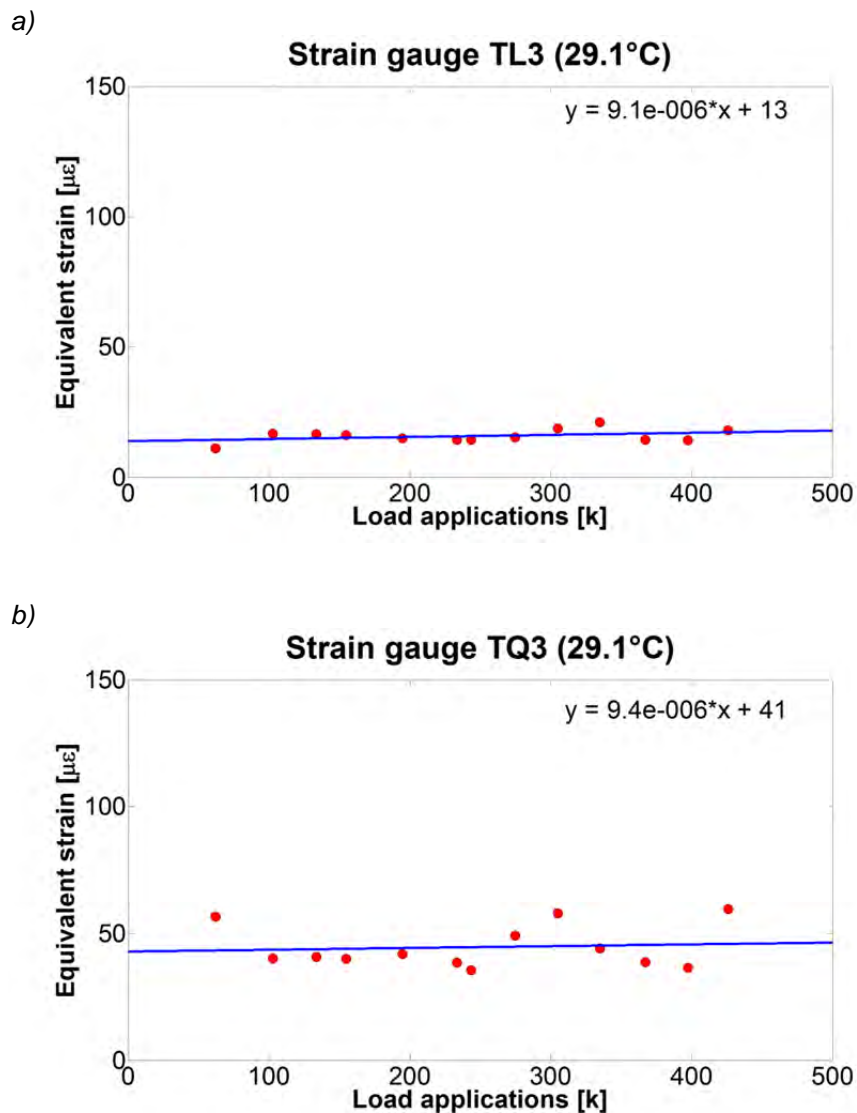
Fig. 5.40 Equivalent strains vs. MLS10 load applications, calculated for the average testing temperature in section F3, for strain gauges a) TL3 and b) TQ3

Section F4

Sensors TQ4 and TL4 installed 11cm below the pavement surface in Section F4, registered very small strains, almost below the resolution of the system; they are therfore not presented in this report.

BL4 and BQ4, 3cm below the surface, show shapes of curves as in section F3 (see Fig. 5.41 and Fig. 5.38): for the strain gauge that is installed in the trafficking direction (BL4), the pavement is "compressed" before the twin tires reach the position of the sensor. Then, when the tires are above the sensors a "tensile" peak occurs that changes to "compressive" when the tires roll away from the position. The gauge BG4 that is positioned perpendicular to the trafficking direction shows only "compressive" strains.
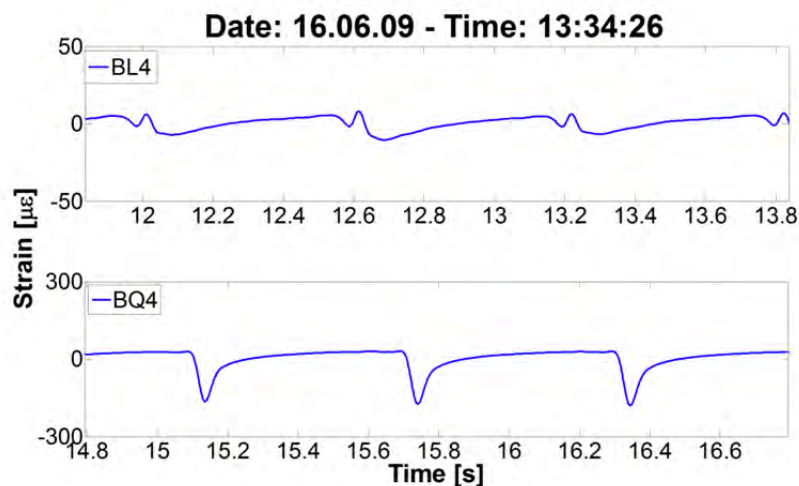
Fig. 5.41 Strains measured in section F4, 3cm below the surface.

The analysis of the results shows that with increasing temperature also the strain amplitude increases. As in section F3, the combination of the equivalent strains throughout the tests also exhibit a good correlation with a sigmoidal curve (see Fig. 5.42). However, in the first part of the tests, the strains seem to scatter slightly from this tendency, at least for sensor BL4. This can be explained as an effect from the interruption of the tests in section F4 which was necessary when trafficking section F3. This interruption may have lead to pavement healing during this period, and therefore to a small change in the measured strains. In addition, the temperature of the pavement decreased dramatically between the first and second period. This might also have played a role in the development of the strains.

a)
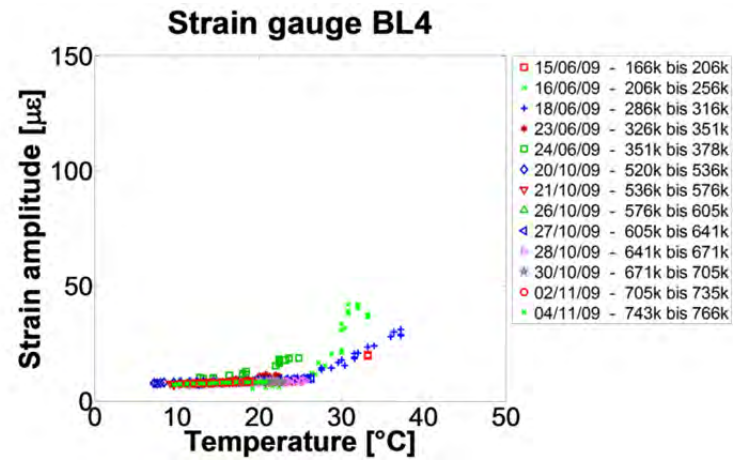
b)
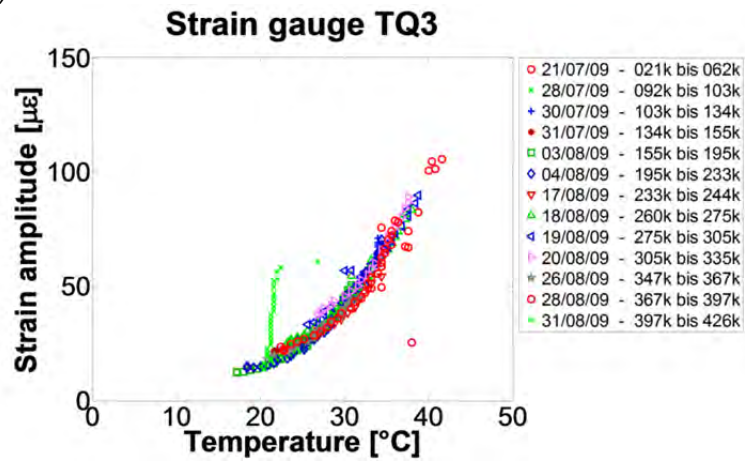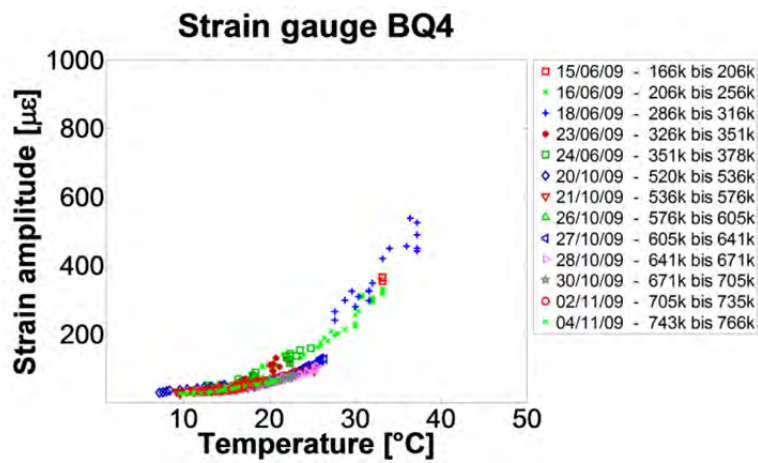

Fig. 5.42 Strain amplitudes during the course of the tests in section F4, for strain gauges
a) BL4 and b) BQ4

Fig. 5.43 presents the calculated equivalent strains vs. the number of MLS10 load cycles. For BL4, the strains remain at around 10$\mu\epsilon$ from the beginning to the end of the tests whereas the BQ4 results show a decrease in the equivalent strains, from around 150$\mu\epsilon$ to 30$\mu\epsilon$. However, this difference seems more related to the sigmoidal curves used for approximating the equivalent strains, rather than to a real change induced by distress. This can be interpreted as a sign that the pavement did not show any type of change in the mechanical properties produced by cracks or other types of distress.

a)

b)

Fig. 5.43 Equivalent strains vs. the number of MLS10 load cycles for the average temperature of 20.3°C, for strain gauges a) BL4 and b) BQ4

Fig. 5.44 presents a summary of the equivalent strain amplitudes in section F3 and F4 at the beginning of the tests and how they would be after 1'000'000 load applications if the linear relationship previously obtained was applied.

Fig. 5.44 Summary of the equivalent strains of section F3 and F4

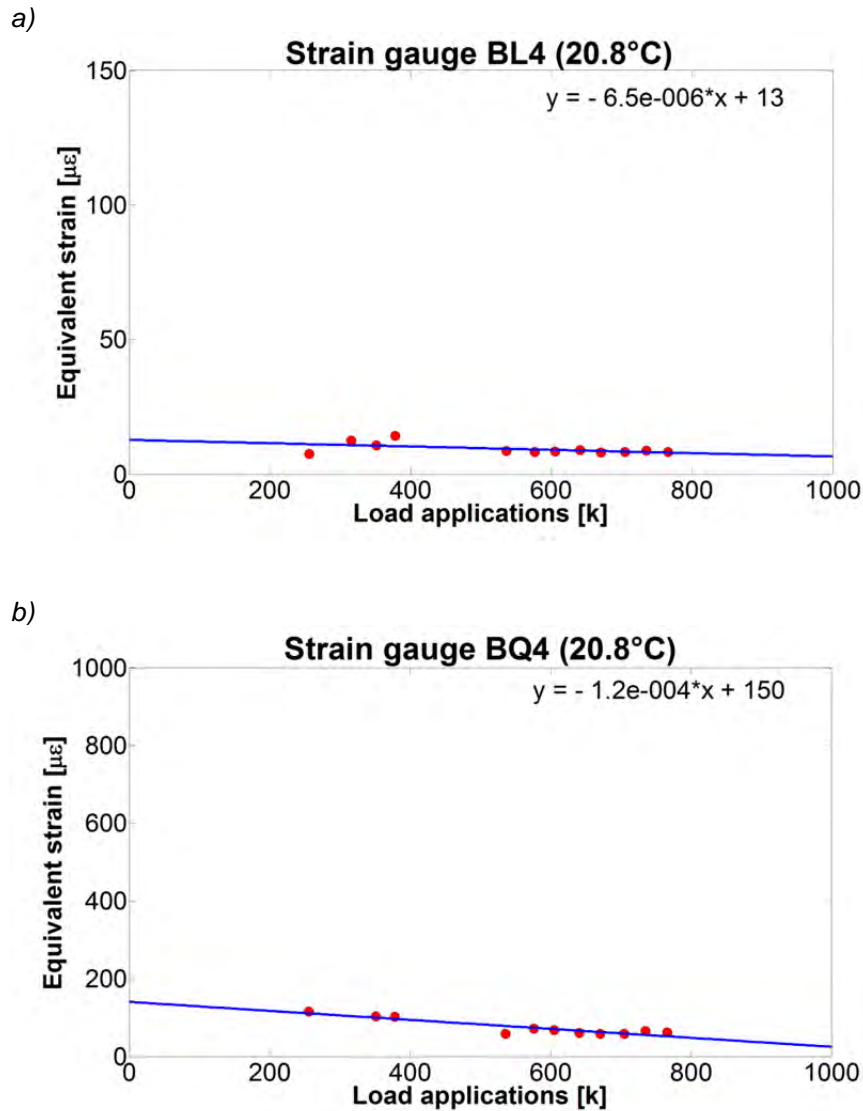| Section	Strain gauge	Depth [cm]	Temp. [°C]	Initial equivalent strain [$\mu\varepsilon$]	1Mio. Load appl. equivalent strain [$\mu\varepsilon$]
F3	TL3	-11	29.1	13	22
	TQ3	-11	29.1	41	50
F4	TL4	-11	20.8		-
	TQ4	-11	20.8		-
	BL4	-3	20.8	13	7
	BQ4	-3	20.8	150	30

5.3.4 Accelerometers

Data Acquisition

Accelerations were recorded every 5 minutes using the same data acquisition system as for the strain gauges. Each of the records comprised blocks of 30s measurements, saved as ASCII files and named with the measurement timestamp. The sampling rate was set to 1200Hz. The measurements were triggered and recorded automatically.

Data Evaluation

The original data evaluation strategy was to obtain pavement deflections from acceleration records and analyse the deflection in the same way than the strain gauge records, as explained in §5.3.3. Hence the deflection amplitudes from each file was calculated in the same way than the strain amplitudes. In this way and from there, to obtain an equivalent deflection value (equivalent strain) for the average temperature was obtained, for every day of analysis. As a result it was expected to obtain a diagram showing the equivalent deflection vs. the number of MLS10 load applications, as described in pages 43 and 43. However, due to the high rigidity of the pavements it was not possible to obtain reliable deflection results. The low acceleration level recorded by the sensors was weaker than the environmental noise (see Fig. 5.45).

Instead, the pure acceleration was used as an indicator of the pavement response to MLS10 loads, under the assumption that a change in deflection amplitudes means also a change in acceleration amplitudes since acceleration is the second derivative of a displacement. The acceleration records were previously low pass filtered with 10Hz cut-off frequency (lower than for strain gauges), as acceleration records are more sensitive to high frequency noise vibrations. Similar to the strain amplitude as explained before, the terms acceleration amplitude and equivalent acceleration are used in the same way as for strains.
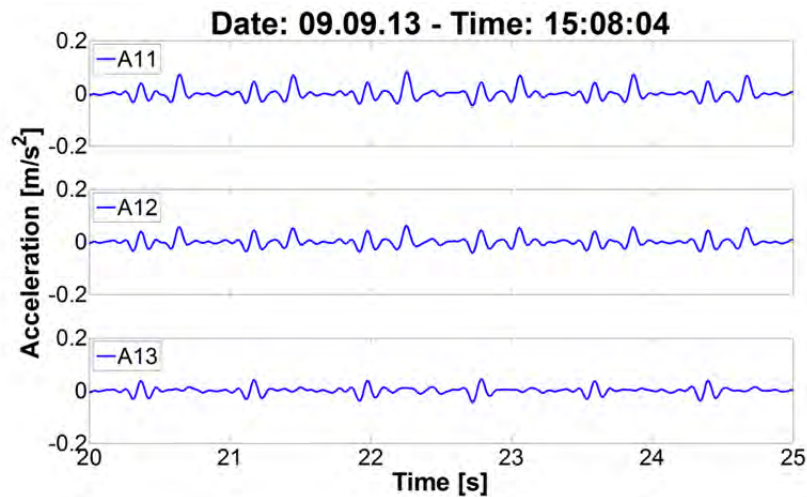
Fig. 5.45 Acceleration measured in section F1.

Summary of the Results

Below, a summary of the results obtained from the 3 accelerometers installed in sections F1, F3 and F4is shown.

<u>Section F1</u>

The analysis of the acceleration records following the method described in the last section shows an increasing strain amplitude with increasing temperature. As expected, the acceleration amplitude close to the load application area recorded by sensor A11 is higher than for the more far accelerometer A13. Fig. 5.46 presents the calculated equivalent accelerations in section F1.

a)

b)

c)

Fig. 5.46 Acceleration amplitudes during the course of the tests in section F1, for accelerometer a) A11 and b) A12 c) A13

Fig. 5.47 presents the calculated equivalent accelerations vs. the number of MLS10 load applications. The values are below $0.1 m/s^2$ and remain almost constant during the tests. This is an indication that the pavement did not change the properties due to MLS10 trafficking.

a)

b)

c)

Fig. 5.47 Equivalent acceleration vs. number of MLS10 load applications for section F1, for accelerometer a) A11 and b) A12 c) A13

<u>Section F3</u>

As expected, the acceleration amplitude close to the load application area recorded by sensor A31 is higher than for the more far accelerometer A33. Fig. 5.48 presents the calculated equivalent accelerations in section F3.
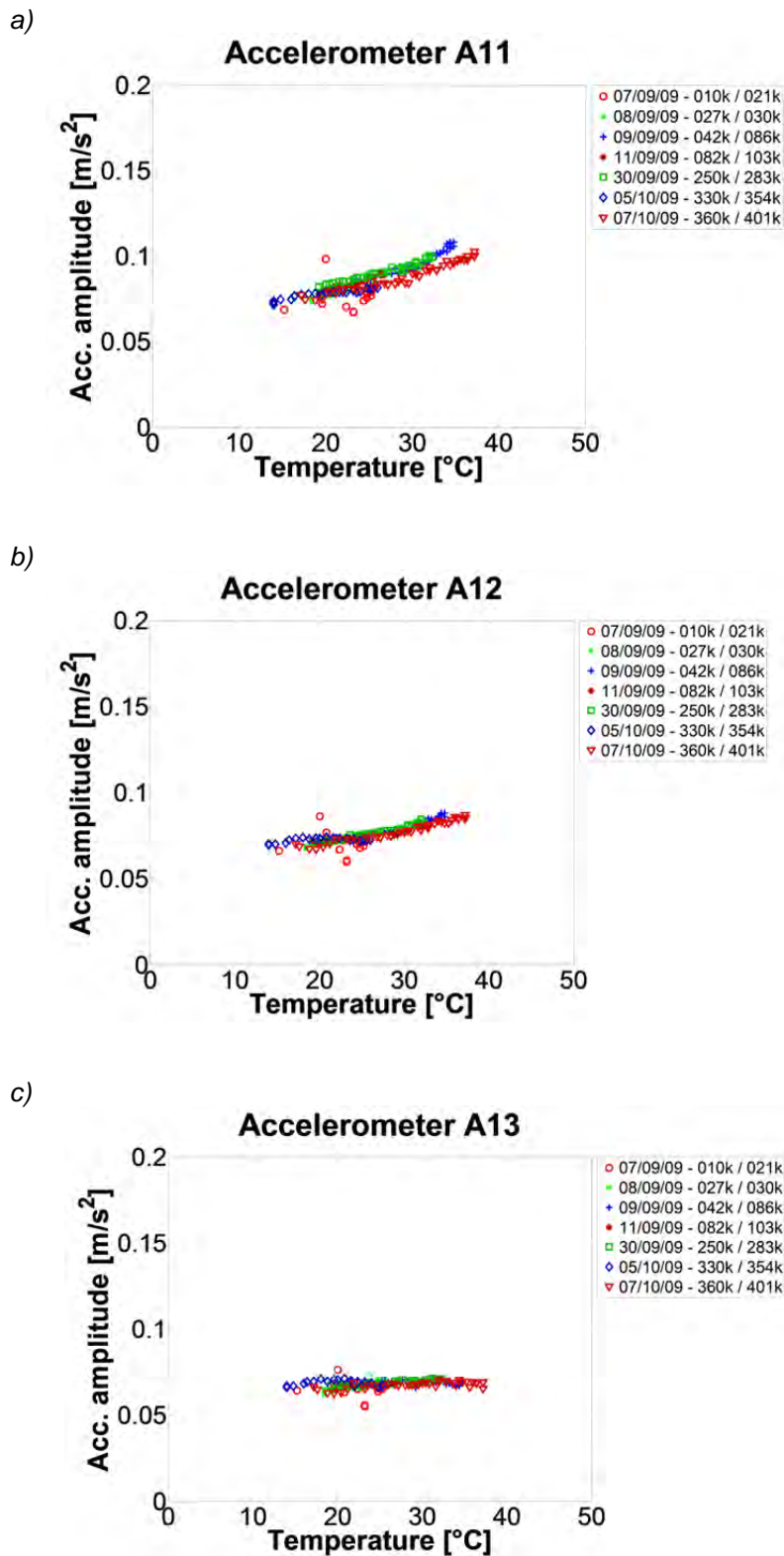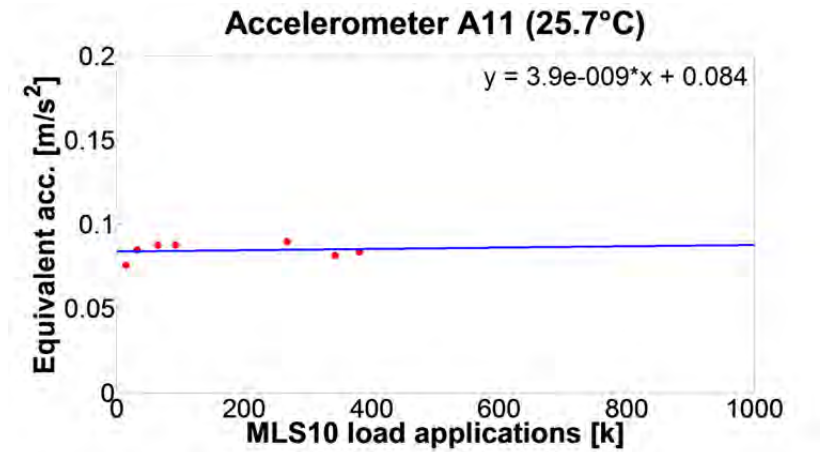
a)

b)

c)

Fig. 5.48 Acceleration amplitudes *during the course of the tests in section F3, for accelerometer a) A31 and b) A32 c) A33.*

Fig. 5.49 presents the calculated equivalent accelerations vs. the number of MLS10 load applications. The values are below 0.03m/s^2 and remain almost constant during the tests.

This is an indication that the pavement did not change the properties due to MLS10 trafficking, confirming the results obtained with the strain gauges.

a)

b)
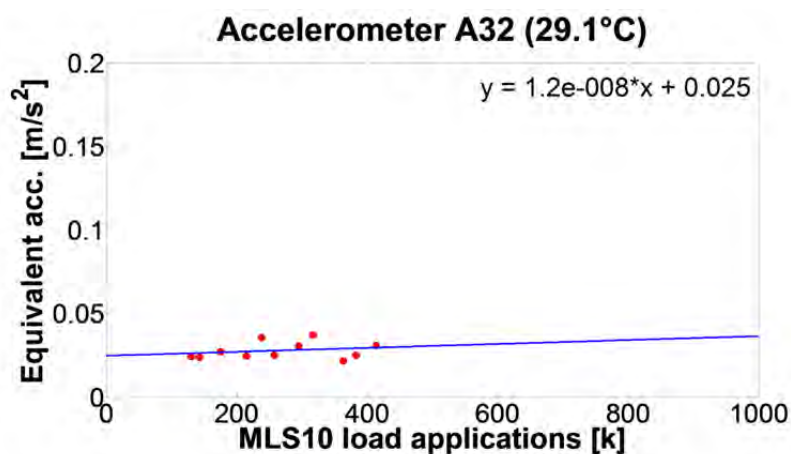
c)
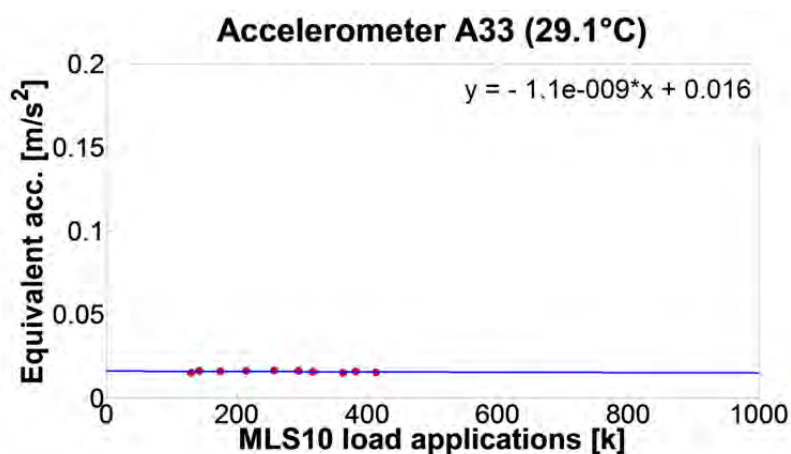
Fig. 5.49 Acceleration vs. number of MLS10 load applications for section F3, for accelerometer a) A31 and b) A32 c) A33

Section F4

As expected, the acceleration amplitude close to the load application area recorded by sensor A41 is higher than for the more far accelerometer A43. Fig. 5.50 presents the calculated equivalent accelerations in section F4.
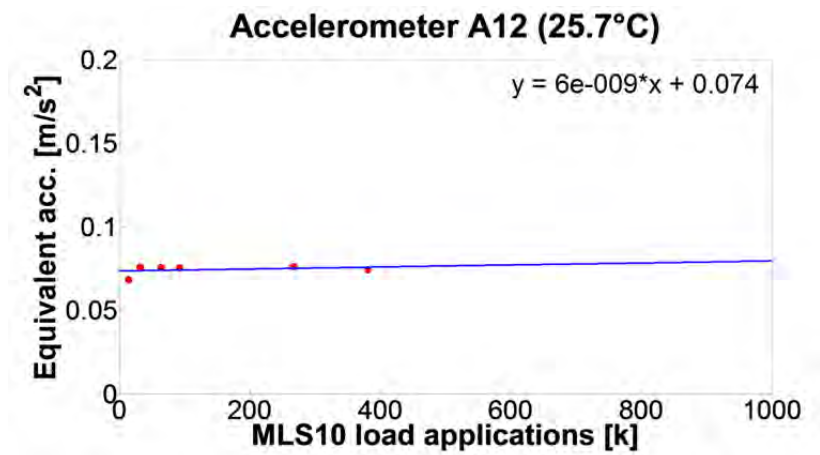
a)

b)

c)
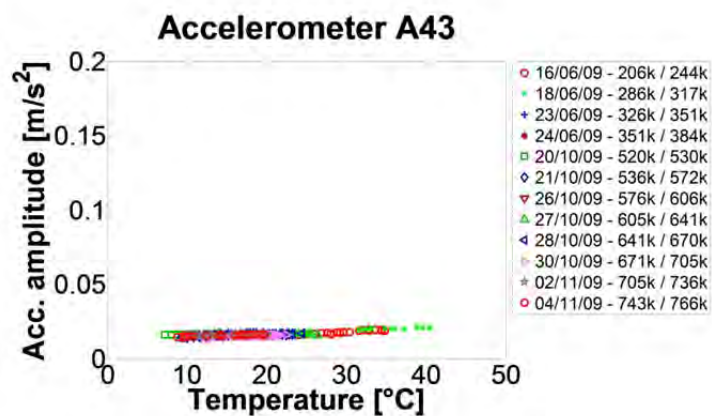
Fig. 5.50 Acceleration amplitudes during the course of the tests in section F4, for accelerometer a) A41 and b) A42 c) A43.

Fig. 5.51 presents the calculated equivalent accelerations vs. the number of MLS10 load applications. The values are below 0.03m/s^2 and remain almost constant during the tests. This is an indication that the pavement did not change the properties due to MLS10 trafficking, verifyying the results obtained with the strain gauges.
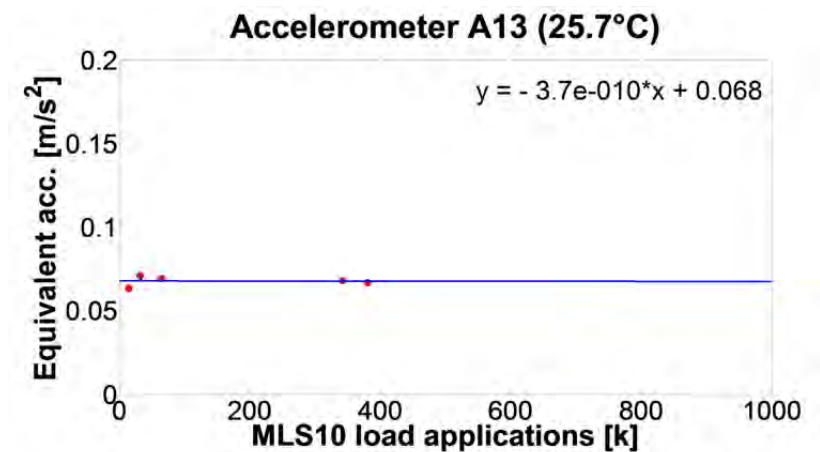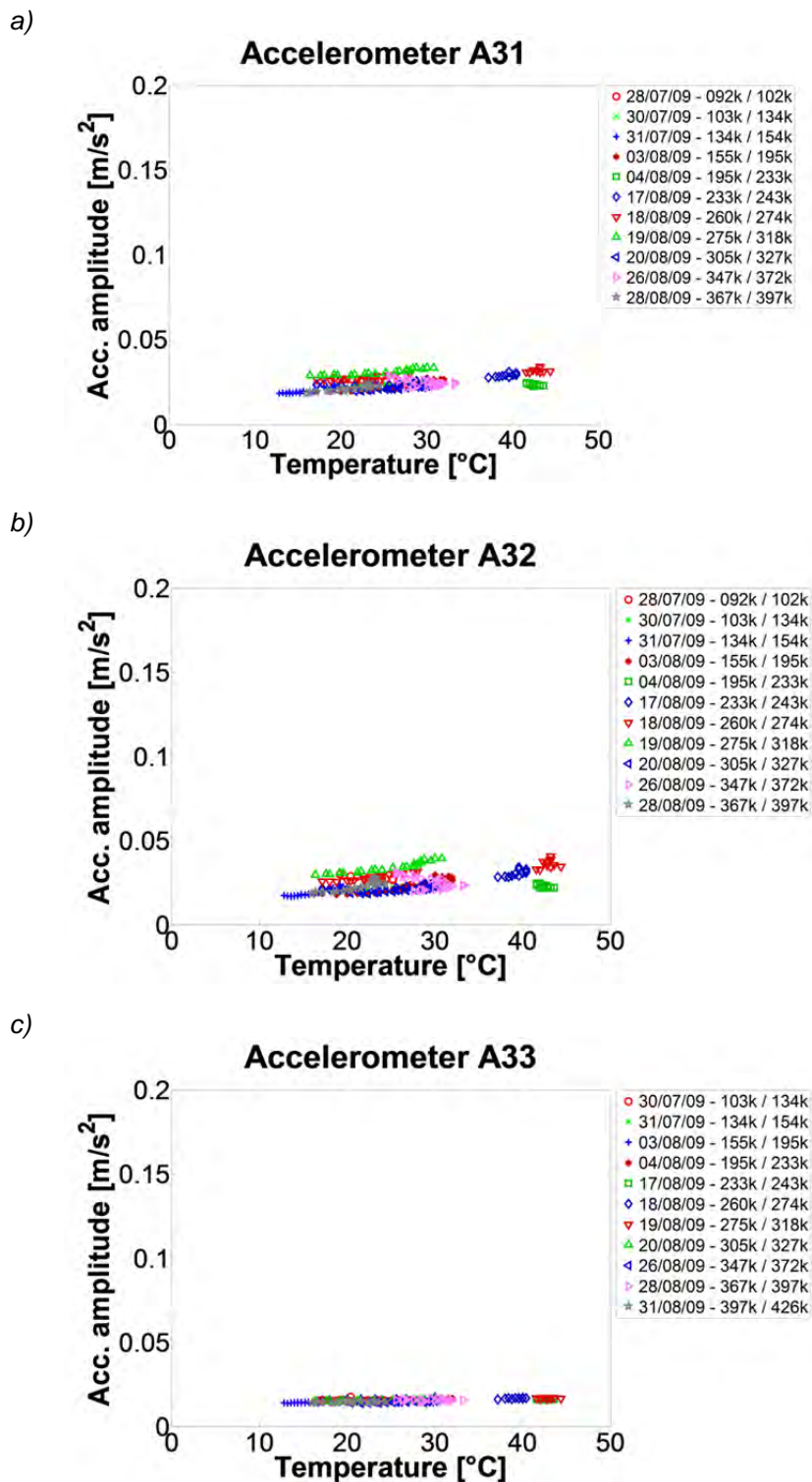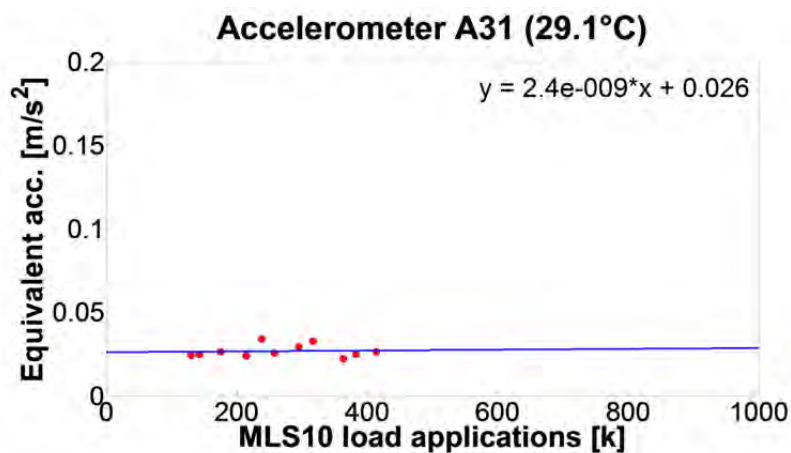
a)
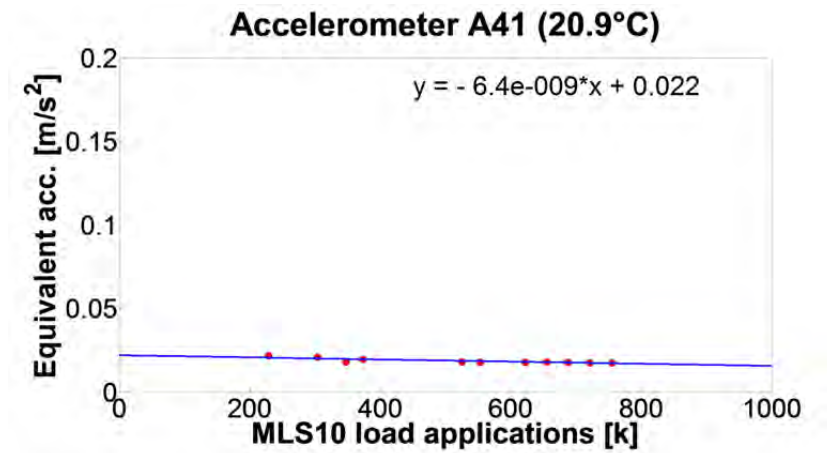
b)
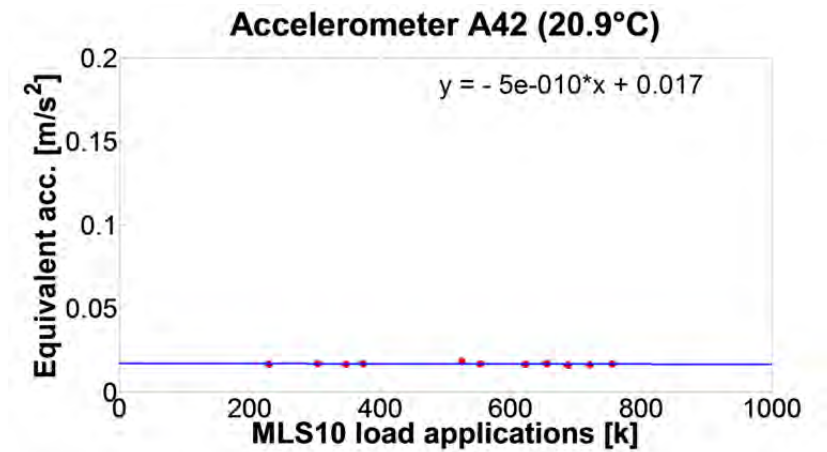
c)

Fig. 5.51 Equivalent acceleration vs. number of MLS10 load applications for section F4, for accelerometer a) A41 and b) A42 c) A43.

Fig. 5.52 presents a summary of the equivalent strains in section F1, F3 and F4 at the beninning of the tests and how they would be after 1'000'000 million load applications if the linear relationship previously obtained was applied.
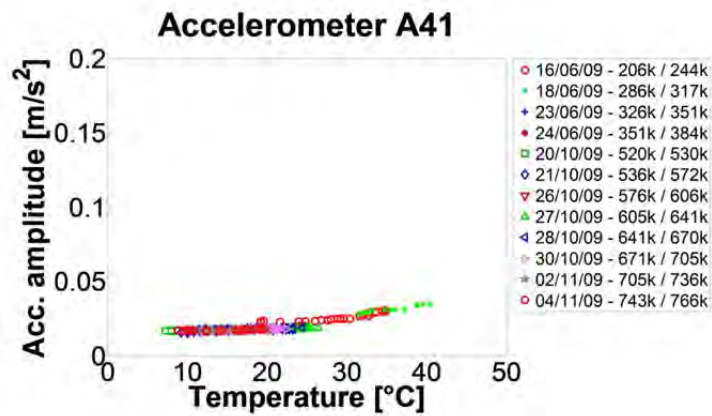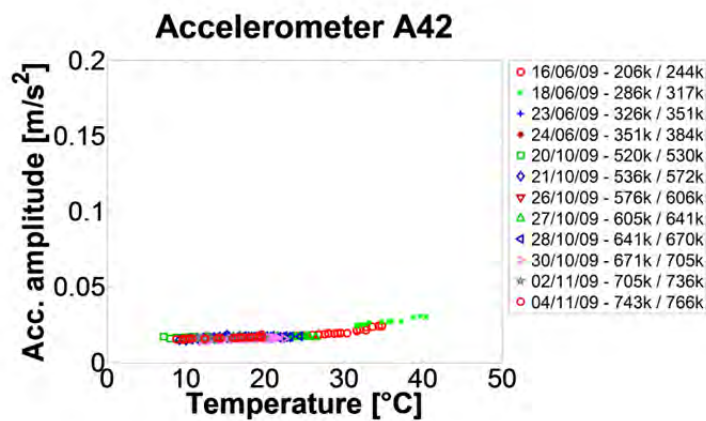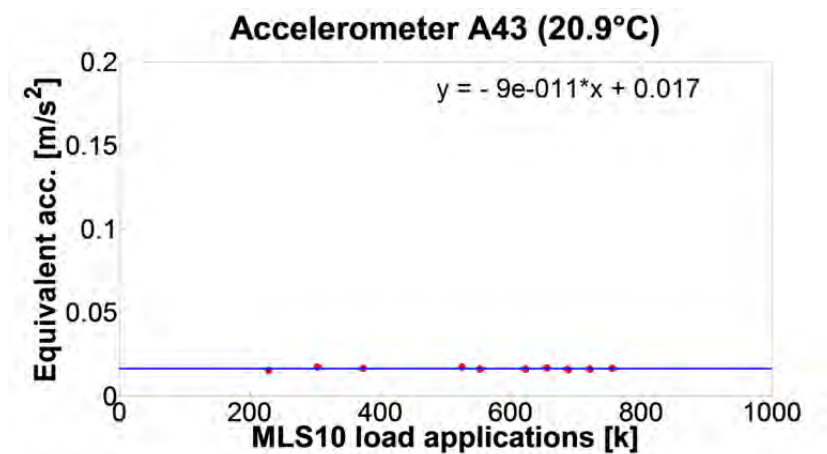
Fig. 5.52 Summary of the equivalent acceleration of section F1, F3 and F4

Section	Accelerometer	Distance to load [cm]	Temp. [°C]	Initial equivalent acc. [m/s²]	1Mio. Load appl. equivalent acc. [m/s²]
	A11	0	25.7	0.084	0.088
F1	A12	30	25.7	0.074	0.080
	A13	60	25.7	0.068	0.068
	A31	0	29.1	0.026	0.028
F3	A32	30	29.1	0.025	0.043
	A33	60	29.1	0.016	0.015
	A41	0	20.8	0.022	0.016
F4	A42	30	20.8	0.017	0.017
	A43	60	20.8	0.017	0.017

Acceleration measurements in all sections show that the deflections under MLS10 loading are extremely low; the highest equivalent acceleration obtained being of about 0.084m/s² for A11 in section F1, which is the weakest section. Accelerations in sections F3 and F4 are of almost the similar oder of magnitude. This is a reasonable result considering that both pavements have almost the same structure and only the AC MR 8 top layer of 3cm is missing in F3. The development of the equivalent accelerations also displays a small change thoroughout the experiments, remaining almost constant. These results confirm the conclusions from strain gauge measurements about the pavement properties remaining almost unaltered after trafficking.

5.3.5   Falling Weight Deflectometer (FWD)

Data acquisition

FWD data was collected by the Karlsruhe Institute of Technology (KIT) in Germany and the data comprised the maximum measured deflection for the nine geophones of the device, the maximum drop loads and the air and surface temperature. The data was saved in spread sheet formate which is editable with Excel.

Data Evaluation

These measurements are considerably influenced by temperature. In order to reduce this influence and detect possible damage areas in the trafficked sector, a special data analysis strategy, different form that suggested by KIT [18] was proposed. The data analysis strategy uses the maximum deflections under FWD impacts for obtaining deflection maps of the grid area where the tests were carried out. Under the assumption that temperature is constant during the tests and the pavement is homogeneous, the deflection should be

equal in each of the measurement points. Still, pavement stiffness is not homogeneous but is expected to change due to trafficking damage. By comparing the maximum deflection of each point of the measurement grid, it is possible to identify comparatively weak zones in the area tested with the FWD. Therefore, deflections maps for each section and measurement campaign were calculated and compared. In order to achieve a better contrast, the deflection at each point was normalized to the maximum deflection of the area and plotted toghether with the deflection maps. If the value at one cell of these normalized deflection matrix is 1, it means that this point has the maximum deflection of the area. If the value was close to 0, then the deflection at this point was small, compared to the highest deflection. The deflection maps show in scale the deflections in different colors. The normalized deflection matrix shows schematically where is the maximum deflection. Red color indicates the position of the maximum deflection whereas green means the lowest deflection of the area. Empty white areas in the matrix indicate that no valid measurement for that point was obtained.

Summary of the Results

<u>Section F1</u>

In Fig. 5.53, deflecion maps and deflection matrices for section F1 at different trafficking times are plotted. Unfortunately, in the initial FWD tests only 2 lines of measurements had valid records. According to the figure, the sector with highest relative deflection remains unchanged throughout the tests and is not located in the loaded area. This suggests that the pavement did not show any type of change in the mechanical properties caused by cracking or any other type of distress in the load application area.

a)
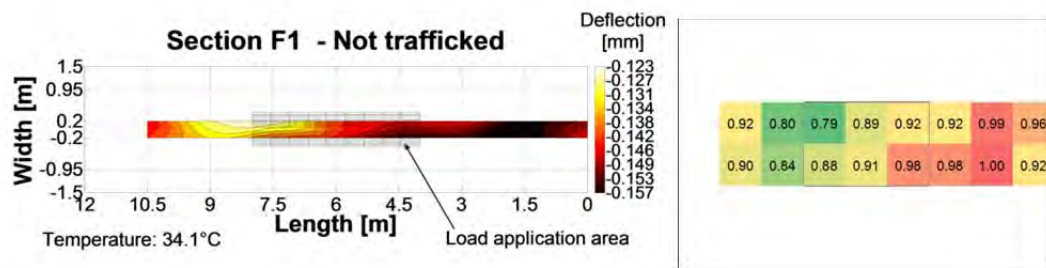
b)
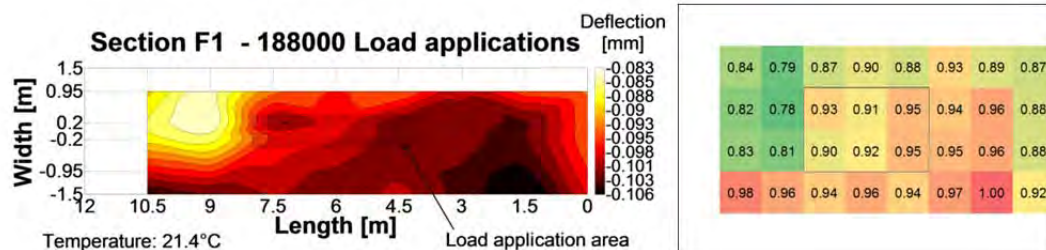
c)
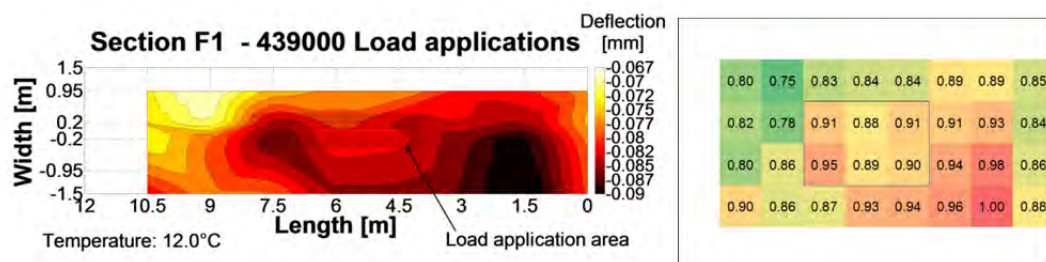
Fig. 5.53 Deflection maps (left) and normalized matrix (right) for section F1 at different trafficking times

Section F3

In Fig. 5.54, deflecion maps and deflection matrices for section F3 at the beginning and end of the trafficking period are plotted. Unfortunately, in the intial FWD tests, only 2 lines of measurements had valid records, making the deflection map a little coarse. According to the figure, the sector with highest relative deflection remains unchanged throughout the tests and is not located in the loaded area. This, again, suggests that the pavement did not show any type of change in the mechanical properties caused by cracking or any other type of distress in the load application area.

a)
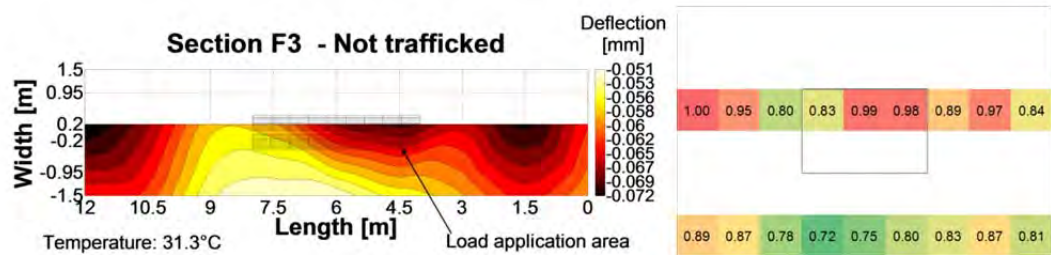
b)
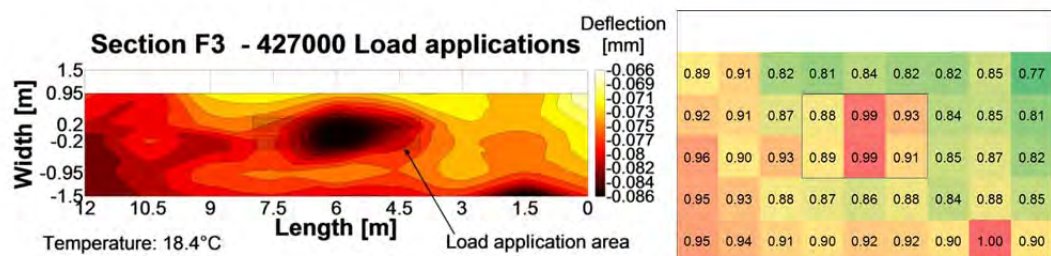
Fig. 5.54 Deflection maps (left) and normalized matrix (right) for section F3 at different trafficking times

Section F4

Fig. 5.55 presents deflecion maps and deflection matrices for section F4 at 3 trafficking times. According to the figure, the sector with the highest relative deflection changed throughout the tests, from the area around coordinates (12m,-1.5m) to the coordinates (6m,-0.2m), which corresponds to the center of the load application area. This change of the position of the highest relative deflection suggests that the pavement might have suffered of a loss of bearing capacity near the load application area at around 550000 load applications.

a)
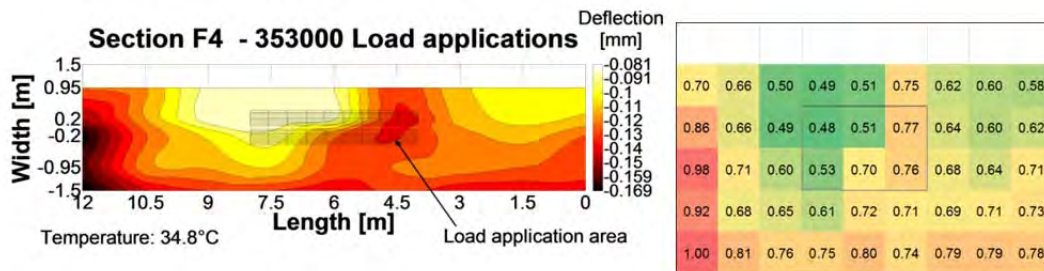
b)
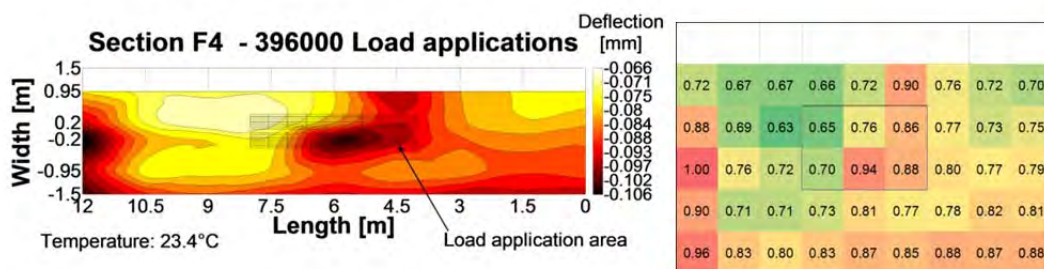
c)
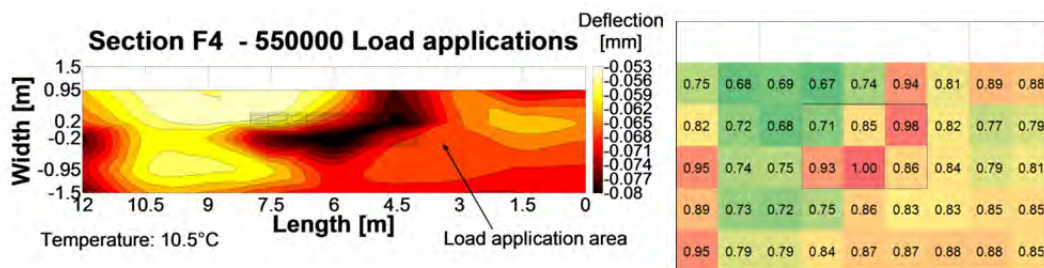
Fig. 5.55 Deflection maps (left) and normalized matrix (right) for section F4 at different trafficking times

5.3.6 ETH Delta

Data acquisition and evaluation

Similar to FWD, the data obtained with the ETH Delta device can be used to prepare 3D deflection maps. In Fig. 5.46Fig. 5.56, Fig. 5.57 and Fig. 5.58, the results for section F1, F3 and F4 are presented respectively.

a)
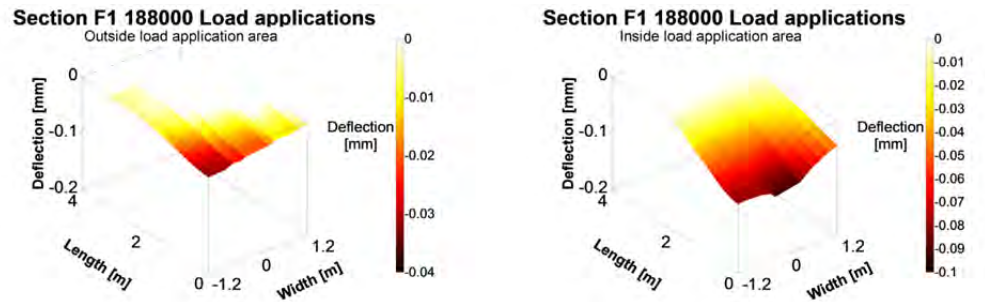
Temperature: 18.5°C

b)
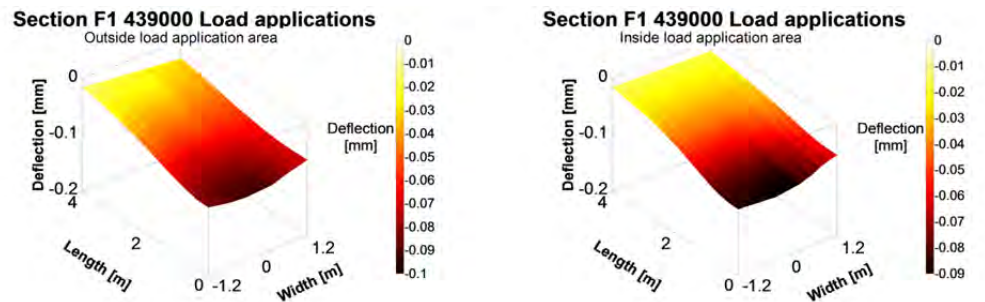
Temperature: 5.5C

Fig. 5.56 3D graph of the deflection measured with ETH Delta for 2 trafficking conditions in section F1, outside (left) and inside (right) the load application area

a)
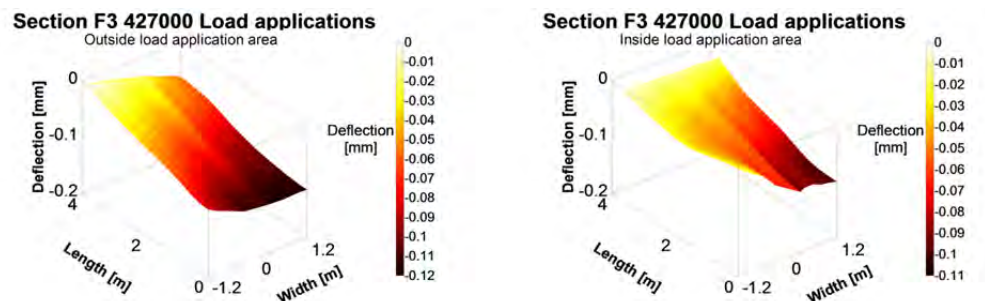
Temperature: 27.4°C

Fig. 5.57 3D graph of the deflection measured with ETH Delta for 2 trafficking conditions in section F3, outside (left) and inside (right) the load application area

a)

Temperature: 23.0°C

b)
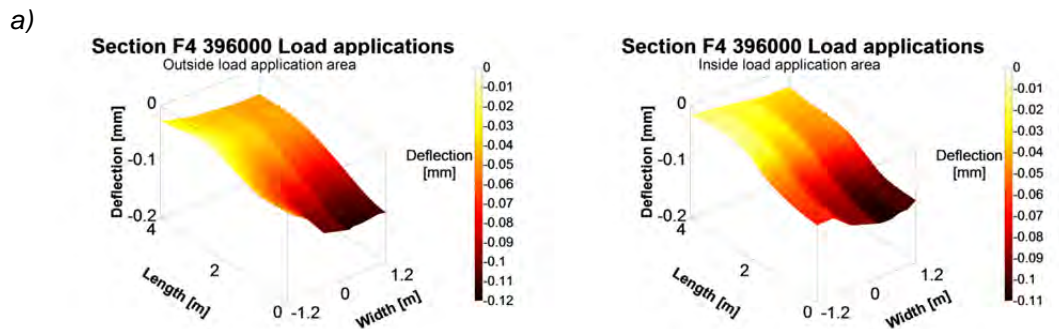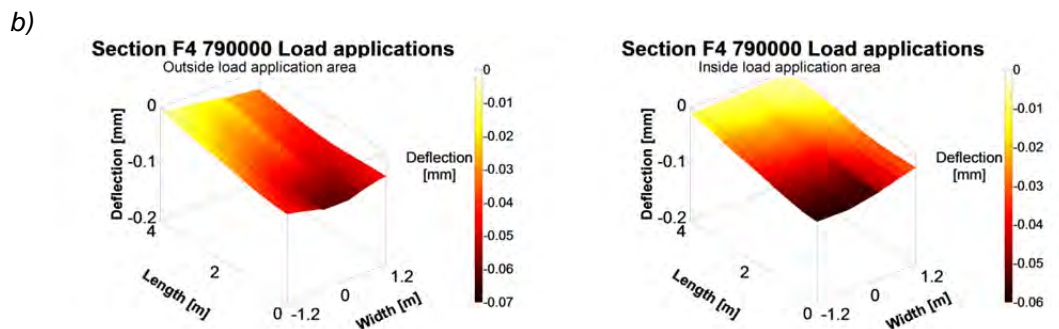
Temperature: 4.8°C

Fig. 5.58 3D graph of the deflection measured with ETH Delta for 2 trafficking conditions in section F4, outside (left) and inside (right) the load application area

The shape and order of magnitude of the deflection bowls don't show clear signs of changes after trafficking. It can be seen that the amount of load applications were not enough to induce a significant change in the structural response.

5.3.7 Portable Seismic Pavement Analyzer (PSPA)

Data acquisition and analysis

In order to reduce the influence of temperature on the results, measurements outside and inside of the trafficking zone were carried out simultaneously. Further, great care was taken to avoid the influence of the sun, affecting differently the measuring spots, i.e. measurements were carried out in the shadow. After data collection, the data is processed by the data acquisition software of the device. Results are plotted in an apparent seismic modulus graph versus depth as shown in the example of Fig. 5.59.
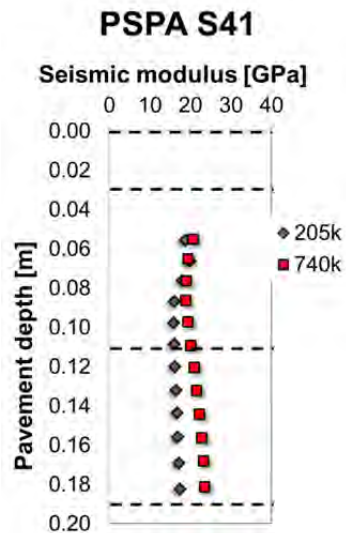
Fig. 5.59 Example of seismic modulus versus depth for different numbers of load applications.

Then, the recorded stiffness in the PSPA measurement at -5 cm, -10 cm, -16 cm (same depth as the temperature sensors) was plotted vs. the number of load applications, to show the evolution during trafficking. Three positions were measured in the field: two of them in the trafficking path and the other one outside, in a not-trafficked area (see Fig. 5.10, Fig. 5.11 and Fig. 5.12). The last one was used as reference, as the stiffness values are expected to change only because of temperature fluctuations and not because of distress. Therefore, as a last step in the evaluation of the data, measurements in the wheel path were normalized to those measurements outside the wheel path. If the normalization gives values near to 1, it means that the stiffness in the trafficked zone is similar to the one in the not-trafficked area. Values above 1 indicate higher stiffness whereas values below it are due to lower stiffness. The assumption for the interpretation of the data was that changes of these initial normalized values over the course of the tests might indicate a change of stiffness induced by the action of the MLS10 loads. A loss of stiffness in the trafficked area due to distress would produce an increment of the normalized values. On the other hand, an increase of the stiffness in the trafficked area would produce a increment in the normalized stiffness.

Summary of the Results

Section F1

Due to a problem in the device while section F1 was trafficked, not enough valid data for the analysis was obtained.

Section F3

The results of the analysis are displayed in *Fig. 5.60*. The analysis of the general evolution at the analyzed depths indicates that the asphalt as well as the stabilization layers have an apparent seismic modulus of around 15-25GPa. There is no clear change in stiffness between the layers. The seismic stiffness measured near the surface (at -5cm) shows the biggest difference among points. However, the normalized values indicate that there is no clear change in both the stiffness trend throughout the tests and the stiffness in the trafficked area (S31 and S32). For the other depths (-10cm and -15cm) stiffness is even more homogenous with no significant change after trafficking.
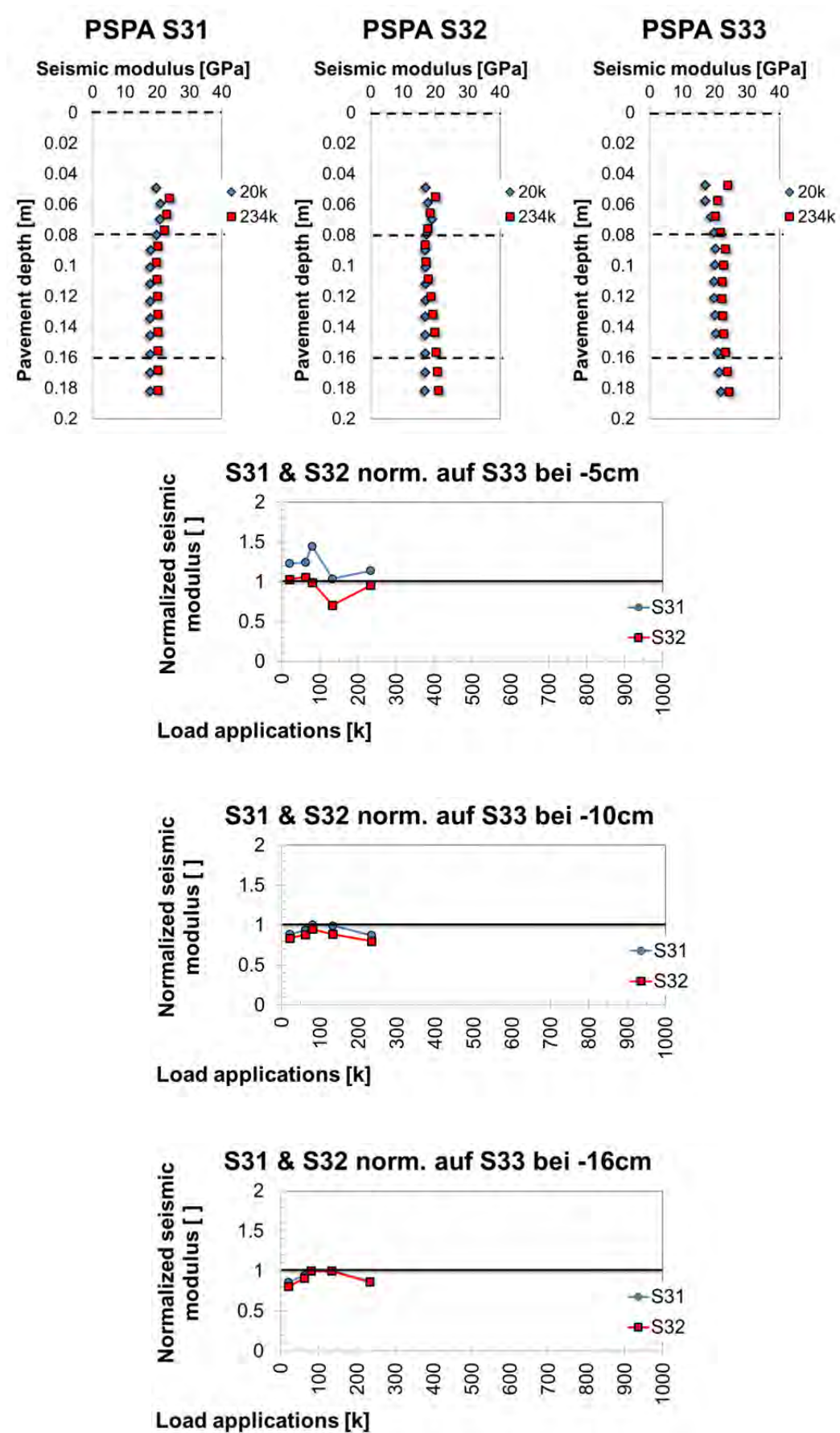
Fig. 5.60 Evolution of seismic modulus vs. depth and number of load applications for section F4.

Section F4

The results of the analysis in section F4 are displayed in Fig. 5.61. The asphalt layers have an apparent seismic modulus of around 15-25GPa, with a peak at S43 of almost 30GPa. If this peak is not considered (the stiffness should not increase that much for the not-trafficked area), it can be seen that there is a small tendency for the stiffness to increase in the trafficking path. However, this change is not significant enough to draw conclusions about changes in the stiffness of the layers after trafficking.
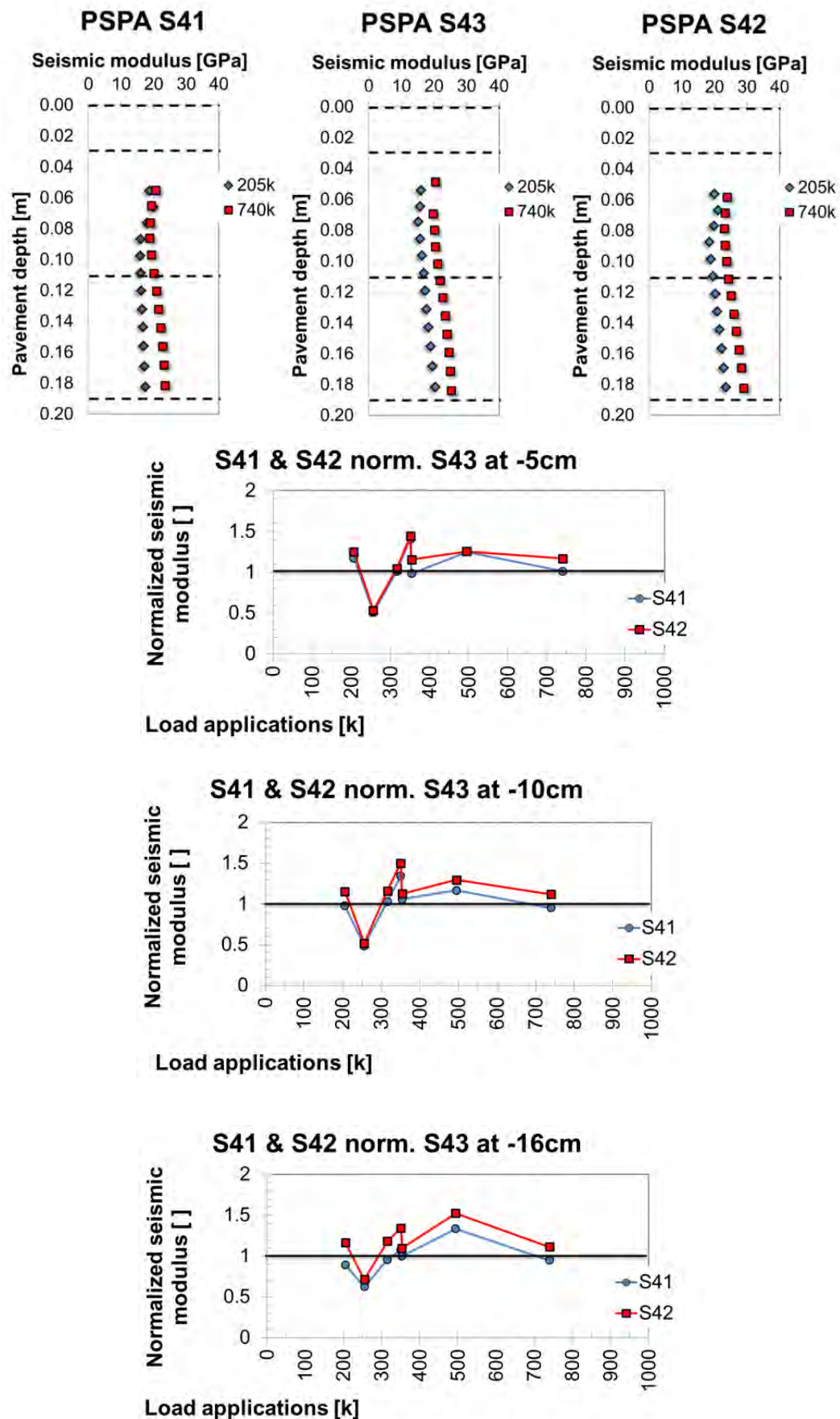
Section F4

Fig. 5.61 Evolution of seismic modulus vs. depth and number of load applications for section F4.

5.3.8 Ground Penetrating Radar (GPR)

The objective of the ground penetrating radar inspections was to detect possible distress mechanisms inside the pavement structure using electromagnetic waves. This non-destructive test method allows to detect changes in the dielectric permeability of the materials composing the pavement and to indirectly link this change to a modification of the material properties due to trafficking. Further, with Ground Penetrating Radar (GPR) it is possible, for example, to detect the exact position of the strain gauges embedded in the pavement, as shown in Fig. 5.62 or to detect areas with possible poor compaction

Therefore, one measurement was carried out before loading the pavement and one at the end of the tests in section F4. Unfortunately, due to a problem in the data acquisition system, the data of the last measurement was not valid and it was not possible to carry out the comparison.
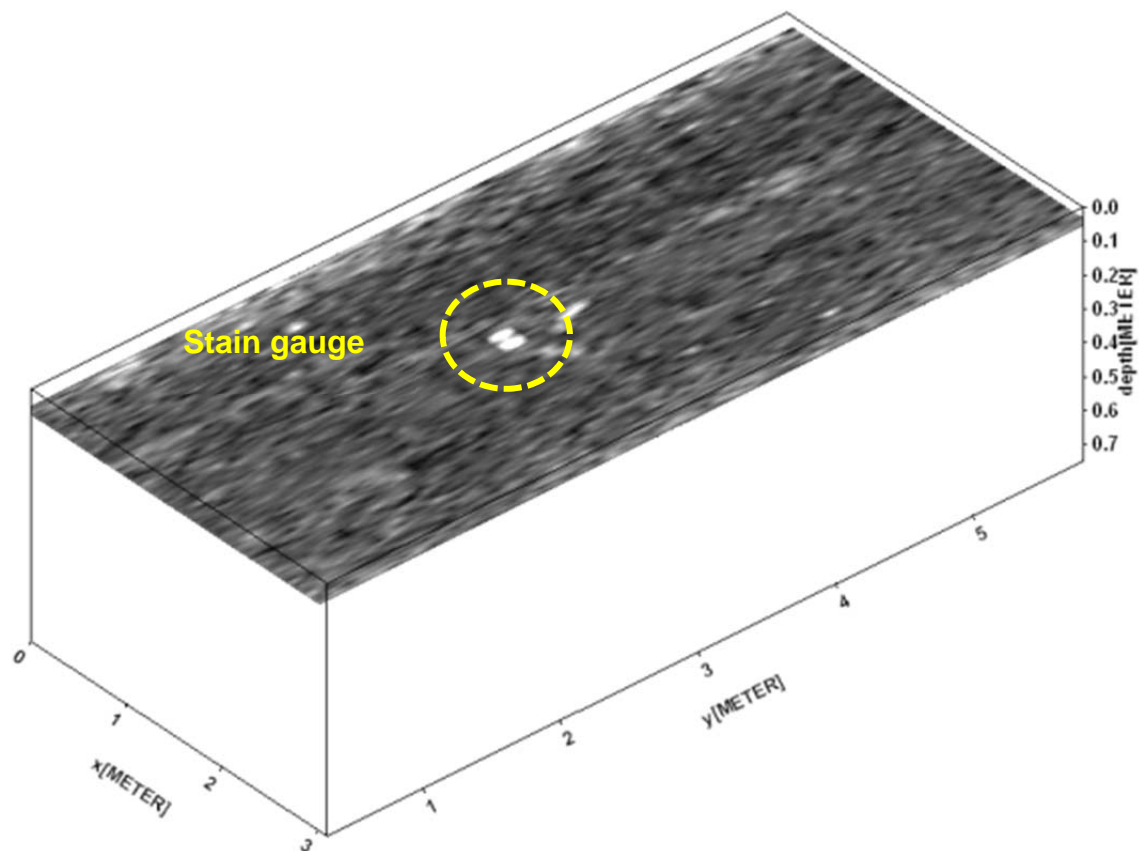
Fig. 5.62 GPR inspection showing the strain gauge BQ4 before loading.

5.3.9 Laboratory tests

Several cores were taken inside and outside the load application area (trafficked and not-trafficked respectively) and different laboratory tests were carried out. The position and names of the cores in section F4 is shown in Fig. 5.63. Coring comprised the bituminous layers. No evaluation of the cement stabilized layers or subgrade was done after the experiments. From GPR inspections at the beginning of the tests, three possible weak areas were detected at a depth of -90mm. These areas, named G1, G2 and G3 are displayed also in Fig. 5.63. Several cores were taken from these areas, in order to verify the GPR results in the laboratory. The laboratory tests on the three top courses included indirect tensile tests and evaluation of interlayer bonding between layers.
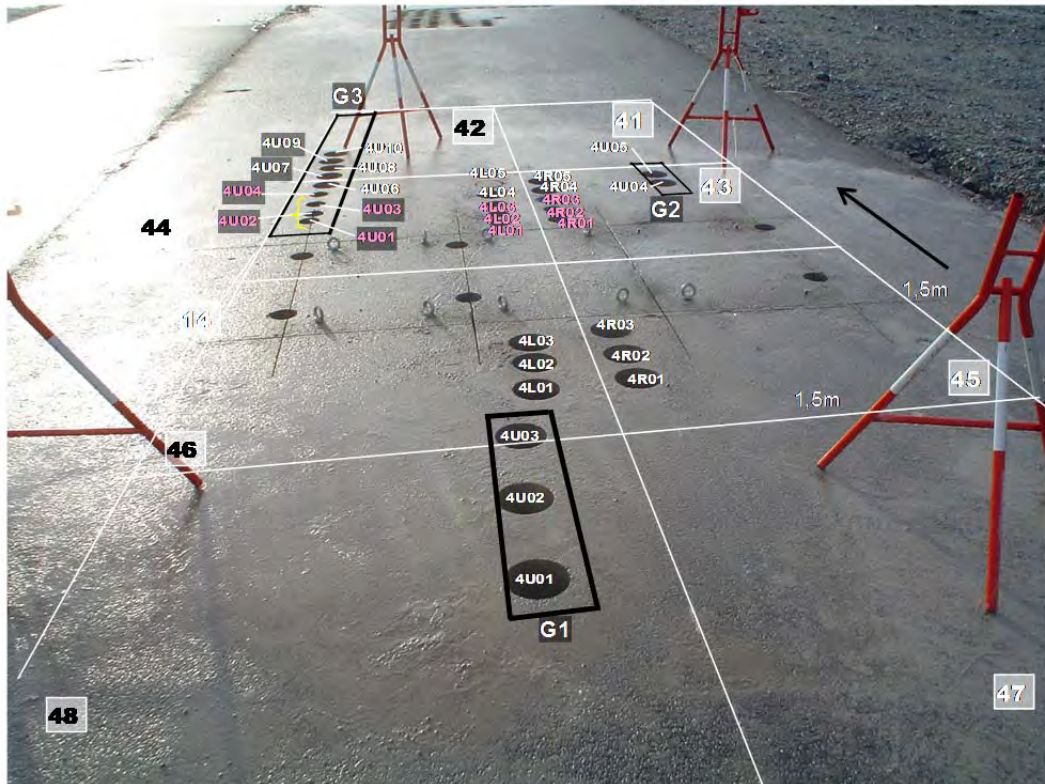
Fig. 5.63 Position and designation of the cores taken from section F4.

5.3.9.1 Bulk Specific Gravity

4 cores of the trafficked area and 4 cores of the not-trafficked area were used to calculate
the bulk specific gravity. Cores of G1, G2 and G3 sectors (see Fig. 5.63) were used for
the tests in the not-trafficked areas. The results were compared to the Marshall compac-
tion values and presented in Fig. 5.64 in terms of degree of compaction.
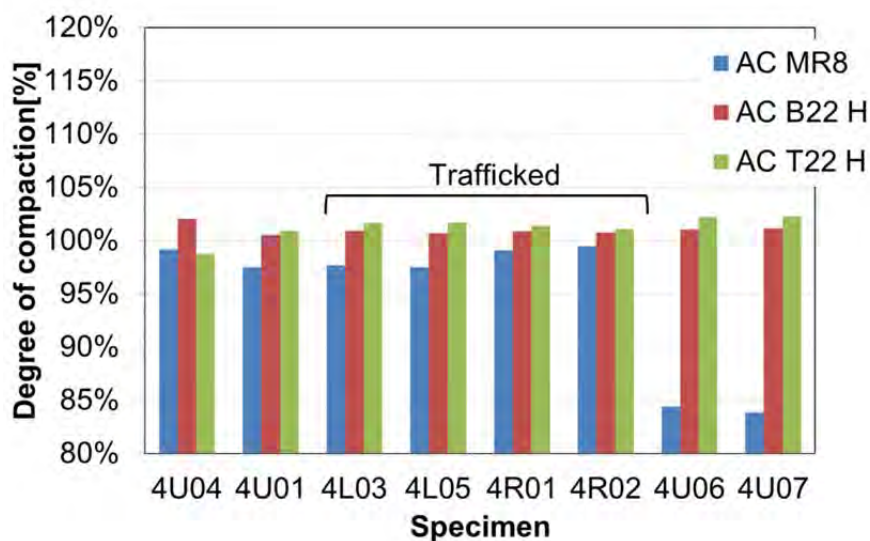
Fig. 5.64 Degree of compaction relative to Marshall values, cores from section F4.

It was expected, that the bulk specific gravity of the cores from the trafficked area would
be higher than in the rest of the cores. However, this did not happened since the traffic

compaction was quite small due to the stiffness of the pavement. Nevertheless, cores 4U06 and 4U07 did not even reach 85% of the Marshall compaction values, probably caused by a poor compaction as confirmed by initial GPR inspections.

5.3.9.2 Indirect tensile test

The elastic resilient moduli of each bituminous layer were calculated from the indirect tensile test results following the European Standard EN 12697-26 [21]. To that end, 3 cores from the load application area (trafficked) and 3 cores from outside the load application area (not-trafficked) were used. An average elastic resilient modulus for each case was calculated and compared. Results are presented in Fig. 5.65 and Fig. 5.66 showing that the difference between both cases is negligible. However, it is interesting to see that the AC MR8 had a much lower modulus. This may be the reason for the rutting results shown in § 5.3.2.

Fig. 5.65 Elastic resilient modulus of not-trafficked and trafficked cores

Layer	Temp.	Elastic resilient modulus Not-trafficked	Elastic resilient modulus Trafficked	Difference
	(°C)	[MPa]	[MPa]	%
	5	9'543	9'395	1.6
	10	6'900	6'622	4.0
	15	4'442	4'594	-3.4
AC MR8	20	3'435	3'481	-1.3
	25	2'367	2'449	-3.5
	30	1'128	1'187	-5.2
	35	859	871	-1.4
	5	18'948	19'490	-2.9
	10	14'668	13'561	7.5
	15	9'925	10'700	-7.8
AC B22 H	20	7'348	7'647	-4.1
	25	4'856	5'019	-3.4
	30	3'268	3'247	0.6
	35	2'231	2'175	2.5
	5	20'248	19'865	1.9
	10	15'985	14'279	10.7
	15	11'295	11'109	1.7
AC T22 H	20	8'060	7'927	1.7
	25	5'170	5'058	2.2
	30	3'522	3'332	5.4
	35	2'315	2'235	3.5

a)

Elastic resilient moduli
Trafficked cores

b)

Elastic resilient moduli
Not-trafficked cores

c)

Comparison not-trafficked and trafficked

Fig. 5.66 Comparison of elastic resilient moduli of not-trafficked and trafficked cores from section F4.

5.3.9.3 Interlayer bonding

The bonding of the interlayers of 4 cores from the load application area (trafficked) and 4 cores from outside the load application area (not-trafficked) were tested with the layer parallel direct shear test (LPDS) according to the Swiss standard SN 670'641 [22]. In total, 2 interlayers were analyzed: between MR8 and AC B 22H (top and second course) and between AC B 22 H and AC T 22 H. The results are presented in Fig. 5.67 and Fig. 5.68 showing that in both cases the interlayer properties of the top interface improved after trafficking in term of both interlayer maximum shear force and stiffness (slope of the curve).

Fig. 5.67 LPDS interlayer shear test results

	Interlayer 1-2 MR8 - AC B 22H		Interlayer 2-3 AC B 22H - AC T 22H	
	Trafficked	**Not-trafficked**	**Trafficked**	**Not-trafficked**
Max. Load [kN]	41.9	32.9	37.1	39.5
Max. Tension [kN/m²]	2373.0	1864.3	2099.5	2235.3
Def. at Max. [mm]	2.7	2.2	1.5	1.3

a)
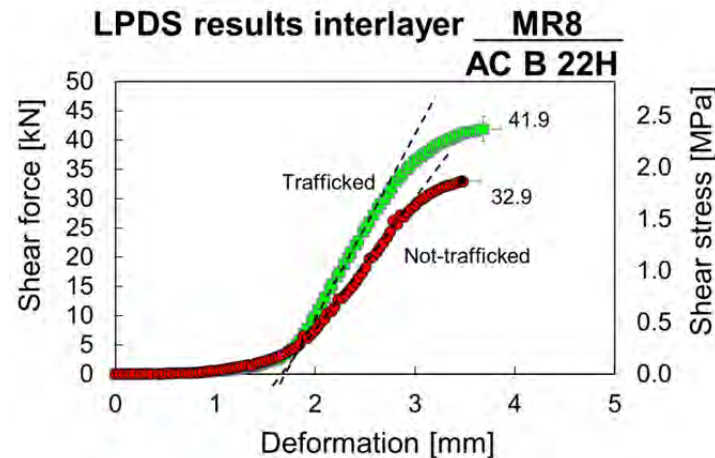
b)
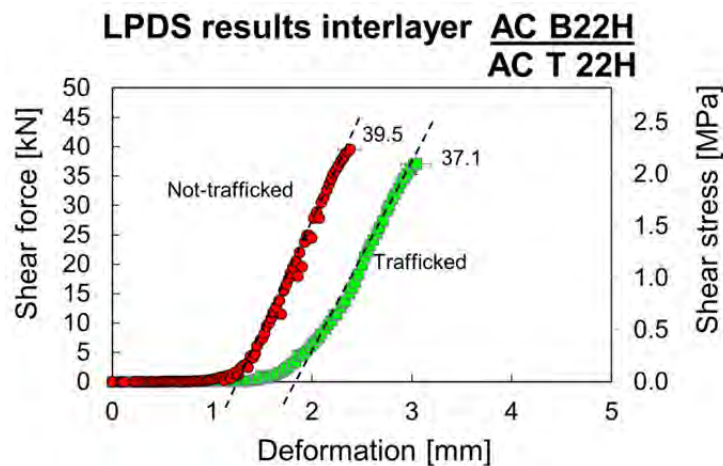
Fig. 5.68 Comparison of the LPDS test results for both not-trafficked and trafficked loading condition in each interlayer.

5.4 Summary and Conclusions

The main goal of the activities summarized in this section was to calibrate the full scaled load simulator MLS10, which is a prototype and was for the first time operated exclusively by personnel from Empa. Hence, the MLS10 was transported to a testing site with three pavement structures of different thicknesses that were trafficked with the load simulator. The thickest structure corresponds to the strongest pavement type of the Swiss design catalogue.

Regular measurements of rutting, static deflections with ETH Delta, etc. were carried out in order to evaluate the pavement response and detect any sign of distress. Finally, cores were taken from the pavement and laboratory tests were performed to determine key material properties of the different pavement layers.

The analysis of the data shows that no clear change in pavement responses occurred during the course of the tests. Profiles show very little rutting, not even reaching 2mm. It is interesting to remark that rutting of the pavement with multiple bituminous layers (section F4) performed the worst. This shows that the permanent deformation was produced mostly by the compaction of the asphalt layers and not by the stabilized and subgrade

courses. FWD measurements in section F4 also indicate that relative deflection increased in the trafficked zone. This can be understood as initiation of a distress mechanism in the structure. As for laboratory tests, the interlayer bonding between the top and second layers appears having increased after MLS10 trafficking. The rest of the laboratory experiments confirmed that the material properties did not change after the tests.

These results show that the pavements were well constructed and did not display unexpected premature failure. With these results it has also been demonstrated that stiff and well-built constructions require quite much trafficking load, and, therefore time, to show clear signs of distress. On the other hand, it means that a pavement that would have shown clear distress after this comparatively limited MLS10 number of loadings ranging from 427'000 to 765'000 would have to be rated of low quality. Hence, on the basis of these results, the MLS10 may well be used as a tool to assess quality right after construction. This may be particularly useful in cases of new materials or uncertainties regarding construction qualities.

Nevertheless, for research purposes and for acquiring information on specific bearing capacity questions (e.g. regarding the effect of overlays in case of maintenance), it is recommended that, in future, the MLS10 is used for evaluating weaker structures since this could give reliable answers in a shorter period of time.

However, acquiring experience during a period of seven month was the most valuable profit of the project. In this time, many shortcomings of the MLS10 and missing operation skills were identified and improved. Moreover, the instrumentation of the pavement, data acquisition and analysis, which were demanding tasks, could be accomplished successfully, since almost all sensors worked as required over the whole time period

5.5 Further experiments: Comparison between the MMLS3 and MLS10

5.5.1 Introduction and objectives

As part of the master thesis of Andrés Pugliessi from University of Rosario (Argentina) [2], a comparison was carried out between the pavement response to the full scale load simulator MLS10 in the field and to the down-scaled model mobile load simulator MMLS3 in the laboratory. The MMLS3 is a one-third scaled version of the MLS10 and the principles of operation are similar. The configuration of the MMLS3 equipment is simple and consists of four wheels of 300mm diameter, each loading the pavement with a maximum of 2.1kN using a spring suspension system, at a maximum speed of 2.5m/s (9km/h). This speed allows reaching up to 7200 load applications per hour. In this case, the wheel load is applied over a length of about 1.0m. A view and schema of the equipment is presented in Fig. 5.69.
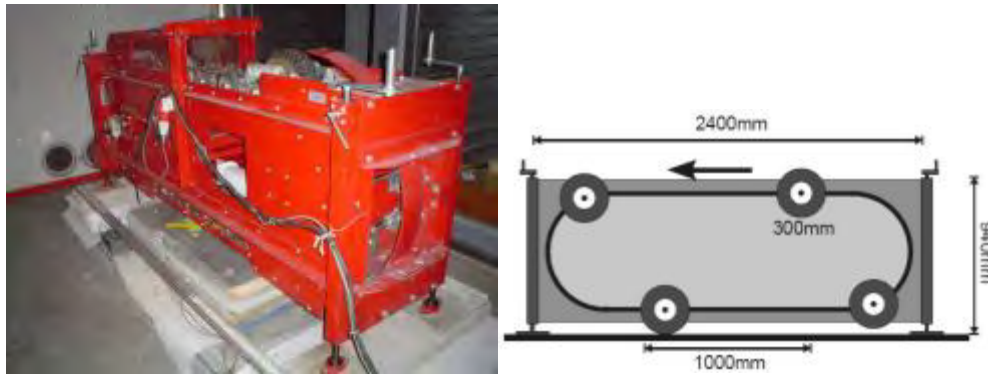
Fig. 5.69 View and schema of the MMLS3.

Because of the different load configurations, both load simulators induce different strain conditions in the same pavement. This might lead to different distress mechanisms. Therefore, the investigation was focused in comparing the effect of both simulators in the same pavement by measuring and simulating the strain levels. Additional reading on this study was published and presented in the APT 2012Accelerated Pavement Testing congress in California [23] and can be found in Anhang III.4.

5.5.2 Experimental setup

After the field experience with MLS10, a total of 6 pavement slabs 1100mm x 700mm were taken out from the trafficked area. Due to the high adhesion of the SAMI between the asphalt and the stabilized layer, the removal was difficult, and as a result the thickness of the slabs was variable (see Fig. 5.70). This was corrected by embedding the slabs in concrete.

Fig. 5.70 Pulling out of one of the pavement blocks

Once in the laboratory, one of the slabs from section F4 was prepared for trafficking with the MML3. The selected slab contained the temperature and strain gauges sensors installed during the construction of the pavement. All the sensors were re-connected to the data acquisition system. When the slab was ready, it was placed in a container with temperature control. The MMLS3 was positioned on top of the slab.

Thermal conditioning of the slab was carried out for 24h and for temperatures of 20°C, 25°C, 30°C and 35°C. After reaching the temperature, the MMLS3 was run at 1.5 km/h, 3.4 km/h, 5.3 Km/h, 7.1 km/h and 9.0 km/h and strain measurements were carried out. Fig. 5.71 presents a comparison of both tests conditions.

Fig. 5.71 Summary of field and laboratory test conditions

	MLS10	**MMLS3**
Pavement		
	Field test	Lab test
Load		
	Twin tires	Single tire
Infl. Pressure [Mpa]		
	0.8	0.6
Speed [km/h]		
	22	1.5
		3.4
		5.3
		7.1
Temperature [°C]		
	variable	20
		25
		30
		35

5.5.3   Simulation of the pavement response

Simulation of the pavement response to the MLS10 and MMLS3 loadings were performed with both finite element (FEM) and analytical models. FEM were used to verify the measurements made in the field.

5.5.3.1   Finite element models

The FEM software Abaqus was used to simulate the response of the pavement to a single tire passing of the MLS10 and MMLS3. The geometry of the models was defined as a piece of the pavement of 2250mm length and 2000mm width (Fig. 5.72). The model of the MLS10 loading included the asphalt and stabilization layers. The geometry simulating the MMLS3 trafficking did not include the stabilization layers because they were not relevant for the testing in the laboratory. Temperature dependent linear elastic and viscoelastic material models were used for the asphalt layers. Linear elastic material was used to model the cement stabilized layer. The values for the material models (temperature dependent elastic modulus) were obtained from laboratory tests, as described in §5.3.9.2. The loads of both load simulators were modeled as a constant vertical pressure, moving along the load application path. Therefore, for each simulation speed, load and size of the tire footprint was taken into account. Further, in order to simulate the material response to dynamic loading, inertia was taken into account.
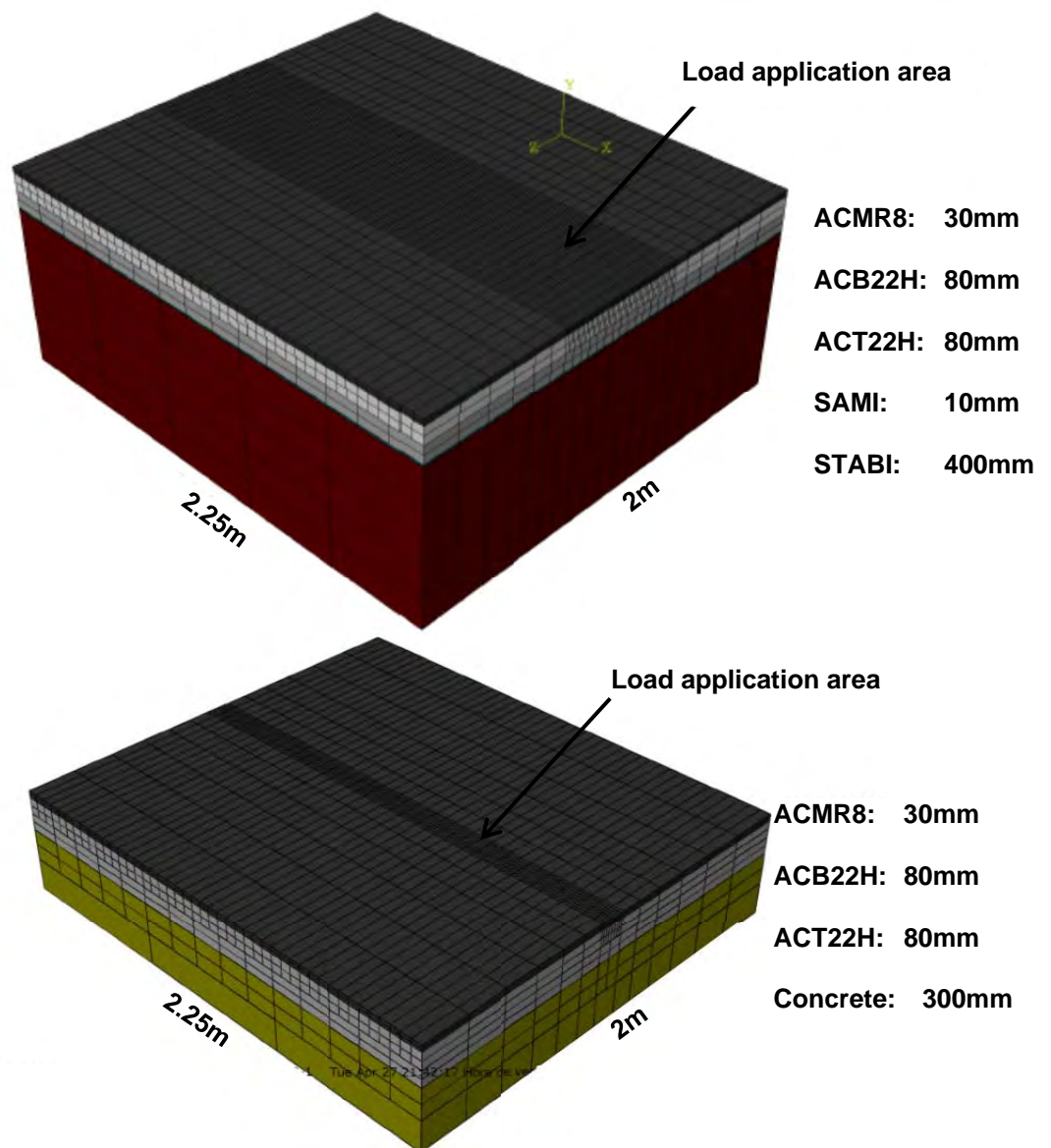
Fig. 5.72 View of the geometry of the models. On top, MLS10 model and on the bottom the MMLS3 model

5.5.4   Summary of the results

5.5.4.1 Measurements with strain gauges

Strain amplitudes were calculated in the same way as explained in § 4.3.3. The results for both load simulators for the longitudinal and transversal strain gauges BL4 and BQ4 are shown in Fig. 5.73 and in Fig. 5.74 respectively.

a)

Strain gauge BL4 - MLS10 load
Speed:22km/h, Load:65kN, Twin tires, Infl. pressure:0.8MPa

◆ 04/11/09 - 743k to 766k

b)

Strain gauge BL4 - MML3 load
Speed:9km/h, Load:2.1kN, Single tire, Infl. pressure:0.6MPa

▲ MMLS3 loading-
long. strains

$y = 4.2959e^{0.0863x}$
$R^2 = 0.9755$
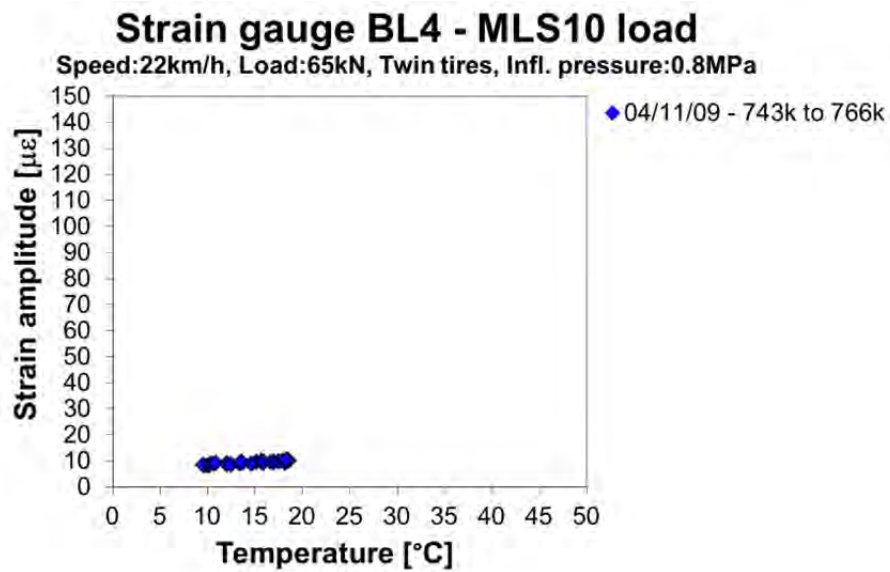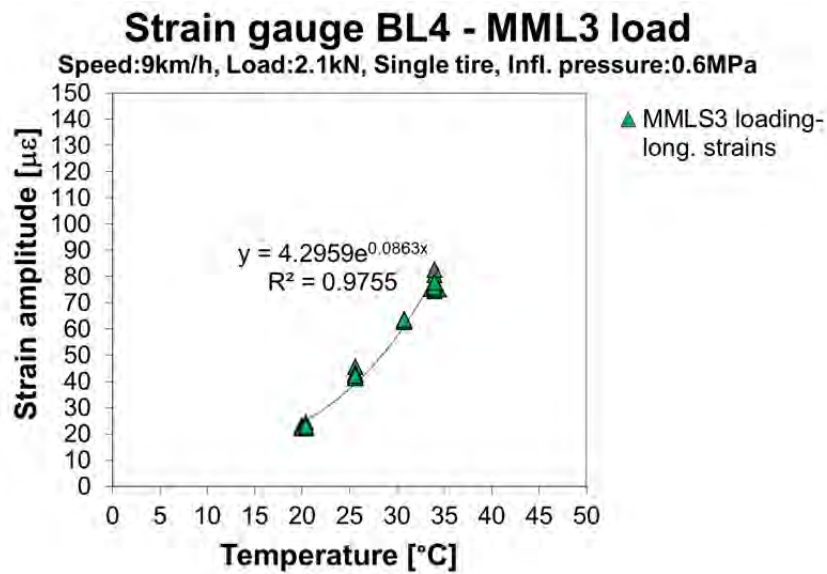
Fig. 5.73 Measured longitudinal strains for a) MLS10 tests at 22km/h and b) MMLS3 tests at 9km/h.

a)
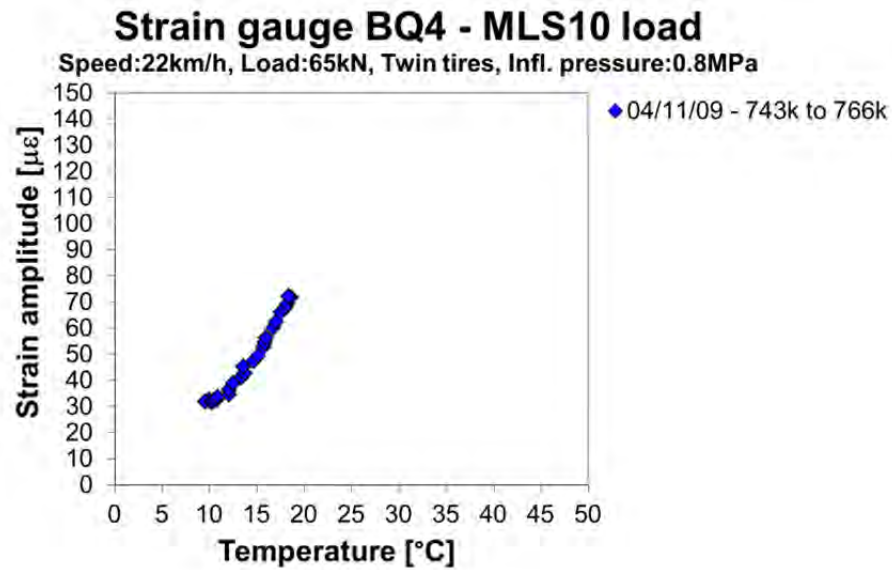
b)
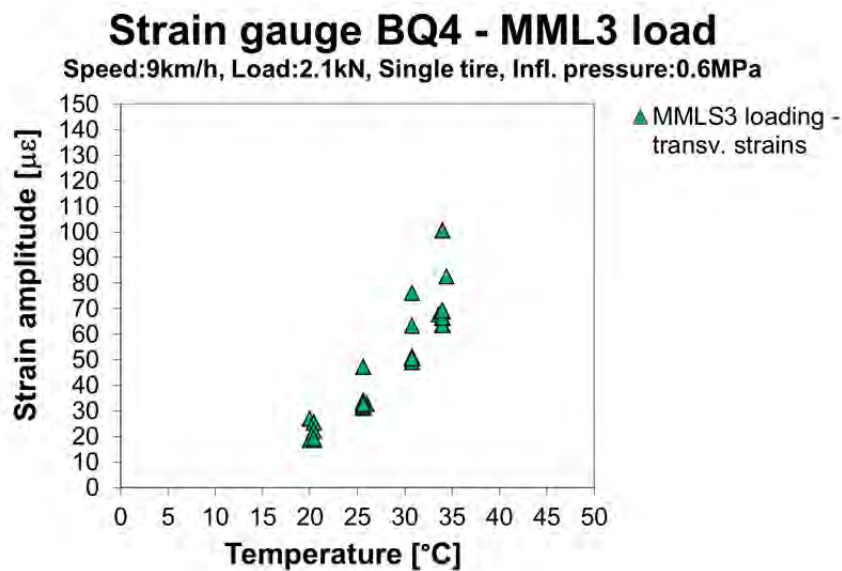
Fig. 5.74 Measured transversal strains for a) MLS10 tests at 22km/h and b) MMLS3 tests at 9km/h.

The relationship between the strains induced by both machines in the same pavement is presented in Fig. 5.75 and Fig. 5.76. To calculate the relationship between MLS10 and MMLS3 responses, the strain values, which are temperature dependent, are approximated with sigmoidal functions. Then, for each temperature, it is possible to calculate the strain amplitudes produced by both machines.

Strain gauge BL4
MMLS3 vs MLS10

$y = 2.62x^{0.48}$
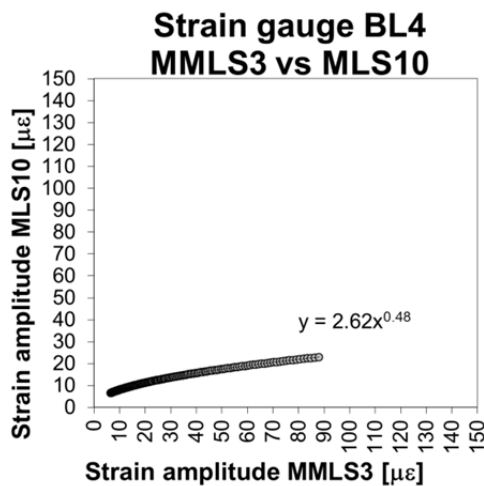
Fig. 5.75 Relationship between the absolute longitudinal strain amplitudes for MLS10 and MMLS3

Strain gauge BQ4
MMLS3 vs MLS10

$y = 2.37x^{1.19}$
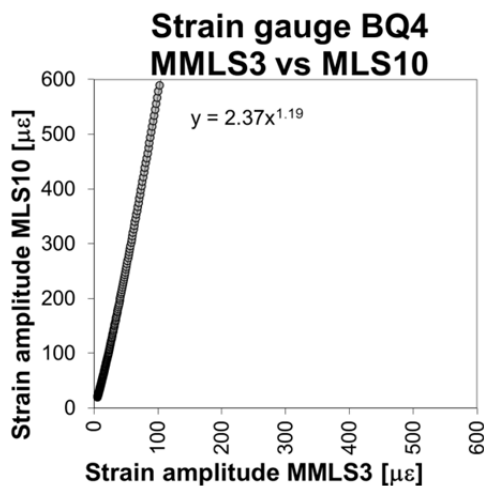
Fig. 5.76 Relationship between the absolute transversal strain amplitudes for MLS10 and MMLS3

Although the load of the MMLS3 is much lower than the MLS10 load (2.1kN to 65kN), the measured longitudinal strains at -30mm are higher for the first one. On the other hand, the transversal strains for the MLS10 are more than double the strains of MMLS3. This can be explained because of the type and size of the tires: the MLS10 has twin tires and the MMLS3 single tires of quite small footprint. This might have a big influence on the strains measured near the application of the load and road surface.

5.5.4.2 Finite Element simulations

The response of the strain gauges was compared with the theoretical strains obtained with the finite element models. After adjusting some material parameter values, the finite element calculations of the MLS10 loading show results that are in good agreement with those obtained in the measurements, as presented in Fig. 5.77 and Fig. 5.78. However, for MMLS3, the finite element calculations have some differences with measured strains (Fig. 5.79 and Fig. 5.80). This might be because the small tire of the MMLS3 produce higher strains concentrated around the footprint area which are more difficult to simulate with the present model. Further investigation should be done in order to refine the finite element models.
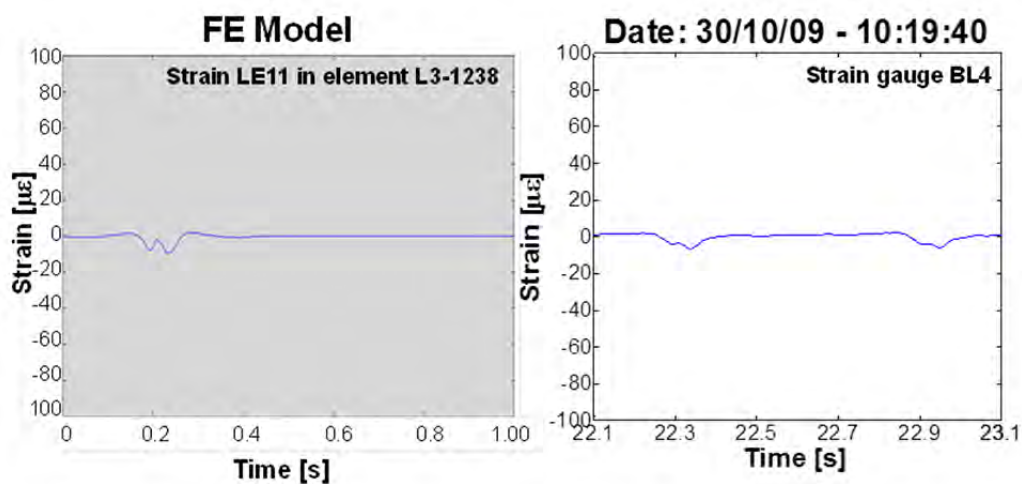
Fig. 5.77 Comparison of strains under the wheel track in the longitudinal direction obtained from the FE model and in situ measurements, for MLS10 loading
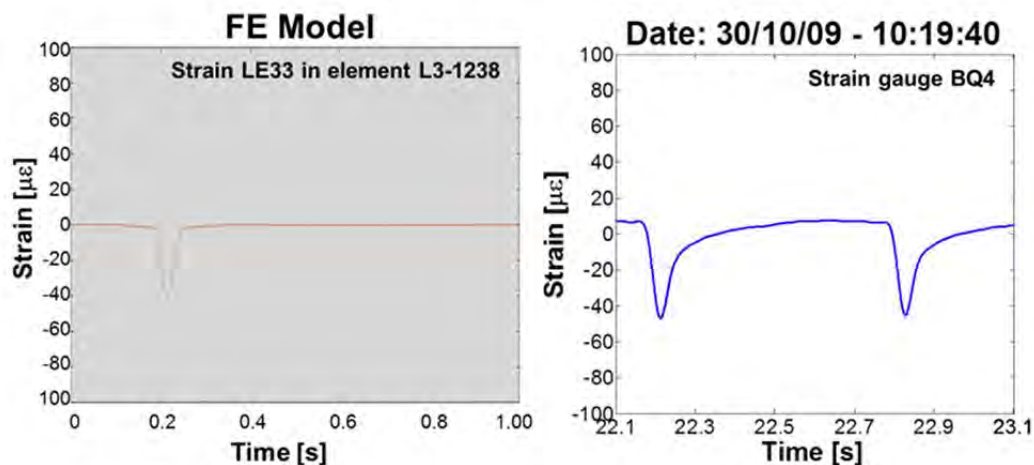
Fig. 5.78 Comparison of strains under the wheel track in the transversal direction obtained from the FE model and in situ measurements, for MLS10 loading
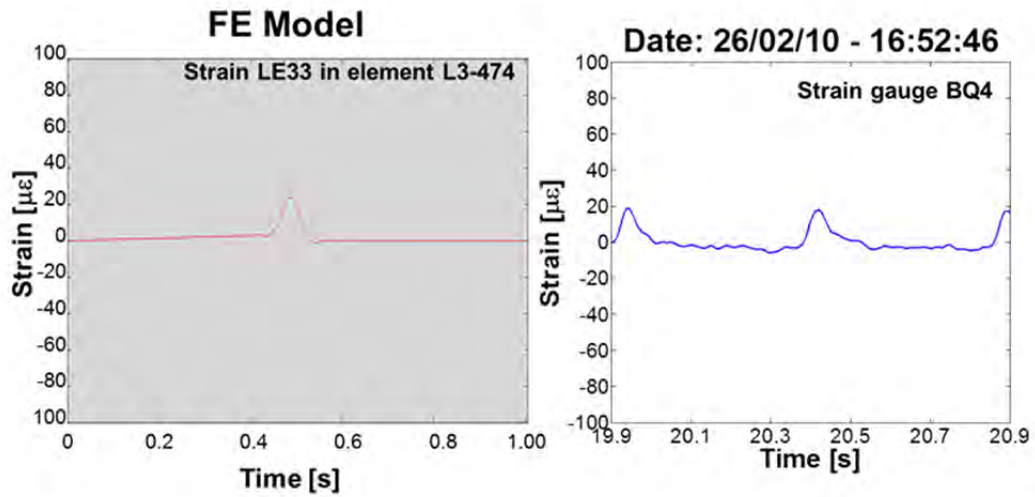
Fig. 5.79 Comparison of strains in the transversal direction obtained from the FE model and in situ measurements, for MML3 loading
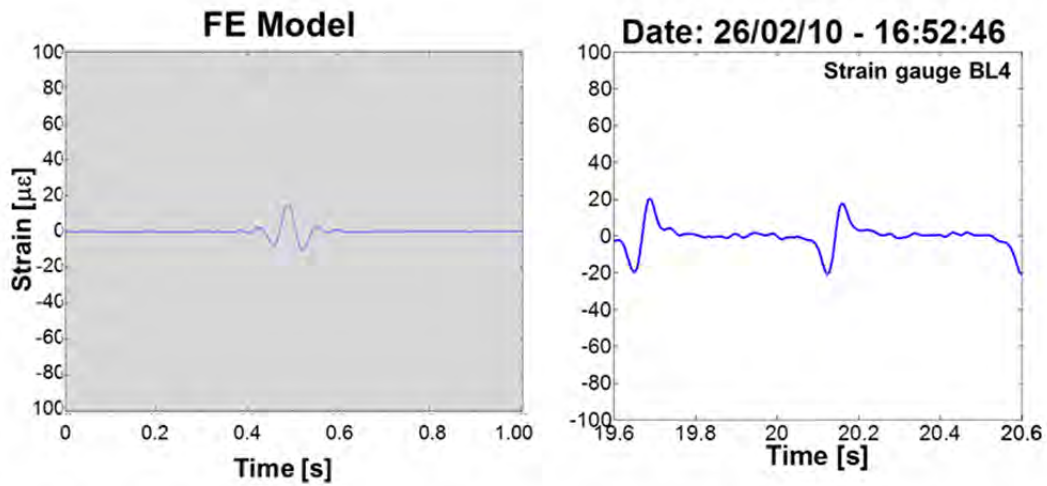
Fig. 5.80 Comparison of strains in the longitudinal direction obtained from the FE model and in situ measurements, for MMLS3loading

6 Test Site 2: Rastplatz Suhr

6.1 Introduction

Between January and March 2010, a major control and reinforcement work was carried out at Empa, looking forward to solving and preventing breakdowns during testing. The bogie chain was taken out of the frame of the machine and several changes were carried out. The most important improvements are listed below:

Reinforcement of the new bogies

Due to the fatigue cracks observed in the bogie frames, a new calculation of the structure was carried out by the South African constructor as part of warranty work. The solution for repairing the cracks consisted of reinforcement plates welded onto the existing frame (see Fig. 6.1)

Fig. 6.1 View of bogie reinforcement

Improvement of bearing setup

All bearings were revised and some pieces of the setup were re-designed, constructed and mounted again.

Changing the frame

Due to the alterations in the geometry of the bogies, the frame of the machine had to be changed to let the running parts move without touching the construction and to make the structure fit for super single tires (Fig. 6.2)

Fig. 6.2 Change in a beam of the frame

After the revision, the machine was prepared for deploying to the motorway rest area "Rastplatz Suhr" where an aged pavement was to be tested.

6.2 Experimental setup

6.2.1 Layout of the test sections

The test site was located on a by-pass road section for a rest area of highway A1, direction Bern (see Fig. 6.3). The rest area called "Rastplatz Suhr" was closed to traffic for a little more than one month in summer 2010.

It is known, that the pavement was built more than 20 years before the tests. However, at the beginning of the tests the pavement structure at the test site was unknown. Later, after trafficking and before rehabilitating the pavement, samples of the bound layers were taken in order to examine the structure and type of construction.

Fig. 6.3 View of testing site and thickness of the pavement

6.2.2 Load configuration

The machine was setup to apply 65kN in each of the four bogies, using a twin tire configuration. This is the maximum load that MLS10 is able to induce with this type of tire and corresponds to a total axle load of 130kN. The loads were calibrated using static scales. The tire pressure was set to 7.5bar. The trafficking speed for the tests was 22km/h. The MLS10 was equipped with Good-year 455/50 R22.5 twin tires with a inflation pressure of 7.5bar.

6.2.3 Evaluation of pavement performance

As explained in § 5.4.1, several stationary sensors and periodic non-destructive tests were used, as listed below:

Stationary sensors embedded in the pavement

- Thermocouples
- Strain gauges
- Accelerometers

Periodic measurements

- Transversal profiles
- Portable Seismic Pavement Analyzer (PSPA)
- ETH Delta

6.2.4 Location of the sensors and non-destructive testing

A schematic of the position of the sensors is depicted in Fig. 6.4.
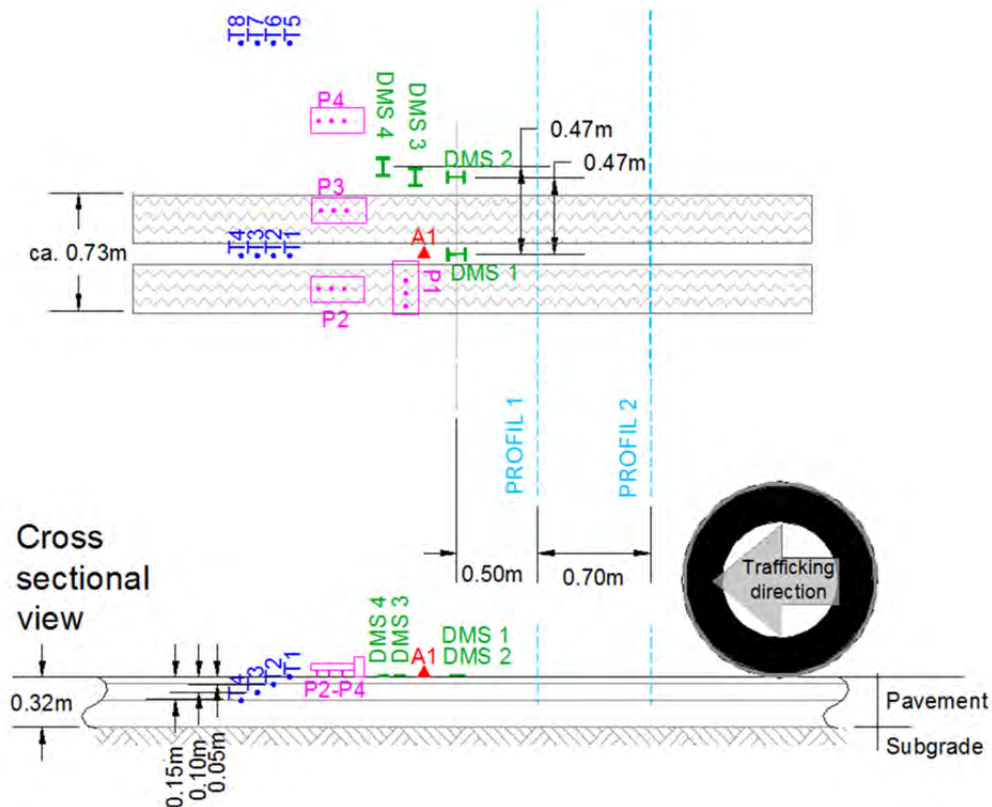
Fig. 6.4 Schema with the position of the stationary sensors and periodic measurements in the pavement showing the designation for different sensors and strain gauges, together with their position and direction:

P: PSPA
A: Accelerometer
DMS: Strain gauge
T: Thermocouple

The strain gauges were glued to the pavement surface, since it was not possible to put them inside the structure of this pavement. DMS 1 was installed along the trafficking axle, between the twin tires. DMS 2 was mounted parallel to DMS 1 but 47cm to the left side from the axle. DMS 3 and DMS 4 were installed on the pavement surface perpendicular to the trafficking direction: the position of DMS 3 was positioned 55cm and DMS 4 was situated 67cm away from the axle.

Thermocouples were installed inside the pavement by drilling small holes at different depths. Thermocouples T1 to T4 were placed in the trafficking axle on the surface and at depths of 50mm, 100mm and 150mm. T5 to T8 were installed at the same depths, but 1m away from the axle.

Only one accelerometer, A1, was installed on the surface between the twin tires.

Two transversal profiles were taken to evaluate permanent surface deformation on one side of the trafficking path.

PSPA measurements were carried out in each tire path (P1 perpendicular to the trafficking direction, P2 and P3 along the wheel path) and outside the trafficking area (P4).

6.3 Operation

6.3.1 Loading history

The goal of the test program was to reach 1'000'000 MLS10 load applications of 65kN. However, the time window when the test section was available was much shorter than expected. Therefore only half of the number of load applications could be conducted.

The MLS10 was deployed on the 10th of May 2010 and was moved away from the site on the 22nd of June 2010. A total of 405'000 load applications was carried out. The accumulated number of loads through the duration of the tests is presented as a line Fig. 6.5. Horizontal segments in the line represent the days where the MLS10 was not operational due to holidays, weekends, breakdowns in the functioning of the machine or because of measurements, installation of sensors, etc. Details regarding the machine performance during this period are described in the next section.
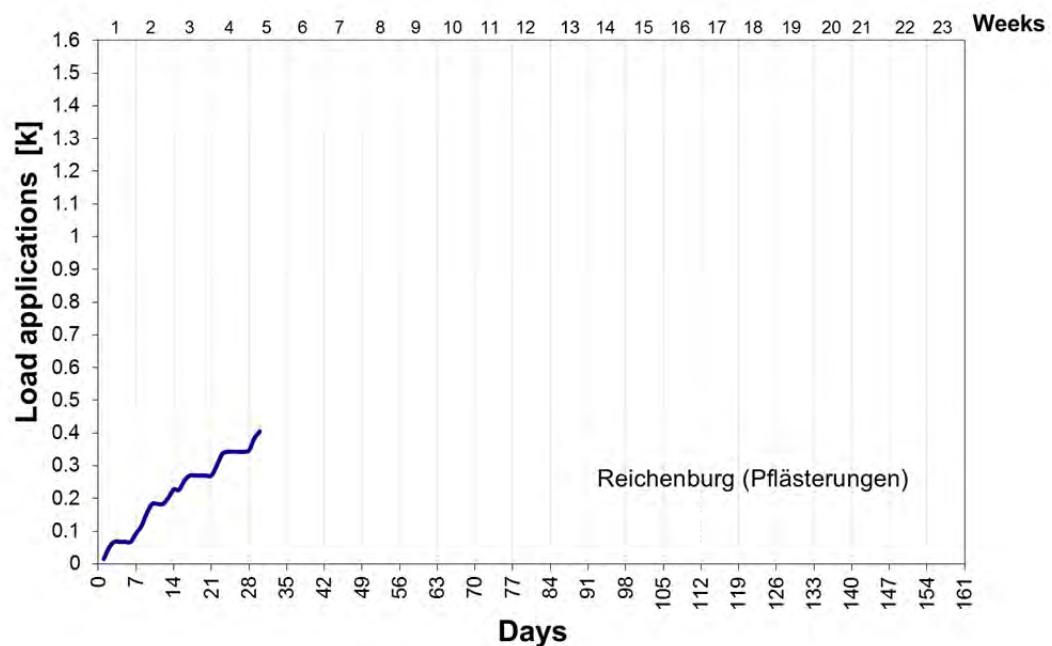
Fig. 6.5 Number of MLS10 accumulated load applications vs. time

6.3.2 Interruptions due to machine malfunctioning

Cracks in diagonal struts

Daily routine checks, allowed to discover small cracks in the bogie chain (see Fig. 6.6). These were welded before having a complete break of the strut.

Fig. 6.6 Crack in a strut connection

Breaking of bolts

After reinforcement of the bogies, an unexpected problem started to occur regularly: Bolts fixing the so called reaction plates to the bogies had to be replaced because the fixation of the brackets holding them to the bogies (called C-Brackets) started failing on a regular basis (see Fig. 6.7). The reaction plates are parts that are responsible for pulling the bogies while trafficking. The reason of the problem was unknown and the policy adopted to deal with the problem was to replace the broken bolts and continuing testing until a final solution could be found. A total of 3 screws broke during these tests.

Fig. 6.7 Failure of a bolt in a C-Bracket

6.3.3   Non-destructive tests

Non-destructive tests were performed at different trafficking times. Fig. 6.8 informas about when ETH Delta measurements were carried out.

Fig. 6.8 Date and number of MLS10 load applications for ETH Delta tests.

Date	Number of MLS10 load applications
17.05.10	0
04.06.10	270178
21.06.10	405'000

ETH Delta tests were carried out by staff of the Institute for Geotechnical Engineering (IGT) of ETH.

6.4 Measurements results

6.4.1 Temperature

Fig. 6.9 presents the temperature profiles measured by sensors T1 to T8.

a)

b)
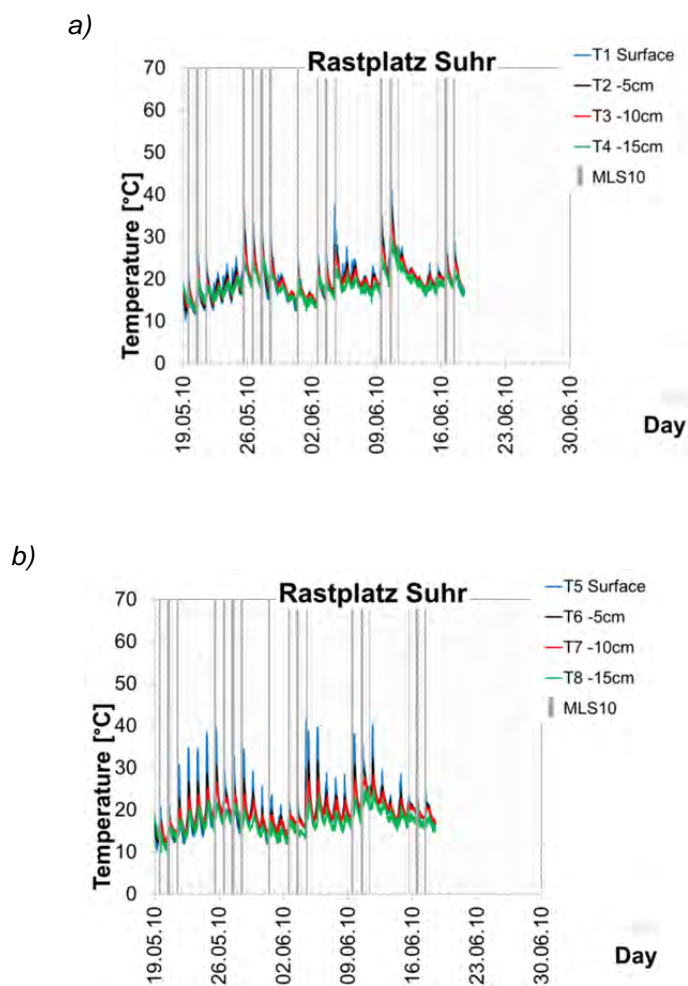
Fig. 6.9 Temperature distribution measured during the testing period; a) T1-T4 in the wheel path below the wheels and b) T5...T8 distance of 1m away from the wheel path.

Fig. 6.10 summarizes the average temperatures over the testing period and the average temperature only while the machine was running. This table shows that the average temperatures near to the rolling tires are higher that the temperatures outside the wheel path.

Fig. 6.10 Average temperatures

Thermocouple	Average temp. over hole testing period [°C]	Average temperature during trafficking [°C]
T1	20.6	24.5
T2	20.1	22.6
T3	19.7	21.0
T4	18.5	20.0
T5	20.7	22.1
T6	19.9	20.0
T7	19.4	19.3
T8	17.3	17.7

6.4.2 Transversal pavement profiles

Data Evaluation

Data evaluation was performed according to § 5.3.2.

Summary of the Results

Fig. 6.11 shows the progressive deformation of the pavement in both measurement positions P01 and P02, obtained with the MLS profiler. The same figure shows the average deformation under and beside the wheels at the end of the tests, relative to the initial measurements.

a)
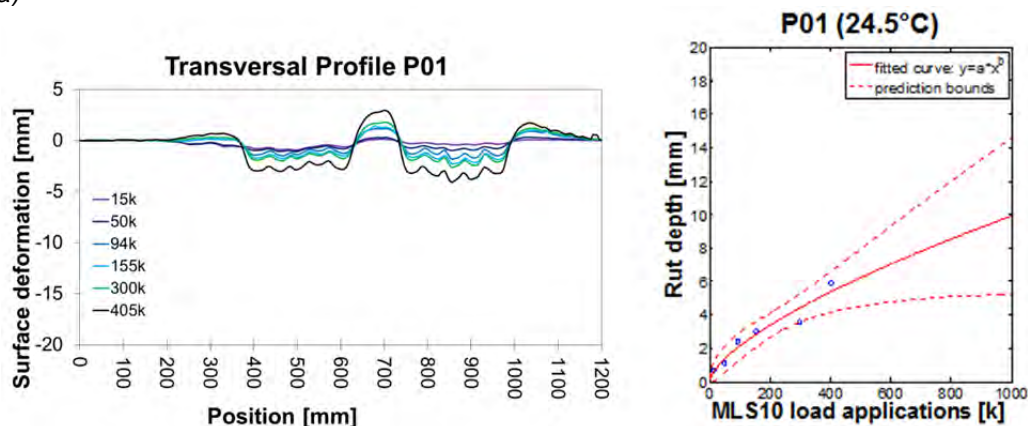
b)
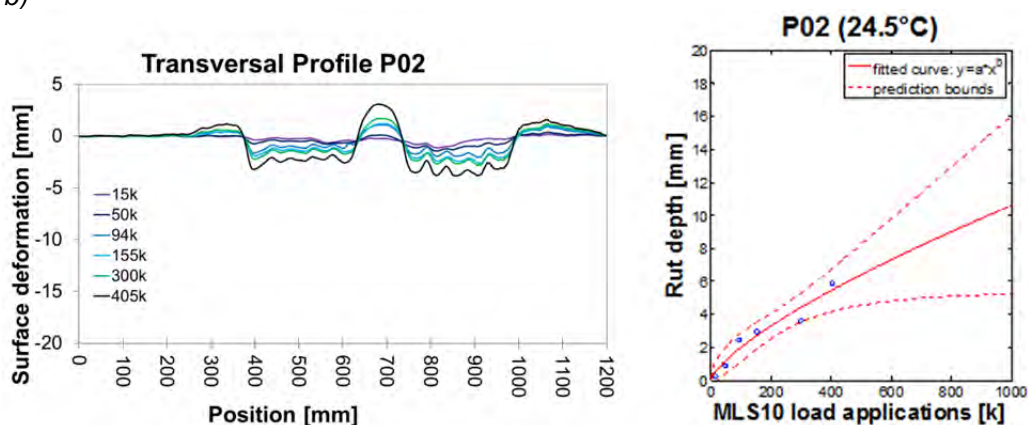
Fig. 6.11 Measured permanent vertical deformation and progressive rut depth vs. number of MLS10 load applications fitted with a power function, including 95% prediction bounds. For positions P01 and P02.

The coefficients for the power functions used to fit the measured data, with the 95% confidence bounds, as well as the coefficient of determination R^2 are presented in Fig. 6.12:

Fig. 6.12 Power function fit parameters

Profile	a (with 95% confidence bounds)	B (with 95% confidence bounds)	R^2
P01	$9.1\ 10^{-4}$ ($-2.9\ 10^{-3}$, $4.7\ 10^{-3}$)	0.67 (0.34, 1.0)	0.94
P02	$4.3\ 10^{-4}$ ($-1.6\ 10^{-3}$, $2.5\ 10^{-3}$)	0.73 (0.36, 1.11)	0.94

The shapes of the transversal profiles show that rutting was produced by a shoving of asphalt material from below to the sides of the tires, showing that there was no compaction of the subgrade. By the end of the tests after ca. 400'000 load applications, the rutting was of about 6mm. In both cases the coefficient of determination R^2 shows that the approximations with power functions are quite accurate.

6.4.3 Strain gauges

Data acquisition and evaluation

Data evaluation was done according to § 5.3.3.

Summary of the results

Fig. 6.13 shows one example of measurements with all strain gauges. As expected, the record of DMS1 and DMS 2 display a tension-compression-tension shape. When the tire arrives to the position of the sensors, the pavement will suffer tension and when the tire is at the same position of the sensor, a compression situation occurs that will reverse when the rolling tire passes by. As anticipated, the values of DMS1 are bigger than those of DMS 2, because DMS1 is closer to the tire. DMS 3 and DMS 4 show purely tensile strains, following the shape of the deflection bowl. DMS 3 values are slightly higher than DMS 4 values, since it is installed closer to the tire.
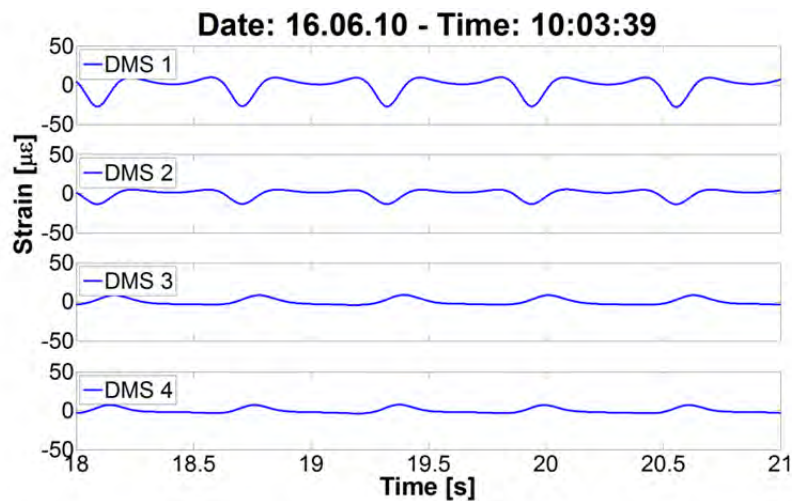
Fig. 6.13 Example of strain gauge measurement.

The sensor DMS 1 installed on the surface, between the trafficking twin tires registered strain amplitudes of $67\mu\varepsilon$ at the beginning of the tests and $71\mu\varepsilon$ at the end (Fig. 6.14). This means that they almost remained equal through trafficking. As explained before, DMS 2 registered lower values of around $29\mu\varepsilon$ which remained stable until the end of trafficking. DMS 3 and DMS 4 measured almost the same values, $15\mu\varepsilon$ and $14\mu\varepsilon$ at the beginning of the tests and slightly increased values of $17\mu\varepsilon$ and $15\mu\varepsilon$ respectively at the end. The tendency shown in these calculations reveal that the strains did almost not change during trafficking (Fig. 6.15). This can be interpreted as a sign that the pavement did not show any significant sign of change in the mechanical properties caused by cracks or other distress types.

Fig. 6.16 presents a summary of the results obtained with the strain gauges.

a)
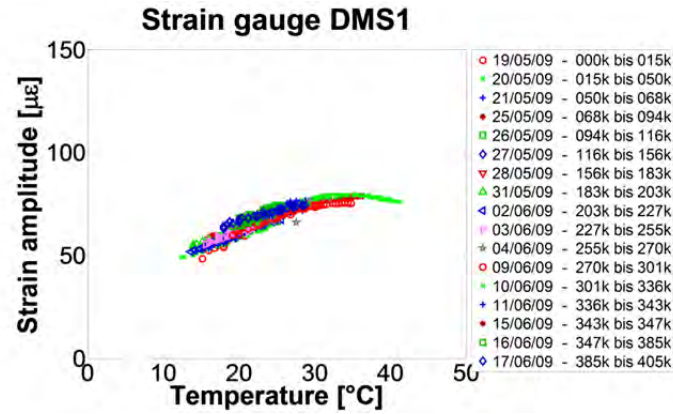
b)
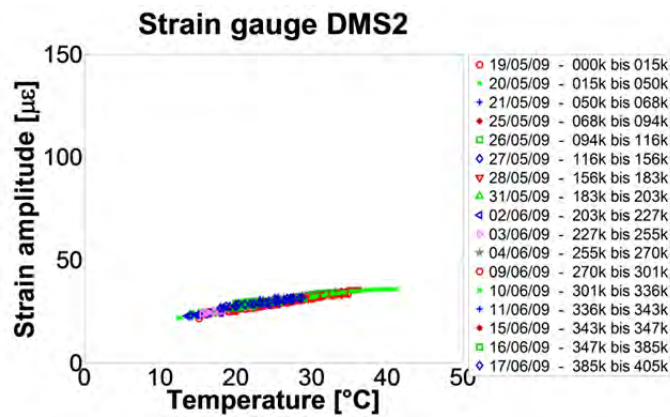
c)
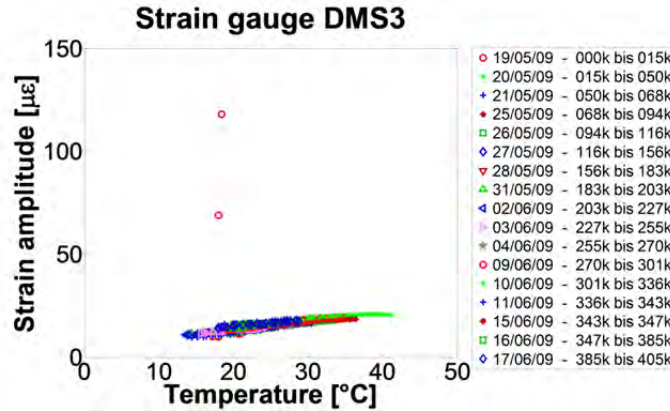
d)
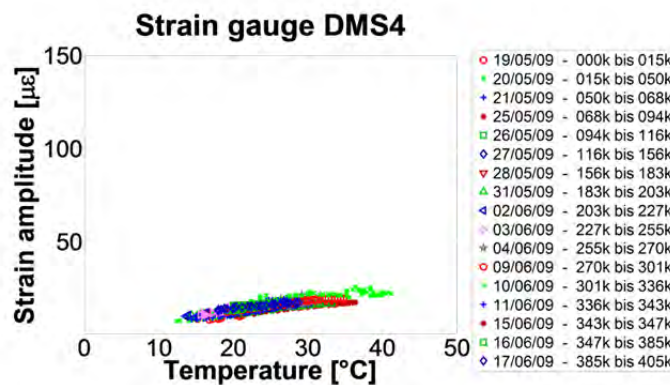
Fig. 6.14 Evolution of strain amplitudes during the course of the tests.

a)

DMS1 (24.5°C)

$y = 7e\text{-}006*x + 71$

b)

DMS2 (24.5°C)

$y = 5.2e\text{-}007*x + 29$

c)

DMS3 (24.5°C)

$y = 8.1e\text{-}006*x + 14$

d)

DMS4 (24.5°C)

$y = 2.6e\text{-}006*x + 16$
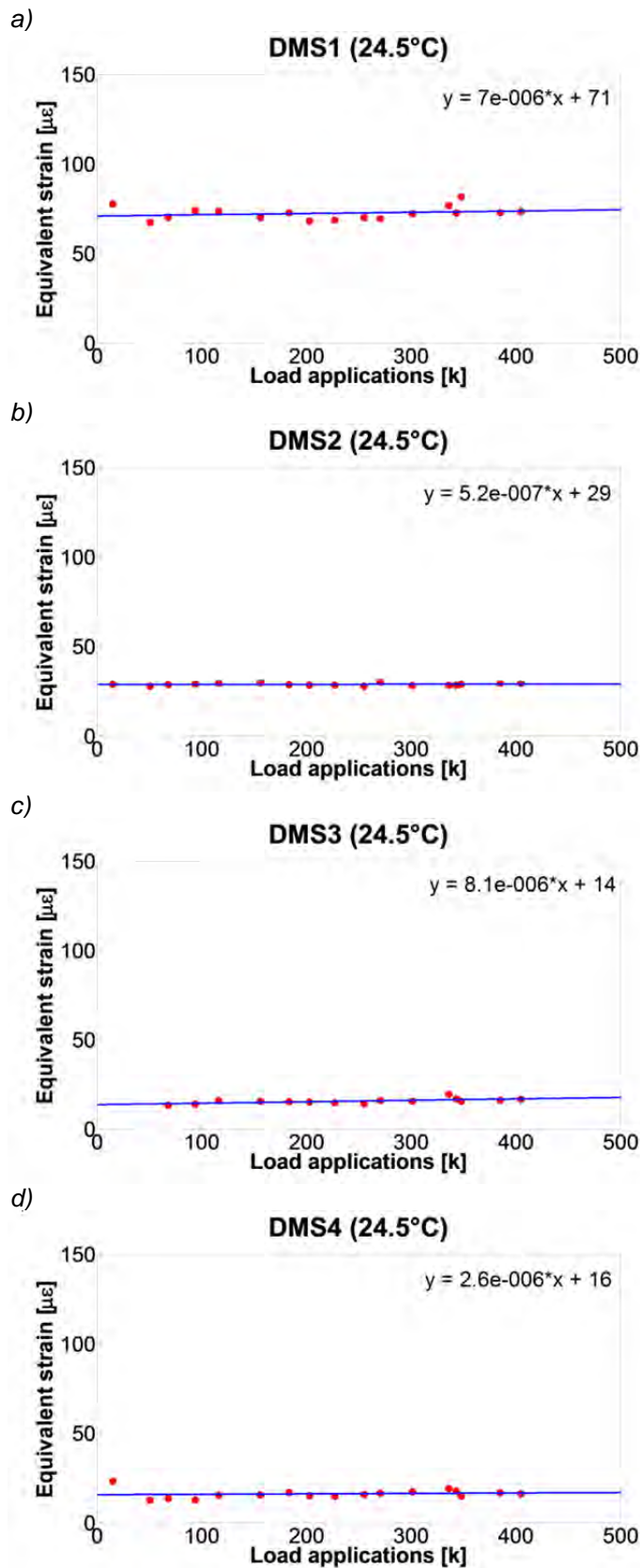
Fig. 6.15 Equivalent strains during the course of the tests and equivalent strains vs. the number of MLS10 load cycles.

Fig. 6.16 Summary of the equivalent strains

Strain gauge	Distance to tire [cm]	Temp. [°C]	Initial equivalent strain [με]	1Mio. equivalent strain [με]
DMS 1	0	24.5	71	78
DMS 2	47	24.5	67	77
DMS 3	55	24.5	14	22
DMS 4	67	24.5	16	19

6.4.4 Accelerometers

Data acquisition and evaluation

Data evaluation was done according to § 4.3.4.

Summary of the Results

Fig. 6.17 shows the results obtained with the accelerometer A1. According to the results, the deflection increases slowly with the amount of load applications. The acceleration amplitudes at the beginning and after 1 million load applications are presented in Fig. 6.18.

The acceleration amplitudes tend to increase with the accumulated number of load applications. However, there is no apparent inflection point in the linear development of the calculated equivalent accelerations, which would indicate a sudden change in the pavement stiffness.

a)
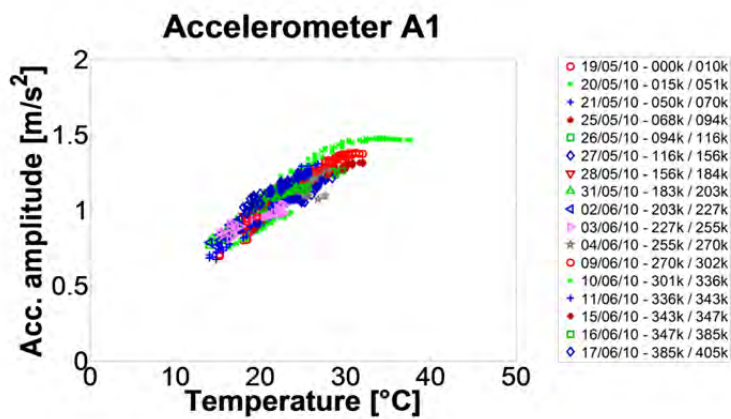
b)
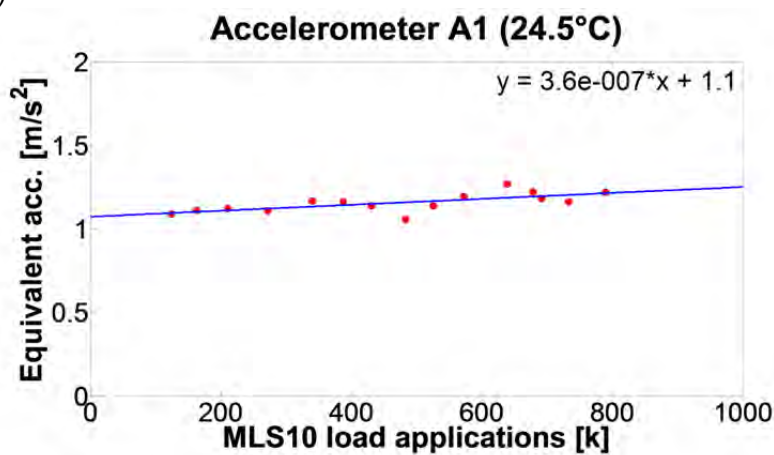
Fig. 6.17 a) Acceleration amplitude vs. temperature and b) equivalent acceleration vs. number of MLS10 load applications.

Fig. 6.18 Summary of the equivalent acceleration

Initial equivalent acc. [m/s^2]	1Mio. load applications equivalent acc. [m/s^2]
1.10	1.46

6.4.5   ETH Delta

Data acquisition and evaluation

The data obtained with the ETH Delta was used to prepare 2D deflection maps. Fig. 6.19 shows the measured deflections at the beginning, in the middle and at the end of the tests.

It can be observed, that the shape and order of magnitude of the deflection bowls do not show clear signs of changes after being trafficked. It can be seen that the amount of 405'000 load applications was not enough to induce a clear change in the structural response.

a)
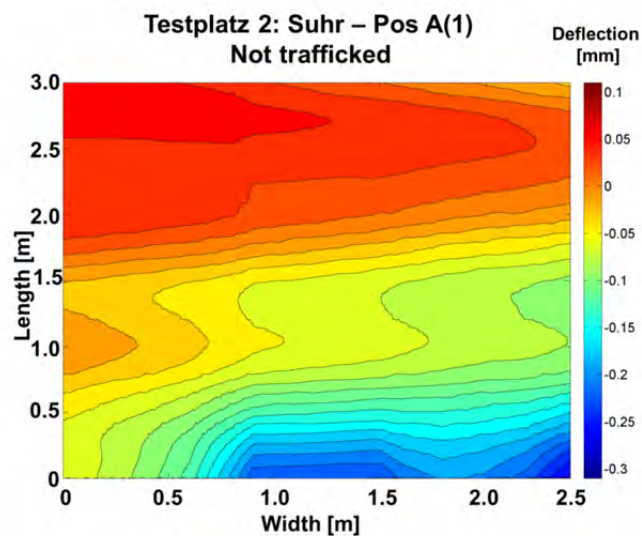
b)
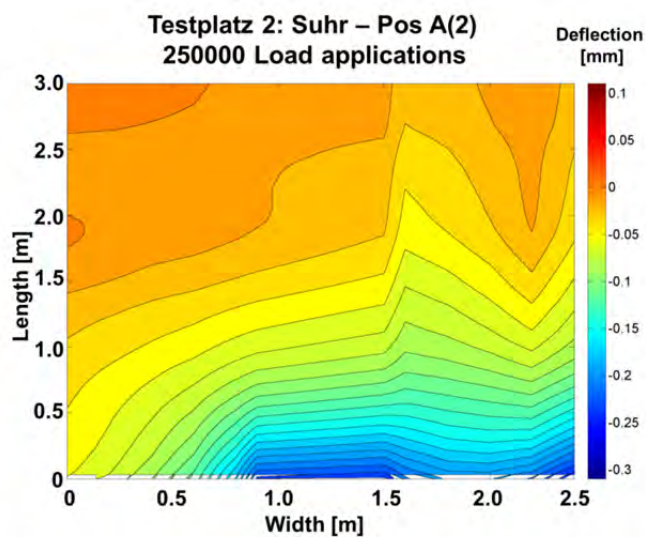
c)
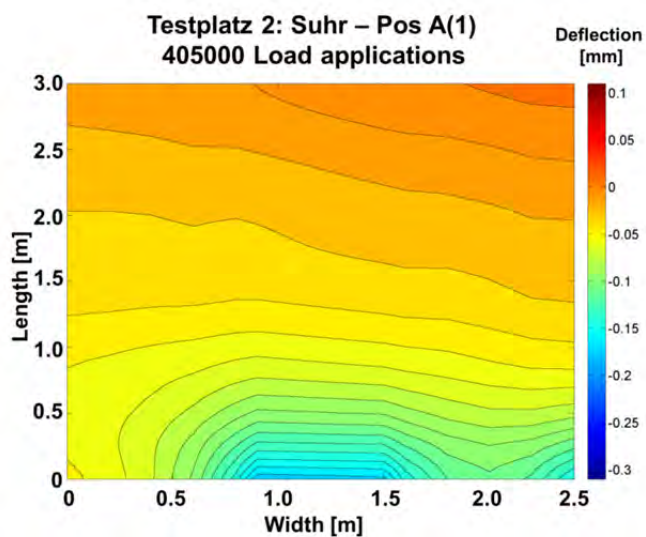
Fig. 6.19 2D deflection maps for different trafficking times obtained with ETH Delta

6.4.6   Portable Seismic Pavement Analyzer (PSPA)

Data acquisition and analysis

Data evaluation was done according to § 5.3.7.

Summary of the Results

The seismic moduli vs. depth before and after trafficking are displayed in Fig. 6.20. The normalized seismic modulus at the reference position P4 is presented in Fig. 6.21. The observation of the general modulus evolution in the analyzed depths indicates that the stiffness of the asphalt layers range between 15 and 25GPa.

There is no clear change in the stiffness between the layers. In fact, the values normalized in Fig. 6.21 with respect to the modulus at position P4 show that there is no clear change in the stiffness trend throughout the tests. For the other depths (-10cm and -16cm) the stiffness is even more homogenous with no significant change after trafficking
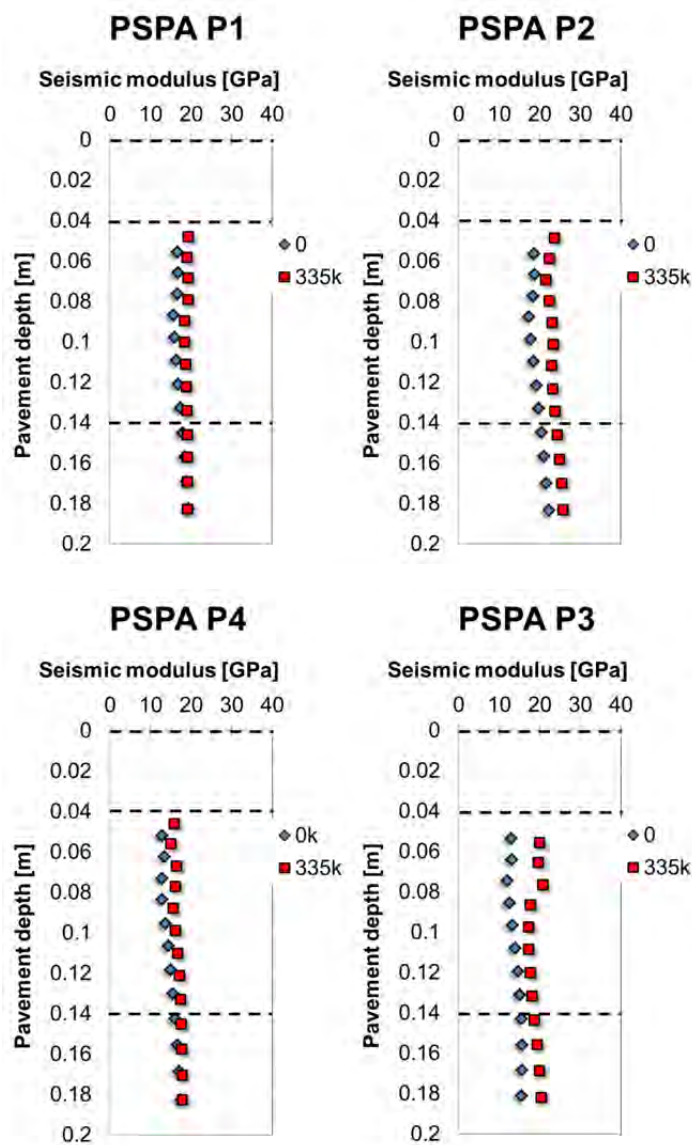
Fig. 6.20 Seismic modulus from PSPA measurements versus depth before and after trafficking at pavement positions P1,…P4

a)
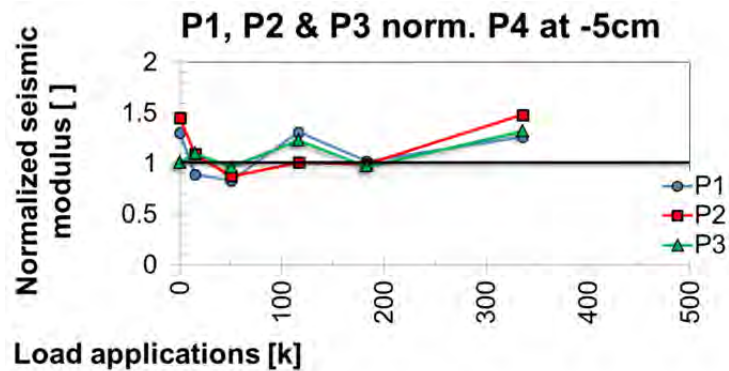
b)
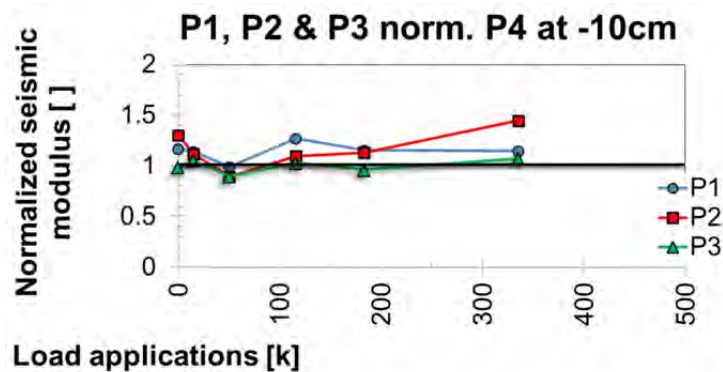
c)
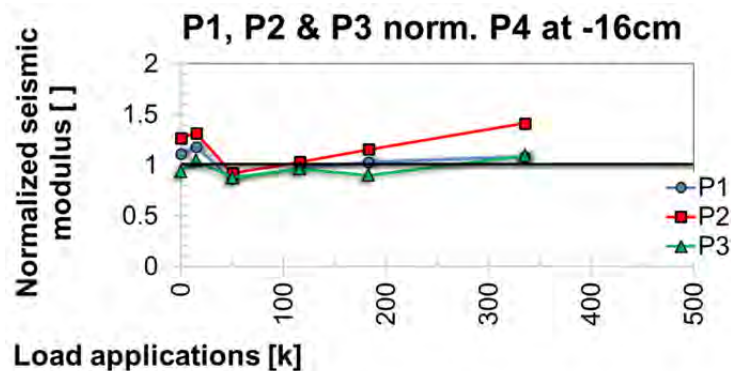
Fig. 6.21 Normalized seismic modulus from PSPA measurements at different depths vs. number of load applications

6.4.7 Laboratory tests

Several cores were taken from the trafficked and not-trafficked areas for conducting different laboratory tests. The position and labelling of the cores is shown in Fig. 6.22. Coring comprised only the bituminous layers. After a visual inspection of the cores and from their smell, it was concluded that the second layer from the top was probably a tar containing mixture. Therefore, it was decided not to carry out any further laboratory test with the cores other than the layer parallel direct shear test (LPDS) to check for interlayer bonding properties.

Fig. 6.22 Position and labelling of the cores

6.4.7.1 Interlayer bonding

Four cores taken from the trafficked area were tested with the layer parallel direct shear test (LPDS) according to the Swiss standard SN 670641 [22] and compared with results obtained from not trafficked cores. Only the interlayer between the top and binder course was tested. Other than in case of Test Site 1 (Filderen) the results show that the interlayer properties got worse after trafficking (see Fig. 6.23). This indicates that the interlayer was considerably weakened during loading eventually increasing the risk of interlayer debonding as observed on Swiss pavements under real traffic [24].
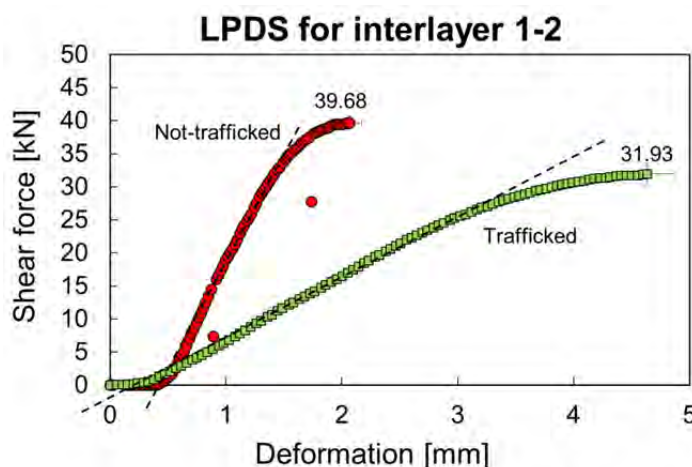
Fig. 6.23 Comparison of the LPDS interface test results between top and binder course for both not-trafficked and trafficked cores.

6.5   Summary and Conclusions

The MLS10 was transported to an old existing T4-S1 pavement on a by-pass road section of a rest area. It turned out that the second layer from the top was probably a tar containing mixture. Regular measurements of rutting profiles, static deflections with ETH Delta, etc. were carried out in order to evaluate the pavement response and detect any sign of distress.

From the analysis of the data it was found that no clear change in the pavement responses occurred during the 405'000 load applications of this test. Profiles show low rutting but

almost twice the rutting obtained at the Test Site 1 in Filderen. In any case, the pavement showed a very stiff behavior and indications of long remaining life expectancy. However, as for the LPDS interlayer shear results on cores after trafficking, a clear reduction of interlayer stiffness was observed, which points to a certain weakening of the structure. This confirms earlier findings in a test section in Hinwil [1].

7 Test Site 3: Neue Staffeleggstrasse

7.1 Experimental setup

7.1.1 Layout of the test sections

The new constructed cantonal road in Aargau was chosen as Test Site 3, prior to its opening to normal traffic (see Fig. 7.1). The road has two segments with different types of pavements. It was decided to install the MLS10 in the area where both types of pavements change, so in case one of the pavements shows strong damage signs, the machine could be easily positioned on the other pavement. However, because of the good performance of the road only the pavement of section F1 was loaded and included in this report..
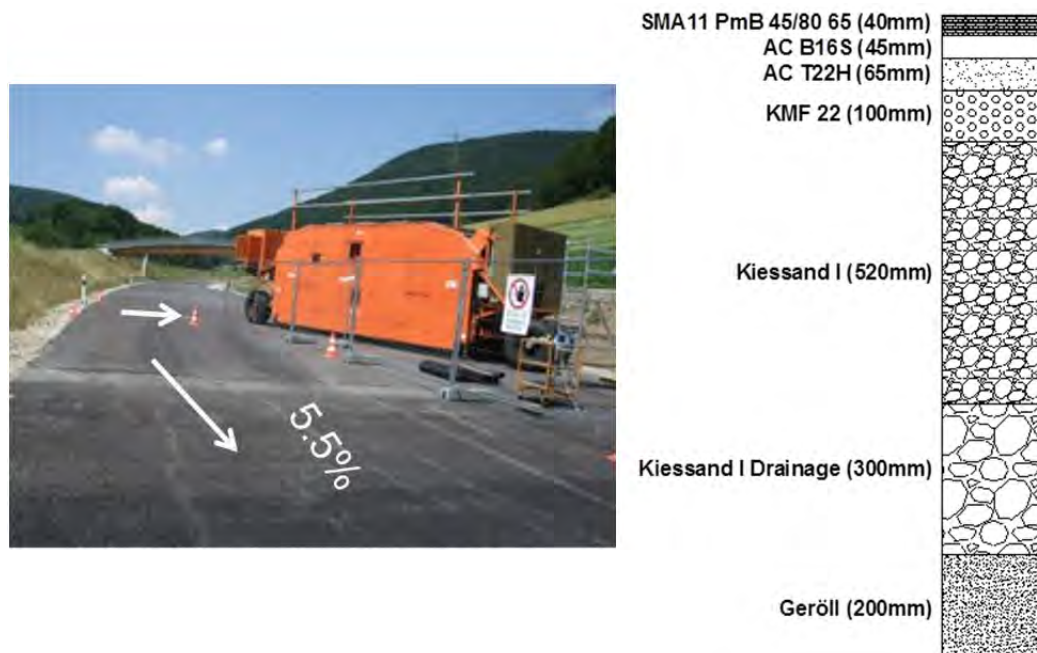
Fig. 7.1 View of testing site and thickness of the pavement.

One disadvantage of this site was that the machine had to be positioned on a section with a comparatively steep slope. Hence, the MLS10 had to be positioned in the direction of the flowing water, i.e. in an angle of about 28° to the road axis in order to allow equal wearing of the bogie rails. This special situation caused some additional unexpected complications that will be briefly explained in the next paragraphs, but allowed to obtain information about the limits of testing pavements in mountainous regions with the MLS10.

7.1.2 Load configuration

The machine was setup to apply 65kN with each of the four bogies, using a twin tire configuration. This is the maximum load that MLS10 is able to induce with this type of tire and corresponds to a total axle load of 130kN. The loads were measured using static scales. The tire pressure was set to 7.5bar. The trafficking speed used for the tests was 22km/h. For these tests, MLS10 was equipped with Good-year 455/50 R22.5 twin tires.

7.1.3 Evaluation of pavement performance

As explained in § 5.1.5, in this test section several sensors and non-destructive tests were carried out, as listed below:

Sensors embedded in the structure

- Thermocouples
- Strain gauges
- Accelerometers

Periodic measurements

- Transversal profiles
- Portable Seismic Pavement Analyser (PSPA)
- Falling Weight Deflectometer (FWD)
- ETH Delta

7.1.4 Location of the measurement devices

A schematic of the position of the sensors is depicted in Fig. 7.2. Almost the same sensor configuration as in Suhr was used.
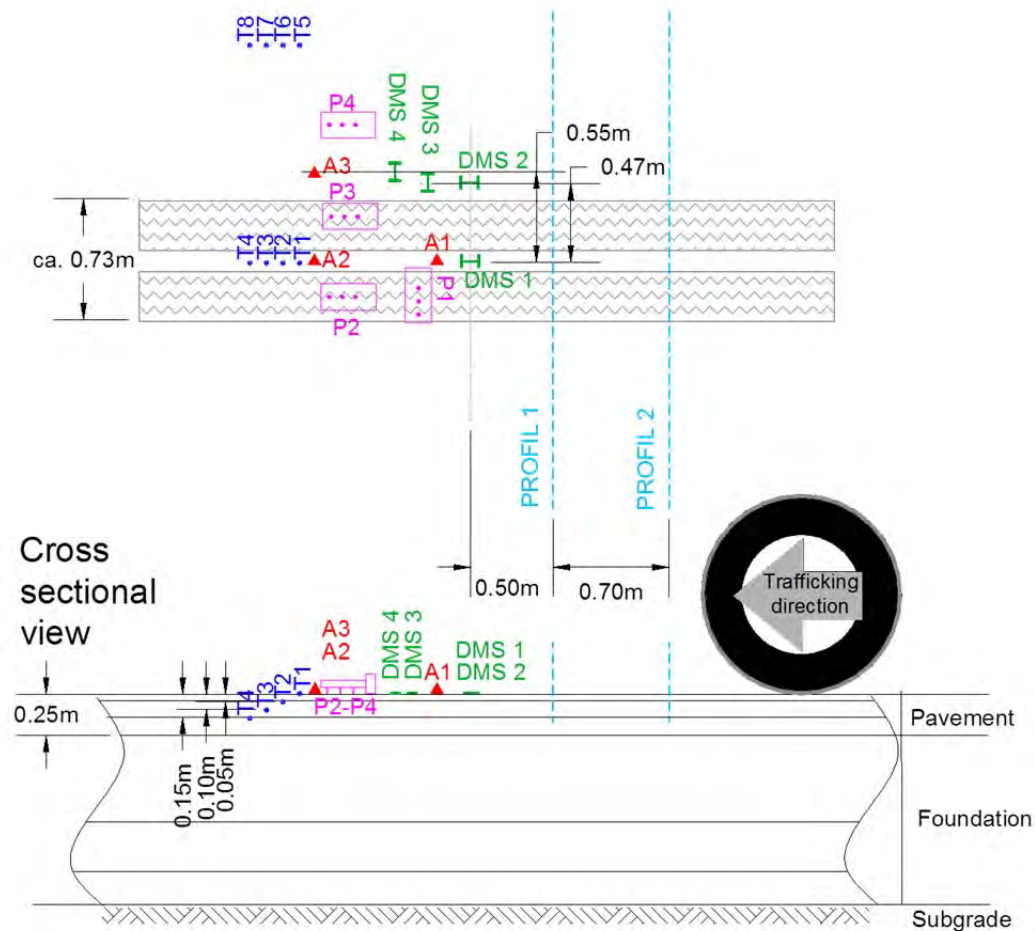
Fig. 7.2 Schema with the position of the stationary sensors and periodic measurements in the pavement showing the designation for different sensors and strain gauges, together with their position and direction:

P: PSPA
A: Accelerometer
DMS: Strain gauge
T: Thermocouple

The strain gauges were glued to the pavement surface, since it was not possible to install them inside the structure. DMS 1 was installed along the trafficking axle, between the twin tires. DMS 4 was mounted parallel to DMS 1 but 47cm to the left side from the axle. DMS 2 and DMS 3 were installed on the pavement surface perpendicular to the trafficking direction; DMS 2 was positioned 55cm and DMS 3 was situated 67cm from the axle.

Thermocouples were installed inside the pavement by drilling small holes at different depths. Thermocouples T1 to T4 were placed in the trafficking axle at the surface and at depths of 50mm, 100mm and 150mm. T5 to T8 were installed at the same depths, but 1m away from the axle.

Three accelerometers, were attached to the surface of the pavement. A1 and A2 were placed along the trafficking axle, between the twin tires and A3 was installed 55cm beside the axle.

Two transversal profiles were taken to evaluate permanent surface deformation on one side of the trafficking path.

PSPA measurements were carried out in each tire path (P1 perpendicular to the trafficking direction, P2 and P3 along the wheel path) and outside the trafficking area (P4).

FWD measurements were carried out according to the grid presented in Fig. 7.3.
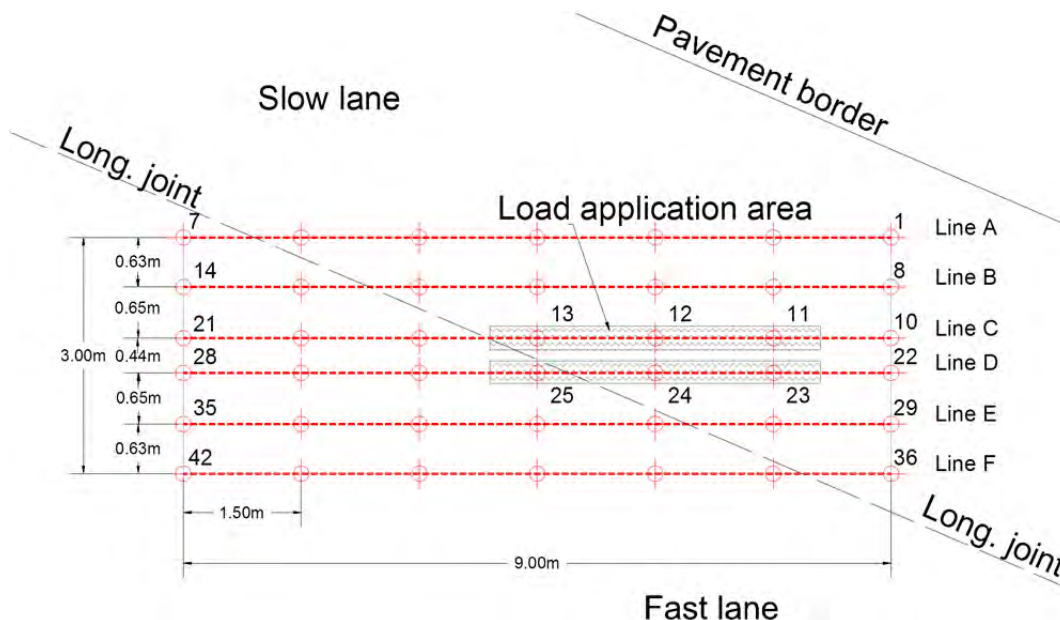
Fig. 7.3 FWD measurement grid.

7.2 Operation

7.2.1 Loading history

The MLS10 was deployed on the 2nd of July 2010 and was moved away on the 2nd of July 2010. A total of 400'000 load applications was carried out. The accumulated number of loads through the duration of the tests is presented as a line in Fig. 7.4. Horizontal segments in the line represent the days where the MLS10 was not operational due to holidays, weekends, breakdowns in the functioning of the machine or because of measurements, installation of sensors, etc. Details regarding the machine performance during this period are described in the next section.
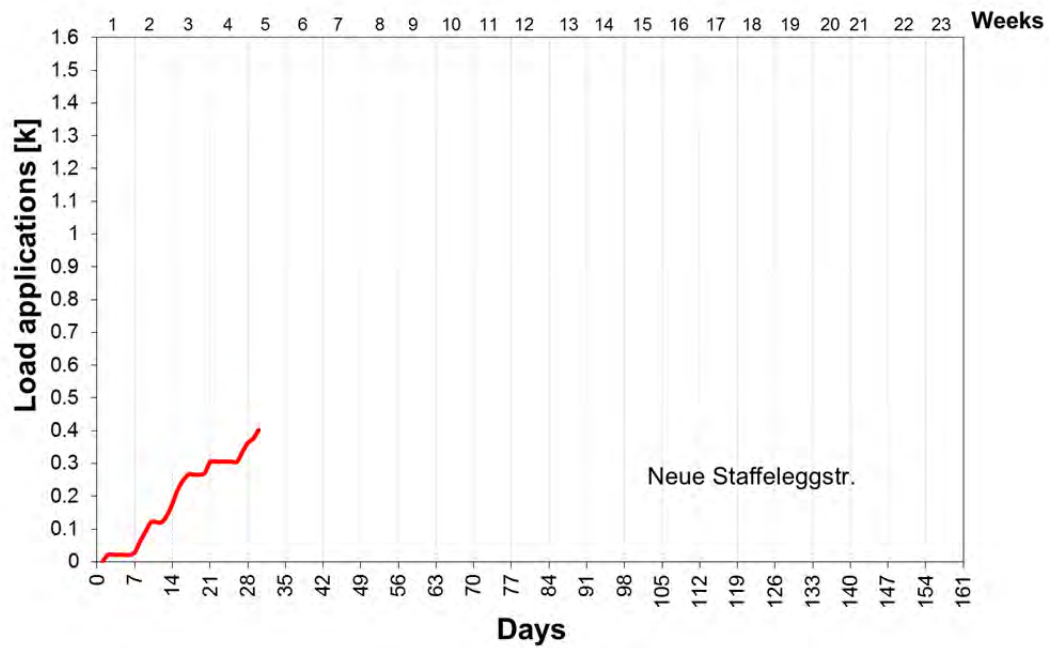
Fig. 7.4 Number of accumulated MLS10 load applications vs. time.

7.2.2 Interruptions due to machine malfunctioning

Change of brakes

The steep slope in which the MLS10 had to operate turned to be highly risky for the safety of the personnel working with the machine. Therefore, the complete breaking system of the machine was revised and replaced for a stronger one (see Fig. 7.5).

Fig. 7.5 Revision of the machine breaks.

Breaking of bolt of the reaction plates

Bolts fixing the reaction plates to the bogies though the C-Brackets continued failing in a regular basis, as described in § 6.3.2. A total of 5 screws broke during these tests.

Cracks in bogies

Small cracks appeared again in the bogies (see Fig. 7.6). However, it was decided to continue the work, making regular visual inspections to evaluate the progress of the cracks and prepare a reinforcement to be carried out after these tests.

Fig. 7.6 Crack in a bolt fixation area

7.3   Measurements results

7.3.1   Temperature

Fig. 7.7 presents the temperature profiles measured by sensors T1 to T8.

a)

b)
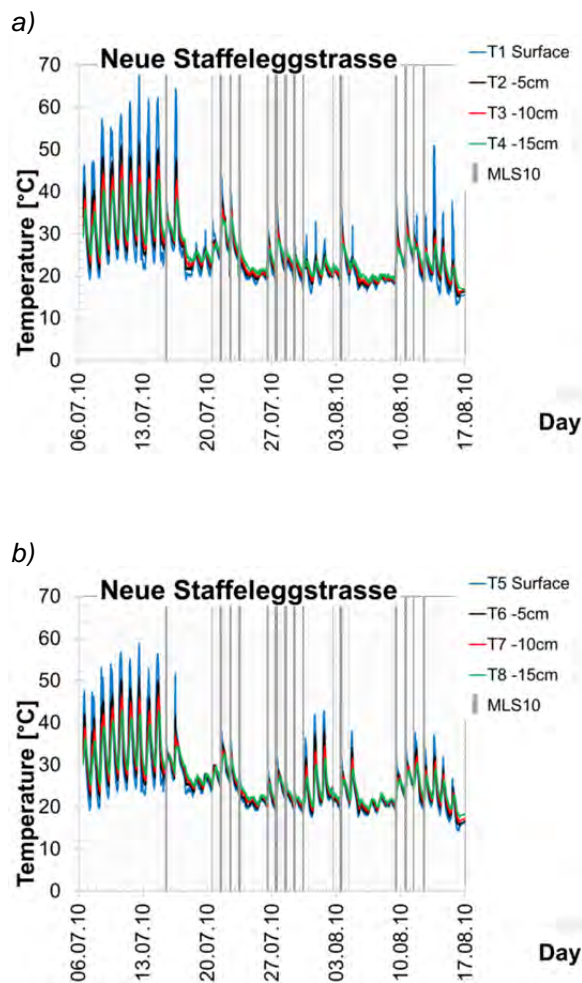
Fig. 7.7 Temperature profile measured during the testing period T1-T4 in the wheel path below the wheels; T5…T8 distance of 1m away from the wheel paths.

Fig. 7.8 summarizes the average temperatures over the testing period and the average temperature only while the machine was running. This table shows that the average temperatures near to the rolling tires are higher that the temperatures outside the wheel path.

Fig. 7.8 Average temperatures

Thermocouple		Average temp. over hole testing period [°C]	Average temperature during trafficking [°C]
T1	26.3		27.9
T2	26.0		25.4
T3	26.0		24.6
T4	26.0		24.4
T5	26.7		25.9
T6	26.7		24.8
T7	26.8		24.3
T8	26.7		24.1

7.3.2 Transversal pavement profiles

Data Evaluation

Data evaluation was done according to § 5.3.2.

Summary of the Results

Fig. 7.9 shows the progressive deformation of the pavement in each section, obtained with the MLS profiler. The same figure shows the average deformation under and beside the wheels at the end of the tests, relative to the initial measurements.

a)

b)
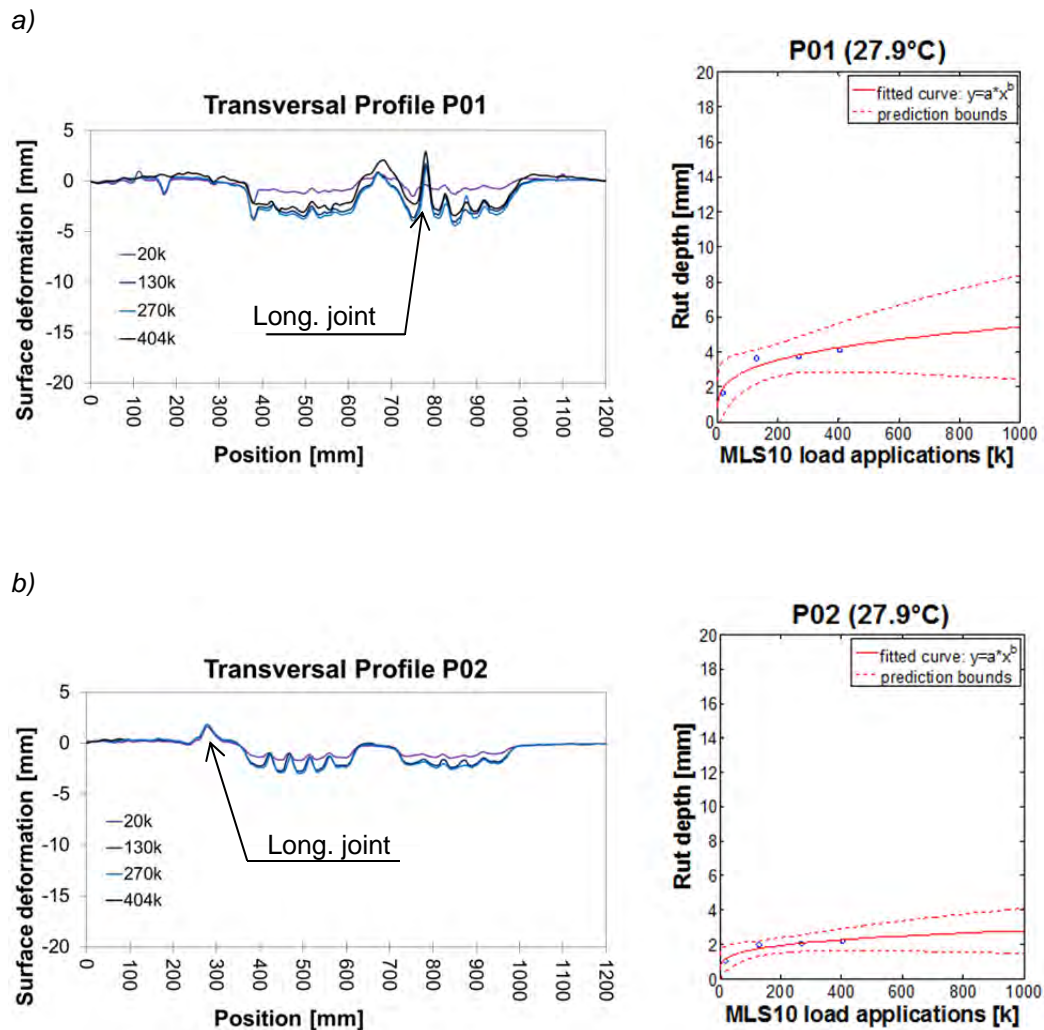
Fig. 7.9 Measured permanent vertical deformation and progressive rut depth vs. number of MLS10 load applications fitted with a power function, including 95% prediction bounds. For positions P01 and P02.

The coefficients for the power functions used to fit the measured data, with the 95% confidence bounds, as well as the coefficient of determination R^2 are presented in Fig. 7.10:

Fig. 7.10 Power function fit parameters

Profile	a (with 95% confidence bounds)	B (with 95% confidence bounds)	R^2
P01	0.14 (-0.40, 0.68)	0.27 (-0.05, 0.68)	0.91
P02	0.12 (-0.27, 0.52)	0.23 (-0.03, 0.48)	0.91

By the end of the tests after ca. 400'000 MLS10 load applications, the rutting was of about 2mm to 4mm, depending on the profile position. From the shapes of the transversal profiles it can be deducted that rutting was produced by a compaction of the material below the tires. In the same figure it is possible to observe the longitudinal joint of the pavement. The material of the joint, flowed between the threads of the tire forming bumps

on the surface of the pavement. In both cases the coefficient of determination R^2 shows that the approximations with power functions are quite accurate.

7.3.3   Strain gauges

Data acquisition and evaluation

Data evaluation was done according to § 5.3.3.

Summary of the Results

Fig. 7.11 shows one of the measurements registered with all strain gauges. As expected, DMS 1 and DMS 4 curves display tension-compression-tension shapes. When the tire arrives to the position of the sensors, the pavement will tension and when the tire is at the same position of the sensor, a compression situation occurs that will reverse when the rolling tire passes by. As anticipated, the values of DMS 1 are higher than DMS 4 values, because DMS 1 is closer to the tire. DMS 2 and DMS 3 show pure tension, following the shape of the deflection bowl. DMS 2 values are slightly above those of DMS 3 values, since DMS 2 is installed closer to the tire.
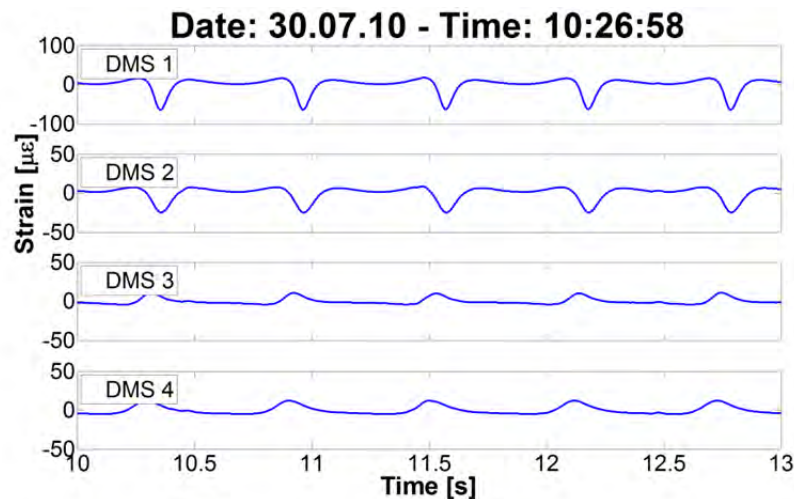
Fig. 7.11 Strain gauge measurement

As presented in Fig. 7.12, sensor DMS 1, installed on the surface between the trafficking twin tires, registered strains of 95$\mu\varepsilon$ at the beginning of the tests and 93$\mu\varepsilon$ at the end. This means that the strains remained almost equal during trafficking. As explained before, DMS 4 registered lower values, of around 38$\mu\varepsilon$, which remained stable until the end of trafficking. DMS 2 and DMS 3 measured almost the same values, 22$\mu\varepsilon$ and 21$\mu\varepsilon$, at the beginning of the tests. DMS 2 strains remained almost the same throughout the tests whereas DMS 3 strains show a light decreasing tendency to 18$\mu\varepsilon$. The trends shown in these calculations reveal that the strains did practically not change during trafficking (Fig. 7.13). This can be interpreted as a sign that the pavement did not change its mechanical properties due to cracking or other distress types.

Fig. 7.14 presents a summary of the results obtained with the strain gauges.

a)

b)

c)

d)
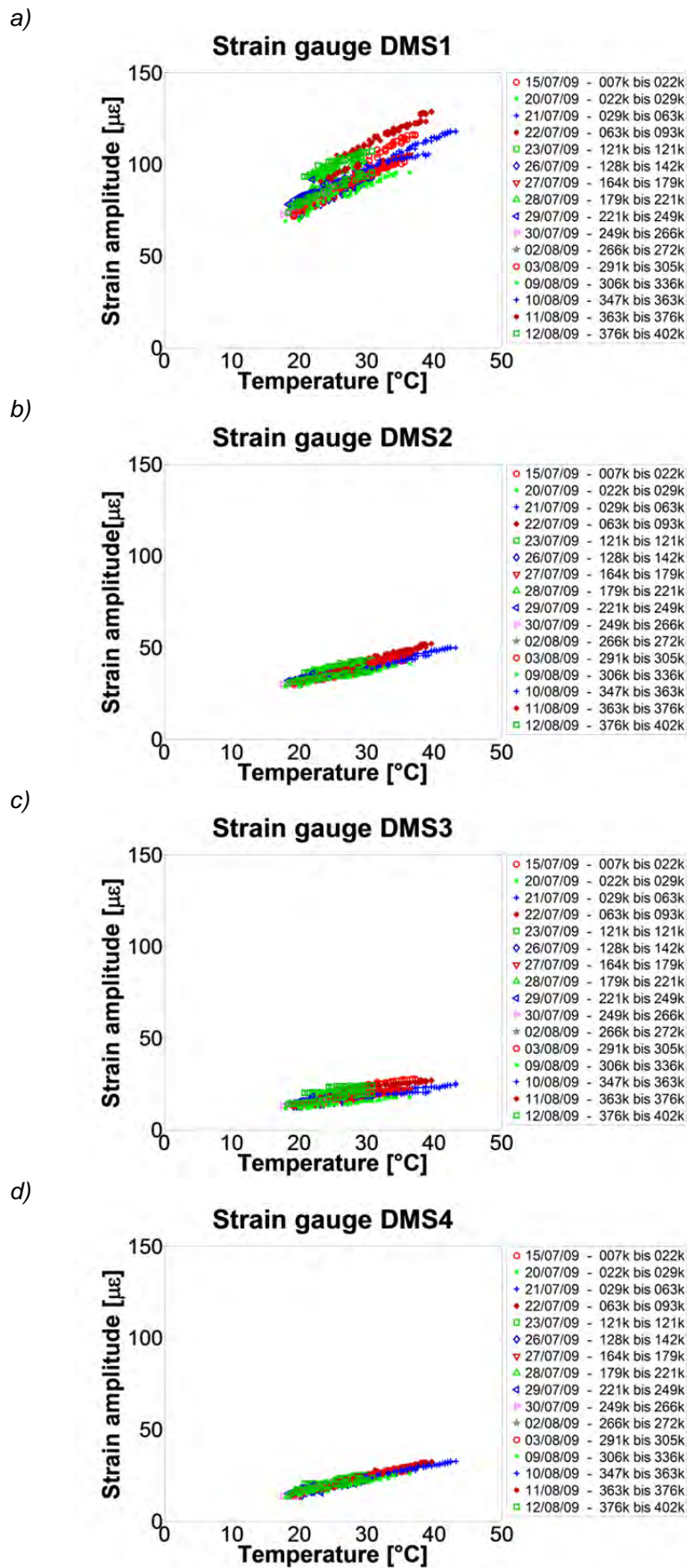
Fig. 7.12 Evolution of strain amplitudes during the course of the tests.

a)
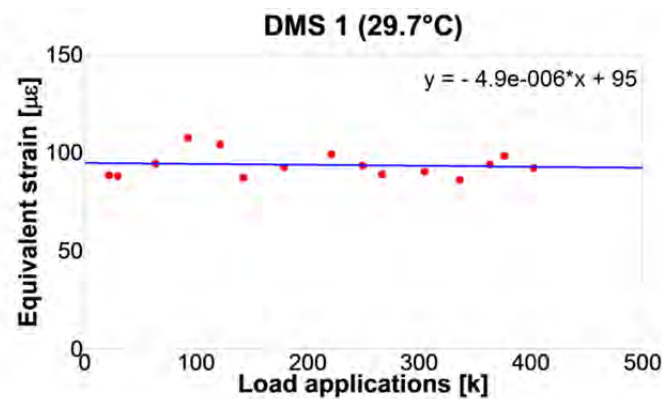
b)
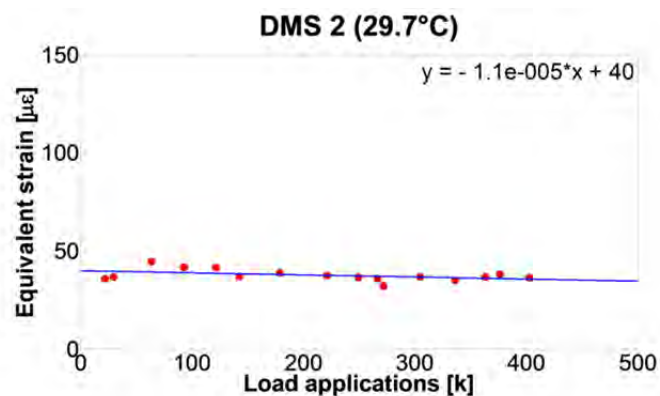
c)
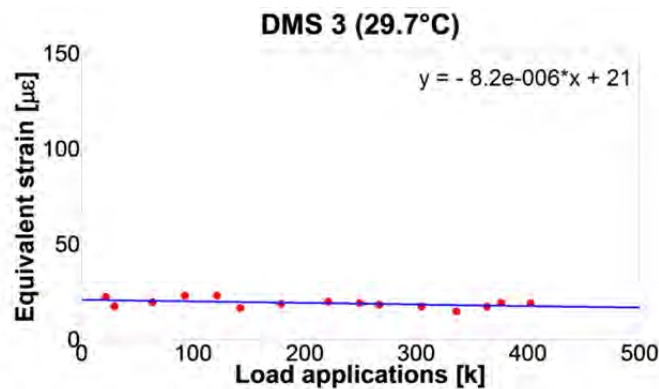
d)
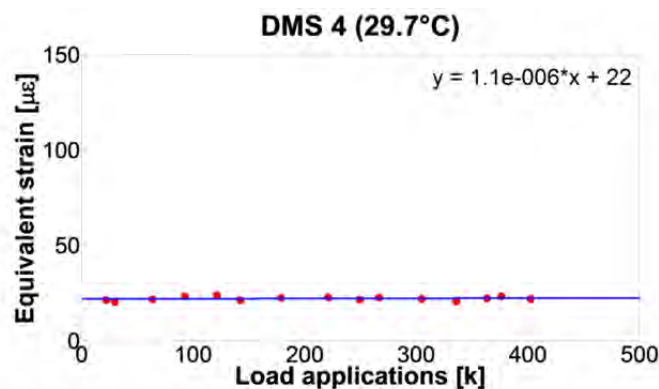
Fig. 7.13 Equivalent strains vs. the number of MLS10 load cycles.

Fig. 7.14 Summary of the equivalent strains

Strain gauge	Distance to tire [cm]	Temp. [°C]	Initial equivalent strain [$\mu\varepsilon$]	1Mio. equivalent strain [$\mu\varepsilon$]
DMS 1	0	27.9	95	93
DMS 2	47	27.9	40	38
DMS 3	55	27.9	21	18
DMS 4	67	27.9	22	23

7.3.4   Accelerometers

Data acquisition and evaluation

Data evaluation was done according to § 4.3.4.

Summary of the Results

Fig. 7.16 shows the results obtained with the accelerometer A1 and A3. Accelerometer A2 was damaged during the tests.

a)
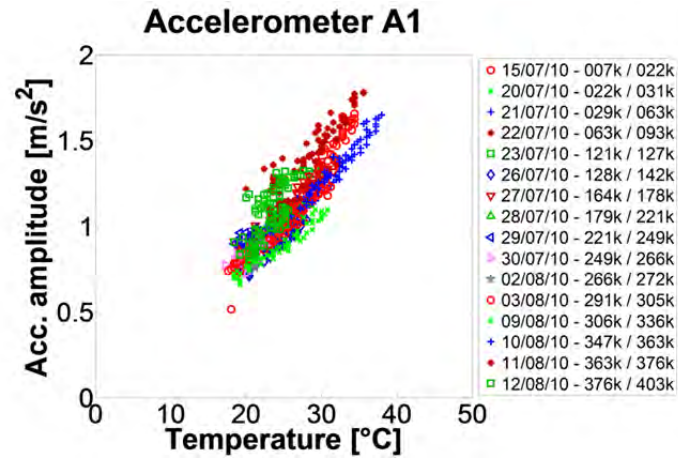
b)
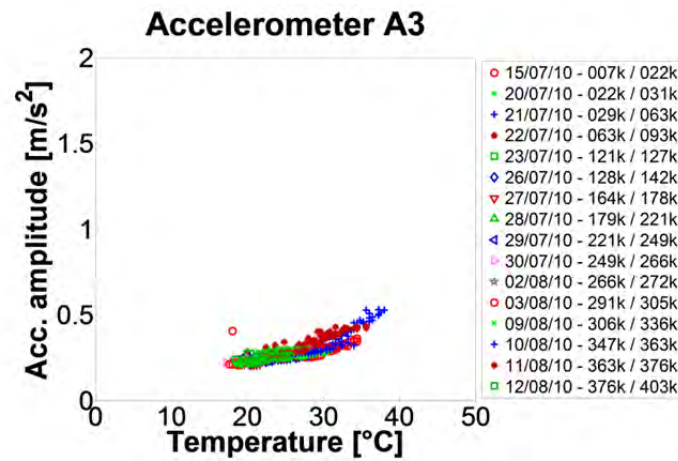
Fig. 7.15 Evolution of acceleration amplitudes during the course of the tests

a)

Accelerometer A1 (29.7°C)

$y = -2.4\text{e-}007*x + 1.2$

b)

Accelerometer A3 (29.7°C)

$y = -6.3\text{e-}008*x + 0.29$
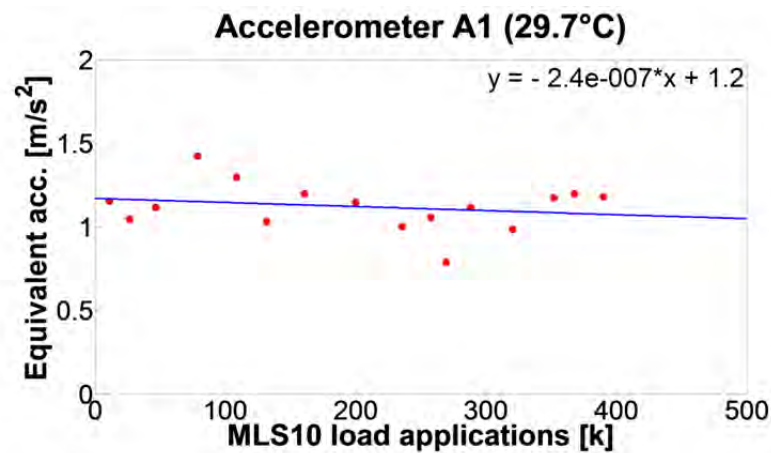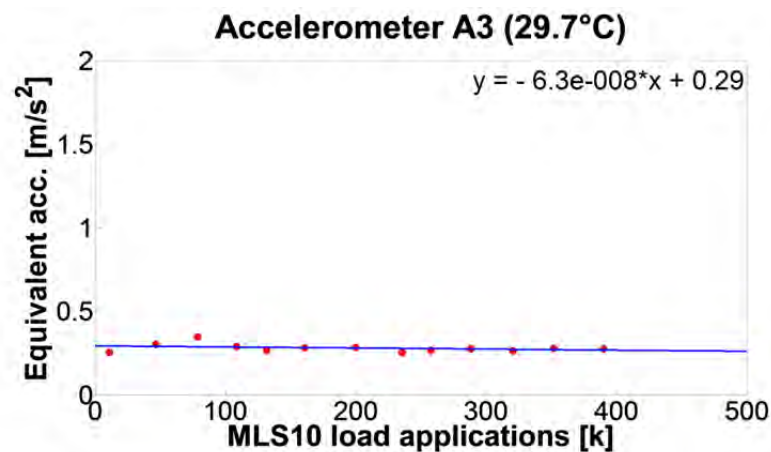
Fig. 7.16 Equivalent accelerations vs. the number of MLS10 load cycles

The scattering in the results for accelerometer A1 might be a sign that the accelerometer was not firmly attached to the pavement. The equivalent accelerations at the beginning and after 1 million load applications are presented in Fig. 7.17.

Although the acceleration, in this case, tends to decrease with the accumulated number of loads, there is no apparent inflection point in the linear development of the calculated equivalent accelerations, which would indicate a sudden change in the pavement stiffness.

Fig. 7.17 Summary of the equivalent acceleration

Accelerometer	Initial equivalent acc. [m/s^2]	1Mio. load applications equivalent acc. [m/s^2]
A1	1.20	0.96
A2	0.29	0.23

7.3.5 ETH Delta

Data acquisition and evaluation

The data obtained with the ETH Delta was used to prepare 2D deflection maps. Fig. 7.18 shows th the measured deflections at the beginning and at the end of the tests at two locations.

However, due to a combination of factors like different climatic conditions during measurements and the generally very stiff pavement, the deflections obtained were extremely small. Therefore, unfortunately the validity of the data is not guaranteed. Nevertheless the results support the observation from other measurements that pavement stiffness remained invariable after the 404'000 load applications also on this test site.

a)
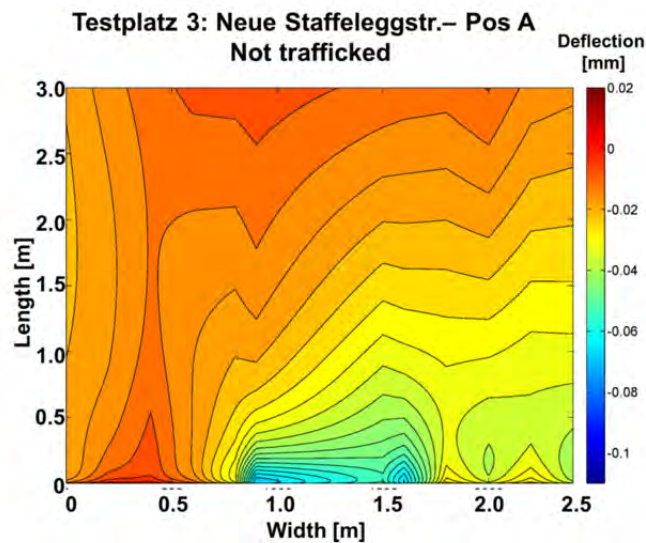
b)
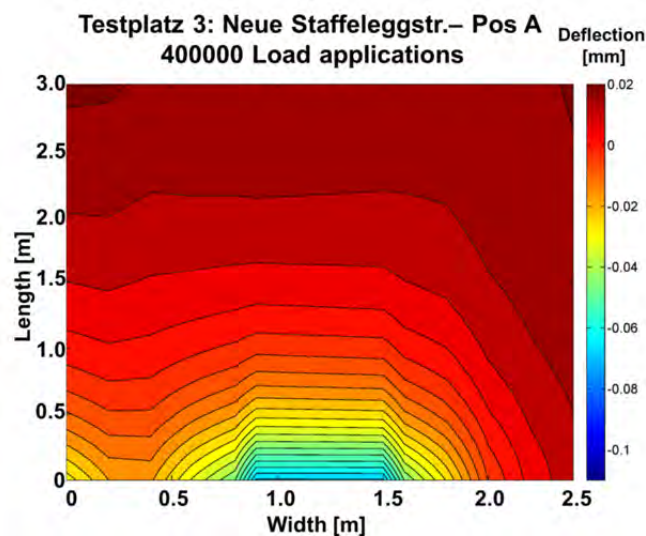
Fig. 7.18 2D deflection maps obtained with ETH Delta device after different numbers of load applications

7.3.6   Falling weight deflectometer (FWD)

Data acquisition and evaluation

Measurements were done only at the end of the tests. Data evaluation was performed following the procedure outlined in § 5.3.5.

Summary of the Results

The deflection map for the measurement carried out at the end of the test is presented in Fig. 7.19. The results show that there is a weak area in one of the corners of the investigated area, corresponding to the border of the road. This is reasonable, because road pavement edges are usually lacking of lateral confinment. However, the trafficked area does not seem weaker or different than the rest of the pavement.
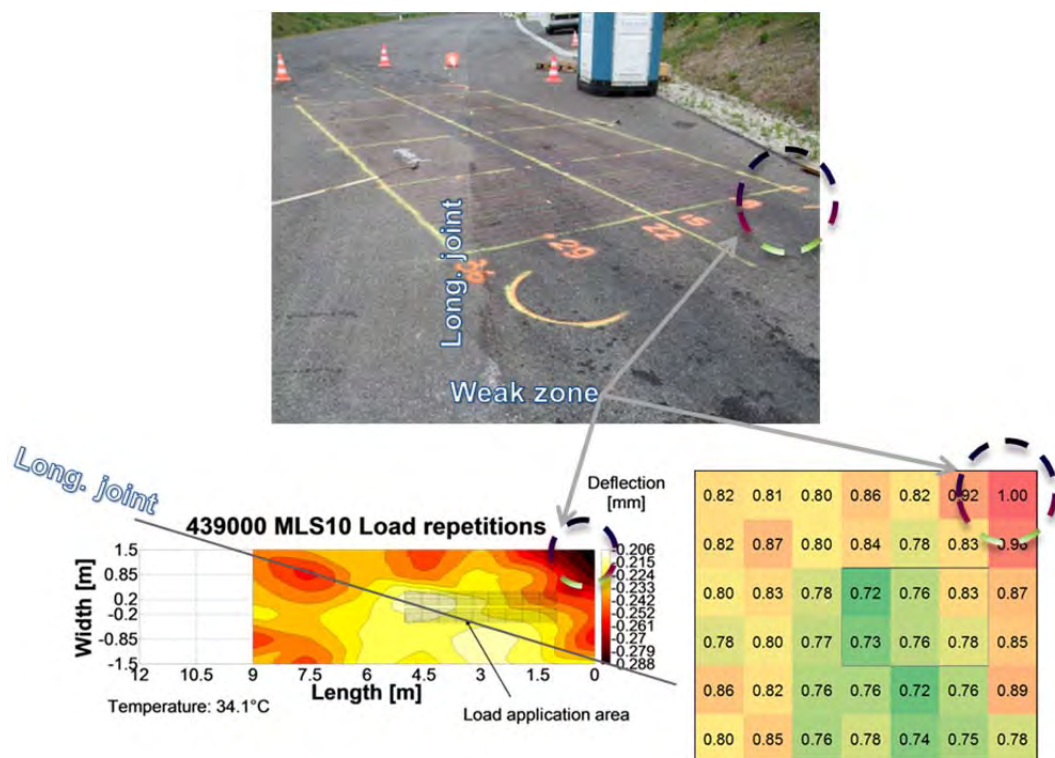
Fig. 7.19 FWD measurement setup (top), deflection maps (below left) and normalized matrix (below right) at the end of the tests. The dotted line shows the weaker area of the pavement

7.3.7   Ground Penetrating Radar (GPR)

Equipment

The equipment used for the measurements was a GSSI SIR-20 control unit, with a 1.5GHz antenna and a 2.6GHz antenna

Section layout

Fig. 7.20 shows the measurement setup. The blue zone in the left picture indicates the loaded area. The picture on the right shows the full surface view after MLS10 traffickin.

Measurements were carried out using a special setup to move the antenna over the pavement surface, covering an area of 6m x 3m. To that end, 60 measurements were done following lines of 3m length. The lines were spaced every 0.1m. All measurements were then combined to prepare 2D and 3D images of the pavement structure.

a)

.

b)
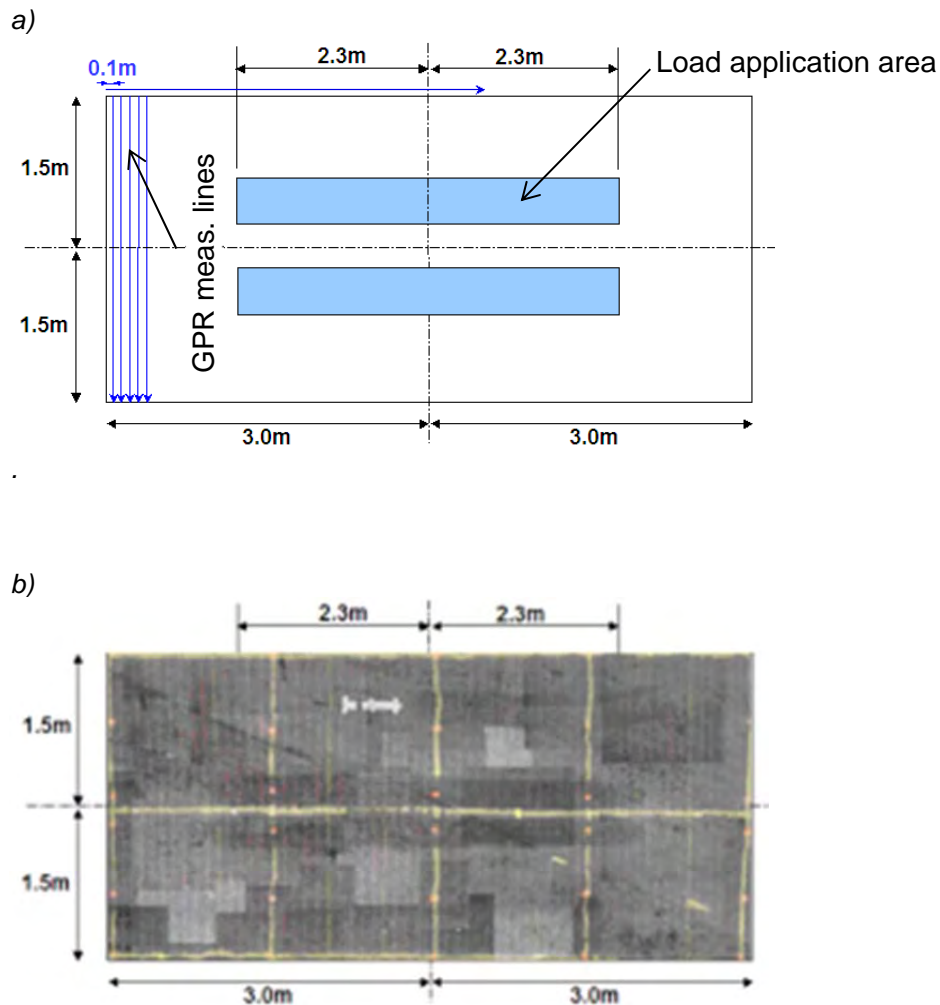
Fig. 7.20 a) setup of GPR measurement and b) view of the pavement surface after MLS10 testing

Data evaluation

Original GPR data is collected in form of a vector, showing wave data in a line. The data has to be converted to 2D format and displayed as figures. This is done by dedicated software to compare measurements with 1.5GHz and 2.6GHz antennas before and after 404'000 load applications with MLS10.

Summary of the Results

Comparison 2D data of GPR

Line 1 (Fig. 7.21) is situated outside the trafficking zone. Fig. 7.22 shows 2D data of Line 1 before and after MLS10 testing with the 1.5GHz antenna. As expected, no difference between measurements before and after testing was found. Fig. 7.23 shows the same Line 1 inspected with the 2.6GHz antenna. Again, no difference between measurements before and after MLS10 testing was observed.

Line 31 (Fig. 7.24) lies in the middle of the trafficking zone. Fig. 7.25 presents 2D data of Line 31 using the 1.5GHz antenna before and after MLS10 testing. Here, it appears possible to detect some rutting of the pavement due to MLS10 testing. The same Line 31 measured with the 2.6GHz antenna is shown in Fig. 7.26. This result shows clearly signs of rutting of the pavement, mostly located near the surface. No other sign of distress can be detected from these images.

Line 61 (Fig. 7.27) is located outside the trafficking zone. Fig. 7.28 shows 2D data of Line 1 before and after MLS10 testing with the 1.5GHz antenna. Again, as expected, no difference between measurements before and after testing was found. Similar follows from Fig. 7.29, where corresponding results from measurements with the 2.6GHz antenna are depicted.

These results also show that the 2.6GHz antenna has an advantage over the 1.5GHz antenna for detecting changes near surface since it provides more detailed information.

Line 1
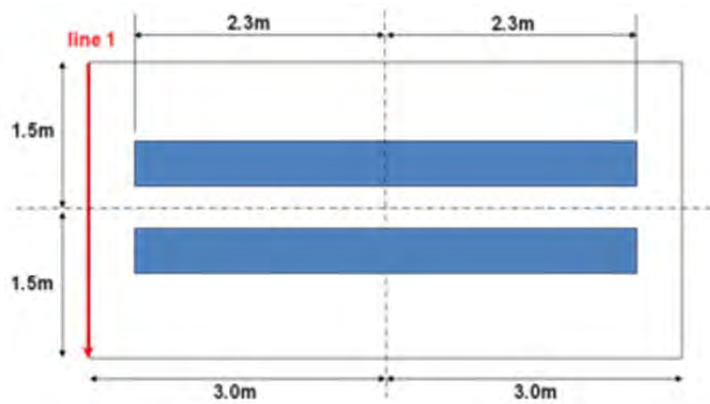
Fig. 7.21 Position of the measurement Line 1
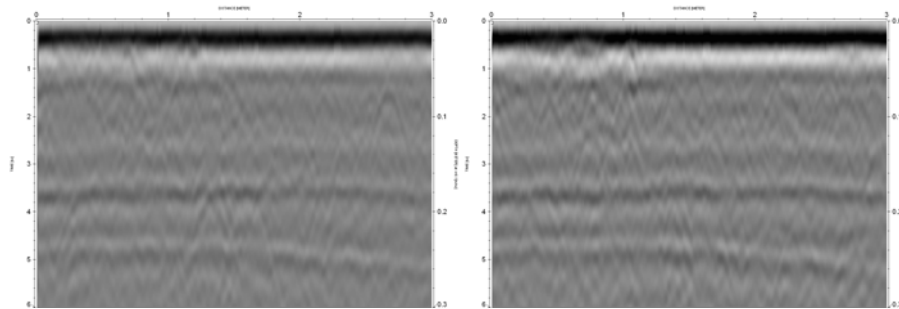
Fig. 7.22 1.5GHz antenna before (left) and after (right) trafficking
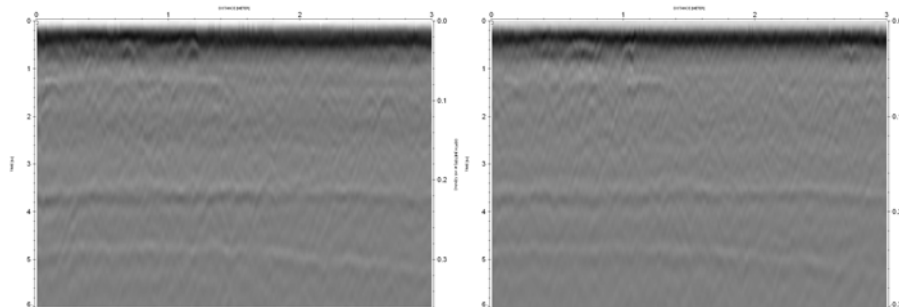
Fig. 7.23 2.6GHz antenna before (left) and after (right) trafficking

Line31
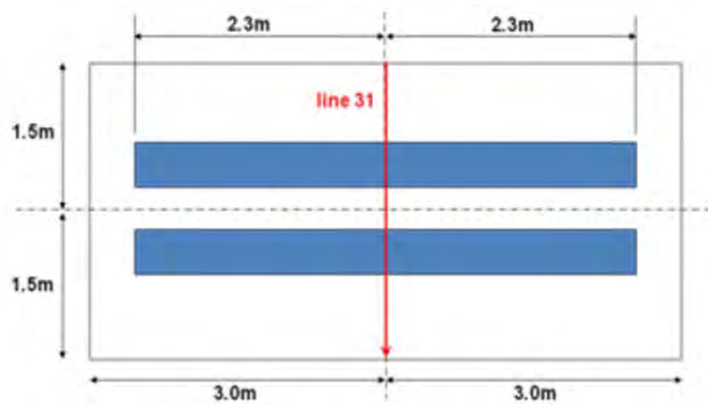
Fig. 7.24 Position of the measurement Line 31
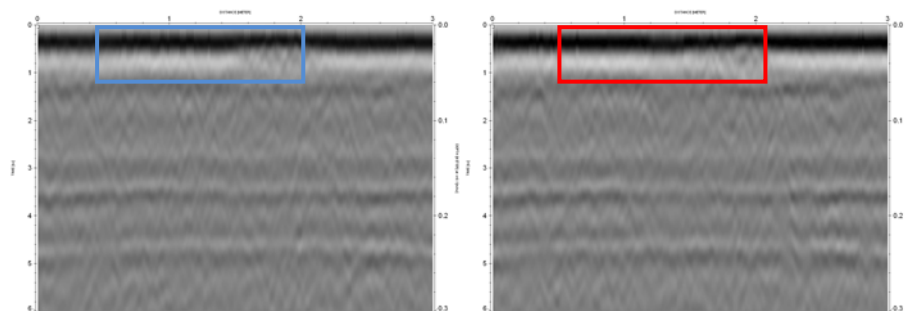
Fig. 7.25 1.5GHz antenna before (left) and after (right) trafficking marking the region with some indication of possible rutting near the surface
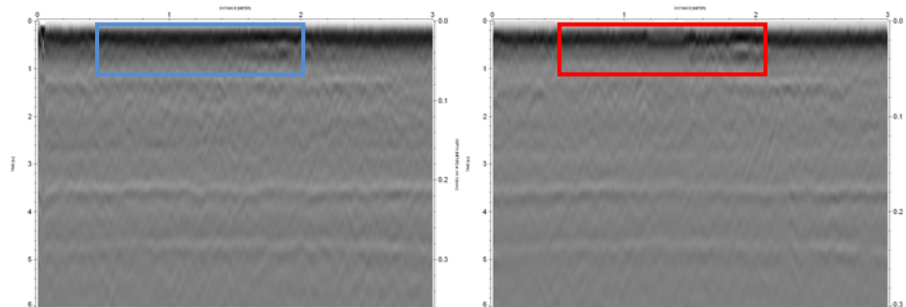
Fig. 7.26 2.6GHz antenna before (left) and after (right) trafficking marking the region where some rutting near the surface appears visible

Line61
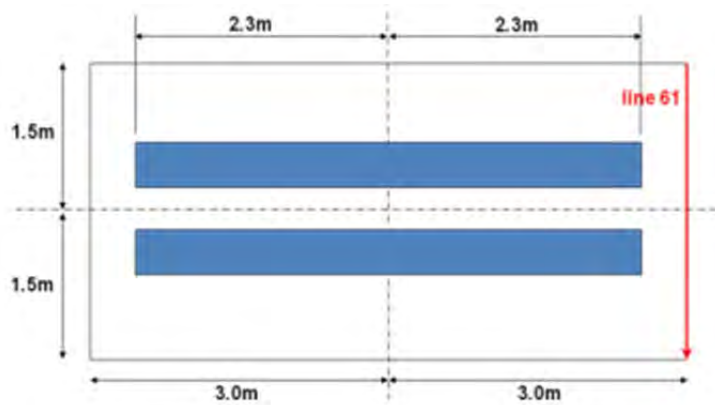
Fig. 7.27 Position of the measurement Line 61
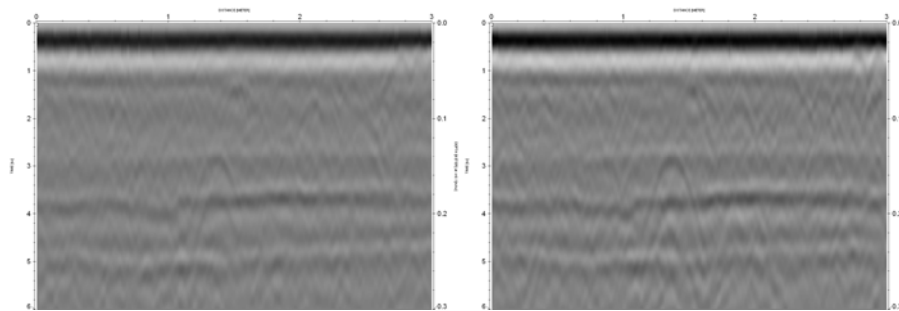
Fig. 7.28 1.5GHz antenna before (left) and after (right) trafficking
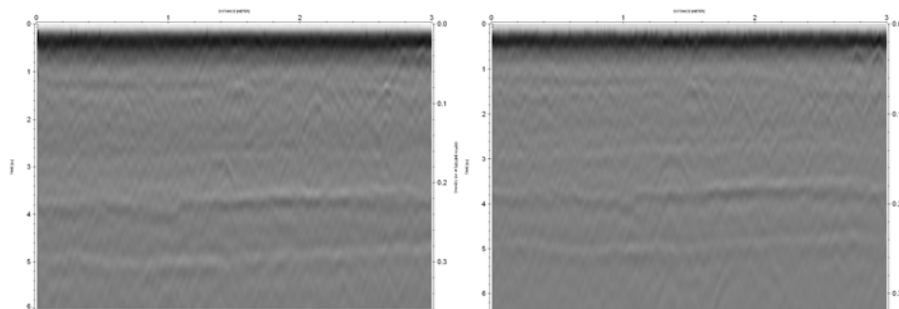
Fig. 7.29 2.6GHz antenna before (left) and after (right) trafficking

Comparing 3D data of GPR

After analyzing the 2D data, data was converted to 3D images with a special software. In order to perform a systematic analysis, slices of the complete scanned area at different depths, were plotted and compared. Then, changes within of the pavement were detected using a simple procedure.

Fig. 7.30 to Fig. 7.43 present 3D analyzed data showing GPR area data in slices at different depths. These figures show clear tire traces from both1.5GHz and 2.6GHz measurements down to 3cm depth from the surface. One diagonal line on all figures (top left to bottom right) shows a pavement joint. The reason for showing the pavement joint parallel to the trafficking direction is due to the fact that the MLS10 had to be positioned in the direction of the flowing water, i.e. in an angle of about 28° to the road axis. The white short line on the top center in the pictures after trafficking is a strain gauge.

These figures show almost no difference between 1.5GHz antenna and 2.6Ghz results. However, 3D data of 2.6GHz antenna near the surface appear to transform into slightly clearer pictures than those of 1.5GHz antenna data.

3D data from the 2.6GHz antenna in about 1,5cm depth from the surface (Fig. 7.33) shows other wheel traces marked by red boxes. These traces may have been caused by the MLS10 driving wheels since the MLS10 had to be moved away to allow GPR measurements. Furthermore, these traces may have been influenced also by moisture because measurements were done just after rain and the surface was still a little wet.

Slice 1, depth 0 (Pavement surface)
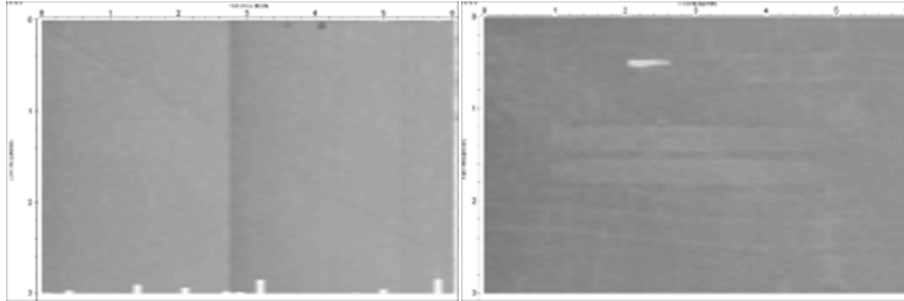
Fig. 7.30 1.5GHz antenna before (left) and after (right) trafficking.
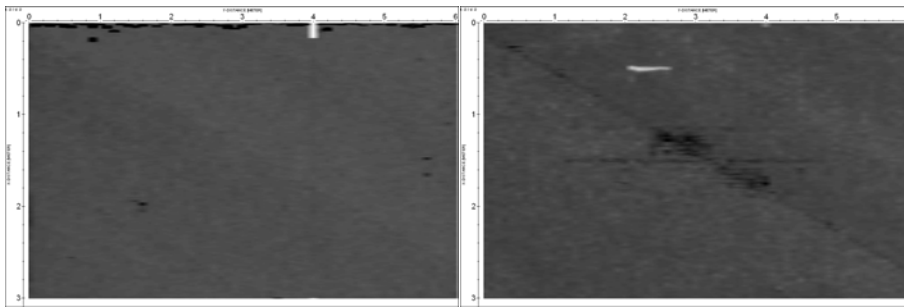
Fig. 7.31 2.6GHz antenna before (left) and after (right) trafficking.

Slice 2, depth -1.5cm
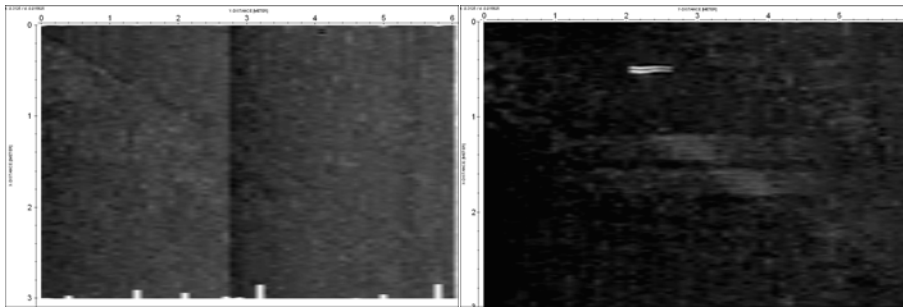
Fig. 7.32 1.5GHz antenna before (left) and after (right) trafficking.
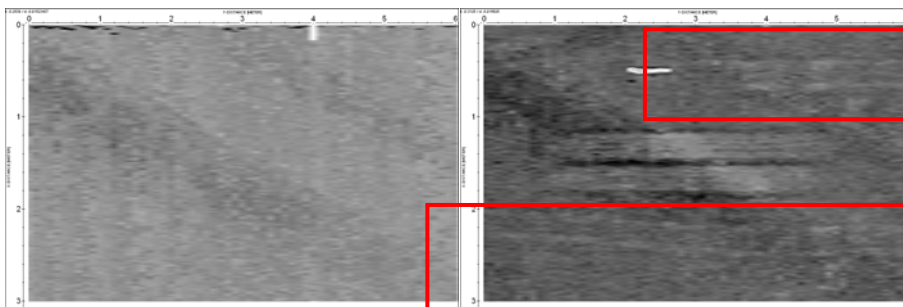
Fig. 7.33 2.6GHz antenna before (left) and after (right) trafficking; square markers show traces from MLS10 driving wheels when moving the machine away from the GPR measurement area.

Slice 3, depth -2cm
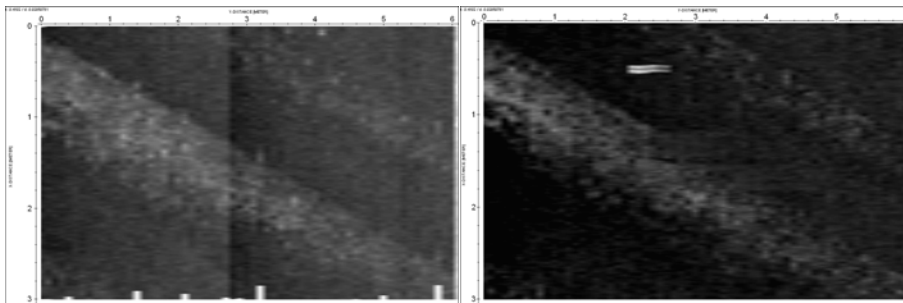
Fig. 7.34 1.5GHz antenna before (left) and after (right) trafficking.
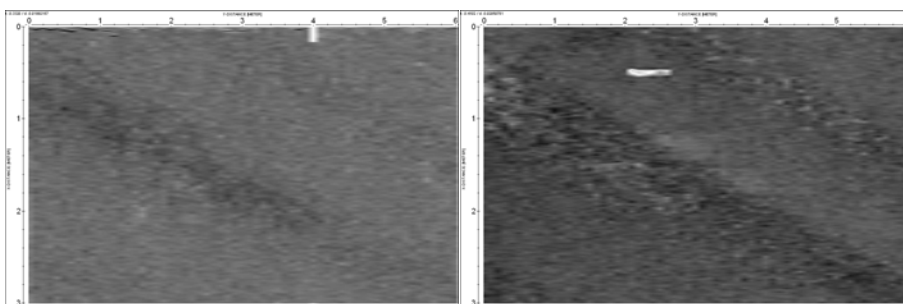
Fig. 7.35 2.6GHz antenna before (left) and after (right) trafficking.

Slice 4, depth -3cm
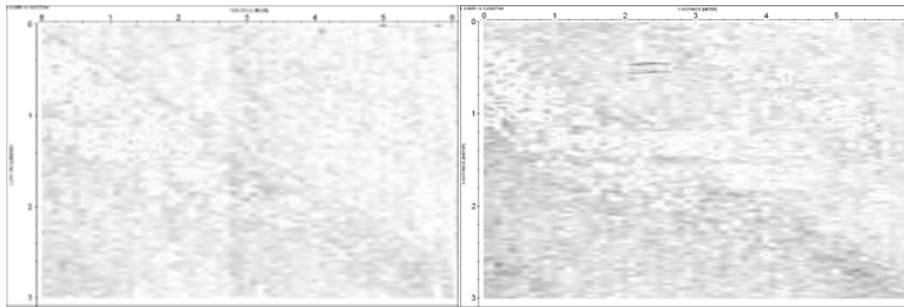
Fig. 7.36 1.5GHz antenna before (left) and after (right) trafficking.
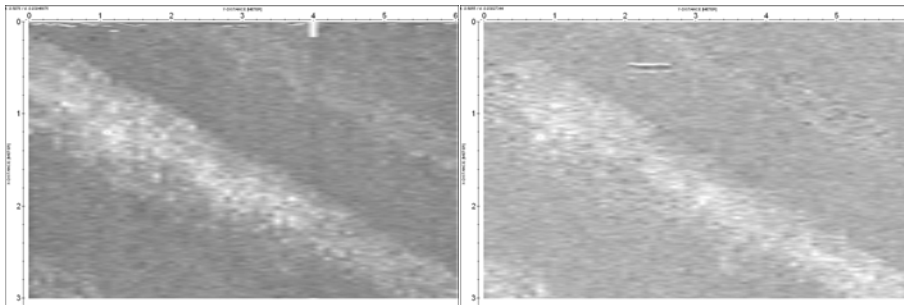
Fig. 7.37 2.6GHz antenna before (left) and after (right) trafficking.

Slice 5, depth -5cm
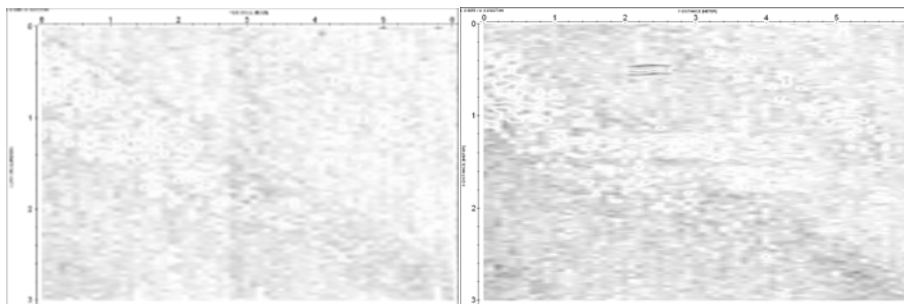
Fig. 7.38 1.5GHz antenna before (left) and after (right) trafficking.
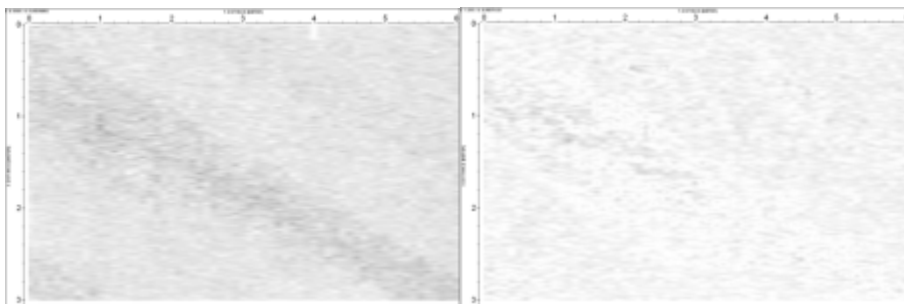
Fig. 7.39 2.6GHz antenna before (left) and after (right) trafficking.

Slice 6, depth -10cm
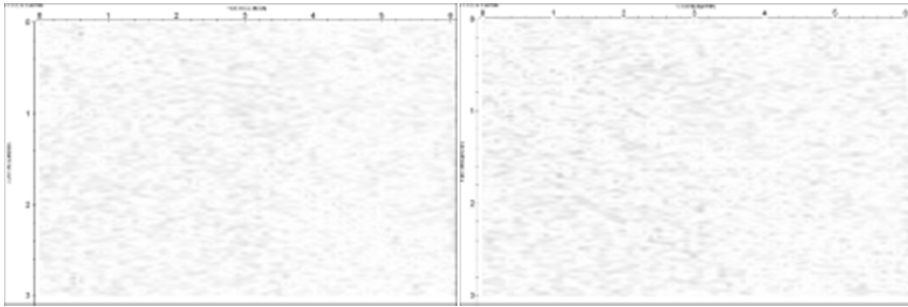
Fig. 7.40 1.5GHz antenna before (left) and after (right) trafficking.
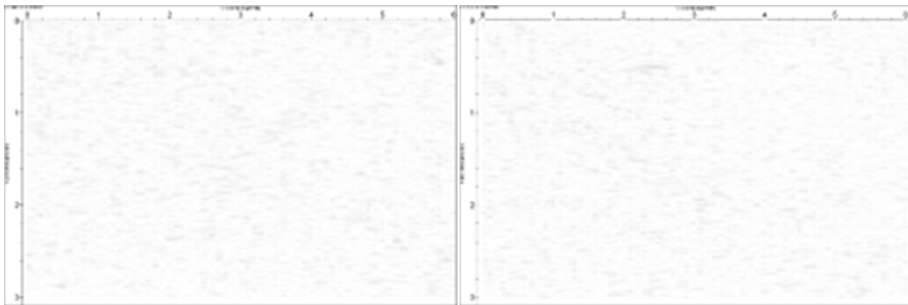
Fig. 7.41 2.6GHz antenna before (left) and after (right) trafficking.

Slice 7, depth -20cm
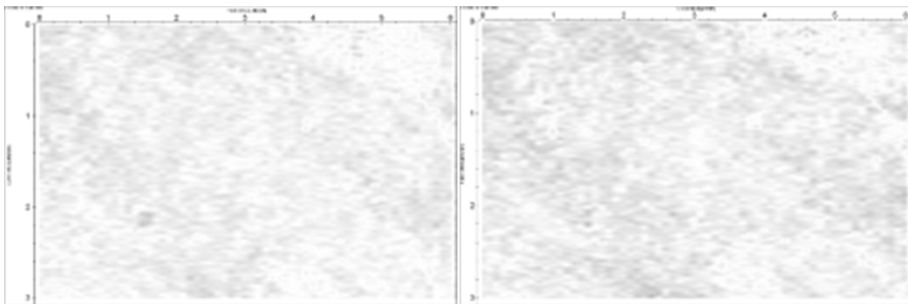
Fig. 7.42 1.5GHz antenna before (left) and after (right) trafficking.
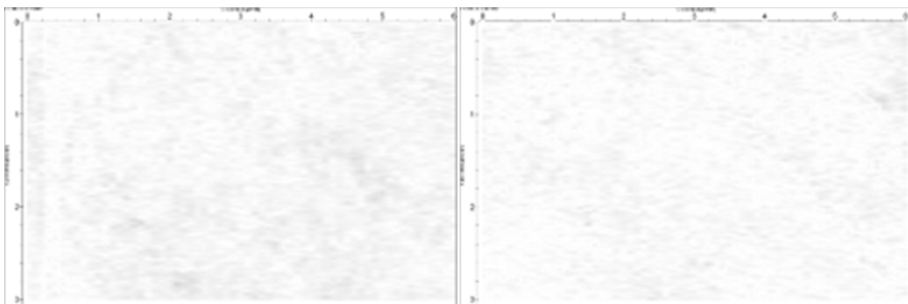
Fig. 7.43 2.6GHz antenna before (left) and after (right) trafficking.

Conclusions

According to this experiment, 2D data and 3D data show various aspects of asphalt pavement conditions. GPR data show clear difference between before and after MLS10 testing. The 2.6GHz antenna is better suited to determine the internal situation near sur-

face than of the 1.5GHz antenna. This is because the electromagnetic wavelength of the 2.6GHz antenna is shorter than the 1.5GHz antenna and therefore the resolution below the surface becomes clearer.

7.3.8 Portable Seismic Pavement Analyser (PSPA)

Data acquisition and analysis

Data evaluation was done according to § 4.3.7.

Summary of the Results

The seismic moduli vs. depth before and after trafficking with 404'000 load applications are displayed in Fig. 7.44. The normalized seismic modulus at the reference position P4 is presented in Fig. 7.45. The observation of the general modulus evolution in the analyzed depths indicates that the stiffness of the asphalt layers range between 10 and 15GPa. Hence, stiffness appears lower than for Test Section 2. There is no clear change in the stiffness between the layers. The values normalized in Fig. 7.45 with respect to the modulus at position P4 show that there is no clear change in the stiffness trend throughout the tests. For the other depths (-10cm and -16cm) the stiffness is even more homogenous with no significant change after trafficking.
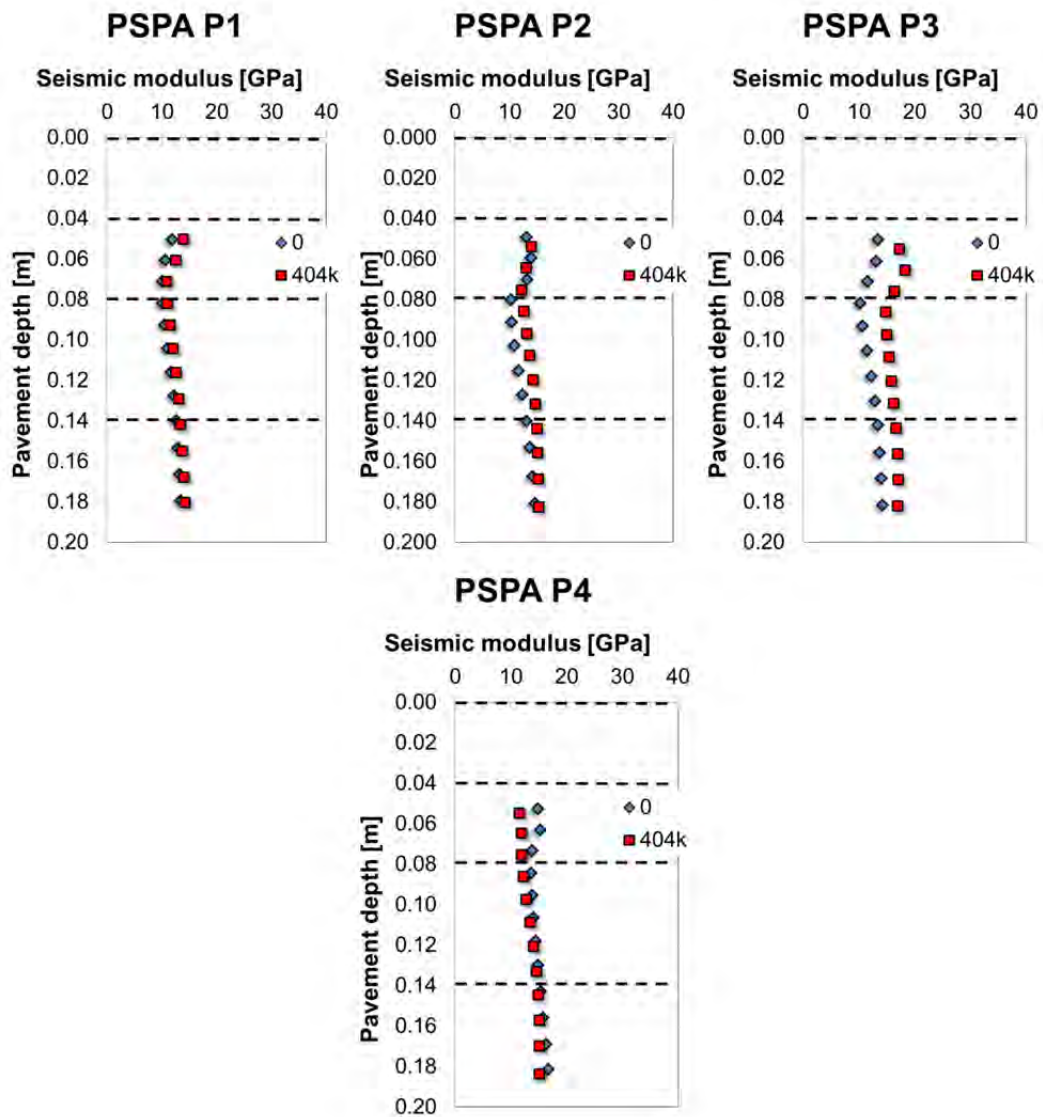
Fig. 7.44 Seismic modulus from PSPA measurements versus depth before and after trafficking with 404'000 load applications at pavement positions P1..P4

a)
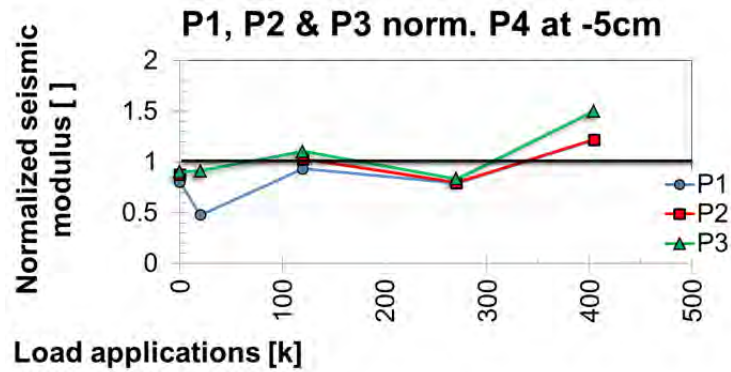
b)
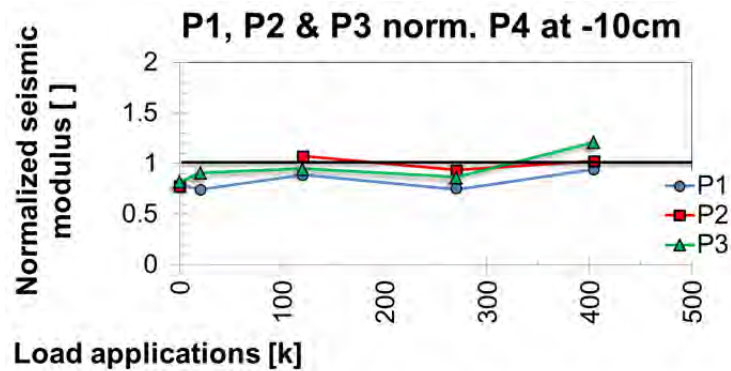
c)
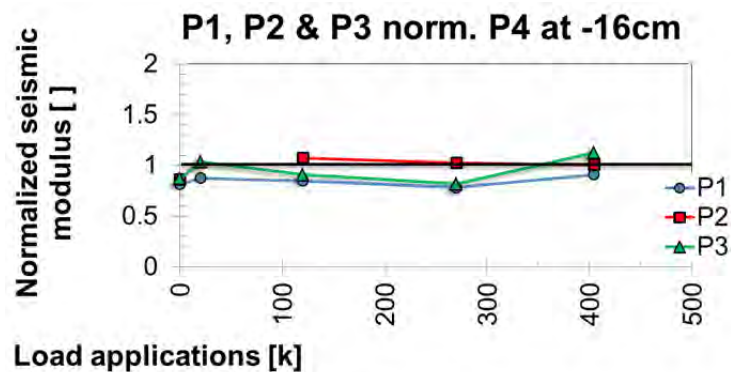
Fig. 7.45 Normalized seismic modulus from PSPA measurements at different depths vs. number of load applications

7.3.9   Laboratory tests

Several cores were taken from the trafficked and not-trafficked areas and different laboratory tests were carried out. The position and labelling of the cores is shown in Fig. 7.46. Coring comprised but the bituminous layers.
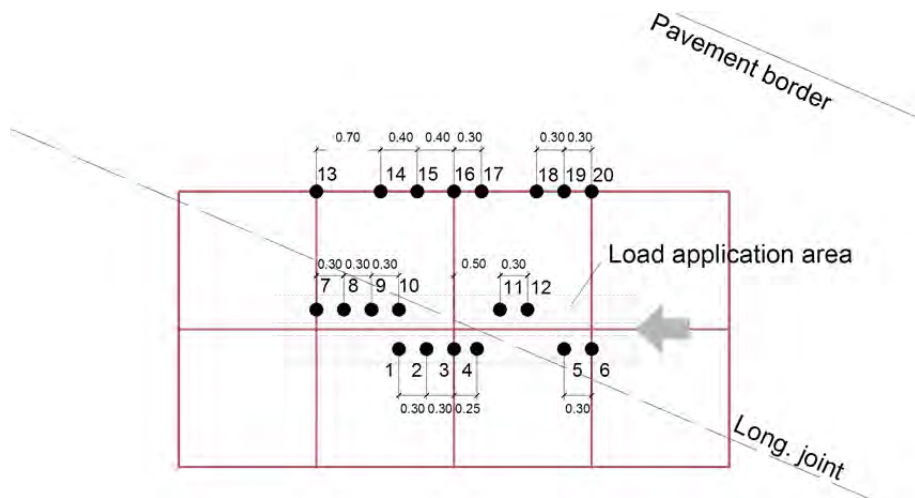
Fig. 7.46 Schema with the position and labelling of the cores.

7.3.9.1 Interlayer bonding

Four cores taken from the trafficked area were tested with the layer parallel direct shear test (LPDS) and compared with results obtained from not-trafficked cores. The results show that the interlayer properties hardly changed after trafficking except for the interlayer between AC B 16S and AC T 22H where trafficking appears related to an increase in the maximum stresses (see Fig. 7.47 and Fig. 7.48)

Fig. 7.47 LPDS interlayer shear test results

	Interlayer 1-2 SMA 11 - AC B16S		Interlayer 2-3 AC B16S - AC T22H		Interlayer 3-4 AC T22H – KMF 22	
	Trafficked	**Not-trafficked**	**Trafficked**	**Not-trafficked**	**Trafficked**	**Not-trafficked**
Max. Load [kN]	38.7	39.3	40.3	30.2	41.4	42.0
Max.Tension [kN/m2]	2190.0	2223.9	1709.0	2280.5	2342.8	2376.7
Def. at Max. [mm]	3.90	3.88	3.4	2.6	5.2	4.2

a)
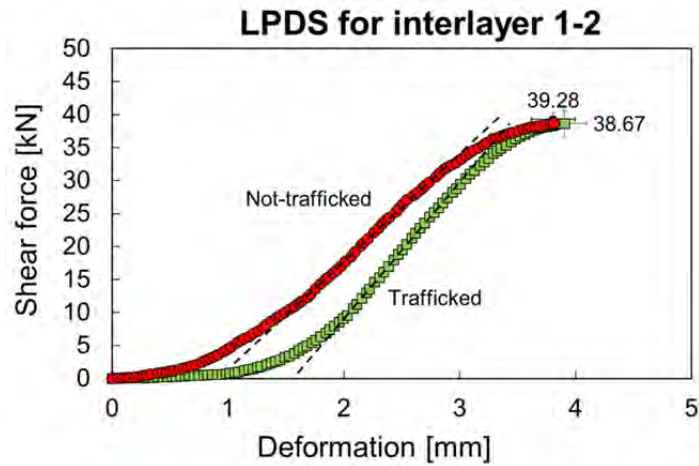
b)
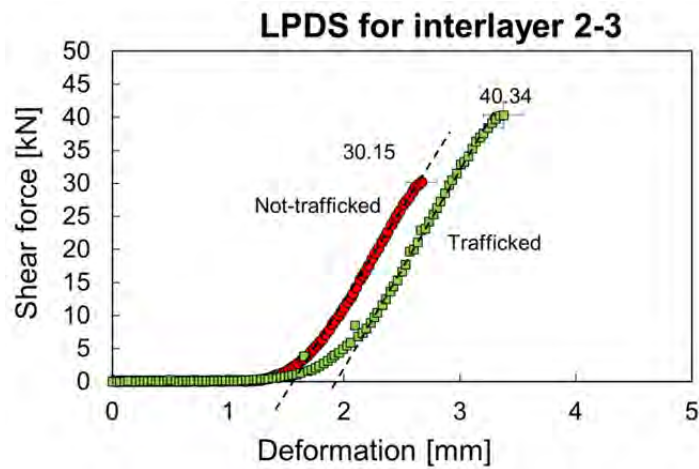
c)
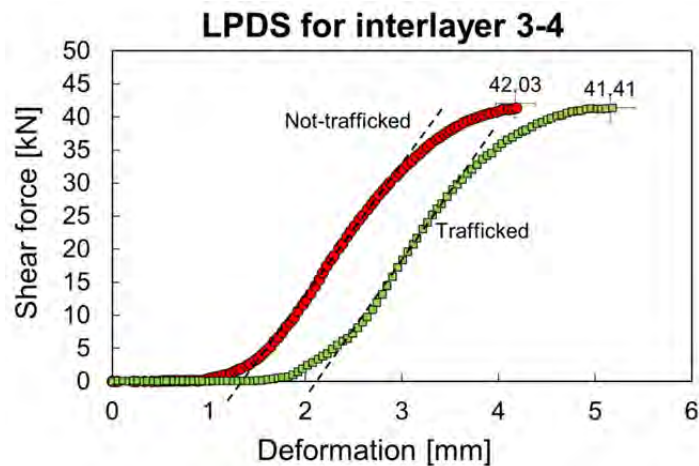
Fig. 7.48 Comparison of the LPDS test results for both not-trafficked and trafficked loading condition in each interlayer.

7.4   Summary and Conclusions

The MLS10 was transported to a testing site for loading a new T4-S1 pavement, still not open for use on a comparatively steep slope. Regular measurements of rutting, static deflections with ETH Delta, etc. were carried out in order to evaluate the pavement response and detect any sign of distress.

The analysis of the data shows that no clear change in the pavement responses occurred during the 404'000 load applications of the test. Profiles show low rutting of the same order of magnitude than in Rastplatz Suhr. The pavement showed a very stiff behavior pointing towards long remaining life expectancy.

8   Conclusions

The experience gathered in the three testing sites with channelized twin tire loading at 22km/h and 65kN half axle load confirm that the MLS10 is an important tool for simulating traffic loading of a pavement with full-scale rolling loads in an accelerated way and validating the construction of pavement and /or confirming the bearing capacity and remaining service life of old pavements.

This work confirmed that the MLS10, in combination with the right type of sensors and pavement evaluation techniques, provides valuable information for evaluating the mechanical service capability of real pavements in a reproducible way. It was demonstrated that the MLS10 can be deployed to many places thanks to its design, which showed high flexibility and mobility. Hence, the device is characterized by the following clear advantages:

- Compact size in comparison with other similar machines. It is relatively easy to transport the MLS10 to the test location and displace it on the site by its own driving wheels.

- Unidirectional loading direction, similar to real traffic.

- High amount of realistic load applications in a relatively short period of time

- With a speed of 22km/h, the load is the most realistic one compared to other mobile machines.

For short periods of time, the machine can work continuously during a day of about 8.5 h and load the pavement with up to 40'000 load applications. For a longer period of time, e.g. in case of stiff pavements this performance reduces since these tests require a high amount of load cycles. Although the MLS10 continuously increased the performance and many of the problems of this prototype were identified and solved, unexpected breakdowns may still occur that can reduce the performance and efficiency of the machine.

One of the most valuables outcomes of these tests was the possibility to improve the functionality of the MLS10, and to learn how to operate the machine in an efficient way. The research also allowed to compare and evaluate different measurement methods optimizing their application in a holistic way, such as combined application of temperature sensors, strain gauges and accelerometers and the use of periodically applied non-destructive sensors, in particular transverse profilometers, portable seismic pavement analyzer (PSPA), falling weigh deflectometer (FWD), ETH Delta deflectometer and ground penetrating radar (GPR).

The tests in "Filderen" revealed that the new structure of the A1 highway, as well as other weaker versions of this pavement, have high stiffness and bearing capacity and require a considerable amount of time and effort to generate significant changes in the response from load induced distress. This confirms that the dimensioning of the pavement and its construction according to actual Swiss Standards is of good quality. In fact, the behavior observed with the MLS10 on the new pavements in Filderen was comparable to the behavior of a 20 year old pavement on the "Rastplatz Suhr" with good long term performance.

These positive findings were also confirmed by the test results of the new pavement in "Neue Staffeleggstrasse", which also showed that the MLS10 can be used on pavements with a slope of 5% provided that it can be positioned such that the loading of the machine frame can be realized in a balanced way. However, it is recommended to avoid such extreme applications for safety reasons. The results found in this research provide a good point of reference for testing new pavements where new construction techniques and

new types of materials are used, since these new pavements would have to show at least similar positive behavior than the pavements investigated in this research.

However, with respect to those new developments it is recommended to improve the significance and validity of MLS10 even under conditions where significant distress has started and where maintenance has been delayed. For next uses of the MLS10 it is also suggested to focus on testing weaker pavements in order to reach the bearing capacity limit within a reasonable period of time and therefore learn what are the most common distress mechanisms present for these types of constructions. In order to be able to conduct such torture tests also for new pavement developments it is advised to perform those test on testing fields specifically devoted for that purpose. Another recommendation would be to investigate the performance under super single loadings (which is known to be more severe) and under lateral wandering conditions.

Appendix

I   Test site 1: Filderen – Results of construction control tests

I.1   Layers

Baudirektion Kanton Zürich

Tiefbauamt
Projektieren + Realisieren

N 20.1.4, Dreieck Zürich-West
Versuchsfeld Stress - Tester
Schichtaufbau

Aufbau	Einbautermin	Belag	Versuchsfeld			
			F 1	F 2	F 3	F 4
Deckbelag	Sep. 08	AC MR 8				30 mm
Binderschicht	Sep. 08 Sep. 08	AC B 22 H AC B 16 H		60 mm	80 mm	80 mm
Tragschicht	Sep. 08	AC T 22 H	80 mm	80 mm	80 mm	80 mm
SAMI-Schicht	Sep. 08		10 mm			
Fundationsschicht Oberschicht	19.09.2008		18 cm HGT mit 65% Belagsgranulat und 35% Kiessand II. Bindemittel Georoc Doroport RB N, 86 kg/m3 fest			
Fundationsschicht Unterschicht	18.09.2008		22 cm HGT mit 65% Belagsgranulat und 35% Kiessand II. Bindemittel Georoc Doroport RB N, 86 kg/m3 fest			
Untergrund mit Materialersatz	14.09.2008		Alte tonige Schüttung, wenig tragfähig, analog dem Trasse Materialersatz mit ca. 50 cm Molassematerial aus Tunnelvortrieb mit TBM. Stabilisiert mit ca. 25 - 30kg/m3 Georoc Dorosol C 30. Anforderungen wieTrasse: Me erf. > 30'000 MN/m2.			

Fig. I.1 Composition of the layers.

I.2 Static plate bearing tests

CONSULTEST AG

Institut für Materialprüfung, Beratung
und Qualitätssicherung im Bauwesen

STS 091

Deisrütistrasse 11
CH - 8472 Ohringen
Tel 052 335 28 21
Fax 052 335 28 24

Seite 1 von 1

Prüfbericht : Plattendruckversuch E_V und M_E

SN 670 317b

Objekt:	Rückbau Bahnanlage Dreieck Zürich-West, Fildern
Versuch-Nr.:	2
Profil:	F 1.1 gem. Angaben Bauleitung
Auftraggeber:	Toneatti AG
Auftrag-Nr.:	2491-08
Messdatum:	17.09.2008 *Nach messung*

Schicht: P (Planum)

		Erst-belastung	Zweit-belastung
σ_{max}	MN/m²	0.25	0.25
a_1	mm/(MN/m²)	5.489	0.714
a_2	mm/(MN²/m⁴)	-1.429	7.429
E_V	MN/m²	43.8	87.5
E_{V2}/E_{V1}		2.00	
Anforderung:		-	-
Kurve	R^2	1.0000	0.9917
Planum			
σ_1	MN/m²	0.05	0.05
σ_2	MN/m²	0.15	0.15
M_E	MN/m²	57.7	136.4
M_{E2}/M_{E1}		2.36	
Anforderung:	30 MN/m²	**erfüllt**	

Plattendurchmesser [mm] 300

Bemerkungen: -

Erstbelastung

n	Laststufe	Spannung MN/m²	Setzung mm
0	0	0.00	0.00
1	1	0.05	0.16
2	2	0.10	0.42
3	3	0.15	0.68
4	4	0.20	0.93
5	5	0.25	1.17
6			
7			
8			

Entlastung

n	Laststufe	Spannung MN/m²	Setzung mm
1	1	0.15	1.11
2	2	0.05	0.86
3	3	0.00	0.66
4			
5			

Zweitbelastung

n	Laststufe	Spannung MN/m²	Setzung mm
0	10	0.00	0.66
1	11	0.05	0.68
2	12	0.10	0.80
3	13	0.15	0.94
4	14	0.20	1.08
5			
6			
7			
8			

Datum/Unterschrift Sachbearbeiter
17.09.2008

Fig. I.2 Static plate bearing test results Nr. 1 of the subgrade in section F1.

CONSULTEST AG

Institut für Materialprüfung, Beratung und Qualitätssicherung im Bauwesen

STS 091

Deisrütistrasse 11
CH - 8472 Ohringen
Tel 052 335 28 21
Fax 052 335 28 24

Seite 1 von 1

Prüfbericht : Plattendruckversuch E_V und M_E
SN 670 317b

Objekt:	**Rückbau Bahnanlage Dreieck Zürich-West, Fildern**
Versuch-Nr.:	3
Profil:	F 1.2 gem. Angaben Bauleitung
Auftraggeber:	Toneatti AG
Auftrag-Nr.:	2491-08
Messdatum:	17.09.2008 *Nachmessung*

Schicht: P (Planum)

		Erst-belastung	Zweit-belastung
σ_{max}	MN/m²	0.25	0.25
a_1	mm/(MN/m²)	13.351	0.789
a_2	mm/(MN²/m⁴)	9.429	22.857
E_V	MN/m²	14.3	34.6
E_{V2}/E_{V1}		2.42	

Anforderung: - -

Kurve	R^2	0.9992	0.9941
Planum			
$\sigma 1$	MN/m³	0.05	0.05
$\sigma 2$	MN/m²	0.15	0.15
M_E	MN/m²	**19.7**	**56.0**
M_{E2}/M_{E1}		2.84	

Anforderung: 30 MN/m² **nicht erfüllt**

Plattendurchmesser [mm] 300

Erstbelastung

n	Laststufe	Spannung MN/m²	Setzung mm
0	0	0.00	0.00
1	1	0.05	0.28
2	2	0.10	0.99
3	3	0.15	1.76
4	4	0.20	2.68
5	5	0.25	3.48
6			
7			
8			

Entlastung

n	Laststufe	Spannung MN/m²	Setzung mm
1	1	0.15	3.36
2	2	0.05	2.72
3	3	0.00	2.21
4			
5			

Zweitbelastung

n	Laststufe	Spannung MN/m²	Setzung mm
0	10	0.00	2.21
1	11	0.05	2.25
2	12	0.10	2.49
3	13	0.15	2.87
4	14	0.20	3.24
5			
6			
7			
8			

Datum/Unterschrift Sachbearbeiter
17.09.2008

Bemerkungen: -

Fig. I.3 Static plate bearing test results Nr. 2 of the subgrade in section F1.

CONSULTEST AG

Institut für Materialprüfung, Beratung
und Qualitätssicherung im Bauwesen

STS 091

Deisrütistrasse 11
CH - 8472 Ohringen
Tel 052 335 28 21
Fax 052 335 28 24

Seite 1 von 1

Prüfbericht : Plattendruckversuch E_V und M_E

SN 670 317b

Objekt:	**Versuchsfeld ETH**
	Dreieck Zürich-West, Fildern
Versuch-Nr.:	**3**
Profil:	F 2.1
Auftraggeber:	Toneatti AG
Auftrag-Nr.:	2465-08
Messdatum:	15.09.2008

Schicht: P   (Planum)

		Erst-belastung	Zweit-belastung
σ_{max}	MN/m^2	0.25	0.25
a_1	mm/(MN/m^2)	19.966	1.491
a_2	mm/(MN^2/m^4)	21.714	9.143
E_V	MN/m^2	8.9	59.6
E_{V2}/E_{V1}		6.72	
Anforderung:	·		·

Kurve	R^2	0.9984	0.9986
Planum			
σ1	MN/m^2	0.05	0.05
σ2	MN/m^2	0.15	0.15
M_E	MN/m^2	**12.3**	**90.4**
M_{E2}/M_{E1}		7.32	
Anforderung:	30 MN/m²	**nicht erfüllt**	

Plattendurchmesser [mm]   300

Erstbelastung

n	Laststufe	Spannung MN/m^2	Setzung mm
0	0	0.00	0.00
1	1	0.05	2.16
2	2	0.10	3.49
3	3	0.15	4.63
4	4	0.20	5.93
5	5	0.25	7.56
6			
7			
8			

Entlastung

n	Laststufe	Spannung MN/m^2	Setzung mm
1	1	0.15	7.54
2	2	0.05	7.29
3	3	0.00	6.89
4			
5			

*Stehendes Wasser auf Fläche
co. 12 Std. nach Einbau
→ Ersatz am 16.09.08
des durchnässten Schicht*

Zweitbelastung

n	Laststufe	Spannung MN/m^2	Setzung mm
0	10	0.00	6.89
1	11	0.05	6.97
2	12	0.10	7.14
3	13	0.15	7.31
4	14	0.20	7.55
5			
6			
7			
8			

Datum/Unterschrift Sachbearbeiter
15.09.2008

Bemerkungen: -
5303 PB, V01.06

Fig. I.4 Static plate bearing test results Nr. 1 of the subgrade in section F2.

13/15

CONSULTEST AG

Institut für Materialprüfung, Beratung
und Qualitätssicherung im Bauwesen

STS 091

Deisrütistrasse   11
CH - 8472 Ohringen
Tel   052 335 28 21
Fax 052 335 28 24

Seite 1 von 1

Prüfbericht : Plattendruckversuch E_V und M_E

SN 670 317b

Objekt:	Rückbau Bahnanlage
	Dreieck Zürich-West, Fildern
Versuch-Nr.:	4
Profil:	F 2.1 gem. Angaben Bauleitung
Auftraggeber:	Toneattl AG
Auftrag-Nr.:	2491-08
Messdatum:	17.09.2008 *Nachmessung*

Schicht: P   (Planum)

		Erst-belastung	Zweit-belastung
σ_{max}	MN/m²	0.25	0.25
a_1	mm/(MN/m²)	11.223	1.009
a_2	mm/(MN²/m⁴)	-5.143	12.857
E_V	MN/m²	22.6	53.3
E_{V2}/E_{V1}		2.35	
Anforderung:		-	-
Kurve	R²	0.9998	0.9949
Planum			
$\sigma 1$	MN/m²	0.05	0.05
$\sigma 2$	MN/m²	0.15	0.15
M_E	MN/m²	29.4	83.8
M_{E2}/M_{E1}		2.85	
Anforderung:	30 MN/m²	**nicht erfüllt**	

Plattendurchmesser [mm]   300

Bemerkungen: -

Erstbelastung

n	Laststufe	Spannung MN/m²	Setzung mm
0	0	0.00	0.00
1	1	0.05	0.28
2	2	0.10	0.82
3	3	0.15	1.31
4	4	0.20	1.76
5	5	0.25	2.23
6			
7			
8			

Entlastung

n	Laststufe	Spannung MN/m²	Setzung mm
1	1	0.15	2.14
2	2	0.05	1.73
3	3	0.00	1.43
4			
5			

*Materialersatz mit Stabilisat
am 16.9.08 ausgeführt
(Alter bei Messung = 24 Std.)*

Zweitbelastung

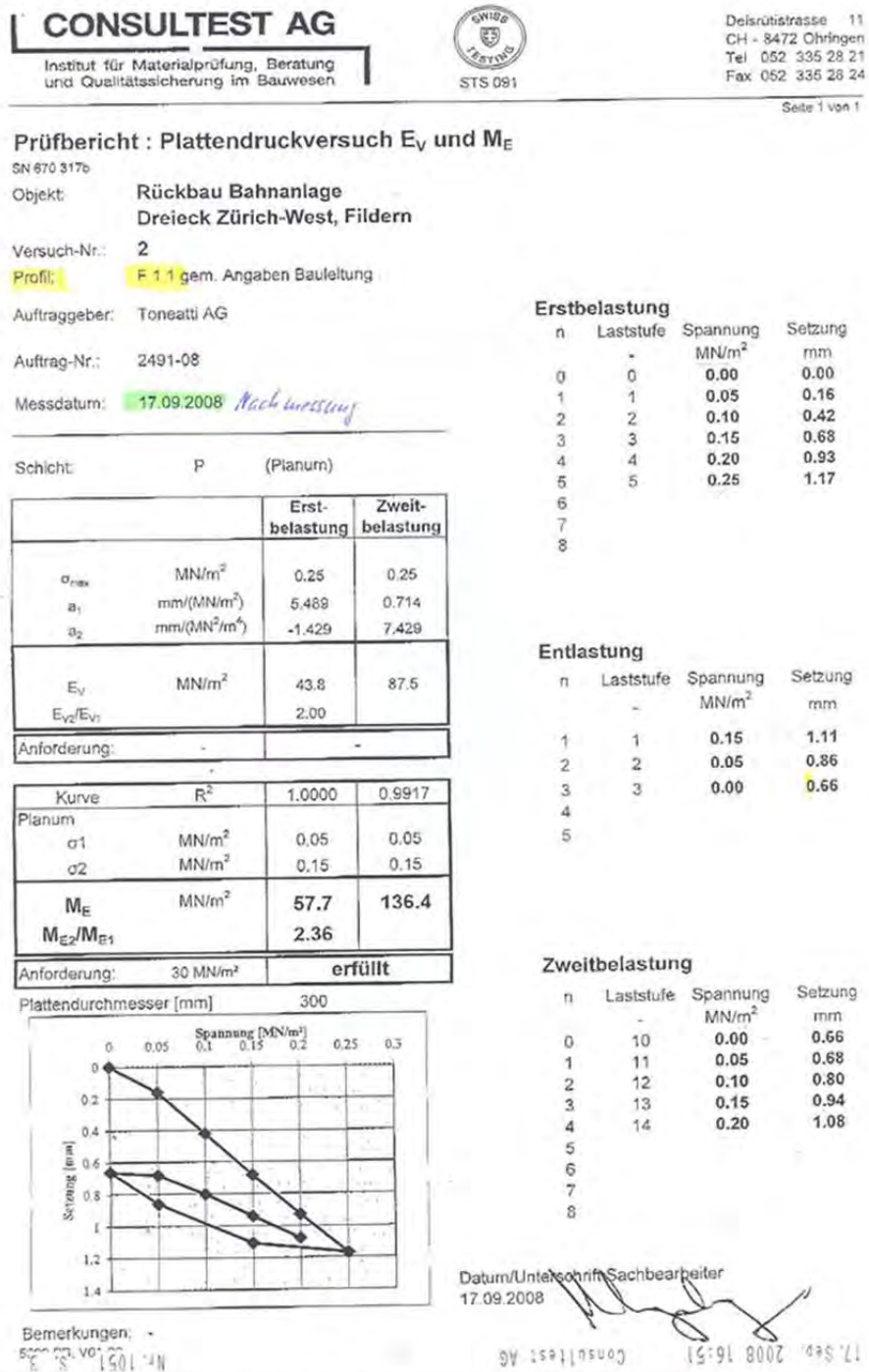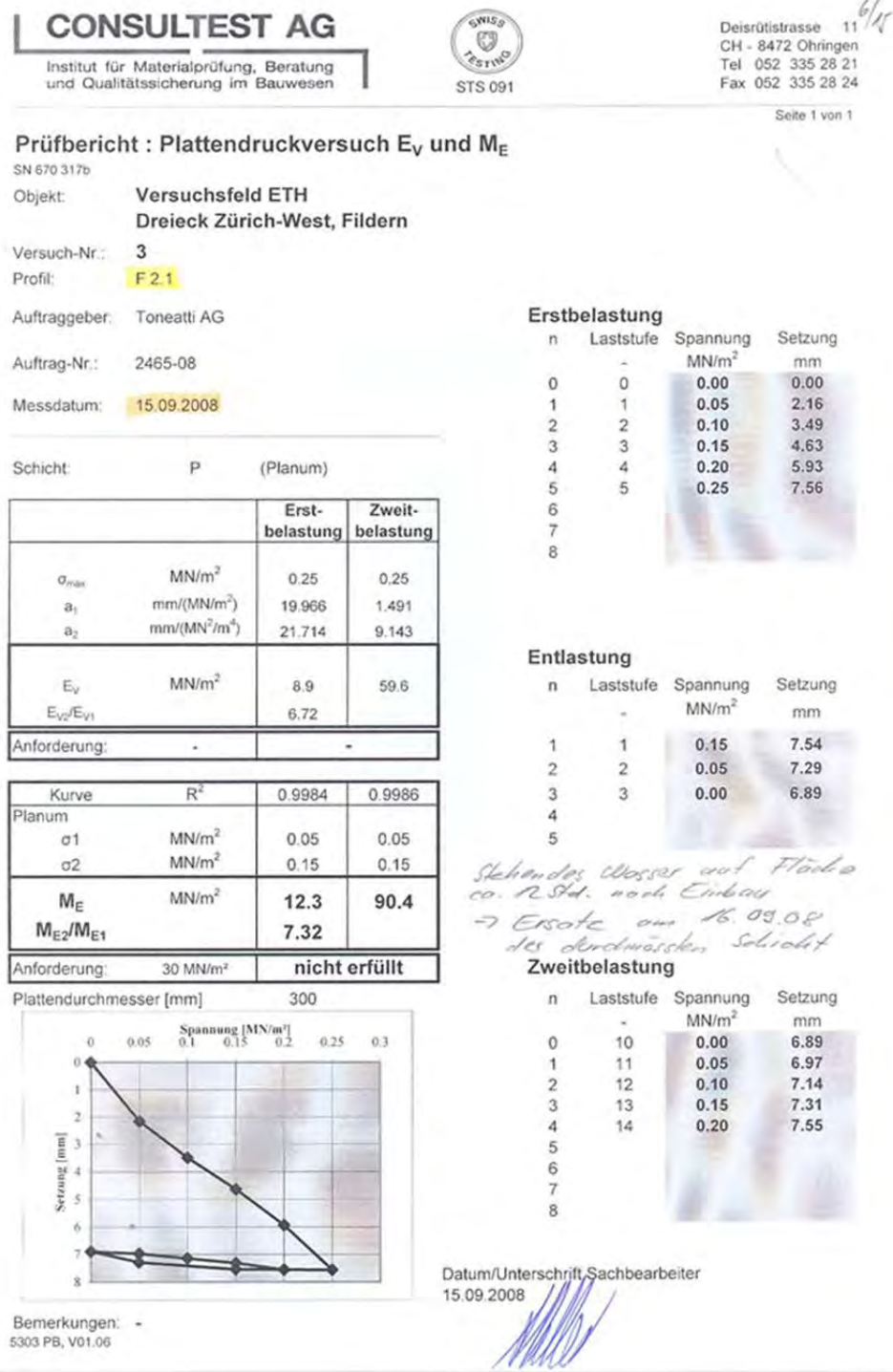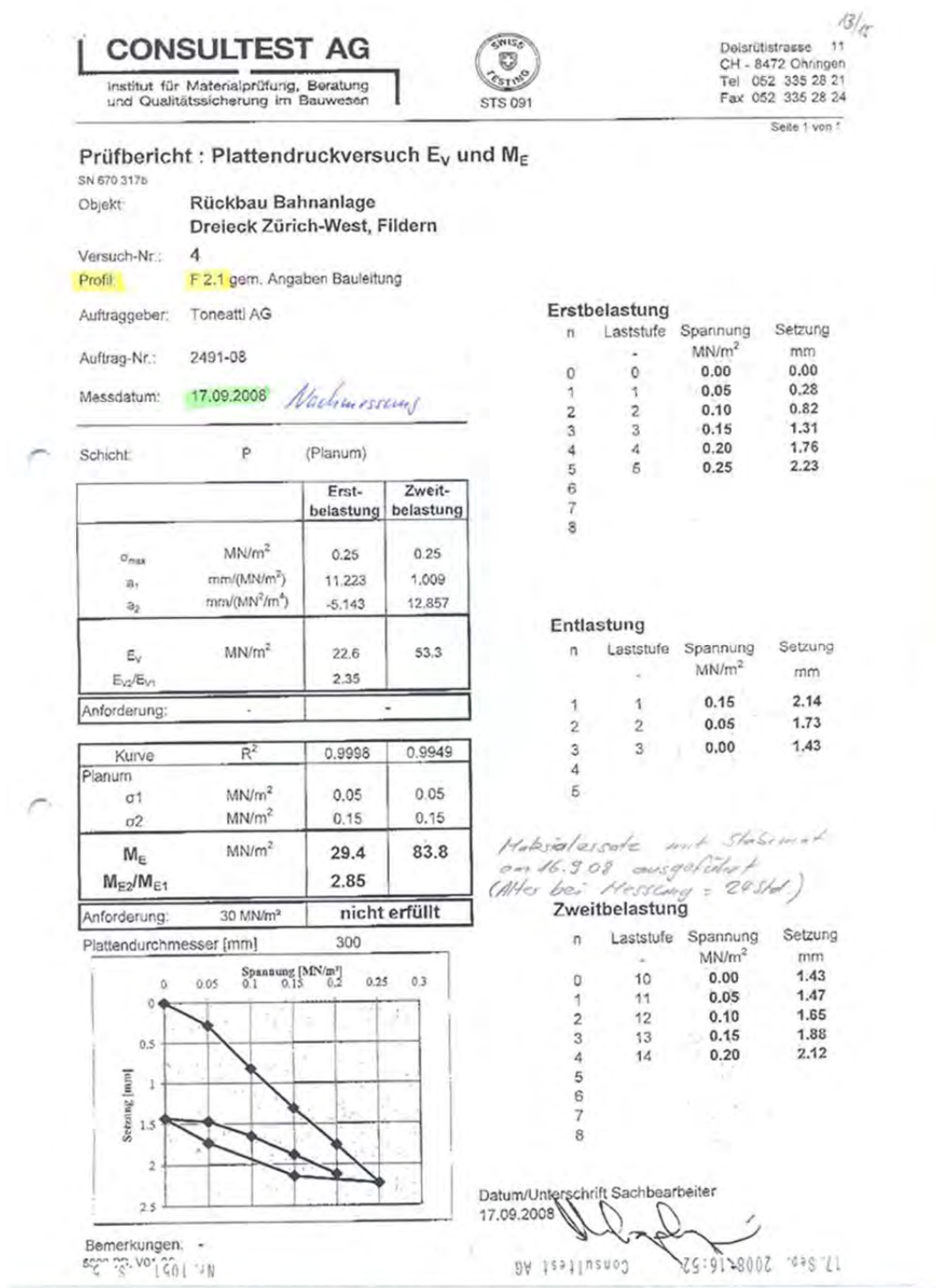| n	Laststufe	Spannung MN/m²	Setzung mm
0	10	0.00	1.43
1	11	0.05	1.47
2	12	0.10	1.65
3	13	0.15	1.88
4	14	0.20	2.12
5			
6			
7			
8			

Datum/Unterschrift Sachbearbeiter
17.09.2008

Fig. I.5 Static plate bearing test results Nr. 2 of the subgrade in section F2.

Fig. I.6 Static plate bearing test results Nr.3 of the subgrade in section F2.

CONSULTEST AG

Institut für Materialprüfung, Beratung
und Qualitätssicherung im Bauwesen

STS 091

Deisrütistrasse 11
CH - 8472 Ohringen
Tel 052 335 28 21
Fax 052 335 28 24

Seite 1 von 1

Prüfbericht : Plattendruckversuch E_V und M_E
SN 670 317b

Objekt:	**Versuchsfeld ETH**
	Dreieck Zürich-West, Fildern
Versuch-Nr.:	**4**
Profil:	F 3.1
Auftraggeber:	Toneatti AG
Auftrag-Nr.:	2465-08
Messdatum:	15.09.2008

Schicht: P   (Planum)

		Erst-belastung	Zweit-belastung
σ_{max}	MN/m²	0.25	0.25
a_1	mm/(MN/m²)	6.097	0.746
a_2	mm/(MN²/m⁴)	5.143	6.571
E_V	MN/m²	30.5	94.2
E_{V2}/E_{V1}			3.09
Anforderung:	-		-

Kurve	R^2	0.9982	0.9959
Planum			
$\sigma1$	MN/m²	0.05	0.05
$\sigma2$	MN/m²	0.15	0.15
M_E	MN/m²	**42.1**	**145.6**
M_{E2}/M_{E1}		**3.46**	
Anforderung:	30 MN/m²	**erfüllt**	
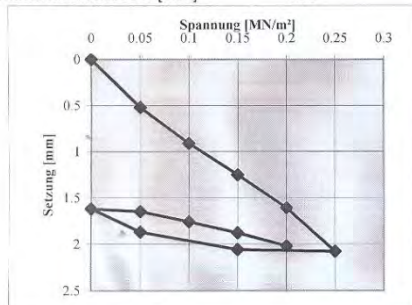
Plattendurchmesser [mm]   300

Erstbelastung

n	Laststufe	Spannung MN/m²	Setzung mm
0	0	0.00	0.00
1	1	0.05	0.52
2	2	0.10	0.91
3	3	0.15	1.25
4	4	0.20	1.61
5	5	0.25	2.08
6			
7			
8			

Entlastung

n	Laststufe	Spannung MN/m²	Setzung mm
1	1	0.15	2.06
2	2	0.05	1.87
3	3	0.00	1.62
4			
5			

Zweitbelastung

n	Laststufe	Spannung MN/m²	Setzung mm
0	10	0.00	1.62
1	11	0.05	1.65
2	12	0.10	1.76
3	13	0.15	1.88
4	14	0.20	2.02
5			
6			
7			
8			

Datum/Unterschrift Sachbearbeiter
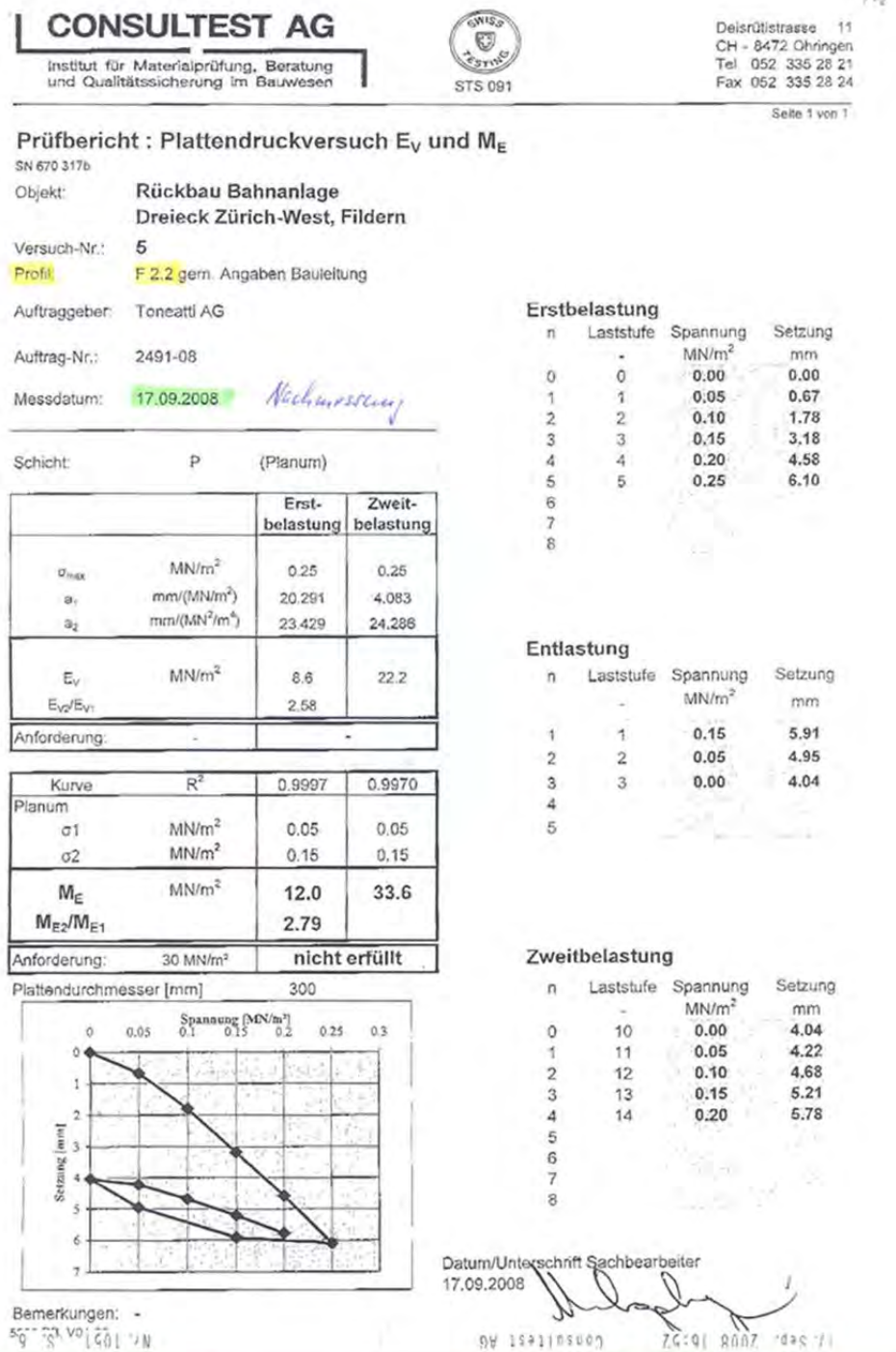15.09.2008

Bemerkungen: -
5303 PB, V01.06

Fig. I.7 Static plate bearing test results Nr.1 of the subgrade in section F3

CONSULTEST AG

Institut für Materialprüfung, Beratung
und Qualitätssicherung im Bauwesen

SWISS TESTING

STS 091

Deisrütistrasse 11
CH - 8472 Ohringen
Tel 052 335 28 21
Fax 052 335 28 24

Seite 1 von 1

Prüfbericht : Plattendruckversuch E_V und M_E

SN 670 317b

Objekt:	**Versuchsfeld ETH**
	Dreieck Zürich-West, Fildern
Versuch-Nr.:	**5**
Profil:	F 3.2
Auftraggeber:	Toneatti AG
Auftrag-Nr.:	2465-08
Messdatum:	15.09.2008

Schicht: P (Planum)

		Erst-belastung	Zweit-belastung
σ_{max}	MN/m²	0.25	0.25
a_1	mm/(MN/m²)	31.789	1.426
a_2	mm/(MN²/m⁴)	4.571	14.571
E_V	MN/m²	6.8	44.4
E_{V2}/E_{V1}		6.50	

Anforderung:	-	-

Kurve	R²	1.0000	0.9983
Planum			
σ1	MN/m²	0.05	0.05
σ2	MN/m²	0.15	0.15
M_E	MN/m²	**9.2**	**69.1**
M_{E2}/M_{E1}		7.54	

Anforderung:	30 MN/m²	**nicht erfüllt**
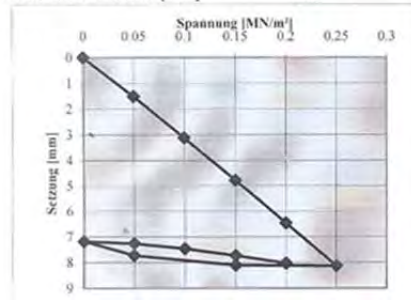
Plattendurchmesser [mm] 300

Bemerkungen: -
5303 PB, V01.06

Erstbelastung

n	Laststufe	Spannung MN/m²	Setzung mm
	-		
0	0	0.00	0.00
1	1	0.05	1.51
2	2	0.10	3.12
3	3	0.15	4.77
4	4	0.20	6.46
5	5	0.25	8.13
6			
7			
8			

Entlastung

n	Laststufe	Spannung MN/m²	Setzung mm
	-		
1	1	0.15	8.10
2	2	0.05	7.73
3	3	0.00	7.18
4			
5			

*Stehendes Wasser auf Fläche
ca. 12 Std. nach Einbau.
→ Ersatz am 16.9.08
der durchnässten Schicht*

Zweitbelastung

n	Laststufe	Spannung MN/m²	Setzung mm
	-		
0	10	0.00	7.18
1	11	0.05	7.26
2	12	0.10	7.46
3	13	0.15	7.73
4	14	0.20	8.03
5			
6			
7			
8			

Datum/Unterschrift Sachbearbeiter
15.09.2008

Fig. I.8 Static plate bearing test results Nr.2 of the subgrade in section F3.

┌ **CONSULTEST AG**

Institut für Materialprüfung, Beratung
und Qualitätssicherung im Bauwesen ┘

(SWISS TESTING / STS 091)

Deisrütistrasse 11
CH - 8472 Ohringen
Tel 052 335 28 21
Fax 052 335 28 24

Seite 1 von 1

Prüfbericht : Plattendruckversuch E_V und M_E

SN 670 317b

Objekt:	**Rückbau Bahnanlage** **Dreieck Zürich-West, Fildern**
Versuch-Nr.:	**1**
Profil:	F 3.2 gem. Angaben Bauleitung
Auftraggeber:	Toneatti AG
Auftrag-Nr.:	2491-08
Messdatum:	17.09.2008 *Abschmessung*

Schicht: P (Planum)

		Erst-belastung	Zweit-belastung
σ_{max}	MN/m^2	0.25	0.25
a_1	mm/(MN/m^2)	11.780	0.823
a_2	mm/(MN^2/m^4)	6.000	14.286
E_V	MN/m^2	16.9	51.2
E_{V2}/E_{V1}		3.02	
Anforderung:		-	-
Kurve	R^2	0.9998	0.9897
Planum			
$\sigma 1$	MN/m^2	0.05	0.05
$\sigma 2$	MN/m^2	0.15	0.15
M_E	MN/m^2	23.1 *	81.5
M_{E2}/M_{E1}		3.53	
Anforderung:	30 MN/m^2	**nicht erfüllt**	

Plattendurchmesser [mm] 300

Erstbelastung

n	Laststufe	Spannung MN/m^2	Setzung mm
0	0	0.00	0.00
1	1	0.05	0.28
2	2	0.10	0.88
3	3	0.15	1.58
4	4	0.20	2.27
5	5	0.25	2.98
6			
7			
8			

Entlastung

n	Laststufe	Spannung MN/m^2	Setzung mm
1	1	0.15	2.91
2	2	0.05	2.41
3	3	0.00	2.13
4			
5			

* *Materialersatz mit SkSi am 16.09.08 ausgeführt (Alter bei Messung = 24 Std.)*

Zweitbelastung

n	Laststufe	Spannung MN/m^2	Setzung mm
0	10	0.00	2.13
1	11	0.05	2.14
2	12	0.10	2.35
3	13	0.15	2.58
4	14	0.20	2.83
5			
6			
7			
8			

Datum/Unterschrift Sachbearbeiter
17.09.2008

Bemerkungen: -

Fig. I.9 Static plate bearing test results Nr.3 of the subgrade in section F3.

CONSULTEST AG

Institut für Materialprüfung, Beratung
und Qualitätssicherung im Bauwesen

SWISS TESTING

STS 091

Deisrütistrasse 11
CH - 8472 Ohringen
Tel 052 335 28 21
Fax 052 335 28 24

Seite 1 von 1

Prüfbericht : Plattendruckversuch E_V und M_E

SN 670 317b

Objekt:	**Versuchsfeld ETH**
	Dreieck Zürich-West, Fildern
Versuch-Nr.:	**1**
Profil:	**F 4.1**
Auftraggeber:	Toneatti AG
Auftrag-Nr.:	2465-08
Messdatum:	15.09.2008

Schicht: P (Planum)

		Erst-belastung	Zweit-belastung
σ_{max}	MN/m²	0.25	0.25
a_1	mm/(MN/m²)	7.509	0.729
a_2	mm/(MN²/m⁴)	-7.429	4.857
E_V	MN/m²	39.8	115.8
E_{V2}/E_{V1}		2.91	
Anforderung:	-		-

Kurve	R^2	0.9994	0.9962
Planum			
$\sigma 1$	MN/m²	0.05	0.05
$\sigma 2$	MN/m²	0.15	0.15
M_E	MN/m²	**49.8**	**176.5**
M_{E2}/M_{E1}		**3.54**	
Anforderung:	30 MN/m²	**erfüllt**	
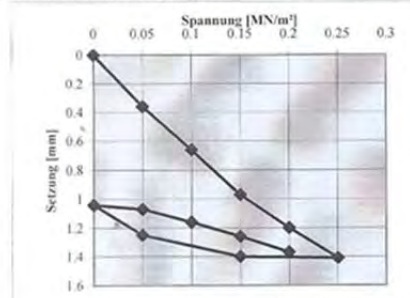
Plattendurchmesser [mm] 300

Erstbelastung

n	Laststufe	Spannung MN/m²	Setzung mm
0	0	0.00	0.00
1	1	0.05	0.36
2	2	0.10	0.66
3	3	0.15	0.97
4	4	0.20	1.20
5	5	0.25	1.41
6			
7			
8			

Entlastung

n	Laststufe	Spannung MN/m²	Setzung mm
1	1	0.15	1.40
2	2	0.05	1.25
3	3	0.00	1.04
4			
5			

Zweitbelastung

n	Laststufe	Spannung MN/m²	Setzung mm
0	10	0.00	1.04
1	11	0.05	1.07
2	12	0.10	1.16
3	13	0.15	1.26
4	14	0.20	1.37
5			
6			
7			
8			

Datum/Unterschrift Sachbearbeiter
15.09.2008

Bemerkungen: -
5303 PB, V01.06

Fig. I.10 Static plate bearing test results Nr.1 of the subgrade in section F4.

CONSULTEST AG

Institut für Materialprüfung, Beratung
und Qualitätssicherung im Bauwesen

STS 091

Deisrütistrasse 11
CH - 8472 Ohringen
Tel 052 335 28 21
Fax 052 335 28 24

Seite 1 von 1

Prüfbericht : Plattendruckversuch E_V und M_E

SN 670 317b

Objekt:	**Versuchsfeld ETH**
	Dreieck Zürich-West, Fildern
Versuch-Nr.:	**2**
Profil:	**F 4.2**
Auftraggeber:	Toneatti AG
Auftrag-Nr.:	2465-08
Messdatum:	15.09.2008

Schicht: P (Planum)

		Erst-belastung	Zweit-belastung
σ_{max}	MN/m^2	0.25	0.25
a_1	mm/(MN/m^2)	7.643	0.769
a_2	mm/(MN^2/m^4)	0.857	8.857
E_V	MN/m^2	28.6	75.4
E_{V2}/E_{V1}		2.63	
Anforderung:	-		-

Kurve	R^2	1.0000	0.9978
Planum			
$\sigma 1$	MN/m^2	0.05	0.05
$\sigma 2$	MN/m^2	0.15	0.15
M_E	MN/m^2	**38.4**	**118.1**
M_{E2}/M_{E1}		**3.08**	
Anforderung:	30 MN/m²	**erfüllt**	

Plattendurchmesser [mm] 300

Bemerkungen: -
5303 PB, V01.06

Erstbelastung

n	Laststufe	Spannung MN/m^2	Setzung mm
0	0	0.00	0.00
1	1	0.05	0.49
2	2	0.10	0.88
3	3	0.15	1.27
4	4	0.20	1.67
5	5	0.25	2.07
6			
7			
8			

Entlastung

n	Laststufe	Spannung MN/m^2	Setzung mm
1	1	0.15	2.06
2	2	0.05	1.82
3	3	0.00	1.52
4			
5			

Zweitbelastung

n	Laststufe	Spannung MN/m^2	Setzung mm
0	10	0.00	1.52
1	11	0.05	1.56
2	12	0.10	1.69
3	13	0.15	1.83
4	14	0.20	2.02
5			
6			
7			
8			

Datum/Unterschrift Sachbearbeiter
15.09.2008

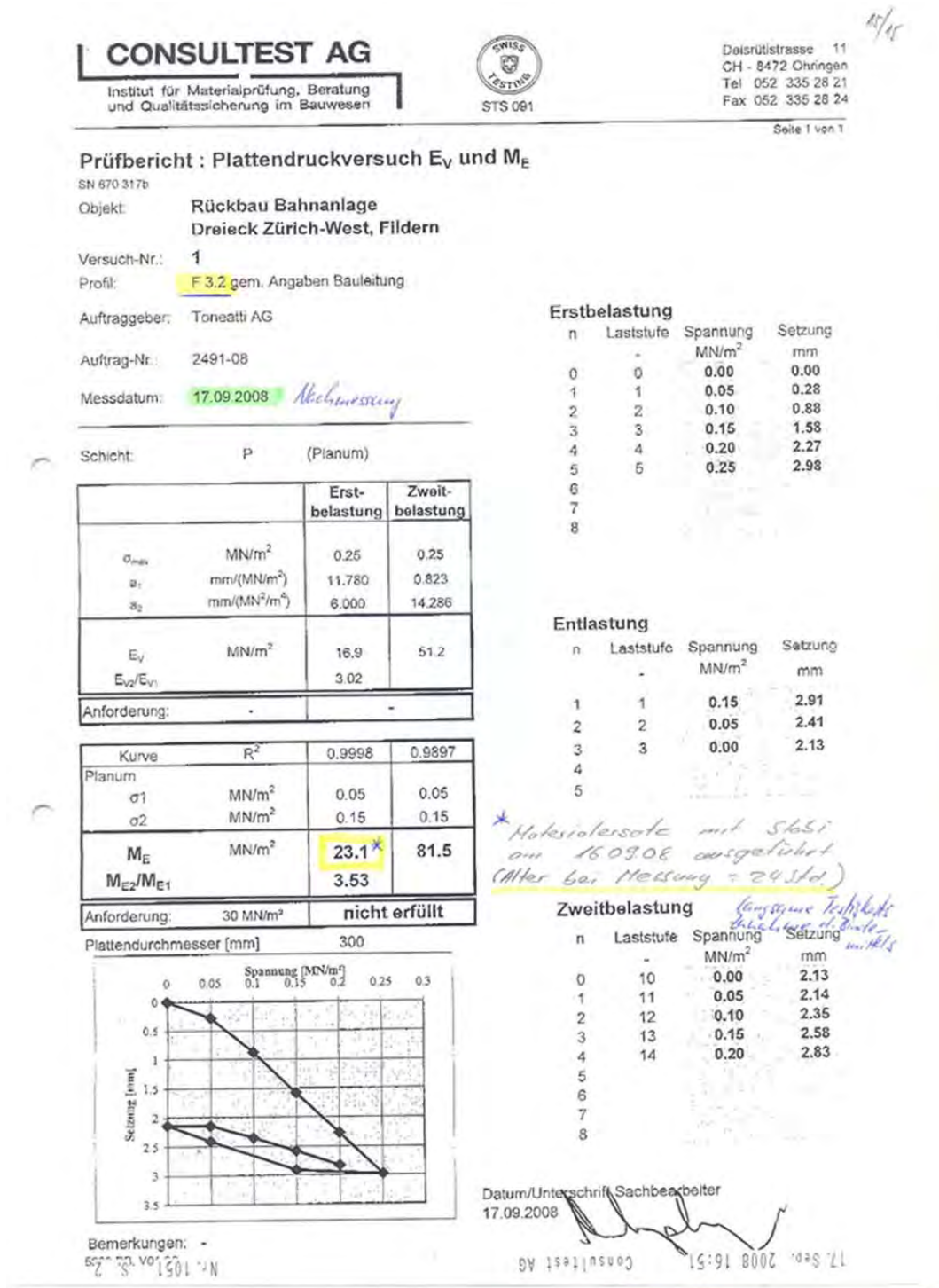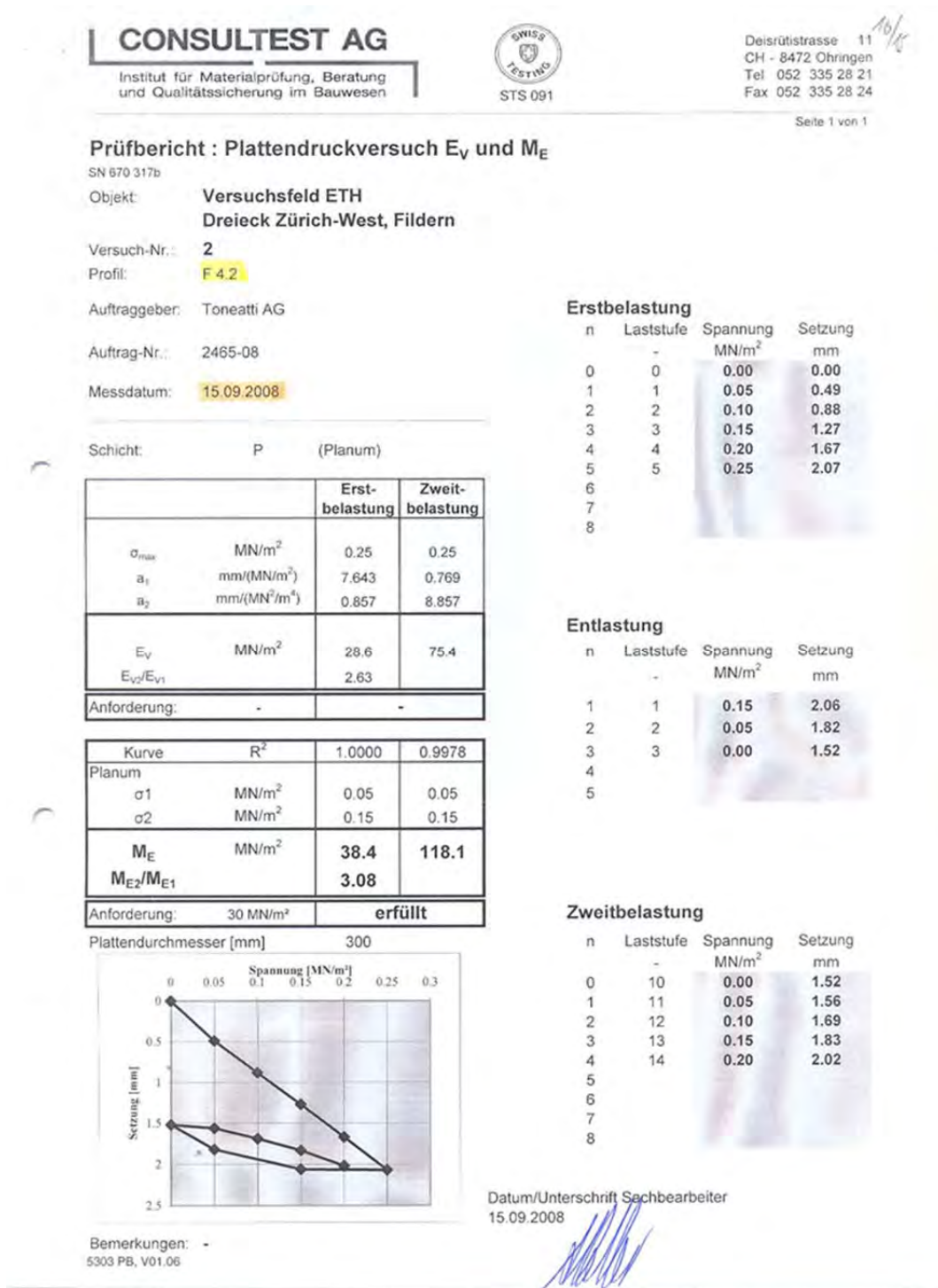*Fig. I.11 Static plate bearing test results Nr.2 of the subgrade in section F4.*

I.3 Asphalt mix: particle size distribution

Tiefbauämter der Kantone
Zürich, Luzern, Uri, Schwyz, Nidwalden, Obwalden und Zug

Lieferwerk:	**Birmensdorf**		Prüfstelle:	**Walo Bertschinger**
			Sollwertdatum:	18.6.08

Walzasphalt - Deklaration 2008			**AC MR 8 PmB**	

Mischgutangaben	Sollwerte	Anforderungen	Code Werk:	6556
Ziel-Bindemittel:	**PmB-E 45/80-65 CH**			
- Art/Sorte:	**Cariphalte 50/70**			
- Dosierung in M-%	6.20	min. 5.7 M-%		
- löslicher Anteil in M-%	6.00	Toleranz EW = ± 0.5	inkl. VIATOP 66	
Zusätze:				
- Art:	**VIATOP + Kalkhydrat**			
- Dosierung in M-%	0.3 + 2.0			
- löslicher Anteil in M-%	0.1			
Rückgewinnung aus Mischgut				
- Penetration: min. [$^1/_{10}$ mm]	30	keine Anforderung		
max. [$^1/_{10}$ mm]	45	keine Anforderung		
- Erweichungspunkt R+K: max.	80.0	keine Anforderung		
- Bindemittelabfluss	-	keine Anforderung		
Mineralstoffe Herkunft:				
- Füller	**Eigenfüller**			
- feine Gesteinskörnung	**Hard AG**			
- grobe Gesteinskörnung	**# 4/8 Gasperini**			
- Mineralanteil Sand ≤ 2.0 mm	28 M-%			
- Mineralanteil Splitte ≥ 2.0 mm	73 M-%			
Mineralkategorie	C 95/1	C 95/1		
Ausbausphalt				
- Kaltzugabe M-%	-	nicht gestattet		
- Warmzugabe M-%	-	nicht gestattet		
Marshall-Werte:				Ja
- Verdichtungstemperatur	155 °C			
- Raumdichte kg/m³	2299		Erstprüfungs-Bericht erfüllt:	
- Rohdichte kg/m³	2459			
- Hohlraumgehalt VM, Vol-%	6.5	6.0...9.0	Konformitätserklärung erfüllt:	
- Hohlraumfüllungsgrad VFB,%	~ 67.4	keine Anforderung		
- Stabilität S kN	-	keine Anforderung	Gültig bis :	
- Fliessen F, mm	-	keine Anforderung		
Bei H und S Belägen:			Stempel / Datum	
Spurbildungstest *)			Unterschrift des Belagswerkes	
- 10000 Prüfzyklen, %	-	---		
- 30000 Prüfzyklen, %	noch ausstehend	≤ 7.5%		
Wasserempfindlichkeit, % **)	noch ausstehend	≥ 70%		

Korngrössenverteilung:	mm			Toleranz	
- Einzelwerte Siebdurchgang	45.0	[M-%]	100.0		
	31.5	[M-%]	100.0		
	22.4	[M-%]	100.0		
	16.0	[M-%]	100.0		
	11.2	[M-%]	100.0		
	8.0	[M-%]	98.0	-8/+5	
	5.6	[M-%]	69.0		
	4.0	[M-%]	39.5	± 7	
	2.0	[M-%]	27.5	± 6	
	1.0	[M-%]	23.5	± 4	
	0.5	[M-%]	19.0		
	0.25	[M-%]	16.0		
	0.125	[M-%]	12.5		
	0.063	[M-%]	10.0	± 2	

Gültigkeit: bis Ende 2008	Bemerkungen: N 20.1.4, Umfahrung Birmensdorf, Dreieck Zürich-West, provisorisc
	Abkühlversuch noch ausstehend

Datum:
Stempel / Unterschrift Belagswerk

Datum: 18.06.2008
akkreditiertes Labor

Datum:
Stempel / Unterschrift Unternehmer

Walo Bertschinger Central AG
Zentrale Labordienste
Postfach 753, 8023 Zürich

Fig. I.12 Aggregate size distribution of the top layer.

Tiefbauämter der Kantone
Zürich, Luzern, Uri, Schwyz, Nidwalden, Obwalden und Zug

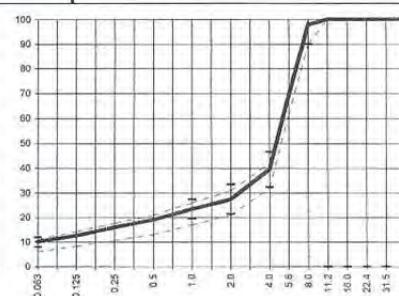| Lieferwerk:	Birmensdorf		Prüfstelle:	Walo Bertschinger
			Sollwertdatum:	30.3.06

Walzasphalt - Deklaration 2006		AC B 22 H	

Mischgutangaben	Sollwerte	Anforderungen	Code Werk:	5408
Ziel-Bindemittel:	PmB-E 10/30-70			
- Art/Sorte:	Cariphalte 25 RC			
- Dosierung in M-%	4.60	* objektspezifisch		
- löslicher Anteil in M-%	4.50	Toleranz EW = ± 0.6		
Zusätze:				
- Art:	-			
- Dosierung in M-%				
- löslicher Anteil in M-%				
Rückgewinnung aus Mischgut				
- Penetration: min. ['/₁₀ mm]	8	* Richtwert		
max. ['/₁₀ mm]	24	* Richtwert		
- Erweichungspunkt R+K: max.	83.0	* Richtwert		
- Bindemittelabfluss	-	—		
Mineralstoffe Herkunft:				1760
- Füller	Eigenfüller			
- feine Gesteinskörnung	-			
- grobe Gesteinskörnung	Kies AG Wil			
- Mineralanteil Sand ≤ 2.0 mm	32 M-%			
- Mineralanteil Splitte ≥ 2.0 mm	68 M-%			
Mineralkategorie	C 95/1	C 50/10		
Ausbauasphalt			PL VF VF 6.9.06	
- Kaltzugabe M-%	-	≤ 15%	CBL JW K̶ 6.9.06	
- Warmzugabe M-%	-	≤ 30%	BL Br K̶ 6.9.06	
Marshall-Werte:				
- Verdichtungstemperatur	155 °C			
- Raumdichte kg/m³	2387			
- Rohdichte kg/m³	2525			
- Hohlraumgehalt VM, Vol-%	5.5	4.0...7.0		
- Hohlraumfüllungsgrad VFB,%	≤ 65.6	—		
- Stabilität S kN	15.0	* Richtwert		
- Fliessen F, mm	4.5	* Richtwert		

	Ja
Erstprüfungs-Bericht erfüllt:	✓
Konformitätserklärung erfüllt:	✓

Gültig bis : 02.04.2011

Stempel / Datum 29.8.06
Unterschrift des Belagswerkes

BAB Belag AG Birmensdorf
Urdorferstrasse
8903 Birmensdorf

Bei H und S Belägen:			
Spurbildungstest *)		—	
- 10000 Prüfzyklen	-	—	
- 30000 Prüfzyklen	noch ausstehend	≤ 10%	
Wasserempfindlichkeit, % **)	noch ausstehend	≥ 70%	

Korngrössenverteilung:	mm				Toleranz
- Einzelwerte Siebdurchgang	45.0	[M-%]	100.0		
	31.5	[M-%]	100.0		
	22.4	[M-%]	98.0	-9/+5	
	16.0	[M-%]	84.0		
	11.2	[M-%]	71.0	± 9	
	8.0	[M-%]	62.0		
	5.6	[M-%]	53.0		
	4.0	[M-%]	44.0	-8/+5	
	2.0	[M-%]	32.0	± 7	
	1.0	[M-%]	21.5	± 5	
	0.5	[M-%]	15.0		
	0.25	[M-%]	12.0		
	0.125	[M-%]	9.5		
	0.063	[M-%]	7.0	± 3	

Gültigkeit: bis Ende 2006   Bemerkungen:

Datum:	Datum: 03.08.2006	Datum: 30.8.06
Stempel / Unterschrift Belagswerk	akkreditiertes Labor	Stempel / Unterschrift Unternehmer

29.8.06

BAB Belag AG Birmensdorf
Urdorferstrasse
8903 Birmensdorf

Walo Bertschinger Central AG
Zentrale Labordienste
Postfach 7534, 8023 Zürich

Anliker AG
Strassen + Tiefbau
Meierhöflistrasse 18
6020 Emmenbrücke

ANLIKER

Fig. I.13 Aggregate size distribution of the binder course.

Tiefbauämter der Kantone
Zürich, Luzern, Uri, Schwyz, Nidwalden, Obwalden und Zug

| Lieferwerk: | Birmensdorf | Prüfstelle: | Walo Bertschinger |
| | | Sollwertdatum: | 11.4.06 |

| Walzasphalt - Deklaration 2006 | | AC T 22 H | |

Mischgutangaben	Sollwerte	Anforderungen	Code Werk: 5858
Ziel-Bindemittel:	PmB-E 10/30-70		
- Art/Sorte:	Cariphalte 25 RC		
- Dosierung in M-%	4.40	* objektspezifisch	
- löslicher Anteil in M-%	4.35	Toleranz EW = ± 0.6	
Zusätze:			
- Art:	32 RA 0/16		
- Dosierung in M-%			
- löslicher Anteil in M-%			
Rückgewinnung aus Mischgut:			
- Penetration: min. [$^1/_{10}$ mm]	8	* Richtwert	
max. [$^1/_{10}$ mm]	24	* Richtwert	
- Erweichungspunkt R+K: max.	83.0	* Richtwert	
- Bindemittelabfluss	-	—	
Mineralstoffe Herkunft:			
- Füller	Eigenfüller		
- feine Gesteinskörnung	-		
- grobe Gesteinskörnung	Kies AG Wil		
- Mineralanteil Sand ≤ 2.0 mm	32 M-%		
- Mineralanteil Splitte ≥ 2.0 mm	68 M-%		
Mineralkategorie	C 95/1	C 50/10	
Ausbauphalt			
- Kaltzugabe M-%	-	≤ 25%	
- Warmzugabe M-%	20	≤ 60%	
Marshall-Werte:			
- Verdichtungstemperatur	155 °C		
- Raumdichte kg/m³	2380		
- Rohdichte kg/m³	2519		
- Hohlraumgehalt VM, Vol-%	5.5	4.0...7.0	
- Hohlraumfüllungsgrad VFB,%	≤ 64.7	—	
- Stabilität S kN	15.0	* Richtwert	
- Fliessen F, mm	4.5	* Richtwert	
Bei H und S Belägen:			
Spurbildungstest *)			
- 10000 Prüfzyklen	-	—	
- 30000 Prüfzyklen	noch ausstehend	≤ 10%	
Wasserempfindlichkeit, % **)	noch ausstehend	≥ 70%	

	Ja
Erstprüfungs-Bericht erfüllt:	✓
Konformitätserklärung erfüllt:	✓
Gültig bis:	02.04.2011

Stempel / Datum 29.8.06
Unterschrift des Belagswerkes
BAB Belag AG Birmensdorf
Urdorferstrasse
8903 Birmensdorf

Korngrössenverteilung:	mm			Toleranz
- Einzelwerte Siebdurchgang	45.0	[M-%]	100.0	
	31.5	[M-%]	100.0	
	22.4	[M-%]	98.0	-9/+5
	16.0	[M-%]	84.0	
	11.2	[M-%]	71.0	± 9
	8.0	[M-%]	62.0	
	5.6	[M-%]	53.0	
	4.0	[M-%]	44.0	-8/+5
	2.0	[M-%]	32.0	± 7
	1.0	[M-%]	21.5	± 5
	0.5	[M-%]	15.0	
	0.25	[M-%]	12.0	
	0.125	[M-%]	9.5	
	0.063	[M-%]	7.0	± 3

Gültigkeit: bis Ende 2006

Bemerkungen:

Datum:
Stempel / Unterschrift Belagswerk

29.8.06
BAB Belag AG Birmensdorf
Urdorferstrasse
8903 Birmensdorf

Datum: 04.08.2006
akkreditiertes Labor

Walo Bertschinger Central AG
Zentrale Labordienste
Postfach 7535, 8023 Zürich

Datum: 30.8.06
Stempel / Unterschrift Unternehmer

Anliker AG
Strassen + Tiefbau
Meierhöflistrasse 18
6020 Emmenbrücke

ANLIKER

Fig. I.14 Aggregate size distribution of the base course.

I.4   Stabilization: compression tests

4/5

Baudirektion Kanton Zürich
STS 339

Tiefbauamt
Oberbau und Geotechnik

Prüfprotokoll

HEIERLI	
Auftrag-Nr.	1760
Freigabe	
Ablage	

Datum 12.3.2007

Auftragsnummer	L07_402/16743

ARGE UP Filderen
Munimatt
8903 Birmensdorf

E   1 4. MRZ. 2007

Funkt.	Vert.	Vis.	Datum

Objekt:	N20.1.4, Dreieck Zürich-West, ARGE UP Filderen, HGT (mit PAK-Belag) Zementstabi
Material:	65% PAK Belag, 35% Kiessand II *(HGT)*
Probenahme ab:	Mischanlage UP Filderen
Zusatzstoffe:	Doroport RB N 70/86 Dosierung: 70kg lose / 86kg/m3 fest
Wassergehalt:	5.2 %
Chargenprotokoll:	111240
Probenbezeichnung des Kunden:	165.999.1
Bemerkungen:	Kunde: Anliker AG Meierhö
	Baustelle: Zementstabilisierung

Druckfestigkeit	SN640509a	Prüfkörper : *Proctor AAHSTO Standard*

Serie Bezeichnung	: 165.999.1	Prüfer	: Vö
Herstelldatum	: 05.03.2007 / 00:00	Probenalter	: 7 Tage 12:42
Prüfdatum	: 12.03.2007 / 12:42	Probenalter nominal :	Tage

Probenbezeichnung	Abmessungen [mm]		Masse	Rohdichte	Bruchlast	Festigkeit
	d	h	[g]	[kg/m³]	[kN]	[N/mm²]
1	101.2	116.2	1998.0	2137.7	15.8	2.0

Prüfung: 1

Die Prüfergebnisse beziehen sich ausschliesslich auf die in diesem Prüfbericht zugrunde liegenden Prüfgegenstände. Kopie auszugsweise nicht erlaubt.
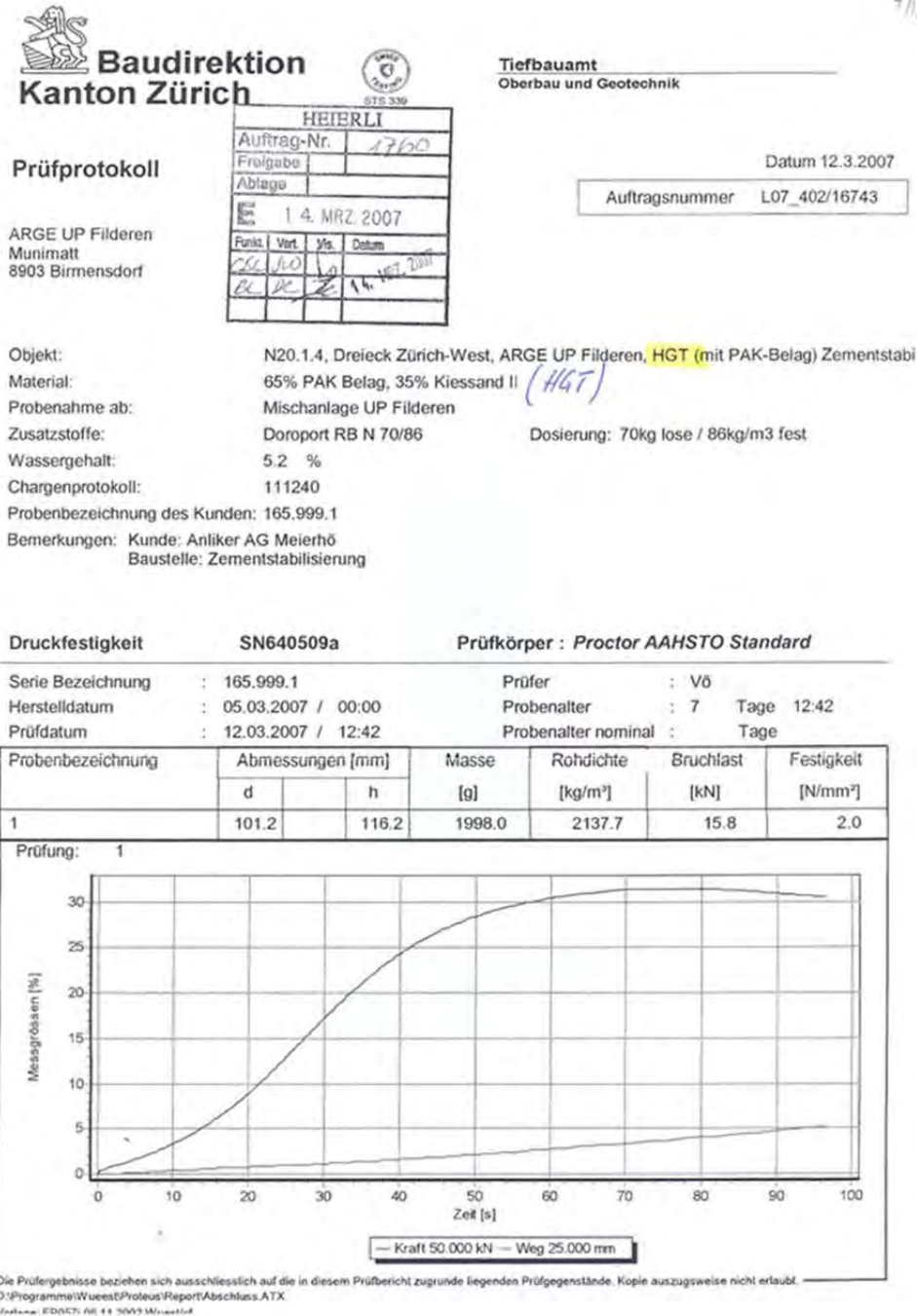D:\Programme\Wueest\Proteus\Report\Abschluss.ATX

Fig. I.15 Compression tests of the cement stabilized material layer

II   Test site 3: Neue Staffeleggstrasse – Results of construction control tests

II.1   Static plate bearing tests

Technische Forschung und Beratung für Zement und Beton

Service de recherches et conseils techniques en matière de ciment et béton
Ricerca e consulenza tecnica per cemento e calcestruzzo
Technical Research and Consulting on Cement and Concrete
Öffnungszeiten: Mo.-Fr.: 7.30-12.00; 13.30-17.00

CH-5103 Wildegg
Lindenstrasse 10
Telefon 062 887 72 72
Fax 062 887 72 70
E-Mail info@tfb.ch

ME direkt : 062 887 72 75
me@tfb.ch

Prüfbericht:

Plattendruckversuch E_v und M_E gemäss SN 670 317b / SOP 3080

Messung mit TFB-LKW als Gegengewicht

Projekt-Nr.:	**106033-01**	
Objekt:	**Tunnel Horental - Staffeleggzubringer**	
Messort:	**Küttigen NK106**	
Witterung:	Tunnel	
Bodenart:	Kies/Sand	
Wassergehalt Boden:	erdfeucht	

Messdatum:	04.03.2010
Beginn erste Messung:	07:40 h
Ende letzte Messung:	13:00 h
Temperatur:	2.1 °C
Korngrösse max.:	63 mm
Prüfung durchgeführt:	ub

Messung 1-6	Erstbelastung						Entlastung			Zweitbelastung				
	1	2	3	4	5	6	E1	E2	E3	1	2	3	4	5
Spannung [MN/m²]	0.05	0.15	0.25	0.35	0.45		0.25	0.12	0.01	0.05	0.15	0.25	0.35	
Setzung [mm]	0.12	0.59	0.87	1.18	1.40		1.40	1.39	1.13	1.14	1.25	1.38	1.45	
Spannung [MN/m²]	0.05	0.15	0.25	0.35	0.45		0.25	0.12	0.01	0.05	0.15	0.25	0.35	
Setzung [mm]	0.23	0.40	0.58	0.74	0.93		0.93	0.92	0.84	0.85	0.85	0.89	0.93	
Spannung [MN/m²]	0.05	0.15	0.25	0.35	0.45		0.25	0.11	0.01	0.05	0.15	0.25	0.35	
Setzung [mm]	0.22	0.53	0.78	1.13	1.34		1.33	1.30	1.09	1.09	1.15	1.23	1.30	
Spannung [MN/m²]														
Setzung [mm]														
Spannung [MN/m²]														
Setzung [mm]														
Spannung [MN/m²]														
Setzung [mm]														

Verlangter M_{E1}-Wert:	nach SN 670'317 b	100 MN/m²	auf Fundationsschicht
	nach SN 670'317 a	(100'000) kN/m²	im Bereich 0.15 - 0.25 MN/m²

Messung Nr.	Profil	E_{V1} [MN/m²]	E_{V2} [MN/m²]	M_{E1} [MN/m²]		[kN/m²]	M_{E2} [MN/m²]	[kN/m²]	M_{E2}/M_{E1} [-]	
13	Block 54/55	67.5	222.8	85.2	!	(107'100)	281.9	(230'800)	3.31	!
14	Km. 1960	129.7	680.7	173.6	ok	(166'700)	1080.6	(750'000)	6.22	!
15	Km. 2040	78.3	312.2	103.1	ok	(120'000)	423.9	(375'000)	4.11	!

Beurteilung der Messwerte:
- M_{E1}:   ok = verlangter M_{E1}-Wert erreicht; ! = verlangter M_{E1}-Wert nicht erreicht
- M_{E2}/M_{E1} = f_E: ok = f_E-Wert erreicht; ! = f_E-Wert nicht erreicht (SN 640 585b, Tab. 1, Strassenbau)

Bemerkungen:

3080aPBd-07 Juli 05   106033-01c.xlsx / 05.03.2010   Seite 1 von 2

Fig. II.16 Static plate bearing tests results of the subgrade.

Technische Forschung und Beratung für Zement und Beton

Service de recherches et conseils techniques en matière de ciment et béton
Ricerca e consulenza tecnica per cemento e calcestruzzo
Technical Research and Consulting on Cement and Concrete

CH-5103 Wildegg
Lindenstrasse 10
Telefon 062 887 72 72
Fax 062 887 72 70
E-Mail info@tfb.ch

Projekt-Nr.:	106033-01	Messdatum :	04.03.2010
Objekt:	Tunnel Horental - Staffeleggzubringer	Beginn 1. Messung:	07:40 h
Messort:	**Küttigen NK106**	Ende letzte Messung:	13:00 h
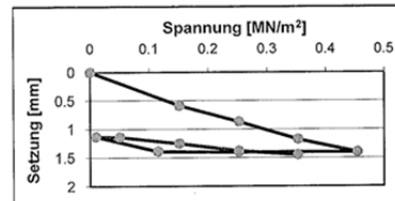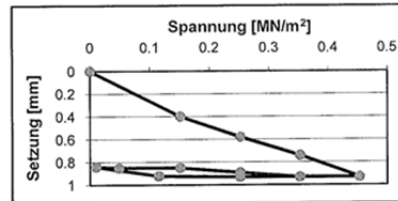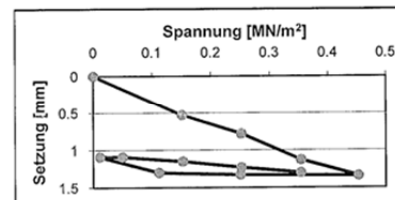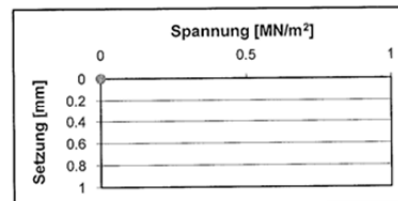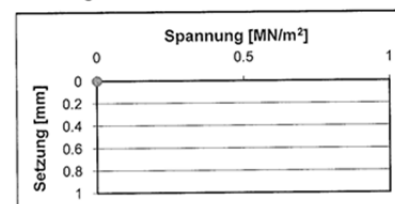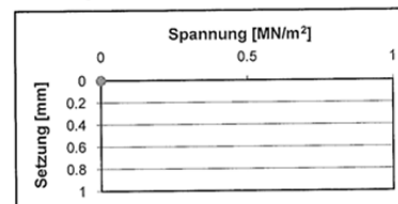
Wildegg, 5. März 2010   ME-Messungen: S. Gumann

Bei Messungen mit dem TFB-LKW als Gegengewicht erfolgt die Setzungsmessung elektronisch. Bei Handmessungen (Gegengewicht bauseitig) ist die Setzungsmessung mechanisch. Für die Plattenunterlage wird trockener Sand verwendet. Die Prüfergebnisse haben nur Gültigkeit für die untersuchten Stellen am Bauobjekt. Die Laststufen sind der jeweiligen Verwendung des untersuchten Bodens (Trag-schicht, Fundation, Planum bzw. Unterbau) angepasst und können auf speziellen Wunsch bei der TFB nachgefragt werden.
Dieser Bericht darf nicht auszugsweise kopiert werden. Das Auftragsdossier wird während 13 Jahren archiviert. Der Auftraggeber kann die Dienstleistungen innerhalb von 30 Tagen beanstanden. Bitte beachten Sie die "Allgemeinen Geschäftsbedingungen". Weitere Informationen: www.tfb.ch.

STS 133

3080aPBd-07 Juli 05   106033-01c.xlsx / 05.03.2010   Seite 2 von 2

Fig. II.17 Static plate bearing tests results of the subgrade. (cont.)

II.2 Asphalt mixes: particle size distribution.

CONSULTEST AG

Institut für Materialprüfung, Beratung
und Qualitätssicherung im Bauwesen

SWISS TESTING
STS 091

Deisrütistrasse 11
CH - 8472 Ohringen
Tel 052 335 28 21
Fax 052 335 28 24

Seite 1 von 1

Prüfbericht : Mischgutuntersuchung

Hinweis : Die Prüfergebnisse beziehen sich ausschliesslich auf die aufgeführten Prüfgegenstände.

Objekt:	NK107 Küttigen AO, Neue Staffeleggstrasse, Knoten Bibersteinerstr.-Knoten Küttigen Nord	
Auftraggeber:	**Kanton Aargau : BVU / ATB**	Auftrag-Nr.: **3051-09**
Oberbauleitung:	**RE / BT / lms**	Labor-Nr.: **10051**
Bauleitung:	**IG PEB Preisig AG, Zürich**	

Probe*:	SMA 11	Probenahme durch:	Consultest AG
Aufbereitungsanlage*:	AMW Grenzach-Wylen	Probenahme Datum / Zeit:	01.10.2009 / 10.00 h
Lieferschein-Nr.*:	-	Mischguttemperatur:	166 °C
Entnahmeort:	km 2.120 links	Probeeingang:	01.10.2009
Unternehmer:	Tozzo AG	Prüfdatum:	02.10.2009

Bindemittel   Art / Sorte*:   PmB 40/80-65 (CH-E) Dosierung* -   lösl. Anteil: **6.07** !   Masse-%
EN 12697-1

Zusätze   Art / Menge*:   Kalkhydrat

* Angaben Dritter

Korngrössenverteilung   EN 12697-2   **SMA 11**

Prüfsieb [mm]	Durchgang Masse-%
45	
31.5	
22.4	
16	100.0
11.2	95.3
8	47.6
5.6	33.9
4	27.3
2	22.1
1	16.8
0.5	13.5
0.25	11.1
0.125	9.2
0.063	7.7

Marshall-Versuch   Verdichtungstemperatur: 155 °C

Raumdichte	EN 12697-6	2'344	kg/m³			
Rohdichte (bestimmt)	EN 12697-5	2'420	kg/m³	Stabilität	S	9.8 kN
Hohlraumgehalt	EN 12697-8	3.1	Vol-% (2 - 5 %)	Fliessen	F	3.2 mm
HM-Füllungsgrad	EN 12697-8	82	%	EN 12697-34		

Eigenschaften des rückgewonnenen Bindemittels

Erweichungspunkt R. u. K.   -   °C
EN 1427

Penetration bei 25°C   -   1/10 mm
EN 1426

Penetrationsindex PI   -
EN 12591

Departement
Bau, Verkehr und Umwelt
Abteilung Tiefbau / Unterhalt
FS Belags- + Geotechnik
12.10.09 HS

Bemerkungen: -

Datum / Unterschrift Sachbearbeiter
02.10.2009

1200a PB, V03.09

Fig. II.18 Aggregate size distribution of the top layer.

CONSULTEST AG

Institut für Materialprüfung, Beratung
und Qualitätssicherung im Bauwesen

STS 091

Deisrütistrasse 11
CH - 8472 Ohringen
Tel 052 335 28 21
Fax 052 335 28 24

Seite 1 von 1

Prüfbericht : Mischgutuntersuchung

Hinweis : Die Prüfergebnisse beziehen sich ausschliesslich auf die aufgeführten Prüfgegenstände.

Objekt:	**K107 Küttigen IO, Neue Staffeleggstrasse**		
Auftraggeber:	**Kanton Aargau : BVU / ATB**	Auftrag-Nr.:	**918-09**
Oberbauleitung:	**RE / BT / lms**	Labor-Nr.:	**3233**
Bauleitung:	**IG PEB Preisig AG, Zürich**		

0 5. Juni 2009

Probe*:	AC T 22 H	Probenahme durch:	Consultest AG
Aufbereitungsanlage*:	AMW Grenzach-Wylen	Probenahme Datum / Zeit:	08.05.2009 / 8.45 h
Lieferschein-Nr.*:	526112	Mischguttemperatur:	168 °C
Entnahmeort:	km 2.120	Probeeingang:	08.05.2009
Unternehmer:	ARGE Erne AG / Tozzo AG, Laufenburg	Prüfdatum:	11.05.2009

Bindemittel   Art / Sorte*:   PmB 25/55-65 (CH-E) Dosierung* -   lösl. Anteil: **4.05** Masse-%
EN 12697-1

Zusätze   Art / Menge*: -

* Angaben Dritter

Korngrössenverteilung   EN 12697-2   AC T 22 H

Prüfsieb [mm]	Durchgang Masse-%
45	
31.5	100.0
22.4	97.5
16	76.8
11.2	65.7
8	53.9
5.6	45.3
4	38.2
2	27.0
1	19.8
0.5	14.9
0.25	10.9
0.125	7.8
0.063	6.1

Marshall-Versuch

				Verdichtungstemperatur:		155 °C	
Raumdichte	EN 12697-6	2'358	kg/m³				
Rohdichte (bestimmt)	EN 12697-5	2'511	kg/m³	Stabilität	S	16.3	kN
Hohlraumgehalt	EN 12697-8	6.1	Vol-% (4-7%)	Fliessen	F	3.1	mm
HM-Füllungsgrad	EN 12697-8	60	%	EN 12697-34			

Eigenschaften des rückgewonnenen Bindemittels

Erweichungspunkt R. u. K. EN 1427	-	°C	
Penetration bei 25°C EN 1426	-	1/10 mm	
Penetrationsindex PI EN 12591	-		

Departement
Bau, Verkehr und Umwelt
Abteilung Tiefbau / Unterhalt
FS Belags- + Geotechnik
29.5.09 MS

Bemerkungen: ersetzt Prüfbericht vom 11.05.2009

Datum / Unterschrift Sachbearbeiter
28.05.2009

1200a PB, V03.09

Fig. II.19 Aggregate size distribution of the binder course.

CONSULTEST AG

Institut für Materialprüfung, Beratung
und Qualitätssicherung im Bauwesen

SWISS TESTING
STS 091

Deisrütistrasse 11
CH - 8472 Ohringen
Tel 052 335 28 21
Fax 052 335 28 24

Seite 1 von 1

Prüfbericht : Mischgutuntersuchung

Hinweis : Die Prüfergebnisse beziehen sich ausschliesslich auf die aufgeführten Prüfgegenstände.

Objekt:	**K107 Küttigen IO, Neue Staffeleggstrasse**		
Auftraggeber:	**Kanton Aargau : BVU / ATB**		Auftrag-Nr.: **942-09**
Oberbauleitung:	**RE / BT / lms**		Labor-Nr.: **3300**
Bauleitung:	**IG PEB Preisig AG, Zürich**		

Probe*:	AC B 16 S	Probenahme durch*:	Tozzo AG
Aufbereitungsanlage*:	AMW Grenzach-Wylen	Probenahme Datum / Zeit*:	09.05.2009 / 9.00 h
Lieferschein-Nr.*:	526187	Mischguttemperatur*:	176 °C
Entnahmeort*:	km 2.120 West	Probeeingang:	11.05.2009
Unternehmer*:	ARGE Erne AG / Tozzo AG, Laufenburg	Prüfdatum:	18.05.2009
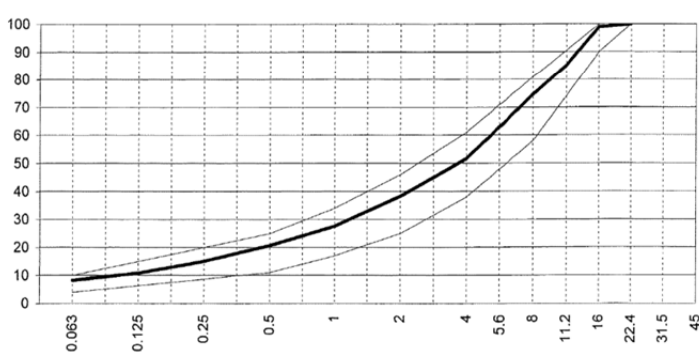
Bindemittel Art / Sorte*: 50/70   Dosierung* -   lösl. Anteil: **5.05** Masse-%
EN 12697-1

Zusätze Art / Menge*: -

* Angaben Dritter

Korngrössenverteilung EN 12697-2   **AC B 16 S**

Prüfsieb [mm]	Durchgang Masse-%
45	
31.5	
22.4	100.0
16	98.9
11.2	85.1
8	74.6
5.6	62.9
4	51.7
2	38.3
1	27.5
0.5	20.7
0.25	15.0
0.125	10.8
0.063	8.3

Marshall-Versuch Verdichtungstemperatur: 135 °C

Raumdichte	EN 12697-6	**2'404**	kg/m³			
Rohdichte (berechnet)	EN 12697-5	**2'481**	kg/m³	Stabilität	S	**13.1** kN
Hohlraumgehalt	EN 12697-8	**3.1**	Vol-% *(3 - 6 %)*	Fliessen	F	**3.4** mm
HM-Füllungsgrad	EN 12697-8	**79**	%	EN 12697-34		

Eigenschaften des rückgewonnenen Bindemittels

Erweichungspunkt R. u. K. EN 1427	-	°C
Penetration bei 25°C EN 1426	-	1/10 mm
Penetrationsindex PI EN 12591	-	

**Departement
Bau, Verkehr und Umwelt**
Abteilung Tiefbau / Unterhalt
FS Belags- + Geotechnik
2o.5.o9 HS

Bemerkungen: -

Datum / Unterschrift Sachbearbeiter
19.05.2009

1200a PB, V03.09

Fig. II.20 Aggregate size distribution of the base course.

CONSULTEST AG

Institut für Materialprüfung, Beratung und Qualitätssicherung im Bauwesen

SWISS TESTING
STS 091

Deisrütistrasse 11
CH - 8472 Ohringen
Tel 052 335 28 21
Fax 052 335 28 24

Seite 1 von 1

Prüfbericht : Mischgutuntersuchung

Hinweis : Die Prüfergebnisse beziehen sich ausschliesslich auf die aufgeführten Prüfgegenstände.

Objekt:	NK107 Küttigen IO, Neue Staffeleggstrasse	
Auftraggeber:	Kanton Aargau : BVU / ATB	Auftrag-Nr. 495-09
Oberbauleitung:	RE / BT / lms	Labor-Nr.: 2330
Bauleitung:	IG PEB Preisig AG, Zürich	

Probe*:	KMF 22	Probenahme durch:	Consultest AG
Aufbereitungsanlage*:	Recycling-Center Frick	Probenahme Datum / Zeit:	03.04.2009 / 9.30 h
Lieferschein-Nr.*:	-	Mischguttemperatur:	-
Entnahmeort:	Trassebau Nord	Probeeingang:	03.04.2009
Unternehmer:	Tozzo AG	Prüfdatum:	07.04.2009

Bindemittel Art / Sorte*: - Dosierung* - lösl. Anteil: **7.66** Masse-%
EN 12697-1

Zusätze Art / Menge*: -

* Angaben Dritter

Korngrössenverteilung EN 12697-2 **KMF 22**
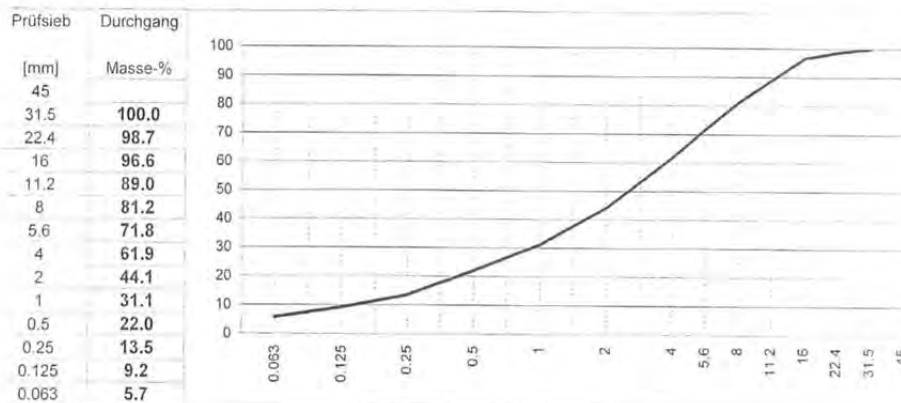
Prüfsieb [mm]	Durchgang Masse-%
45	
31.5	100.0
22.4	98.7
16	96.6
11.2	89.0
8	81.2
5.6	71.8
4	61.9
2	44.1
1	31.1
0.5	22.0
0.25	13.5
0.125	9.2
0.063	5.7

Marshall-Versuch

Verdichtungstemperatur: -

Raumdichte	EN 12697-6	-	kg/m³
Rohdichte (berechnet)	EN 12697-5	-	kg/m³
Hohlraumgehalt	EN 12697-8	-	Vol-%
HM-Füllungsgrad	EN 12697-8	-	%

Stabilität S - kN
Fliessen F - mm
EN 12697-34

Eigenschaften des rückgewonnenen Bindemittels

Erweichungspunkt R. u. K. EN 1427	-	°C
Penetration bei 25°C EN 1426	-	1/10 mm
Penetrationsindex PI EN 12591	-	

**Departement
Bau, Verkehr und Umwelt**
Abteilung Tiefbau / Unterhalt
FS Belags- + Geotechnik
14.04.09

Bemerkungen: **Wassergehalt : 7.1 M-%** ✓

Datum / Unterschrift Sachbearbeiter
07.04.2009

1200a PB, V03.09

Fig. II.21 Aggregate size distribution of the sub-base course.

II.3   Control of compaction KMF

CONSULTEST AG
Institut für Materialprüfung, Beratung und Qualitätssicherung im Bauwesen

SWISS TESTING

STS 091

Deisrütistrasse   11
CH - 8472   Ohringen
Tel   052 / 335 28 21
Fax   052 / 335 28 24

Verdichtungskontrolle mit Troxler Isotopensonde
SN 670 335a

Objekt:	NK107 Neue Staffeleggstrasse Trassebau Nord
Auftraggeber:	Kanton Aargau : BVU / ATB
Oberbauleitung:	RE / BT / lms
Bauleitung:	F. Preisig AG
Unternehmer:	Tozzo AG

Auftrag-Nr.: 509-09

**Departement
Bau, Verkehr und Umwelt**
Abteilung Tiefbau / Unterhalt
FS Belags- + Geotechnik
14.04.09

Messdatum:	03.04.2009
Messstelle:	siehe Tabelle
Messtiefe:	Oberfläche
Material:	KMF 22 ab Recycling-Center Frick

H₂O-Gehalt: -
[%] (Sollwert)

Trockenrohdichte: 2185
[kg/m³] (Sollwert)

Mess-punkt	Profil [m]	ab Axe links	ab Axe rechts	D feucht [kg/m³]	D trocken [kg/m³]	Wassergehalt [%]	Verdichtungsgrad [%]	Sättigungsgrad [%]
1	2075	3		2067	1963	5.3	89.8	38
2	2100		2	2013	1906	5.6	87.2	36
3	2125	x		2031	1903	6.7	87.1	43
4	2150	2		2108	2010	4.9	92.0	39
5	2175	4		2033	1927	5.5	88.2	37
6	2200		4	2081	1932	7.7	88.4	52
7	2225		2	2075	1989	4.3	91.1	33
8	2250	1		2136	2042	4.6	93.5	39
9	2275	3		2070	1935	7.0	88.5	48
10	2300		3	2167	2070	4.7	94.7	42
11	2325		1	2067	1970	4.9	90.2	36
12	2350	2		2163	2016	7.3	92.3	58
13	2375	4		2119	2018	5.0	92.4	40
14	2400	x		2046	1954	4.7	89.4	33
15	2425		4	2061	1980	4.1	90.6	30
16	2450		2	1997	1884	6.0	86.2	37
17	2475	1		2233	2097	6.5	96.0	61
18	2500	3		2030	1911	6.2	87.5	41
19	2525		3	2048	1930	6.1	88.3	41
20	2550		1	2066	1964	5.2	89.9	37
21	2575	2		2118	1968	7.6	90.1	55
22	2600	4		1978	1831	8.0	83.8	46

5301 PB, Version 5   509-09   Seite 1 von 2

Fig. II.22 Compaction of the sub-base course.
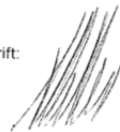
Mess- punkt	Profil [m]	ab Axe links	ab Axe rechts	D feucht [kg/m³]	D trocken [kg/m³]	Wassergehalt [%]	Verdichtungsgrad [%]	Sättigungsgrad [%]
23	2625	x		2052	1932	6.2	88.4	42
24	2650		4	2082	1985	4.9	90.8	37
25	2675		2	2008	1900	5.7	86.9	37
26	2700	1		2064	1929	7.0	88.3	47
27	2725	3		2133	1997	6.8	91.4	52
28	2750		3	2037	1909	6.7	87.4	44
29	2775		1	2299	2163	6.3	99.0	68
30	2800	2		2029	1886	7.6	86.3	48

	Mittelwert	2080	1963	6.0	89.9	43.2

Bemerkungen: -

Datum: 06.04.2009   Unterschrift:

Departement
Bau, Verkehr und Umwelt
Abteilung Tiefbau / Unterhalt
FS Belags- + Geotechnik

5301 PB, Version 5   509-09   Seite 2 von 2

Fig. II.23 Compaction of the sub-base course (cont.).

III   Publications

III.1   APT congress in Davis, California (2012), paper 1

Initial tests results from the MLS10 Mobile Load Simulator in Switzerland

M. Arraigada & M.N. Partl
Empa, Swiss Federal Laboratories for Materials Science and Technology, Duebendorf, Switzerland

A. Pugliessi
ITYAC S.A., Rosario, Argentina

ABSTRACT: The Mobile Load Simulator (MLS10) is a new type of Accelerated Pavement Testing (APT) equipment recently purchased by Empa, Swiss Federal Laboratories for Materials Science and Technology. This paper summarizes the results of the first calibration tests of the MLS10 in Switzerland. The objective was to evaluate the performance of the machine for testing pavements constructed with local materials under local guidelines. The focus of the study was the structure of the A4 motorway near Zürich. Three pavements were constructed and trafficked with a total of 1.6 million 65 kN load passes over a period of approximately seven months. To access the structural response throughout the loading history, the pavements were instrumented with different sensors. Transverse profiles of the surface were periodically taken. Falling Weight Deflectometer (FWD) and static deflection bowl measurements were taken before, during, and after trafficking to evaluate the structural condition. Finally, pavement samples were obtained from the section and tested in the laboratory. The pavement response was analyzed and validated with a model using the Finite Element Method (FEM). At the end of the tests almost no sign of distress was observed, showing the durability of the pavement.

1   INTRODUCTION

1.1   *Background and motivation*

In 2006, the University of Stellenbosch in South Africa developed a prototype APT device. In 2008 the Swiss Federal Laboratories of Material Science and Technology (Empa) purchased the prototype device, known as the MLS10 Mobile Load Simulator, a new APT technology that can apply 6,000 unidirectional load applications in one hour. This device is composed of four loading bogies running in a closed loop and powered by contactless linear induction motors (LIM) (Partl and Arraigada, 2011). Further, the machine is mobile and can be transported on standard low bed trucks. It also has the ability to move autonomously at walking speed to change position within the testing site. With the MLS10 it is possible to consider real climatic and construction conditions.

Since no previous experience with a mobile load simulator of this type was available in Switzerland, an experimental project to evaluate the performance of the machine with pavements constructed following local guidelines, with local materials and construction was planned. The primary objective was to test a typical Swiss pavement in order to know how many MLS10 loading cycles were necessary to produce distress in the structure. In addition, it was expected that these tests would provide some basic information about the design norms used in the country.

A second but equally important objective was to learn the operation of the MLS10 itself, detect possible operational shortcomings and technical defects, and to improve the performance of the machine, which is a prototype and the first of its class in the world.

Finally, the project was used to propose and evaluate pavement testing procedures as well as instrumentation and software to collect research data. Establishment and formalization of the data handling, formatting, processing, storage and backup protocols and software was also a goal.

A new motorway was chosen for the experiment. A dedicated testing site was constructed using the same materials and design used in the Zürich A4 motorway, considering four variations, as explained in the next section. The site was located just beside the motorway area to keep subgrade materials and climate as close as possible to real conditions.

Due to the restricted time window, problems with the prototype machine, and the lack of experience of the personnel in charge of the tests, the number of load repetitions applied to the test sections was limited to 1.6 million over a period of approximately seven months. Testing was carried out on three of the four test sections.

277
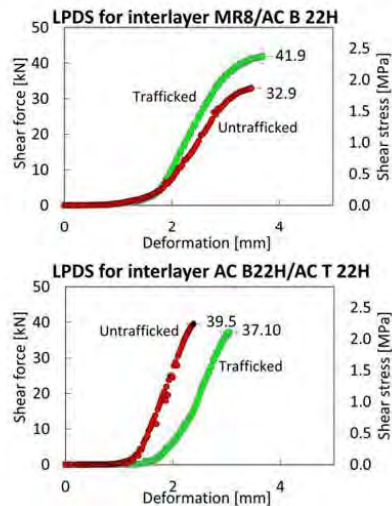
Figure 13. Comparison of the LPDS for both interlayers and loading condition.

Figure 14. Geometry of the FE model.

Figure 15. On left, the FE calculated strains. In the window, the measured strain. (Strain gauge BL4).

Figure 16. On left, the FE calculated strains. In the window, the measured strain. (Strain gauge BQ4).

possible to specify a coefficient of friction and tangential contact stiffness normal to the surfaces involved. It is also possible to select whether the simulated layers are bonded, creating a situation where no relative motion between them is possible.

An eight-node cubic element linear C3D8R was used to define the mesh. This form allows defining a refined element mesh directly under the load footprint and setting the number of elements in each direction of the model. In the last form Job + Visualization, the user can name the simulation and select the type of solver to use for resolution.

Figure 14 presents the FE model geometry for the Section F4 test. The four layers of the structure are displayed in different colors. By having similar characteristics, stabilized granular layer bonding (HGT) is considered as a single 400 mm (180 mm + 220 mm). The overall dimensions of the model are 2,250 mm long and 2,000 mm wide. These dimensions were defined during different runs to achieve an appropriate balance between accuracy and computation. The computing time for these models was on the order of four hours.

The mesh was designed to provide greater definition in areas where a reasonable accuracy is required. In total, 13,662 items were used to define the geometry of the pavement.

Figures 15 and 16 present two examples of calculated and measured strains. Figure 15 shows longitudinal strains at −30 mm depth with a pavement temperature of approximately 20° C. The curve calculated with the FE model is on the left. The window on the right shows one measured loading cycle. In Figure 16 the curve shows transverse strains for the same temperature and position.

Table 6 summarizes the results of the strain (absolute values) for each case: the real, as an average of several measurements, and the simulated for the same mentioned conditions of load speed and pavement temperature. The results show that, although there are still differences between the measured and calculated values, they are small and the model developed here can be used to estimate the pavement response. Further research on this topic will be presented elsewhere (Pugliessi, in prep.).

284

Table 6.   Summary of measured and simulated strains.

Modeled strains ($\mu\varepsilon$)		Simulated strains ($\mu\varepsilon$)	
Longitudinal	Transverse	Longitudinal	Transverse
10	60	11	42

6   SUMMARY AND CONCLUSIONS

The main goal of the activities summarized in this paper was to calibrate the MLS10 which is a prototype for which there was no previous experience in Switzerland. To that end, the objective was to use MLS10 to traffic a typical Swiss pavement structure until signs of distress were observed. However, due to limited testing time, this objective could only be partially fulfilled, as there was no conclusive sign of distress shown in the data presented. An exception was the interlayer bonding between the top and second layers, where results show that bonding increased after MLS10 trafficking. FWD measurements on Section F4 also showed that relative deflection increased in the trafficked zone, which can be understood as the initiation of a distress mechanism in the structure. Almost no rutting was recorded on any of the sections, with measured deformation never exceeding 2 mm. It is interesting to note that rutting was worst on the pavement with multiple bituminous layers (Section F4). This shows that the permanent deformation resulted mostly from compaction of the asphalt layers and did not occur in the stabilized and subgrade layers.

Experience gained over the seven-month test period was, however, the most valuable offering of the project. During this time many shortcomings of the MLS10 were identified and improved. Instrumentation, data acquisition and analysis were all accomplished successfully, given that all sensors worked as required.

Finally, the development of a FE model capable of simulating the MLS10 loading with increasing accuracy was another asset of this project.

REFERENCES

Partl, M.N. and Arraigada, M. 2011. Der neue Mobile Load Simulator (MLS10), *Strasse und Autobahn* 62(4):252–257 April 2011.

Pugliessi, A. in prep. *Relationship between Mobile Load Simulators MMLS3 and MLS10*, M Eng thesis, National University of Rosario (UNR), Argentina.

Raab, C. and Partl, M.N. 2008. Investigation on Long-Term Interlayer Bonding of Asphalt Pavements. *Baltic Journal of Road and Bridge Engineering*. 3(2):65–70.

Rabaiotti, C., Partl, M.N., Caprez, M. and Puzrin, A.M. 2008. APT device evaluation for road research in Switzerland: test campaign on a Swiss Highway with the MLS10, *3rd International Conference on Accelerated Pavement Testing*, Madrid October 2008.

VSS, 1997. *Schweizer Norm (SN) 640324a: Dimensionierung Strassenaufbaus, Unterbau und Oberbau*. Schweizerischer Verband der Strassen- und Verkehrsfachleute (VSS) VSS-Expertenkommission 5.03.

VSS, 2000. *Schweizer Norm (SN) 670461: Bituminöses Mischgut – Bestimmung des Schichtenverbunds (nach Leutner)*. Schweizerischer Verband der Strassen- und Verkehrsfachleute (VSS) VSS-Expertenkommission 5.09.

VSS, 2008. Schweizer Norm (SN) 640430b: Walzasphalt – Konzeption, Ausführung und Anforderungen an die eingebauten Schichten. Schweizerischer Verband der Strassen- und Verkehrsfachleute (VSS). VSS-Expertenkommission 5.01.

285
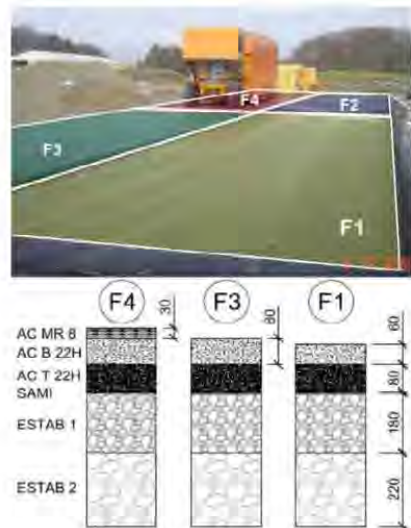
Figure 1. Layout of the sections and layers of the three pavements trafficked with the MLS10.

In situ tests were carried out to establish the subgrade properties before starting with trafficking. In order to evaluate the pavement deterioration, pavement response to MLS10 loading was monitored using strain gauges and accelerometers, as described later. Since temperature cannot be controlled while loading, several temperature sensors were installed in the structure. Other non-destructive pavement testing procedures were carried out on a regular basis, as described later.

After completion of trafficking of the sections, the pavement was cored and samples were tested in the laboratory. Parameters including temperature dependent elastic modulus and interlayer bonding between the asphalt layers of the trafficked and non-trafficked areas were assessed.

The analysis of all of these combined data was used to establish the degree of deterioration of the structure after APT with the MLS10. A finite element model was prepared to evaluate the stress conditions under load and compared with measured values.

2 EXPERIMENTAL SETUP

2.1 Test section layout and construction

The test site was constructed in September 2008 and comprised four different test sections. Each section consisted of a rectangular area 20 m × 5 m, totaling a paved surface of 10 m × 40 m, as shown in Figure 1a. The materials used in each section (Figure 1b)

correspond to a heavy duty full-depth asphalt pavement described in the Swiss Norms (VSS, 1997; VSS, 2008). This pavement is the thickest structure in the design catalogue, prepared for the highest traffic loading calculated in Switzerland. The difference between each of the four sections was the number of layers. Section F4 was constructed following the exact design of the motorway pavement. Section F3 was built in the same way as Section F4, but without the top layer (AC MR 8). Finally, Section F1 was constructed with no top and second layers (AC B 22H). The base layer of all sections (AC T 22H) was placed on top of a stress absorbing membrane interlayer (SAMI) separating the asphalt layers from the two cement stabilized layers of 18 cm and 22 cm thickness, respectively. The concept behind test plan was to compare the response of each of the structures to evaluate the validity of the design norms. Each of the pavements in Section F1, Section F3 and Section F4 corresponds to a Structural Number (SN) of 128, 160 and 172, respectively.

For the tests, the MLS10 was regularly moved through the testing site to have, on average, the same temperature profile in each section. Due to time restrictions, Section F2 was not trafficked and therefore, is not discussed in this paper.

2.2 Subgrade and base layer material properties

During pavement construction, standard tests were carried out to evaluate the subgrade and base course performance. Load bearing capacity tests on the subgrade and compressive strength of the cement stabilization were performed prior to construction of the pavement.

2.3 Test section instrumentation

The response and deterioration of the pavement was evaluated using different methods. Sensors were installed in the structure to monitor the temperature of the materials and measure the deformation and deflection under the MLS10 loading. A schematic of the location of the sensors with their names is depicted in Figure 2 (only for Section F4). The name and the installation depth in all sections are shown in Table 1. Deflection was measured indirectly using capacitive accelerometers (A41 to A43 in the figure). Strain gauges were installed during construction to monitor deformation between the asphalt layers (BQ4, TQ4, BL4 and TL4). No strain gauges were installed in Section F1.

Kyowa (120 mm long) strain gauges were used. These are covered with acrylic and use three conductors for compensating resistance change due to temperature. The cables of the original sensor were changed for stranded silver-plated copper wires with Teflon insulation, capable of withstanding the high temperatures of the hot asphalt concrete during construction. Data acquisition was done with a *Spider 8* system. *Catman* software was used to control the system. Data was collected continuously and recorded every five minutes.

278
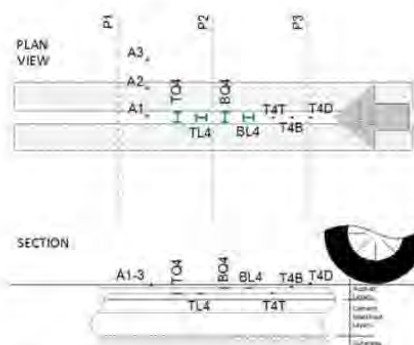
Figure 2. Schematic of the position of the sensors in Section F4.

Table 1. Location and naming of the sensors.

Section	Temp.	Depth (cm)	Strain gauge	Depth (cm)	Direction
F1	T1T	0	-	-	-
	T1S	-8	-	-	-
F3	T3B	0	TQ3	-8	
	T3T	-8	TL3	-8	
F4	T4D	0	BQ4	-3	
	T4B	-3	BL4	-3	
	T4T	-11	TQ4	-11	
	-	-	TL4	-11	

2.4 Periodic measurements

Permanent deformation of the structure was evaluated during periodic measurements with a profilometer in three transverse locations along the wheel path (P41 to P43 in Figure 2). Rutting profiles for each pavement were then calculated. Visual inspections of the pavement surface were carried out simultaneously with the profile measurements.

2.5 Non-destructive tests

Two types of non-destructive tests were carried out, before, during and after trafficking (Table 2). A Falling weight deflectometer (FWD) was used to measure pavement deflection using a grid of 45 points distributed in an area of 12 m × 2.5 m. Deflection bowl measurements were also taken with an ETH Delta device, which determines the deflection bowl produced by a static axle load. It has 12 high precision lasers that measure the rebound of the road surface

Table 2. Date and number of MLS10 load repetitions for each non-destructive test.

Date (2009)	FWD tests			ETH delta tests		
	Section					
	1	3	4	1	3	4
29/06	0	0	353,000	–	–	–
15/09	188,000	427,000	396,000	–	–	–
16/09	–	–	–	188,000	427,000	396,000
22/10	439,000	427,000	550,000	–	–	–
10/11	–	–	–	439,000	–	740,000

when the loading axle moves away from the device (Rabaiotti, 2008). Measurements were taken in both the trafficked area and outside the trafficked area. Results are in the form of three dimensional deflection bowls that can be compared or can be used for backcalculation purposes.

3 TEST PROGRAM

The MLS10 is able to apply a maximum load of 65 kN, corresponding to a full-scale axle load of 130 kN. It can be converted to an equivalent single axle load with a destructive amplification factor of 8.46. In theory, to simulate 20 years of traffic it would be necessary to load the pavement with 8,630,000 MLS10 load repetitions. The goal of the first phase of the test program was to apply 3 million MLS10 65 kN load repetitions and after this, decide if an extension of the test period was required to fulfill the main objective of the project. Unfortunately, due to reasons already explained, a total of only 1,606,000 load applications were reached before the end of the project time period. Of that total, the load applications were distributed in each of the sections as summarized below:

- Section F1: 439,000 load repetitions
- Section F3: 427,000 load repetitions
- Section F4: 740,000 load repetitions

For these tests, the MLS10 was equipped with Goodyear 455/50 R22.5 dual tires. The speed of the moving tires was 22 km/h. In order to test under similar temperature profiles and have the results comparable, the machine was moved regularly from one section to the other.

4 DATA ANALYSIS AND INTERPRETATION

4.1 Temperature

Table 3 summarizes the average temperatures measured for the duration of the tests. The first column presents the total average temperature in the entire testing period whereas the second column considers only the temperature measured when the MLS10 was in

279

Table 3. Temperature in each section.

Sensor	Average temperature (°C)	Average temperature while trafficking (°C)
T4D	22.6	23.4
T4B	22.8	20.3
T4T	22.5	18.7
T3B	23.2	28.5
T3T	23.8	29.6
T1T	19.7	27.5
T1S	20.0	23.8
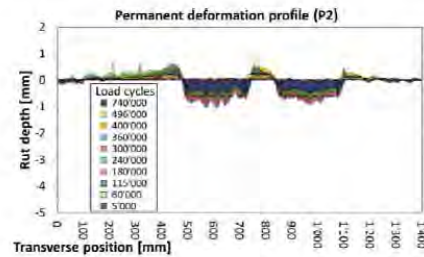
Figure 3. Example of one transverse pavement profile for different trafficking intervals.
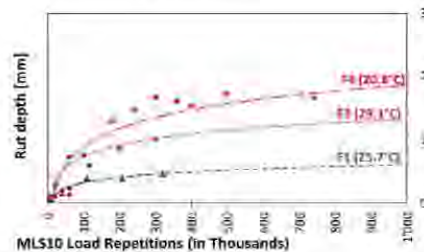
Figure 4. Progressive comparative rutting of all the sections.

service. Average surface temperatures in Section F3 were the highest of all sections, whereas Section F4 recorded the lowest temperature with 23.4°C.

4.2 Transverse pavement profile

Pavement permanent deformation for each section was calculated by analyzing the three profiles taken with the MLS profilometer. Figure 3 presents the accumulated deformation of the pavement surface of profile P42, corresponding to the second profile of Section F4. Figure 4 shows the progressive rutting in terms of load applications for all the test sections. The curves extrapolated to one million loading cycles show very small rutting depths of less than 2 mm for all sections trafficked. Section F4 had the highest rutting,
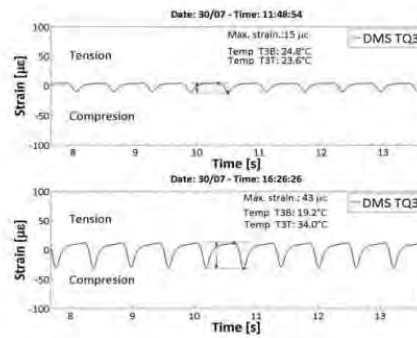
Figure 5. Deformation measured with the TQ3 strain gauge showing the deformation with increase in pavement temperature.
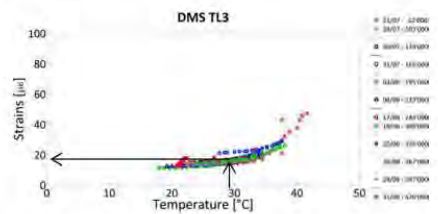
Figure 6a. Temperature dependent absolute deformation obtained with sensor TL3. Every marker type represents a day and a certain number of MLS10 loads.

despite the pavement having the most layers and lowest temperature during the tests.

4.3 Strain gauges

In order to analyze the deformation obtained with the strain gauges it was necessary to take into account the influence of speed of the MLS10 loads and the pavement temperature. Measurements were filtered and only those records taken at a trafficking speed of 22 km/h were considered. Temperature change during the day and the influence of tire friction on temperature were both taken into consideration as they both had an effect on strain under the same load, as shown in the example in Figure 5.

The average difference between tension and compression peaks was calculated for every valid file recorded and stored in a table together with the measured temperature, the timestamp and the number of accumulated loads. Then, for every day with records, curves of temperature dependent deformation were drawn and fitted with sigmoidal functions (Figure 6a). By repeating this procedure for everyday of the test, it was possible to build deformation curves dependent of the number of trafficking loads. An average temperature for all measurements was determined and the

280
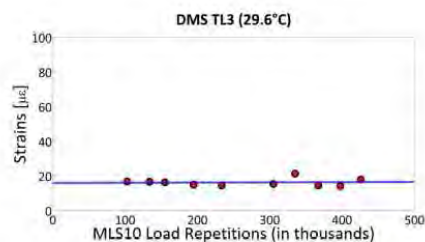
Figure 6b. Deformation vs. number of MLS10 load repetitions for average temperature.
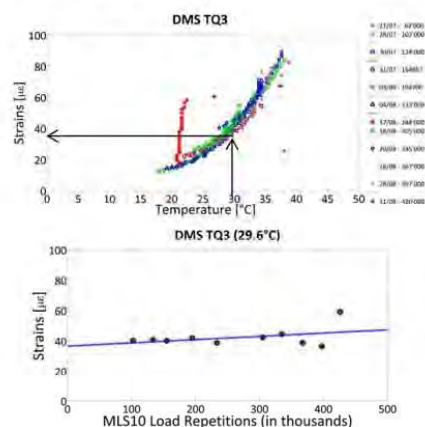
Figure 7. Strain gauge analysis for TQ3.

Figure 8. Strain gauge results for BL4 and BQ4.

The investigation revealed that no clear change could be detected in Section F1. On Section F4, however, relative deflection increased on the trafficked sector. Unfortunately, no further data could be collected in order to confirm this tendency.

4.5 *ETH Delta*

The data obtained with the ETH Delta device was used to prepare three-dimensional (3-D) deflection maps. Deflection maps for Section F1 and Section F4 are provided Figure 10 and Figure 11, respectively.

The shape and order of magnitude of the deflection bowls do not show clear signs of change after being trafficked. It can be seen that the amount of load repetitions were insufficient to induce a change in the structural response.

4.6 *Laboratory tests*

Bituminous layers on all sections were cored. No evaluation of the cement stabilized layers or subgrade was done after trafficking.

Laboratory testing on the three top layers included indirect tensile tests and evaluation of interlayer bonding.

4.6.1 *Indirect tensile test*

Temperature dependent elastic moduli of the bituminous layers were calculated for six cores taken from the wheel path and outside the trafficked area. An average elastic modulus for each condition was calculated and compared. Results are presented in Table 4 and Figure 12, and show that the difference between both loading conditions was negligible.

deformation was again calculated. This deformation was then plotted against the accumulated number of loads (Figure 6b). By evaluating the data in this way, it was possible to reduce the influence of temperature in the results.

Other calculations for Section F3 and Section F4 are presented in Figure 7 and Figure 8, respectively.

None of the strain gauge measurements showed a significant change in the deformation values. This can be interpreted as evidence that the structures tested with the MLS10 did not show any kind of distress after trafficking.

4.4 *Falling weight deflectometer*

Data obtained with the FWD was used to prepare deflection maps of the areas were the tests were carried out. This area, about 12 m long and 2.5 m wide had the MLS10 loading sector in its center (wheelpath). By taking the maximum deflection of each point of the measurement grid, the authors expected to identify relatively weak zones in the scoped area. Deflection maps for Section F1 and Section F4 are shown in Figure 9.

281

Figure 9. 3-D deflection maps for FWD tests on Section F1 and Section F4. The footprint of the dual tires is marked in the centre of the area.
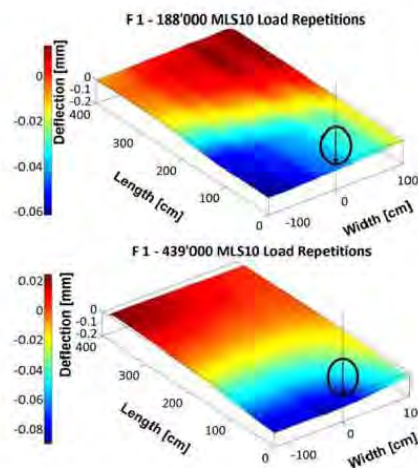
Figure 10. 3D deflection measured with ETH Delta for two trafficking conditions on Section F1.
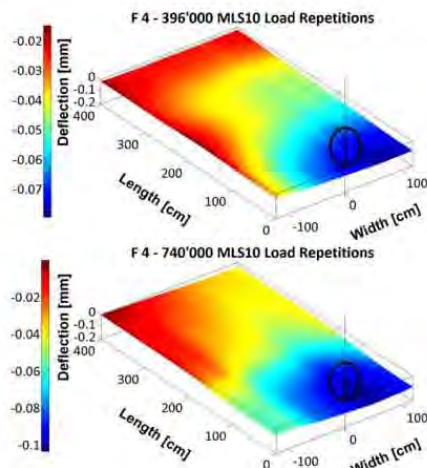
Figure 11. 3-D deflection measured with ETH Delta for two trafficking conditions on Section F4.

4.7 Interlayer bonding

Four cores taken from the loaded area were tested with the layer parallel shear test (LPDS) according to Leutner (VSS, 2000), and then compared with results obtained from untrafficked cores. Two interlayers were analyzed: between MR8 and AC B 22 H (top and second course) and between AC B 22 H and AC T 22 H. The results, summarized in Table 5, and plotted in Figure 13, show that the MR8 and AC B 22 H interlayer properties improved after trafficking. This confirms earlier research findings on this topic (Raab and Partl, 2007).

282

Table 4. Elastic moduli of the top layers.

Layer	Temp. (°C)	Non-trafficked (MPa)	Trafficked (MPa)	Difference %
AC MR8	5	9,543	9,395	1.6
	10	6,900	6,622	4.0
	15	4,442	4,594	−3.4
	20	3,435	3,481	−1.3
	25	2,367	2,449	−3.5
	30	1,128	1,187	−5.2
	35	859	871	−1.4
AC B22 H	5	18,948	19,490	−2.9
	10	14,668	13,561	7.5
	15	9,925	10,700	−7.8
	20	7,348	7,647	−4.1
	25	4,856	5,019	−3.4
	30	3,268	3,247	0.6
	35	2,231	2,175	2.5
AC T22 H	5	20,248	19,865	1.9
	10	15,985	14,279	10.7
	15	11,295	11,109	1.7
	20	8,060	7,927	1.7
	25	5,170	5,058	2.2
	30	3,522	3,332	5.4
	35	2,315	2,235	3.5

5 FINITE ELEMENT MODEL

In this section, a finite element (FE) model of the experimental phase is briefly discussed. The goal was to establish a relationship between the measured deformation on the test sections and the stress-strain field of the structure. The simulation attempts to represent as closely as possible the conditions of load dimension (footprint), speed, temperature of the structure, materials, etc. To that end, the commercial finite element software *ABAQUS* was used.

To take field conditions into consideration, a plug-in of *ABAQUS 6.8* was developed. A GUI (Graphical User Interface) coded in *Python* was used to generate and simulate the experiments automatically, as detailed below.

The GUI form was created in a way that the parameters were incorporated in each field through the different tabs. Data entry was arranged by completing five different forms, related to different stages of the organization of the model. The names of the forms, which are activated by selecting the appropriate tab are: Geometry and Materials, Loads, Interactions, Element Types + Mesh and Job + Visualization. This plug-in has the ability to create a structure of four layers with different thicknesses.

The material properties of each layer are stored in a file establishing a library of materials. A drop down menu in the materials form allows access to the list of materials available in the library. The form also allows incorporation of the influence of temperature in each layer separately.
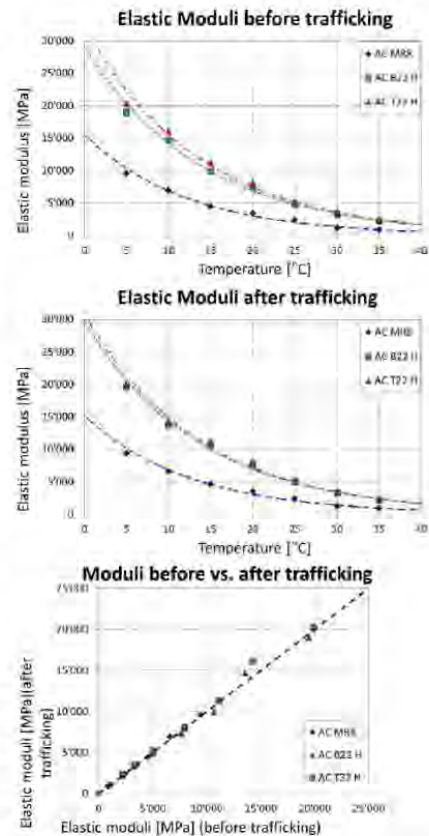
Figure 12. Top two diagrams show the moduli of trafficked and non-trafficked cores. Bottom diagram shows a comparison of both modules, with good correlation.

Table 5. Average results of the LPDS.

Parameter	MR8-AC B 22H		AC B 22H-AC T 22H	
	Trafficked	Un trafficked	Trafficked	Un trafficked
Load (kN)	41.9	32.9	37.1	39.5
Tension (kN/m²)	2,373.0	1,864.3	2,099.5	2,235.3
Deform. (mm)	2.7	2.2	1.5	1.3

Loads were also stored in a load library. The GUI user chooses from a menu of loads of different type, shape, amplitude and speed. In the Interactions menu, different types of contact models are chosen. It is

283

III.2   APT congress in Davis, California (2012), paper 2

International case studies in support of successful applications of accelerated pavement testing in pavement engineering

F. Hugo
Stellenbosch University, Stellenbosch, South Africa

M. Arraigada
Swiss Federal Laboratories for Materials Science and Technology, Switzerland

L. Shu-ming
Tongji University, Shanghai, China

T. Zefeng
Communication Research Institute of Liaoning Province, China

R.Y. Kim
Construction and Environmental Engineering, North Carolina State University, US

ABSTRACT: Accelerated Pavement Testing (APT) offers a unique proven methodology to investigate performance of different material and pavement structures under various conditions. Case studies using Mobile Load Simulator (MLS) equipment provide well-documented information in support of this statement. The international selection of typical cases provides pavement engineers (and managers) insight into some of the lessons learned and application of the knowledge gained in respect of distress and failure mechanisms. Case studies from China, Europe, and United States are presented. These cover applications of asphalt materials including pavement surfacing, stone matrix asphalt, Guss asphalt, and full-depth asphalt. Trafficking under wet and dry as well as artificially heated conditions, are discussed. Structural compositions include a steel bridge deck surfacing, a full-scale and comparative scaled pavement, and a sandy subbase subjected to the influence of a high water table. The paper reports on a synthesis of facets of analyses and findings from the case studies including both laboratory and field applications.

1 INTRODUCTION

At the Third International Accelerated Pavement Testing (APT) Conference in 2008, the findings of three APT case studies were reported and discussed by Hugo et al., (2008). The same procedure was used in a paper presented at the recent Conference on Asphalt Pavements in Southern Africa (CAPSA) conference in South Africa for reporting on a number of APT case studies (Hugo et al., 2011). In particular, the effect of slow moving traffic resulting in harsh operational conditions for asphalt materials was discussed. It was apparent that there was considerable benefit gained from conducting syntheses of APT studies.

Full-scale Mobile Load Simulator (MLS) equipment, developed after the 2006 MLS prototype, was recently used for APT studies in Europe and China during 2009 and 2010. In two of the case studies, the one-third scale model mobile load simulator (MMLS3) was incorporated in the studies. The findings that were reported by the respective researchers provide noteworthy information (Pugliessi et al., 2010). This paper will provide a synthesis of the findings from selected case studies. It will include a review of findings from an earlier Accelerated Loading Facility (ALF) study in the USA that was linked to APT with the MMLS3. The information should provide a useful basis for application by pavement design engineers. The case studies were selected to relate to monitoring and evaluation of distress and failure mechanisms impacting on pavement performance in APT studies.

Fifteen distress mechanisms that were identified in the course of the synthesis study are shown in Table 1. The extent of this is apparent. Twelve of these features in the case studies were selected for discussion in this paper.

Details pertaining to each of the case studies will not be presented except where appropriate for the purpose of supporting the conclusions in the case study. Readers are referred to the respective references that were reviewed for more information. The broad spectrum of the distress mechanisms covered by the case studies is apparent from the extent to which each relates to a number of distress or failure mechanisms.

93

Table 1. Summary of distress and failure mechanisms relating to pavement performance identified during the APT case studies

Distress/failure mechanism	Case study/location				
	1 – CRILP Bridge deck	2 – CRILP HMA study	3 – EMPA Full-depth HMA	4 – NCSU Fatigue study	5 – Tongji Full-depth HMA
Fatigue cracking		X			
Stiffness				X	X
GPR response (voids)			X		
Debonding	X				
Response	X	X	X		X
Friction loss	X				
Surface degradation	X	X			
Rutting/deformation	X	X	X		
Scaled performance			X	X	X
Heating	X	X			X
Bleeding		X			
Stripping	X	X			
Water table					X

Against the background of the case studies in Table 1, the following primary objectives were selected for review:

Evaluation of surfacing options for a steel bridge deck in China (CS1).
Trafficking of stiff full-depth pavements under both wet and dry conditions as well as artificially heated conditions in China (CS2) and Switzerland (CS3).
Comparison of fatigue distress on a model pavement and a full-scale test pavement in USA (CS4).
Influence of a high water table on the structural performance of a stiff full-depth pavement in China (CS5).

Details relating to the respective APT facilities will not be presented unless required for better understanding of the respective case studies. In this regard the following general information relating to the full-scale MLS testing system is provided.

2 MLS APT EQUIPMENT

The MLS full-scale equipment is fully described on the MLS website (www.mlstestsystems.com), but can be summarized as follows:

Two full-scale machine sizes are available, MLS10 and MLS66. The operational systems are identical except for the respective lengths of the machines. The MLS66 has six bogies with load wheels, while the MLS10 has four. They have similar test wheel load capacity but, due to the differences in length, the MLS10 only has one load wheel on the pavement surface at a time.

The MLS66 has two load wheels on the pavement for part of the rotational cycle. The system comprises an endless chain of test wheels rotating in a vertical plane at nominally 22 km/h. The bogie chain is housed in a structure with travelling wheels back and front

and is capable of manoeuvring on the test site using a hydraulic powered motor. The structural shell can be lifted to allow testing and inspection of the pavement during stoppages. Heaters can be used internally to heat and control the pavement to a maximum surface temperature of 70°C. The pavement can also be wetted artificially to simulate rain conditions during trafficking. The entire machine can be shifted sideways during trafficking by hydraulic power to simulate lateral wander of traffic. The load on the pavement can be monitored as the bogie traverses the test section and the pavement surface can be monitored to track surface deformation.

The full-scale MLS machines have been utilized for APT studies in Mozambique, South Africa, Switzerland, Austria, and China. In several instances the studies included the use of the MMLS3 a one-third scaled version of the MLS to supplement the full-scale APT. In the same vein the MMLS3 has been used in conjunction with other full-scale APT equipment such as the Accelerated Load Facility (ALF) and the Heavy Vehicle Simulator (HVS).

3 CASE STUDY 1: BRIDGE DECK SURFACING IN LIAONING PROVINCE, CHINA

The Communication Research Institute of Liaoning Province (CRILP) in China acquired a MLS66 full-scale and a one-third scale MMLS3 machine. These were delivered in August 2009. Two major contract studies have been completed by CRILP to date. The details in their reports on the projects serve as the basis for the first two case studies discussed below.

3.1 Study background

The steel bridge deck surfacing (SBD) project was undertaken to compare the performance of two types

94
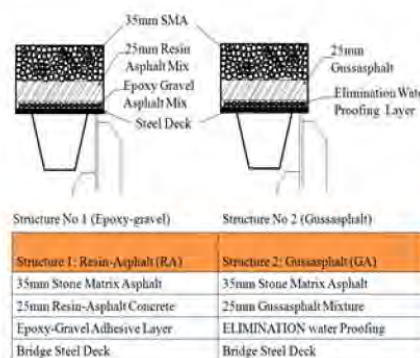
Figure 1. Details of the bridge deck surfacing tested in the Shenyang laboratory in Liaoning.

Figure 2. Typical transverse pavement profile of the two adjacent overlays relative to trafficking intervals.

Figure 3. Comparative rutting of RA and GA on the BDS under MLS66 trafficking.

of pavement surfacing for the deck of a steel bridge that will serve for the coastal road crossing the Liao River. This was the first full-scale APT study by CRILP. The SBD-project was carried out indoors in the CRILP laboratory in Shenyang.

The project client built the bridge section before the formal test and the suppliers of the two pavement types placed the layers on the steel deck of the bridge section between March and June, 2010. A schematic of the construction is shown in Figure 1.

The surfacing layers tested were a Liaoning rut resistant resin asphalt concrete (RA) and Guss asphalt (GA). The latter is a high temperature mix, hot poured asphalt extensively used in Germany. After placement it cools to an impervious deformation resistant layer.

The objective of the test was to compare performance of the two pavement structures for rut-resistance, water-proofing and skid resistance. A special foundation pit was excavated in the laboratory floor with retaining walls alongside to enable the MLS66 to travel longitudinally. The suspended bridge sections were supported at both ends. After completion of the bridge structure, 2.9 million APT load applications were applied on the two surfacings.

3.2 Test results

Figure 2 shows one of the transverse pavement profiles after zero, 100,000, 600,000, 1.1 million, 1.5 million, 2.3 million, and 2.9 million 75 kN load repetitions on dual tires mounted on each of the six bogies. Profiles of the respective pavements on the deck were recorded with the MLS profilometer and calculated.

The progressive rutting in terms of load applications on the two bridge surfacings is shown in Figure 3. There was a "step" jump in the curves between 1.1 and 1.3 million repetitions. This was due to the effect of different temperatures applied during the test. The first 800,000 load applications were applied at ambient temperature (i.e. $10 - 25°C$) and the next 400,000 load applications at $45°C$. The pavement profile did not
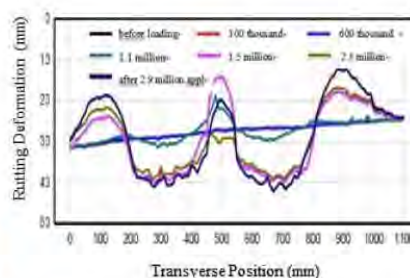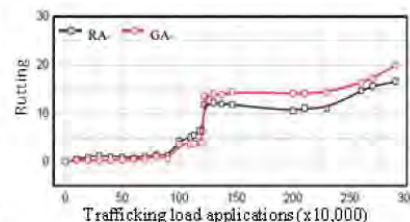
change as much as expected during this period, and the temperature was therefore increased to $55°C$. At this temperature, the rutting rate increased suddenly and consequently the temperature was reduced back to $45°C$ until completion of the test.

3.3 Findings from the SBD surfacing performance

Findings from the SBD surfacing study include:

- The rut-resistant resin-asphalt pavement structure had better comparative rutting performance than the Guss-asphalt pavement.
- The artificial heating successfully controlled the testing conditions.
- Waterproofing and skid resistance of the two structures was similar.
- There was no evidence of stripping but the Guss-asphalt showed some evidence of bleeding.
- There was no evidence of debonding of the pavement layers.

3.4 Case study 1 conclusions

The following conclusions were drawn from the study:

- The study provided confidence for selecting the rut-resistant resin-asphalt pavement structure as the better surfacing for the bridge, subject to economic evaluation.

95

— The APT test protocol was considered reasonable as a basis for similar future studies.
— The testing efficiency of the project was considered cost-effective in terms of time and lessons learned.

4 CASE STUDY 2: TWO HIGHWAY ASPHALT PAVEMENT STRUCTURES IN LIAONING PROVINCE, CHINA

This project was the first field APT after the MLS66 arrived in Liaoning. The project site is located in Xinbin County, Liaoning Province.

The project compared the performance of two highway structures; a rubberized asphalt pavement and a conventional provincial highway pavement. Details on the two test sections constructed are summarized in Table 2. Four test sections were displaced longitudinally and constructed adjacent to each other.

Trafficking was conducted under ambient conditions on each pavement structure with no temperature control. This was followed by a limited number of load applications on sections of each pavement structure under controlled temperature with traffic wander. The test site and equipment is shown in Figure 4 and test results are summarized in Table 3.

4.1 Findings from structural performance

The two pavement structures were evaluated in terms of rut-resistance, fatigue-resistance, and shoving

under comparable conditions. Direct comparisons between the two sections could not be made because of the different pavement structures; however the following observations were made:

— The conventional section had better performance in terms of rut-resistance than the rubberized asphalt section under channelized trafficking.
— Shoving performance was similar on both sections.
— The rubberized asphalt exhibited cracking after about 1.7 million load applications (Figure 5). In contrast there was no cracking on the conventional section.

Table 3. Case Study 2 rutting performance summary.

Test details	Temp. (°C)	Repetitions	Max. Rut Depth (mm)
Conventional			
Ambient temp.	8~41	2,240,000	8
Controlled temp.	45	110,000	4
	50	360,000	15
Total repetitions		2,710,000	
Rubberized asphalt			
Ambient temp.	3~40	2,200,000	20
Controlled temp.	35	13,000	12
	45	20,000	17
	55	24,000	23
Total repetitions		2,257,000	

Figure 5. Close-up view of transverse crack on rubberized asphalt.

Figure 4. MLS66 on the RubAP/LAC test sections at Nanzamu.

Table 2. Case Study 2 test section description (on in situ subgrade with resilient modulus not less than 70 MPa).

Layer		Material and layer thickness (mm)			
		Conventional (LAC) 730 mm		Rubber Asphalt (RubAP) 540 mm	
Asphalt	Upper	Stone matrix asphalt-13L (13 mm)	35	Rubber asphalt (ARAC-16)	50
Surface	Middle	LAC-20 (20 mm)	60		
	Lower	LAC-25 (25 mm)	80		
Seal coat		Slurry seal on emulsified asphalt prime	5	Rubber asphalt chip seal	10
Binder course				Graded crushed macadam	120
Subbase		Cement stabilized macadam	200	Cement stabilized macadam	180
Bottom subbase		Cement stabilized sand and gravel	200	Cement stabilized sand and gravel	180
Cushion layer		Graded sand gravel	150		

96

– The performance provided useful information on failure mechanisms of the two pavement structures and differences in performance provided good information for exploring fatigue designs for the two pavement systems.

– The rubberized asphalt experiment provided adequate performance to justify further research on the use of this material. It also exposed the team to aspects of construction quality that need to be monitored.

5 CASE STUDY 3: STIFF FULL-DEPTH PAVEMENTS IN SWITZERLAND

This case study focuses on a synthesis of data obtained through the interactive relationship between full-scale and scaled APT with specific emphasis on the strains in the top asphalt layer. It relates to field APT trials by the Federal Institute for Materials Testing and Research (EMPA) as a part of its efforts to gain confidence in its ability to conduct APT with the MLS10 it had acquired. In a joint venture between EMPA and the National University of Rosario (UNR) in Argentina, MMLS3 tests were used to evaluate the ability of the scaled trafficking system to measure strains under the scaled wheel load for comparison with strains that were measured under the full-scale trafficking (Pugliessi et al., 2010; Pugliessi, 2011).

5.1 Study background

Three pavement structures were constructed near the A4 Westring motorway close to Zürich (Figure 6), and instrumented with horizontal strain gauges, temperature sensors, and accelerometers. The primary purpose of the study was to evaluate the response and performance of a heavy duty full-depth asphalt pavement subjected to trafficking by an MLS10.

A series of 120-mm long *Kyowa* strain gauges were installed (transversal and longitudinal) 30 mm and 110 mm deep in the asphalt during the construction of the test sections (Figure 7). The three sections were tested with the MLS10 (Arraigada et al., 2012).

After completion of the tests a 190 mm asphalt slab was cut from Section F4 (Figure 8) of the full-scale pavement and transported to the laboratory for temperature conditioning and subsequent MMLS3 testing. A 10 mm interlayer of cement/sand mix was spread between the 190 mm asphalt block and an underlying 300 mm concrete block prior to seating the slab on it. The slab was instrumented to measure strains (Figure 9). The MMLS3 was then straddled over the asphalt block for trafficking (Figure 10).

The strain gauges were reconnected and the block tested at different temperatures and speeds, under limited load applications. Only strain measurements were

Figure 7. Strain gauges prior to asphalt covering.

Figure 8. Extraction of asphalt slab from test pavement.

Figure 9. Cables for monitoring strains under lab trafficking.

Figure 6. Schematic of three pavement structures at Filderen (Pugliessi et al., 2010).

97

Figure 10. MMLS3 trafficking of extracted slab.

Table 4. Input parameters for *BISAR* linear-elastic analyses of MMLS3 and MLS10 wheel loads.

Temp. °C	Layer stiffnesses for *BISAR* analyses (MPa)		
	Layer 1	Layer 2	Layer 3
1,200 reps/hour (both machines)			
20	1,000	3,000	3,000
25	870	2,200	2,230
35	700	1,500	1,500
7,200 reps/hr (MMLS3), 6,000 reps/hr (MLS10)			
20	3,480	7,645	7,930
25	2,480	5,020	5,060
35	870	2,200	2,230

MMLS3 Wheel Load: 2.1 kN at 600 kPa.
MLS10 Wheel Load: 65 kN at 800 kPa.

taken since rutting was minimal and stresses were not considered. Comparisons were made between the strains measured under the scaled and full-scale tests and those predicted by analytical procedures, specifically finite element analyses and *BISAR* linear elastic analyses (Pugliessi, 2011; Arraigada et al., 2012).

Strain data under MLS10 trafficking were collected at different ambient temperatures (no artificial heating was used) and trafficking speeds. In contrast, the MMLS3 trafficking was done at predetermined temperature levels. The temperature was controlled manually at the predetermined levels.

Cores from the test pavement samples were tested in the laboratory to measure indirect tensile stiffness of the asphalt under different temperatures and trafficking frequencies.

Elastic strains were analyzed with *BISAR*, using the input parameters listed in Table 4. Results are summarized in Tables 5 and 6 (Partl and Arraigada, 2011; Arraigada et al., 2012).

5.2 *Summary of findings*

Findings from the study are summarized as follows:

– All strains increased as the temperature was increased, as expected.

– At 20°C and trafficking at 1,200 reps/hr and 7,200 reps/hr, all measured longitudinal strains under full-scale and MMLS3 were closely related to values calculated by *BISAR*. The Indirect Tensile stiffness measurements by Pugliessi (2011) according to EN 12697-26 (2004) Annex C were used as input data for the analyses.

– At 25°C and 35°C and 7,200 reps/hr the longitudinal strain correlation was slightly less than those recorded at 20°C.

– At 25°C and 35°C and 1,200 reps/hr, the discrepancy between calculated and measured MMLS3 longitudinal strains became much larger especially as the temperature increased. The reason for this is not clear and requires further investigation. No 1,200 reps/hr tests were done under MLS10 trafficking.

– At 20°C, 25°C, and 35°C at 7,200 reps/hr, the transverse strains under MMLS3 trafficking were closely related to values that were calculated by *BISAR*. In contrast the transverse strains under MMLS3 trafficking at 1,200 reps/hr did not correlate as well.

– The transverse strains under the MLS10 did not correlate at any of the three temperatures at 6,000 reps/hr. Furthermore, the discrepancy increased as the temperature increased. The reason for this was not investigated.

– It is, however, noteworthy that this is somewhat similar to the response of the longitudinal strain under the MMLS3 at 25°C and 35°C. The increase in strain in both scenarios (MLS10 and MMLS3) would naturally lead to harsh conditions for rutting performance. In the one case due to increased temperature but in the other also as a result of slow trafficking. The importance of performance evaluation under slow heavy trafficking is apparent (Hugo et al., 2011).

– From a critical surveillance of the data in Table 5, the question arose whether some of the discrepancies between strains could be related to the strain gauges being slightly out of line. To evaluate this hypothesis, strains were measured with the MMLS3 offset 50 mm from the identified gauge positions. The elastic strains were calculated to reflect measurement 4 mm on either side of the identified position as well as on it. The analytical calculated strain values were used as a guideline for estimating the perceived position of the gauges. It was concluded that the strain gauges were about 4 mm further from the identified position (i.e. at 54 mm).

5.3 *Case study 3 conclusions*

There was close agreement between measured and calculated strains under both MMLS3 and MLS10 trafficking. It was apparent that the strain measurements at a depth of 30 mm under the MMLS3 trafficking, were compatible with strains that had been measured under the full-scale MLS10 at the same

98

Table 5. Measured and calculated strains under MMLS3 wheel centre and between MLS10 dual tires (longitudinal and transverse).

Temp (°C)	Calculated Strain (με)		Measured Strain (με)		Calculated Strainr (με)		Measured Strain (με)	
	Long.	Trans.	Long.	Trans.	Long.	Trans.	Long.	Trans.
MMLS3	1,200 repetitions/hour				7,200 repetitions/hour			
20	−56	56	−66	30	−20	−20	−23	22
25	−74	74	−121	54	−30	−30	−43	32
35	−104	104	−207	105	−74	−74	−77	67
MLS10	1200 reps/hr				7200 reps/hr			
20	−28	−28	Not	Not	−8	15	−12	87
25	−38	−38	tested	tested	−14	22	−15	143
35	−57	−57			−38	51	−23	382

Table 6. Comparative MMLS3 strains with machine off-set from strain gauge (measured and calculated).

Temp (°C)	Offset (mm)	Stiffness* (MPa)	Calculated Strain (με)		Measured Strain (με)		Measured Strain (με)	
			Long.	Trans.	Long.	Trans.	Long.	Trans.
MMLS3			3,600 reps/hour		2,720 reps/hour		4,240 reps/hour	
20	46	2,200	−14	14				
	50		−12	14	−9	9	−8	8
	54		−10	14				
25	46	2,200	−19	18				
	50		−16	20	−13	15	−10	11
	54		−14	19				

*Layer stiffness: 2,200 MPa/5,000 MPa/5,500 MPa

depth in the pavement structure. This is considered to be a significant advance in the knowledge required to be able to monitor strain levels within pavement structures under MMLS3 trafficking. Overall, the findings serve as a basis for application in asphalt pavement evaluation and related future research.

6 CASE STUDY 4: FATIGUE PERFORMANCE AND CRACKING

Fatigue performance is a primary aspect that normally requires extensive trafficking that can become expensive. As a result such tests are generally fewer in number. Failure mechanisms related to cracking include changes in stiffness of the structure, and debonding. In an APT study of the performance of a pavement that was constructed at the FHWA Turner-Fairbank Highway Research Center in McLean, Virginia (Kim, 1997), stress wave tests were conducted on a 100 mm thick pavement with an AC-5 surface layer. Trafficking was carried out with the FHWA Accelerated Load Facility (ALF).

In a subsequent study of a scaled pavement using the MMLS3 at North Carolina State University, Lee (2003), compared the trend of the stress wave results on a local pavement structure to those reported by Kim and Kim (1996). Figure 11 compares the phase velocities at the center of the wheel-trafficked area and the cumulative crack length in terms of the number of wheel applications for both the MMLS3 and ALF. It can be seen that the phase velocity (and therefore AC stiffness) decreases as the number of loading cycles increase in both cases of the MMLS3 and ALF.

6.1 Findings related to the full-scale and scaled APT fatigue

The physical characteristics of the performance of the two pavements were very similar. This is evident from the study findings.

Figure 11 demonstrates that prior to the appearance of visible surface cracks, after 125,000 load applications, the phase velocities had already significantly reduced. The reduction in phase velocity indicates that the structural degradation in the model pavement test is similar in character, although at a somewhat slower initial rate than observed for the ALF results. This observation suggests that the proposed non-destructive evaluation technique (NDE) using stress wave technique measurements (WCM) could be successfully implemented to investigate fatigue damage evaluation especially for thin AC layers and overlays.

This process may allow the optimum time for maintenance/rehabilitation of a thin AC layer pavement to be determined before cracks appear on the pavement surface.

99
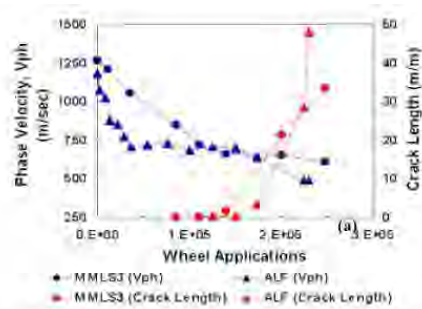
Figure 11. Phase velocity and cumulative surface crack length as a function of wheel applications (Lee, 2003).

The early reduction is attributed to structural degradation of the pavements due to the initiation, propagation, and densification of micro-cracks (Kim and Kim, 1996). Figure 11 also demonstrates that the phase velocity decreases significantly prior to appearance of surface macro cracks. This observation suggests that the optimum time for maintenance/rehabilitation may be long before cracks appear on the pavement surface. Lee and Kim (2004) commented on this phenomenon and stated that the optimum time may be better determined by the change in the phase velocity than by a visual condition survey of the pavement surface. Similar findings were reported by (Lee et al., 1997) in full-scale studies with the TxMLS on Highway 59 in Victoria, Texas where PSPA was used.

6.2 Case study 4 conclusions

It is apparent that transfer of findings between APT systems is feasible and likely to be cost beneficial provided the test systems are compatible. Furthermore, the available tools for monitoring progressive change during APT trafficking are invaluable for detecting micro-fracturing before distress becomes visible at the surface.

7 CASE STUDY 5: FULL-DEPTH ASPHALT PAVEMENTS ON SAND SUBGRADE IN CHINA

The Tongji University MLS66 was initially commissioned in the new APT laboratory. Subsequently it was deployed to conduct a field test to determine the effect of a variation in the water table depth on rutting of a full-depth asphalt pavement supported by cement stabilised subsurface layers. An experimental pavement was constructed on the G40 highway on Chong-ming Island. This highway will connect Shanghai and the inland city of Xi'an. The scope of the experiment included evaluation of the performance of a fine sand subbase with a high water table in the pavement structure. The fine sand is abundant in this region, but it has not been widely used as road subbase.

7.1 Background to the field study

The APT project was undertaken in July, 2010. The APT experiments involved both full-scale MLS66 and the MMLS3 tests. Comprehensive details pertaining to the MLS66 study are presented in the paper by Wu et al. (2012). The laboratory MMLS3 tests were used to assist with the selection of appropriate asphalt mixes for the study.

The test pavements were constructed concurrently as Track I and II. Both had similar asphalt and cemented layers. These were supported on imported fine sand subbase layers placed on a graded macadam layer overlying the in situ clay. Track I had a 1.5 m sand layer and Track II a 3 m sand layer. After construction, the average ground water table was about 2 m below the pavement surface.

The asphalt structure consisted of a surface layer of 40 mm SMA-13 (PG70 penetration grade) binder modified with SBS mixed rubber particles), an intermediate layer of 80 mm AC-20C (modified with 15% by weight rock asphalt), and 80 mm AC-25C (modified with 20% rock asphalt). The bitumen content of the natural rock asphalt was on average 22.3% with a penetration value of 6.1 and a softening point of 84.5°C. The binder in the AC-20C and AC-25C layers was unmodified PG70. The rock asphalt was added during mix production.

The imported base consisted of 540 mm aggregate stabilized with 4% cement. The top 600 to 800 mm of the sand subbase was treated with 3.5% cement, giving the material a resilient modulus of at least 40 MPa. The sand layers were compacted to 93% of laboratory density.

Trafficking with the MLS66 was carried out with an axle load of 75 kN, which is 50% heavier than the standard axle load in China, and a tire pressure of 800 kPa. The MMLS3 laboratory study was done on gyratory compacted briquettes in the conventional test bed, and 2.8 kN axle load and 710 kPa tyre pressure. Four asphalt mixtures were evaluated namely SMA13, OGFC13, AC13 and AC20 (AC is a traditional dense-graded asphalt mixture and the number in the mix type represents the maximum nominal aggregate size in mm). Track I was heated intermittently during trafficking. Track II was tested at ambient temperature.

7.2 Test results

The following test results are relevant to the context of this case study. Readers are also referred to (Wu et al. 2012) for more detailed information.

- After more than one million MLS66 APT applications, the total vertical displacement of the fine sand subbase was about 1.5 mm. Strain data showed that the modulus of the sand had remained constant.
- The temperature range of Track I was controlled and less variable than that of Track II, where temperatures varied with ambient temperature. Despite the MLS66 being covered by a structural

100

Table 7. Temperature range in MLS66 test tracks.

Depth (mm)	T_I (°C)	Average T_I(°C)	T_II (°C)	Average T_II(°C)
40	43 58	53	22~46	31
80	43 59	52	16~39	27
120	45 65	56		
160	43 59	53	24~36	29
200	37 48	44	25~35	30
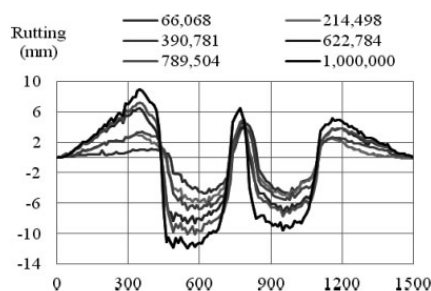
Figure 12. A typical MLS66 transverse profile for Track 1 (Wu et al., 2012).

shell, the weather affected the temperature and the water level especially when during rain. During trafficking the water table depth varied between 1.9 and 2.3 m. The temperature range of the two tracks during trafficking is presented in Table 7.

– The temperature of the MMLS3 test bed was controlled by a closed loop water circulation system set at 60 C. A thermocouple was laid in the middle of two samples 25 mm below the surface of the asphalt to measure the central section temperature in one test. Actual temperatures were found to have varied between 55 and 65°C.

7.3 Analyses of performance and rut data

Both Tracks I and II had two measuring positions referenced as 3 and 4. A typical transverse profile of one of these positions is shown in Figure 12 as it developed during the trafficking. Two maximum points, across the test section were chosen, namely Max1 and Max2. Max1 is defined as the peak rut depth made by trafficking wheel 1 or 2 at the specific measuring position. Max2 is defined as the peak rut depth of the adjacent dual wheel.

The rut depth points were first normalised to a zero reading then normalised with a line across the rut depth values at 0 mm and 1,500 mm across the test section. The Max1 and Max2 points were then selected as the baseline, yielding a total of eight sets of data, respectively, four sets per track. The eight sets of data were consolidated into a single composite averaged curve respectively for heated and ambient performance.
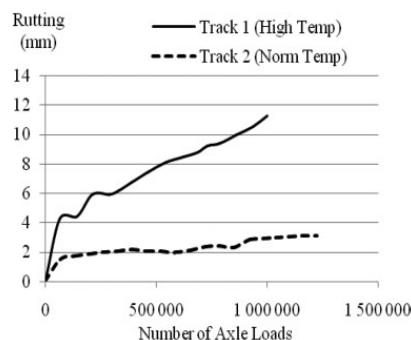
Figure 13. Composite of averaged rutting performance under heated and ambient temperature.
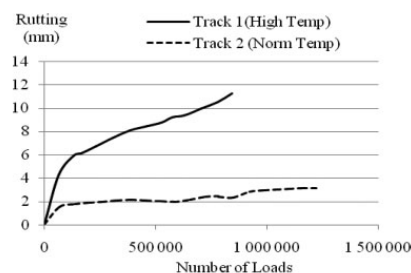
Figure 14. Averaged rutting performance after removal of the axle loads when no rutting occurred under heated trafficking.

The final rut depth at 1 million load repetitions for Track I was 11.3 mm and that of Track II was 3.1 mm.

In Figure 13, two periods where no rutting occurred (i.e., 50 to 100,000 repetitions and 200,000 to 300,000 load repetitions) during trafficking under controlled temperatures are apparent. The reason for this was not clear and was not considered important. It was decided to remove these loading periods from the analyses of the rutting performance (Figure 14). An example of a similar experience treated in a similar manner was found in the NCAT test track literature (Smit et al., 2003).

The modified data points for the two tracks are shown in Figure 15, with plotted power trend lines. Two trend lines, namely 1 and 2, were plotted on Track I. Trend line 1 was plotted by using an appropriate mathematical function. The final predicted rutting was the same as the observed line (predicted 11.1 mm at 1 million axle loads compared to observed of 11.3 mm) before the deletion of the "no-rutting" areas. As an alternative Trend line 2 was plotted on the data which gave a final rut depth of 12 mm at 1 million axle loads. It is apparent that the final rut depth is dependent on the course of events in the early trafficking life of the pavement.

101
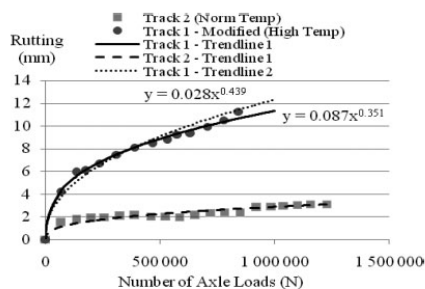
Figure 15. Averaged rutting performance based on extension of the trend line of the heated conditions to compensate for the deleted axle loads.

Wu et al. (2012) further summarized the findings as follows:

— Rutting performance on Track I was influenced by the artificially heated conditions. Two stages are apparent: (1) from 0 to about 66,000 repetitions, where the rate of rutting was 0.6 mm per 10,000 repetitions, and (2) from 66, 000 to 1 million repetitions when the rate of rutting was 0.2 mm per 10,000 repetitions.

— Less rutting was recorded on Track II due to the lower temperatures. The same to distinct periods as Track I were observed, but rates were rutting rates were 0.4 mm and 0.05 mm per 10,000 load repetitions, respectively.

— During trafficking, no fatigue cracking was observed on the surface. A forensic trench through the pavement revealed that the vertical deformation originated from the surface material's deformation and shear flow.

MMLS3 rutting profiles in terms of load applications were compiled for the four laboratory mixes and results of the SMA-13 and AC-20C mixes are shown in Figure 16. The AC-25C was not tested and was assumed to be similar to the AC-20C since this was reported to be the case with the AC-13C that was tested. It should be noted that these values reflect only downward deformation in line with regular rut definitions. This is in contrast to the peak-to-peak maximum rut values that were used as the basis of the analysis by Wu et al. (2012).

7.4 Analyses and findings from field and laboratory APT result comparisons

The rut information from Track I was analyzed to enable a comparison between actual full-scale rutting and MMLS3 predicted rutting from the tests on gyratory compacted specimens. Comparisons with Track II were not made due to varying pavement temperatures on this test. Ruting data of the asphalt mixes under MMLS3 trafficking were analysed by a method akin to the so-called "Direct Method" described by Huang
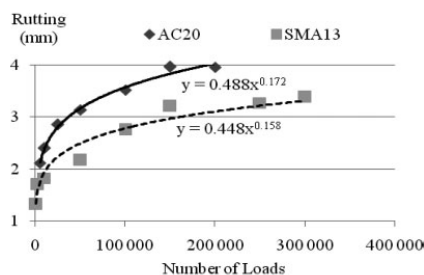
Figure 16. MMLS3 rutting profiles of SMA13 and AC-20C mixes.

Table 8. Actual vs predicted rut rates for Track 1 (mm/10,000 load applications).

Load period	Actual (mm)	Predicted (mm)
0 66,000	0.64	1.88
66,000 330,000	0.12	0.15
330,000 1,000,000	0.07	0.05
66,000 1,000,000	0.08	0.08

(1993). This approach has been used successfully in a variety of rutting studies (Hugo et al. 2011; DPG, 2008).

Two factors are relevant in this method. In principle the dynamic trafficking stress in the briquette under MMLS3 trafficking and the linear elastic stress at the midpoint of the respective asphalt layers is taken as the basis for the vertical stress correlation factor (VSCF). The other factor is the ratio between briquette thickness and the respective layers defined as the thickness correlation factor (TCF). The actual rutting under the MMLS3 trafficking, for each mix, is extrapolated by fitting a trend line to reach the anticipated design number of highway traffic axles. This is generally determined by a power function (Rutmmls). These functions are used as the basis for calculating the predicted rutting (Rut_{pred}) of the different pavement layers.

$$Rut_{pred} = VSCF \times TCF \times Rut_{mmls} \qquad (1)$$

The predicted rutting for Track I was calculated by summing the first three layers, whilst bringing the rutting factors into consideration. By using the predicted rutting, a trend line was taken as the basis to predict the rutting at 1 million load repetitions. The results of the analyses are shown in Figure 17. This prediction was then compared to the adapted full-scale performance of Track I (Figure 15) in Figure 18. The rutting rates for the adapted full-scale performance and the adapted predicted performance on the basis of the MMLS3 tests were calculated as shown in Table 8.

It is apparent that the respective rutting rates matched poorly for the initial test period when most of

102
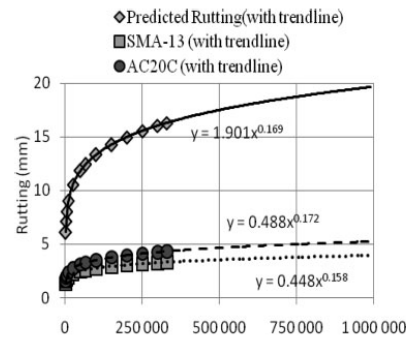
Figure 17. Performance prediction of Track 1 on the basis of analytical procedures using MMLS3 data.
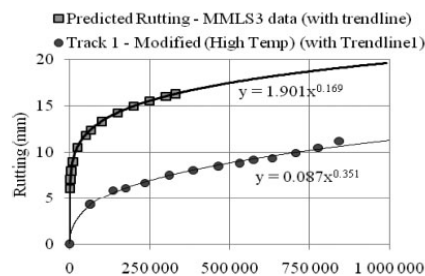
Figure 18. Comparison of the adapted rutting performance on Track 1 to the predicted rutting from MMLS3 laboratory tests.

the rutting occurred (i.e., 0 – 66,000). Thereafter the deformation rate trends matched relatively well during the secondary phase of rutting.

There are two possible reasons for the discrepancy in performance prediction. The MMLS3 rutting test results presented in Figure 16 show that the rut depths of the mixes after 100,000 load applications exceeded the limit of 2.4 mm for rut depth that would probably apply for the trafficking conditions prevalent at the test site according to the MMLS3 Test Protocol (DPGI.2008). This would have categorized both the SMA mix and the AC-20C mix as unsuitable. However, these results were most likely exacerbated, if not primarily caused by the temperature differences between the field and the laboratory studies discussed above. This appears to be the same conclusion reached by Wu et al (2012).

7.5 Case study 5 conclusions

The following conclusions are made based on the observations in this case study:

− The rutting performance predicted from the MMLS3 tests (approximately 20 mm), did not

match full-scale performance (approximately 12 mm). It was concluded that the primary reason for the discrepancy was related to the differences in heated temperature of the laboratory tests (55 to 65 C) compared to those under the MLS66 trafficking (on average 53 to 56°C).

− The independent downward rutting analyses yielded comparative results that differentiated more between Track I (4 mm) with controlled heating than Track II tested at ambient temperatures (2.5 mm). This is ascribed to the differences in upward heave on Track I during early trafficking compared to Track II (Wu et al., 2012).

− The findings and related discussions on rates of rutting by Wu et al (2012), who analysed in terms of peak-to-peak rut, differ from those discussed in this paper, which focussed on downward rutting only.

− The exclusion of the 150,000 load applications that had not caused any rutting during the early trafficking phase with supplement at the end of trafficking appeared to have only minimal effect on the final rut depth (11.3 mm vs. 12 mm). This was despite the virtual increased rate of rutting during the early trafficking phase.

− The results of the rutting study with the MLS66 on Chong-ming Island provided an opportunity for further evaluation of the rutting limits set for the MMLS3 Protocol (DPGI.2008). It also served to compare "rates of deformation" under MMLS3 and MLS66 trafficking particularly during the secondary phase of rutting.

8   CONCLUSIONS FROM THE SYNTHESES OF THE FIVE CASE STUDIES

The five APT case studies discussed in this paper provided valuable information pertaining to the evaluation of performance and failure mechanisms of asphalt pavements, including:

− The results from the APT on the bridge structure demonstrated the benefit of evaluating solutions for deck surfacing prior to embarking on full-scale bridge construction.

− The case studies provided a better understanding of the benefit of APT in evaluating design procedures with materials not yet used in a region or country such as China.

− Evaluation of response of asphalt through strain measurements proved feasible with scaled and full-scale MLS APT trafficking.

− Extraordinary strains arising from slow trafficking and increased temperature in terms of longitudinal and transverse strains observed under MLS APT warrants investigation.

− Stiffness monitoring during APT and surveillance of field performance of pavements was once again confirmed as an invaluable tool.

− It is apparent that transfer of findings between different APT systems is feasible and likely to be cost beneficial.

103

The beneficial use of "rates of deformation" for evaluating rutting was apparent both for full-scale and scaled APT.

REFERENCES

Arraigada, M., Pugliessi, A. and Partl, M. 2012. *Initial Test Results of the New Mobile Load Simulator MLS10 in Switzerland*. Submitted for publication in APT 2012 proceedings.

DPG1. 2008.*Method for evaluation of permanent deformation and susceptibility to moisture damage of bituminous road paving mixtures using the Model Mobile Load Simulator (MMLS3)*. Best Practice document developed under the auspices of the Road Pavement Forum (RPF) and approved for use and distribution at the bi-annual meeting held in Pretoria, South Africa.

Huang, Y.H. 1993. *Pavement Analysis and Design.*, New York, NY: Prentice Hall Inc.

Hugo, F., Bowker, I., Liebenberg, J. and Rossmann, D. 2011. Evaluation of Performance of Asphalt Paving Mixes under Harsh Conditions using the MMLS3, In *10th Conference on Asphalt Pavements for Southern Africa*, CAPSA.

Hugo, F, De Vos, E.R., Tayob, H., Kannemeyer, L. and Partl, M. 2008. Innovative Applications of the MLS10 for Developing Pavement Design Systems, In *Third International Conference on APT in Madrid*.

Kim, Y. and Kim, Y.R. 1997. In-situ evaluation of fatigue damage growth and healing of asphalt concrete pavements using stress wave method, *Transportation Research Record, No. 1568*, Transportation Research Board of the National Academies, pp. 106–113.

Kim, Y. 1997. *Nondestructive Evaluation of Damage Growth and Healing in Asphaltic Surface Layers Using Stress Wave Technique* Dept. of Civil Engineering, North Carolina State University.

Lee, S.J. and Kim, Y.R. 2004. Development of Fatigue Cracking Test Protocol and Life Prediction Methodology Using the Third Scale Model mobile Load Simulator, In *Fifth Intl RILEM Conference on Cracking in Pavements – Mitigation, Risk Assessment and Prevention*, pp. 29–36, Limoges, France.

Lee, N.K.J., Hugo, F. and Stokoe, K.H. 1997. Detection and Monitoring of Cracks in Asphalt Pavements under Texas Mobile Simulator Testing, *Transportation Research Record, No 1570*, Journal of the Transportation Research Board, pp. 10–22, Washington, D.C.

Lee, S.J. 2003. *Long-Term Performance Assessment of Asphalt Concrete Pavements Using the Third Scale Model Mobile Loading Simulator and Fiber Reinforced Asphalt Concrete*, PhD Dissertation. North Carolina State University.

Partl, M.N. and Arraigada, M. 2011. Der neue Mobile Load Simulator MLS10. *Strasse u Autobahn*, 62, Nr 4, pp. 252–257.

Pugliessi, A. 2011. *Relationship between Mobile Load Simulators MMLS3 and MLS10*, M Eng thesis, National University of Rosario (UNR), Argentina.

Pugliessi, A. et al. 2010. Utilización de Simuladores Móviles de Carga MMLS3 y MLS10 para el Estudio de Pavimentos, *XXXVI Asphalt Meeting Buenos Aires*, 2010.

Smit, A.dF., Hugo, F., Rand, D. and Powell, B. 2007. Model Mobile Load Simulator Testing at National Centre for Asphalt Technology Test Track, *Transportation Research Record No 1832*, Journal of the Transportation Research Board, Washington, D. C.

Wu, J. et al. 2012. *Rutting Resistance of Asphalt Pavements with Semi-rigid Base under Full-scale Trafficking of High and Normal Temperature*, Paper submitted for publication in APT 2012 Proceedings.

104

III.3 Strasse und Autobahn

Der neue Mobile Load Simulator (MLS10)

Manfred N. Partl und Martin Arraigada

Beschleunigte Verkehrslastsimulationen (Accelerated Pavement Tests, APT) unter möglichst realen Bedingungen im Massstab 1:1 sind heutzutage ein wesentliches Element, um angewandte Forschung und Entwicklung im Bereich Straßenbaustoffe und Belagsaufbauten betreiben und hinsichtlich ihrer praktischen Tauglichkeit und Umsetzung ohne Behinderung von Verkehrsteilnehmern in sicherer und rascher Weise validieren und optimieren zu können. Damit lassen sich letztlich sowohl Bau- und Unterhaltskosten reduzieren als auch Gebrauchstauglichkeit und Nachhaltigkeit von Straßenbelägen weiter verbessern. An der Empa wurde kürzlich ein neuartiger transportabler Mobile Load Simulator (MLS10) in Betrieb genommen. Es handelt sich dabei um den großmaßstäblichen Prototyp eines kleineren transportablen Laborgerätes aus Südafrika, welches die Empa bereits seit über einem Jahrzehnt erfolgreich in Labor und Feld einsetzt. So leistungsfähig und vielseitig die Maschine auch ist, so anspruchsvoll ist auch ihr Betrieb. Nicht zuletzt auch aus Sicherheitsgründen erfordert die spezielle Technik des neuartigen Systems hoch qualifiziertes Bedienungspersonal. Dies zeigen die bisherigen positiven Erfahrungen in der Schweiz mit dem MLS10, die anhand ausgewählter Ergebnisse an Asphaltbelägen beispielhaft vorgestellt und diskutiert werden.

Accelerated traffic load simulation (Accelerated Pavement Tests, APT) under most realistic full-scale conditions plays an important role nowadays in research and development for road materials and structural pavement design. It is a tool for safe and fast validation and optimization of research products with respect to practical performance and implementation without creating traffic obstructions. This allows reduction of construction and maintenance costs as well as further improvement of performance and sustainability of pavements. Recently, at Empa, a novel transportable Mobile Load Simulator (MLS10) has been put into operation. It is a full-scale prototype version of a smaller transportable lab simulator from South Africa which is used successfully in the lab and in the field by Empa for over more than one decade. The new machine is very efficient and versatile but also non-trivial with respect to operation. Not least for safety reasons the special technique of the novel system requires highly qualified operating personnel. This is confirmed by the positive experience in Switzerland with MLS10, so far. Selected examples of this positive experience with asphalt pavements are presented and discussed in the following.

Verfasseranschriften:
Prof. Dr.-Ing. ETH/SIA M. N. Partl,
Dr.-Ing. M. Arraigada,
Empa, Abteilung Straßenbau/Abdichtungen,
Überlandstraße 129,
8600 Dübendorf/Schweiz,
manfred.partl@empa.ch

1 Einleitung

Die im Asphaltstraßenbau angestrebte rasche und zuverlässige, praxisgerechte Abschätzung der langzeitigen strukturellen Tragfähigkeit von Straßenbelägen ist gekennzeichnet durch das Dilemma, Labor und Praxis in möglichst zuverlässiger Weise zu verknüpfen. Die Schwierigkeit besteht vor allem darin, das unter idealisierenden gut definierten Laborbedingungen bestimmte Stoff- bzw. Systemverhalten mit möglichst einfachen empirisch-mechanistischen Modellen deterministisch oder probabilistisch in möglichst allgemeingültiger Weise auf die realen in situ Bedingungen zu übertragen, die von einer Vielzahl teilweise gegenseitig abhängiger Faktoren geprägt werden. Dies führt in der Praxis zu einem Stoff- bzw. Systemverhalten, welches nicht zuletzt auch wegen den deutlich differierenden geschichtlichen Abfolgen und zeitlichen Maßstäben, aber auch wegen den geometrischen und pro-

duktionsbedingten Unterschieden, weit komplexer und unbestimmbarer ist als dies im Labormaßstab mit vertretbarem Aufwand abgebildet werden kann.

Durch beschleunigte Verkehrslastsimulationen (Accelerated Pavement Testing, APT) unter möglichst realen Bedingungen im Maßstab 1:1 besteht eine gute Chance, dass zumindest teilweise ein Beitrag zur Schließung der noch offenen Erkenntniskette geleistet und damit gleichzeitig sowohl eine Reduktion der Bau und Unterhaltskosten als auch eine weitere Verbesserung der Leistungsfähigkeit von Asphaltbelägen erzielt werden kann. Darauf weisen auch die intensiven weltweiten Arbeiten im Bereich APT hin, wie sie beispielsweise in den internationalen Konferenzen über APT 1999 in Reno, 2004 in Minneapolis und 2008 in Madrid zum Ausdruck kamen. Entsprechend sind von APT rasche, zuverlässige und praxisgerechte Antworten zur Abschätzung der strukturellen Trag- bzw. Resttragfähigkeit

im Rahmen der Zustandserfassung sowie zur Fällung von Entscheiden über Erhaltungsmaßnahmen zu erwarten. Unmittelbar nach dem Einbau können Verkehrslastsimulationen zudem wertvolle Hinweise auf die erreichte Einbauqualität liefern. Im Rahmen von Forschung und Entwicklung kann APT als Validierungstool für Innovationen eingesetzt werden und damit zur Vermeidung teurer, risikoreicher Fehlentwicklungen beitragen.

Aus dieser Erkenntnis heraus wurde kürzlich in der Schweiz durch die Empa in Dübendorf und unterstützt durch das Institut für Geotechnik der ETH Zürich, ETH-IGT, sowie das Bundesamt für Strassen in Bern, ASTRA, ein neuartiger transportabler mobiler Verkehrslastsimulator MLS10 in Betrieb genommen, der nach den Plänen der Universität Stellenbosch in Südafrika hergestellt wurde (Hugo, de Vos et al. 2008). Das Gerät erlaubt die zeitraffende Überrollung des Belages im Maßstab 1:1 und unterscheidet sich von bisher ge-

Der neue Mobile Load Simulator (MLS10) · Verkehrslastsimulation

bräuchlichen Anlagen durch die erhöhte Geschwindigkeit und die Tatsache, dass die Überrollung mit realistischen Radlasten entweder mit Doppel- oder Super-single-Bereifung verkehrsgerecht in unidirektionaler Rollrichtung, also nicht durch Hin- und Her-Rollen, erfolgt. Zudem ist der MLS verglichen mit existierenden Anlagen deutlich kompakter und daher leichter transportierbar und manövrierbar. Dies ist für schweizerische Raumverhältnisse besonders vorteilhaft. Nachstehend werden einige erste praktische Erfahrungen vorgestellt, die im bisherigen Betrieb mit dieser Prototypanlage in der Schweiz gemacht wurden (Arraigada, Kalogeropoulos et al. 2009).

2 MLS10 Funktionsweise

Der MLS10 beruht auf einem neuartigen Konzept (Bild 1). Kernstück bildet eine mit 24 elektromagnetischen linearen Induktions-Motoren LIM angetriebene vertikal umlaufende Endlos-Kette aus vier Schienenwagen (sog. Bogies), die ähnlich einer vertikalen Kettensäge, ellipsenförmig in einer Richtung umlaufen. Diese Bogies sind jeweils mit einer hydraulisch gelagerten, doppel- oder einzelbereiften Halbachse zum Aufbringen der Verkehrslast bestückt. Die Bereifung der Lasträder kann mit 285/70 R19.5 bzw. 495/45 R22.5 erfolgen. Jeder Bogie rollt auf der Umlaufschiene mit 12 Stahl-Doppelrädern. Diese weisen einen Durchmesser von 250 mm auf und sind derart konstruiert, dass je nach Position der Bogies in der oberen oder unteren Hälfte der Umlaufstrecke zur Gewährleistung der Kraftübertragung jeweils eines der beiden Stahl-Doppelräder aktiv ist. Die Form der Laufschienen im Umlenkbereich ist derart optimiert, dass die Lasträder möglichst stoßfrei auf den Belag aufsetzen.

Mit den hydraulisch gegen die Belagsoberfläche gepressten Reifen des jeweils untersten Bogie wird die Straße mit einer Halbachs-Last bis zu 65 kN belastet (entsprechend einer Achslast von 130 kN) und über eine Länge von ca. 4,2 m mit einer maximalen Geschwindigkeit von 22 km/h überrollt. Damit zeichnet sich das Gerät durch eine hohe Leistungsfähigkeit von 6 000 unidirektionalen Überrollungen pro Stunde aus. Jeder Bogie ist mit einem autonomen Messsystem zur Ermittlung der dynamischen Bewegungen zwischen Lastradaufhängung und Bogie ausgestattet. Damit kann die Anpresscharakteristik der Lasträder während des Überrollvorganges gemessen und via Bluetooth an den Kontroll-PC übertragen werden.

Im Betrieb benötigt der MSL10 eine Leistung von 50 kW/h, die von einem integrierten Dieselgenerator mit Partikelfilter erbracht wird. Die Anlage ist mit 3 Dieseltanks à 1 300 l bestückt, die einerseits die statische Steifigkeit der Maschine und anderseits deren Energie-Autonomie sicherstellen. Die Lärmentwicklung beträgt ca. 83 dB(A) und liegt damit im Bereich der am Tage in der Schweiz tolerierbaren Lärmemissionen des Straßenverkehrs.

Um die einseitige Abnutzung der Laufschienen zu vermeiden, ist die maximal zulässige Straßenneigung im Betriebszustand auf 3 % beschränkt. Der MLS10 ist mit einem Zusatzsystem ausgerüstet, welches auch die Simulation des in der Praxis vorkommenden seitlichen Spurdriftens um ± 400 mm erlaubt. Bedingt durch das Antriebssystem wird beim Überrollen kein definierter Horizontalschub aufgebracht, weshalb beispielsweise der Effekt des Bremsens nicht simuliert werden kann. Gewisse Untersuchungen des Abriebverhaltens lassen sich aber durchführen (vgl. Abschnitt 3.2). Die Anlage kann auch mit künstlicher Beregnung der Belagsoberfläche betrieben werden. Dies kann sich in jenen Fällen als zweckmäßig erweisen, wo die Wirkung von Wasser auf das Verhalten des Straßenbelages untersucht werden soll.

Der MLS 10 ist ca. 11 m lang, 3 m hoch und 2,5 m breit. Er hat ein Gewicht von ca. 34 t und kann auf einem Spezialtieflader zur Prüfstelle transportiert werden.

Einmal dort angekommen, kann der MLS 10 selbstständig mit einem Zusatzmotor auf eigenen Transporträdern im Schritttempo von einer Prüfstelle zur anderen manövriert werden. Dieses Fahrsystem erlaubt auch das selbstständige Beladen des Tiefladers über eine maximal 10 % geneigte Rampe. Für periodische Messungen und Inspektionen der Belagsoberfläche lässt sich die Anlage mittels der hydraulisch beweglichen Arme für die Transporträder um ca. 80 cm anheben.

3 Teststrecken

Im Folgenden wird eine kurze Übersicht über verschiedene in der Schweiz untersuchte Teststrecken vermittelt.

3.1 Zürcher Oberlandautobahn A 53 bei Hinwil

Erste Tests wurden im Zeitraum von August bis November 2007 auf der Zürcher Oberlandautobahn A 53 durchgeführt, wo im Hinblick auf die spätere geplante Linienführung im Bereich Betzholz/Hinwil ein kurzes unbefahrenes 20 Jahre altes Fortsetzungsstück zur Verfügung stand, welches hauptsächlich als Deponie von Schnee aus der Schneeräumung im Winter genutzt wurde. Das Straßenstück besaß denselben halbstarren Aufbau aus Zementstabilisierung und Asphaltbeton wie die unter Verkehr stehende Originalausführung der Oberlandautobahn, die nach ca. 10 Jahren hinsichtlich Deckschicht erneuert werden musste. Der Aufbau bestand aus 40 mm Asphaltbeton-Deckschicht auf

Bild 1: Mobile Load Simulator MLS10; a) Prinzip; b) Umlaufsystem mit Bogies; c) Ansicht

Verkehrslastsimulation · Der neue Mobile Load Simulator (MLS10)
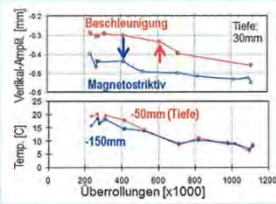
Bild 2: Amplituden der Vertikaldeflexionen beim Überrollen mit Beschleunigungs-Sensoren und magnetostriktiver Relativmessung inklusive Belagstemperatur in verschiedenen Tiefen; die Pfeile bezeichnen den mutmaßlichen Beginn maßgeblicher Schädigung

80 bis 100 mm Asphaltbeton Binderschicht und zwei ca. 180 mm dicken zementstabilisierten Tragschichten. Die Strecke wies ein Quergefälle von 3% auf und war durch zahlreiche klimabedingte Risse charakterisiert. Insgesamt wurde 1 Million (= 1 000k) unidirektionaler Überrollungen (Ürlg.) aufgebracht. Auf ein Spurdriften wurde verzichtet, um einen möglichst hohen Beschleunigungsgrad der künstlichen Verkehrseinwirkung zu erzielen.

Es wurden verschiedene Sensoren stationär eingebaut und periodische Messungen mit verschiedenen anderen Verfahren durchgeführt. Erwähnt seien hier namentlich:
– Spurbildung mittels Profilometermessung
– Statische und dynamische Deflexion mit dem ETH-DELTA Gerät, einem neuen am ETH-IGT entwickelten elektronischem Messsystem (Rabaiotti 2008)
– Seismischer dynamischer Modul mit dem Portable Seismic Pavement Analyzer PSPA (Hugo, de Vos et al. 2008)

– Georadar GPR (Hugenschmidt 2008)
– Ausbildung von Oberflächenrissen durch visuelle Inspektion
– Vertikalbeschleunigung in den Belagsschichten (Arraigada, Partl et al. 2009)
– Vertikalverformung in den Belagsschichten mit magnetostriktivem Sensor (Raab, Partl et al. 2005)

Einzelheiten über die einzelnen Messverfahren sowie die im konkreten Fall angewendeten detaillierten Auswertungen sind in der oben erwähnten Literatur und im entsprechenden Schlussbericht enthalten (Arraigada, Kalogeropoulos et al. 2009). Die Untersuchungen ergaben eine kontinuierliche rasch einsetzende Spurbildung, die nach ca. 50k Ürlg. bereits ein Drittel jener nach 1 000k Ürlg. erreichte und, der Querneigung der Straße entsprechend, in den beiden Roll-Spuren der Doppelbereifung etwas unterschiedlich waren. Gemäß kontinuierlicher Messungen mit den Beschleunigungs- und Magnetostriktiv-Sensoren nahmen die Vertikalverformungen unter Last trotz klimatisch bedingt sinkender Belagstemperaturen nach 400k bis 600k Ürlg. sukzessive zu, was auf eine einsetzende Schädigung hindeutete (siehe Markierungspfeile im Bild 2). Tatsächlich lieferten die Untersuchungen mit GPR nach ca. 600k Ürlg. Anzeichen für horizontale Anomalien in 4,5 cm Tiefe (dunkle Zonen im Bild 3), also etwa auf dem Niveau des Übergangs von Deckschicht zur Binderschicht, die sich bis zu 1000k Ürlg. noch verstärkten und sich nach der forensischen Entnahme von Belagsriegeln als Lagentrennung erwiesen.

Die Messungen mit dem ETH-DELTA Gerät ließen nach 1 000k Ürlg. deutlich kanalisierte Einsenkungsmulden erkennen, was auf einen Funktionsverlust der zement-

stabilisierten Tragschichten hindeutete (Bild 4). Entsprechend erwies sich die Zementstabilisierung bei der Riegelentnahme als nahezu pulverisiert, konnte sie doch leicht mit einem Schraubendreher von Hand durchstoßen werden. Dass die beschleunigte Verkehrslastwirkung des MLS10 nicht nur eine bleibende Verformung in den Asphaltschichten sondern vor allem auch ein Durchstanzen des Asphalts verursachte, wurde durch die an den entnommenen Riegeln festgestellte Schubrissbildung an den Flanken der Roll-Spuren bestätigt.

Aufgrund der Verkehrszählungen dürfte die während der letzten 20 Betriebsjahre auf der Oberlandautobahn aufgetretene Verkehrsbelastung bei ca. 5,5 bis 6,5 Millionen Einheitsachslasten à 81,6 kN liegen; dies unter der Annahme eines Lastwagenanteils von 6,3% und einer jährlichen Zuwachsrate von 4,45%. Die vor 10 Jahren erneuerte Deckschicht wies in der befahrenen Normalspur starke Risse auf. Dies deutet darauf hin, dass eine Verkehrsbelastung in der erwähnten Größenordnung tatsächlich einen Grenzwert für die Tragfähigkeit der Strecke darstellt. In den MLS10 Versuchen mit einer Halbachsen-Last von 65 kN (entsprechend einer Achslast von 130 kN) war daher mit einer strukturellen Schädigung nach ca. 750k Ürlg. zu rechnen, eine Größenordnung, die sich in den Tests bestätigte.

3.2 Empa Abrasionstests

Im Rahmen des Forschungsprojektes APART (Abriebspartikel des Straßenverkehrs) über nicht auspuffbedingte PM10-Emissionen wurden im Auftrag des Bundesamtes für Strassen ASTRA und des Bundesamtes für Umwelt BAFU neben Feinstaubemissionen unter Normalverkehr auch solche infolge MLS10 gemessen (Gehrig, Zeyer et al. 2010); dies nicht zuletzt, um den Anteil der Feinstpartikel infolge Straßenabrieb und Staub-Aufwirbelung trotz chemischer Ähnlichkeit jeweils quantitativ zuordnen zu können. Die Messungen erfolgten auf einem oberflächlich leicht vorbeanspruchten AC 11 Belag auf dem Empa-Gelände. Ermittelt wurden die Partikel der Fraktion 0,5 bis 20 µm mit einem aerodynamischen Partikelgrößen Analysator (TSI APS Modell 3321). Gleichzeitig wurde die Verdünnung eines genau dosierten Tracer Gases SF6 (Schwefelhexafluorid) bestimmt, welches zur rechnerischen Berücksichtigung der Strömungsverhältnisse im MLS10 während des
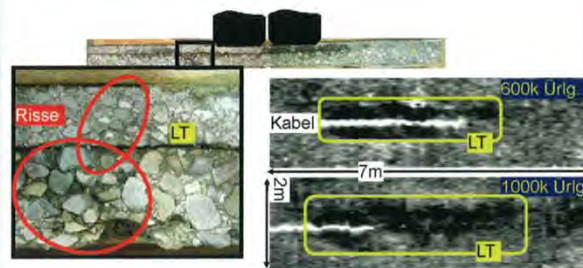
Bild 3: Lagetrennung (LT) und Risszone im entnommenen Riegel nach 1 000k Überrollungen (links unten); GPR Landkarte in 4,5 cm Tiefe nach 600k und 1 000k Überrollungen (rechts unten)
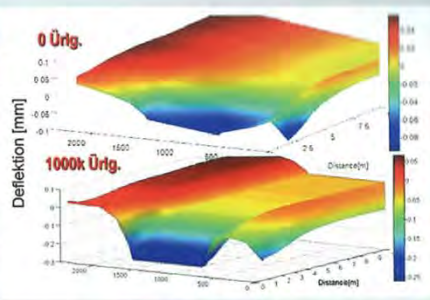
Bild 4: ETH-DELTA Gerät mit gemessenen Deflexionsmulden nach 0 und 1000k Überrollungen

Überrollvorganges diente. Das Bild 5 zeigt die Partikelkonzentration in der Außenluft und während des MLS10 Betriebes in Funktion der Partikelgröße. Da sich die Aufwirbelung im vorliegenden Fall als vernachlässigbare Größe erwies, stellt die Differenz der beiden Messungen den Abrieb dar. Verglichen mit der Verteilung der Partikelgröße in der Außenluft ist die Verteilung der Abriebspartikel deutlich in Richtung der gröberen Partikel verschoben.

3.3 Anschluss an die neue Zürcher Westumfahrung A 20

Zur Untersuchung des Belagskonzeptes der A 4 im Anschluss an die neue Westumfahrung A 20 von Zürich wurden von November 2008 bis September 2009 mit dem MLS10 auf separatem Gelände drei entsprechende Testfelder mit unterschiedlich vollständigem Belagsaufbau untersucht. Die Schichtfolge des Vollaufbaus von unten nach oben umfasste zwei hydraulisch stabilisierte Schichten von insgesamt 480 mm Dicke, eine SAMI Schicht, eine 80 mm Tragschicht AC T 22 H, eine 80 mm Binderschicht AC B 22 H und eine 30 mm Deckschicht aus Rauasphalt AC MR 8. Auf dem Feld 4 mit dem Vollaufbau wurden insgesamt 740k Ürlg. durchgeführt. Bei Feld 3 ohne Deckschicht wurden 427k Ürlg. aufgebracht, während Feld 1 nur noch die Tragschicht umfasste und mit 439k Ürlg belastet wurde. Erneut wurden Spurbildung, statische Deflexionsmulde mit ETH-DELTA Gerät, seismischer Modul mit PSPA, Lagentrennung mit GPR und die Deflexionen über Beschleunigungssensoren erfasst. Zudem wurden in verschiedenen Tiefen die Längs- und Querdehnungen über Dehnmess-Sensoren (DMS) ermittelt und durch das Institut für Straßen- und Eisenbahnwesen (ISE) des Karlsruher Instituts für Technologie (KIT)

an drei Messkampagnen Tragfähigkeitsmessungen mit dem Falling Weight Deflectometer (FWD) durchgeführt (Karcher, Partl et al. 2010).

Die Ergebnisse zeigen, dass der Belag verglichen mit der Strecke bei Hinwil extrem steif und tragfähig ist. Die Längsdehnungen im Bereich von 10 bis 70 µm/m, die bei sommerlichen Temperaturen zwischen dem 21. Juli und 19. August 2008 im

deckschichtlosen Feld 3 unmittelbar unter der Roll-Spur in einer Tiefe von 8 cm (d. h. auf der Tragschichtoberfläche) ermittelt wurden, lassen in Funktion der Überrollungen mit einer Halbachs-Last von 65 kN unabhängig von der Belagstemperatur keinen Dehnungszuwachs erkennen (Bild 6). Im Feld 4 wurde auch nach 740k Ürlg. für den vorliegenden Aufbau eine praktisch unverändert hohe Stabilität festgestellt.

Bild 5: Typische Partikelgrößenverteilung bei AC11 während des MLS10 Betriebes
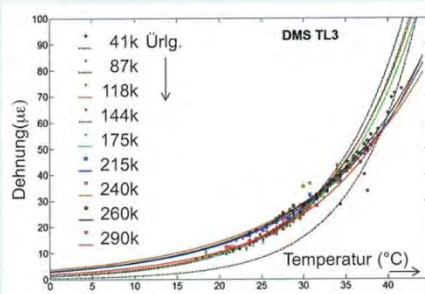
Bild 6: Längsdehnungen in Testfeld 3 unter der Rollstrecke in 8 cm Tiefe in Abhängigkeit der Belags-Temperaturen bei zunehmender Anzahl Überrollungen

Verkehrslastsimulation · Der neue Mobile Load Simulator (MLS10)
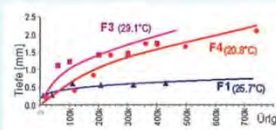
Bild 7: Zunahme der maximalen Spurbildung in den verschiedenen Testfeldern F1, F3, F4. Ebenfalls angegeben ist die mittlere Prüftemperatur

Durch die FWD-Messungen konnte ebenfalls keine Verringerung der Tragfähigkeit infolge der MLS10-Beanspruchung festgestellt werden.

Der im Bild 7 angegebenen Spurbildungsentwicklung in den drei Testfeldern bei mittleren Temperaturen von 20,8 bis 29,1°C ist zu entnehmen, dass die bleibenden Deformationen vor allem den Asphaltschichten zuzuordnen sind und nicht, wie im Falle der Strecke bei Hinwil, dem Versagen der Stabilisierungsschichten. Entsprechend ist die Spurbildung bei Feld F1 mit nur alleiniger Tragschicht deutlich geringer als bei den Feldern F3 und F4 mit Binderschicht und Vollaufbau; dies obwohl die mittlere Temperatur bei Feld F1 sogar etwas höher war als während der Prüfung des Vollaufbaus. Es bleibt jedoch festzustellen, dass die Spurrinnentiefe mit lediglich 2 mm am Ende des Versuchsprogrammes, trotz Prüfung während der Sommermonate, als sehr gering einzustufen ist. Somit kann gefolgert werden, dass die gewählte Dimensionierung erfolgreich war und der Belag eine gute Qualität aufweist.

3.4 Rastplatz der A 1 bei Suhr und neue Staffeleggstrasse

Die Steifigkeit der aktuell in der Schweiz für Hochleistungsstraßen angewendeten Belagskonzepte bestätigte sich auch in den

beiden jüngsten Einsätzen des MLS10 auf einem Fahrstreifen im Bereich des Rastplatzes der A 1 (Bern–Zürich) bei Suhr sowie auf der neuen Staffeleggstrasse, welche Teil der neuen Nord-Umfahrung der Kantonshauptstadt Aarau bildet. Verglichen mit den Messungen auf dem Belag der Zürcher Westumfahrung wurden auf dem Rastplatz Suhr nach 405k Ürlg. mit ca. 3 mm etwa doppelt so tiefe Spurrinnen festgestellt. Trotzdem darf der Belag generell noch als recht steif bezeichnet werden. Im Falle der Staffeleggstrasse erwies sich das relativ große Längs- und Quer-Gefälle von 6 bzw. 5,5% als kritisch für die Versuchsdurchführung, weil die Laufschienen des MLS10 ungleichmäßig belastet werden und die Gefahr der einseitigen Abnutzung besteht. Um diese Problematik zu lösen, wurde der MLS10 in Fallrichtung, d.h. mit einem leichten Winkel zur Richtung des Straßenverkehrs, positioniert. Die festgestellten Änderungen der Belagseigenschaften waren auch in diesem Falle relativ gering. Wie aus Bild 8 ersichtlich, wurden mittels ETH-DELTA Messungen gewisse Unterschiede im Deflexionsverhalten festgestellt. Generell konnte aber auch dieser moderne Belag im Vergleich zur Strecke in Hinwil als bedeutend tragfähiger eingestuft werden.

4 Schlussfolgerungen

Die bisherigen Erfahrungen mit dem MLS10 bestätigen, dass die beschleunigte Verkehrslastsimulation im 1:1 Maßstab ein wichtiges Forschungs- und Validierungsinstrument darstellt, welches allgemein noch zu wenig eingesetzt wird, um die Übertragung von Laborergebnissen und Modellen auf das tatsächliche Verhalten unter Verkehr wissenschaftlich zu beglei-

ten und dadurch dem Risiko von technischen Fehlentwicklungen entgegenzuwirken.

Die mobile von der Empa betriebene zukunftsweisende MLS10-Anlage hat sich in Kombination mit geeigneter Sensorik und Messverfahren als vielversprechendes, praktisches Hilfsmittel zur Erfassung der mechanischen Leistungsfähigkeit von real eingebauten Asphaltbelägen erwiesen, dessen Einsatzbereich dank der hohen Mobilität nachgewiesenermaßen nicht nur auf die Schweiz beschränkt ist. Der MLS 10 zeichnet sich somit durch folgende klare Vorteile aus:

- Kompakte Größe; daher vergleichsweise gut transportierbar, auch bei engen Kurvenradien (z.B. wie Kreisel) und engem Lichtraumprofil; zudem auf engem Raum im Selbstfahrmodus übersichtlich manövrierbar.
- Unidirektionale Überrollrichtung; d.h. keine realitätsfremde Hin- und Her-Überrollung.
- Hohe Anzahl realistischer Halbachs-Lasten in relativ kurzer Zeit möglich; daher ist die Prüfzeit und das Staurisiko in Feldversuchen minimal.
- Mit 22 km/h Überrollgeschwindigkeit erlaubt der MLS10 bei vertretbarem Zeitaufwand Ermüdungsprüfungen unter realistischen dynamischen Lasten, sodass das Risiko von Fehlschlüssen durch Überhöhung der Achslasten zwecks Reduktion der Anzahl Überrollungen entfällt.

Nach den bisherigen Erfahrungen mit nahezu 10 Mio. Überrollungen beträgt die durchschnittliche Leistungsfähigkeit bei normalem 8,5 Stunden Betrieb ca. 40 000 unidirektionale Überrollungen pro Tag mit einer Halbachs-Last von 65 kN. Allerdings darf nicht vergessen werden, dass der von der Empa betriebene MLS10 noch ein Prototyp ist, der im gegenwärtigen Zustand einen relativ aufwendigen Unterhalt durch gut geschultes Personal erfordert und im Rahmen seiner Weiterentwicklung einem kontinuierlichen konstruktiven und betrieblichen Optimierungsprozess unterworfen ist.

Die bisherigen Anwendungen des MLS10 in der Schweiz dürfen als vielversprechend bezeichnet werden, da wichtige – wenn auch noch nicht abschließende – Hinweise über die Einsatzmöglichkeiten der beschleunigten Verkehrslastsimulation zur großmaßstäblichen Beurteilung der Leistungsfähigkeit realer Strecken gewonnen werden konnten. Namentlich konnte bei den Tests auf der A 53 bei Hinwil nach ca.
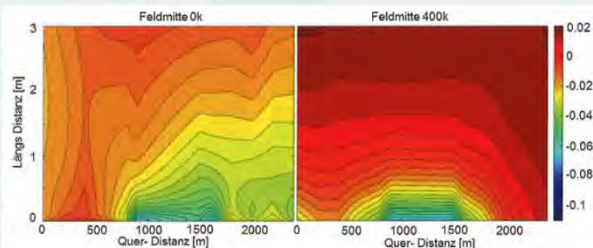
Bild 8: Veränderung der ETH-DELTA Deflexions-Isohypsen auf der Staffeleggstrasse nach 0k und 400k Überrollungen

0,4 bis 0,6 Mio. Überrollungen mit E130 (Einheitsachslasten von 130 kN) Versagen infolge Lagentrennung und Durchstanzen der Zementstabilisierung festgestellt werden. Dies entspricht etwa dem reellen Versagen nach ca. 0,74 Mio. E130, welche in der 40-jährigen Betriebsperiode zwischen 1967 und 2007 aufgebracht wurden.

Als unerwartete positive Erkenntnis zu werten ist das im Rahmen von Partikelgrößen Untersuchungen gefundene Resultat, dass der MLS10 trotz der passiv angetriebenen Lasträder zu Partikelabriebs-Messungen herangezogen werden kann, insbesondere auch zur Unterscheidung von Straßenabrieb und Staubaufwirbelung.

Hinsichtlich moderner schweizerischer Belagskonzepte ist zu erwähnen, dass sich gegenüber der Strecke bei Hinwil die moderne Belagsstruktur der A 4 im Anschluss an die neue Zürcher Westumfahrung A 20 als extrem steif und tragfähig erwiesen hat. Auch nach 0,8 Mio. Überrollungen des Vollaufbaus waren keine deutlichen Veränderungen im Verhalten feststellbar und die Spurbildung betrug lediglich 2 mm. Somit konnte gefolgert werden, dass die gewählte Dimensionierung erfolgreich war und der Belag eine gute Qualität aufweist. Dass mit den gegenwärtigen modernen Belagskonzepten in der Schweiz eine hohe Tragfähigkeit erreicht werden kann, wurde aber auch in den MLS10 Tests im Bereich des Rastplatzes der A 1 (Bern-Zürich) bei Suhr sowie der Nordumfahrung Aarau auf der neuen Staffeleggstrasse deutlich. Letztere bestätigte, dass ein Einsatz des MLS10 bei Gefällen von mehr als 3% aus maschinentechnischen Gründen problematisch ist.

Bis heute ergab sich noch keine Gelegenheit, mit dem MLS10 einen modernen schweizerischen Autobahnbelag bis zum vollständigen Versagen zu beanspruchen und durch Kombination der erwähnten Messverfahren die Veränderung der mechanischen Leistungsfähigkeit solcher Belagsstrukturen zu erfassen und zu beurteilen. Auch war es noch nicht möglich, Restfestigkeiten von Belägen vor und nach der Erneuerung zu bestimmen, um Hinweise über die Dimensionierung von Belagsverstärkungen zu erhalten. Dies wird sicherlich Gegenstand künftiger Einsätze des MLS10 sein.

Literaturverzeichnis

Arraigada, M.; Kalogeropoulos, A.; Hugenschmidt, J.; Partl, M.N.; Caprez, M.; Rabaiotti, C. (2009): Pilotstudie zur Evaluation einer mobilen Großversuchsanlage für beschleunigte Verkehrslastsimulation auf Straßenbelägen. Eidgenössisches Departement für Umwelt, Verkehr, Energie und Kommunikation, Bundesamt für Strassen. Forschungsauftrag ASTRA 2004/018, Bericht Nr 1261

Arraigada, M.; Partl, M.N.; Angelone, S.M.; Martinez, F (2009): Evaluation of Accelerometers to Determine Pavement Deflections under traffic Loads. Material and Structures, 42, 6, Springer Verlag, 779–790

Gehrig, R.; Zeyer, K.; Bukowiecki, N.; Lienemann, P.; Poulikakos, L.D.; Furger, M.; Buchmann, B. (2010): Mobile Load Simulators – a tool to distinguish between the emissions due to abrasion and resuspension of PM10 from road surfaces. Atmospheric Environment, 44, 38 Elsevier Verlag, 4937–4943

Hugenschmidt, J. (2008): Georadar zur zerstörungsfreien Prüfung von Verkehrsbauwerken. Strasse und Verkehr, Nr. 1–2, Verlag Vereinigung Schweizerischer Strassen- und Verkehrsfachleute, 26–35

Hugenschmidt, J. (2010): Geophysics and non-destructive testing for transport infrastructure, with emphasis on ground penetrating radar. Doktorarbeit, Diss ETH Nr 19225

Hugo, F.; de Vos, E.; Tayob, H.; Kannemeyer, L.; Partl, M.N. (2008): Innovative Applications of the MLS10 for Developing Pavement Design Systems. Proceedings of 3rd International Conference on Accelerated Pavement Testing, APT 2008, Madrid

Karcher, C.; Partl, M.N.; Plachkova, P.; Arraigada, M.; Umminger, M. (2010): Untersuchung der Veränderung der strukturellen Substanz von Asphaltkonstruktionen. Straße und Autobahn, 61, 9, Kirschbaum Verlag, 631–637

Raab, C.; Partl, M.N.; Anderegg, P.; Brönnimann, R. (2005): A LTPP Study with a new Device for Vertical Deformation Measurements. Int. Journal of Pavement Engineering, 6, 3, Taylor and Francis Verlag, 211–216

Rabaiotti, C. (2008): Inverse Analysis in Geotechnics. Doktorarbeit, Diss ETH Nr 18135

Rabaiotti, C.; Partl, M.N.; Caprez, M. (2008): APT device evaluation for road research in Switzerland: test campaign on a Swiss Highway with the MLS10. Proceedings of 3rd Int. Conf. on Accelerated Pavement Testing, APT08, Madrid

III.4   Strasse und Verkehr

Beschleunigte Verkehrslastsimulation mit dem Mobile Load Simulator MLS10

Beschleunigte Verkehrslastsimulationen (Accelerated Pavement Tests, APT) unter möglichst realen Bedingungen im Massstab 1:1 sind heutzutage ein wesentliches Element, um angewandte Forschung und Entwicklung im Bereich Strassenbaustoffe und Belagsaufbauten betreiben zu können. An der Eidgenössischen Materialprüfungs- und Forschungsanstalt (EMPA) wurde kürzlich ein neuartiger transportabler Mobile Load Simulator (MLS10) in Betrieb genommen. So leistungsfähig und vielseitig die Maschine auch ist, so anspruchsvoll ist auch ihr Betrieb. Dies zeigen die bisherigen positiven Erfahrungen in der Schweiz mit dem MLS10, die anhand ausgewählter Ergebnisse an Asphaltbelägen beispielhaft vorgestellt und diskutiert werden.

*Von Manfred N. Partl und Martin Arraigada ***

Die im Asphaltstrassenbau angestrebte rasche und zuverlässige, praxisgerechte Abschätzung der langzeitigen strukturellen Tragfähigkeit von Strassenbelägen ist gekennzeichnet durch das Dilemma, Labor und Praxis in möglichst zuverlässiger Weise zu verknüpfen. Die Schwierigkeit besteht vor allem darin, das unter idealisierenden gut definierten Laborbedingungen bestimmte Stoff- bzw. Systemverhalten mit möglichst einfachen empirisch-mechanistischen Modellen deterministisch oder probabilistisch in möglichst allgemeingültiger Weise auf die realen in situ Bedingungen zu übertragen, die von einer Vielzahl teilweise gegenseitig abhängiger Faktoren geprägt werden. Dies führt in der Praxis zu einem Stoff- bzw. Systemverhalten, welches nicht zuletzt auch wegen den deutlich differierenden geschichtlichen Abfolgen und zeitlichen Massstäben, aber auch wegen den geometrischen und produktionsbedingten Unterschieden, weit komplexer und unbe-

stimmbarer ist als dies im Labormassstab mit vertretbarem Aufwand abgebildet werden kann.

Durch beschleunigte Verkehrslastsimulationen (Accelerated Pavement Testing, APT) unter möglichst realen Bedingungen im Massstab 1:1 besteht eine gute Chance, dass zumindest teilweise ein Beitrag zur Schliessung der noch offenen Erkenntniskette geleistet und damit gleichzeitig sowohl eine Reduktion der Bau und Unterhaltskosten als auch eine weitere Verbesserung der Leistungsfähigkeit von Asphaltbelägen erzielt werden kann. Darauf weisen auch die intensiven weltweiten Arbeiten im Bereich APT hin, wie sie beispielsweise in den internationalen Konferenzen über APT 1999 in Reno, 2004 in Minneapolis und 2008 in Madrid zum Ausdruck kamen. Entsprechend sind von APT rasche, zuverlässige und praxisgerechte Antworten zur Abschätzung der strukturellen Trag- bzw. Resttragfähigkeit im Rahmen der Zustandserfassung sowie zur

* Manfred Partl, Prof. Dr. Ing. ETH/SIA, Leiter Empa Abteilung Strassenbau/ Abdichtungen Empa, Dübendorf

* Martin Arraigada, Dr. Ing., Bauingenieur, Projektleiter Empa Abteilung Strassenbau/Abdichtungen Empa

Essais accélérés sur les revêtements avec le Mobile Load Simulator MLS10

La réalisation d'essais accélérés sur les revêtements (Accelerated Pavement Tests, APT) dans des conditions proches de la réalité à l'échelle 1:1 est essentielle pour mener les travaux de R&D appliquée dans le domaine des matériaux de construction des routes et des enrobés. Un simulateur mobile de charge d'un genre nouveau (Mobile Load Simulator, MLS10) vient d'être mis en service au Laboratoire fédéral d'essai des matériaux et de recherche Empa. L'appareil est performant et polyvalent, mais d'utilisation complexe. Les résultats des premières expériences réalisées jusqu'ici sur différents enrobés sont positifs.

Fällung von Entscheiden über Erhaltungsmassnahmen zu erwarten. Unmittelbar nach dem Einbau können Verkehrslastsimulationen zudem wertvolle Hinweise auf die erreichte Einbauqualität liefern. Im Rahmen von Forschung und Entwicklung kann APT als Validierungstools für Innovationen eingesetzt werden und damit zur Vermeidung teurer, risikoreicher Fehlentwicklungen beitragen.

Aus dieser Erkenntnis heraus wurde vor Kurzem durch die Empa in Dübendorf zusammen mit dem Institut für Geotechnik der ETH Zürich, ETH-IGT, und unterstützt durch das Bundesamt für Strassen in Bern, ASTRA, ein neuartiger, transportabler, mobiler Verkehrslastsimulator MLS10 in Betrieb genommen, der nach den Plänen der Universität Stellenbosch in Südafrika hergestellt wurde (Hugo et al. 2008). Das Gerät erlaubt die zeitraffende Überrollung des Belages im Massstab 1:1 und unterscheidet sich von bisher gebräuchlichen Anlagen durch die erhöhte Geschwindigkeit und die Tatsache, dass die Überrollung mit realistischen Radlasten entweder mit Doppel- oder Supersingle-Bereifung verkehrsgerecht in unidirektionaler Rollrichtung, also nicht durch Hin- und Herrollen, erfolgt. Zudem ist der MLS verglichen mit existierenden Anlagen deutlich kompakter und daher leichter transportier- und manövrierbar. Dies ist für schweizerische Raumverhältnisse besonders vorteilhaft. Nachstehend werden einige erste praktische Erfahrungen vorgestellt, die im bisherigen Betrieb mit dieser Prototypanlage in der Schweiz gemacht wurden (Arraigada et al. 2009).

MLS10: Funktionsweise

Der MLS10 beruht auf einem neuartigen Konzept (Abb. 1). Kernstück bildet eine mit 24 elektromagnetischen linearen Induktionsmotoren LIM angetriebene vertikal umlaufende Endloskette aus vier Schienenwagen (sog. Bogies), die ähnlich einer vertikalen Kettensäge, ellipsenförmig in einer Richtung umlaufen. Diese Bogies sind jeweils mit einer hydraulisch gelagerten, doppel- oder einzelbereiften Halbachse zum Aufbringen der Verkehrslast bestückt. Die Bereifung der Lasträder kann mit 285/70 R19.5 bzw. 495/45 R22.5 erfolgen. Jeder Bogie rollt auf der Umlaufschiene mit 12 Stahldoppelrädern. Diese weisen einen Durchmesser von 250 mm auf und sind derart konstruiert, dass je nach Position der Bogies in der oberen oder unteren Hälfte der Umlaufstrecke zur Gewährleistung der Kraftübertragung jeweils eines der beiden Stahldoppelräder aktiv ist. Die Form der Laufschienen im Umlenkbereich ist derart optimiert, dass die Lasträder möglichst stossfrei auf den Belag aufsetzen.

Mit den hydraulisch gegen die Belagsoberfläche gepressten Reifen des jeweils untersten Bogie wird die Strasse mit einer Halbachslast bis zu 65 kN belastet (entsprechend einer Achslast von 130 kN) und über eine Länge von ca. 4,2 m mit einer maximalen Geschwindigkeit von 22 km/h überrollt. Damit zeichnet sich das Gerät durch eine hohe Leistungsfähigkeit von 6000 unidirektionalen Überrollungen pro Stunde aus. Jeder Bogie ist mit einem autonomen Messsystem zur Ermittlung der dynamischen Bewegungen zwischen Lastradaufhängung und Bogie ausgestattet. Damit kann die Anpresscharakteristik der Lasträder während des Überrollvorganges gemessen und via Bluetooth an den Kontroll-PC übertragen werden.

Im Betrieb benötigt der MSL10 eine Leistung von 50 kW/h, die von einem integrierten Dieselgenerator mit Partikelfilter erbracht wird. Die Anlage ist mit 3 Dieseltanks à 1300 Liter bestückt, die einerseits die statische Steifigkeit der Maschine und andererseits deren Energieautonomie sicher-
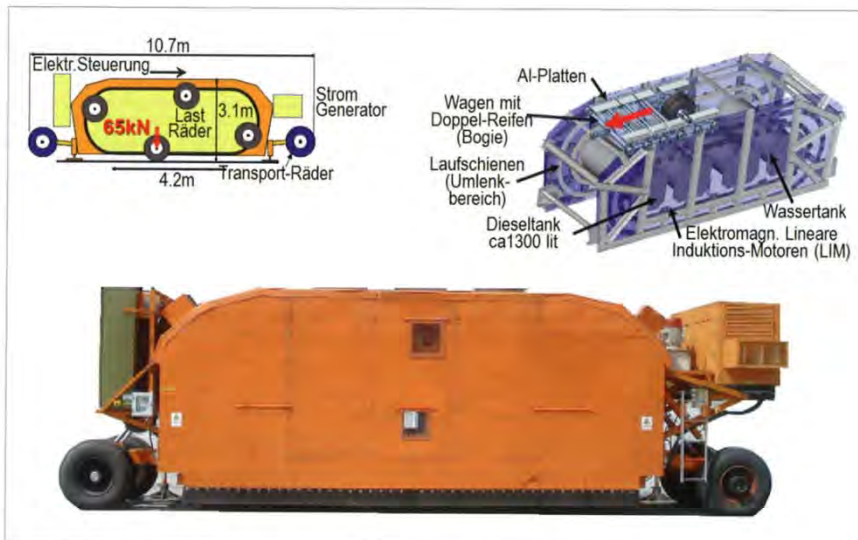
1: Mobile Load Simulator MLS10: Prinzip (oben links), Umlaufsystem mit Bogies (oben rechts), Ansicht (unten).

1: Mobile Load Simulator MLS10: principe (en haut à gauche), système de circulation avec bogies (en haut à droite), vue d'ensemble (en bas).

stellen. Die Lärmentwicklung beträgt ca. 83 dB(A) und liegt damit im Bereich der am Tage in der Schweiz tolerierbaren Lärmemissionen des Strassenverkehrs.

Um die einseitige Abnutzung der Laufschienen zu vermeiden, ist die maximal zulässige Strassenneigung im Betriebszustand auf 3 % beschränkt. Der MLS10 ist mit einem Zusatzsystem ausgerüstet, welches auch die Simulation des in der Praxis vorkommenden seitlichen Spurdriftens um ±400 mm erlaubt. Bedingt durch das Antriebssystem wird beim Überrollen kein definierter Horizontalschub aufgebracht, weshalb beispielsweise der Effekt des Bremsens nicht simuliert werden kann. Gewisse Untersuchungen des Abriebverhaltens lassen sich aber durchführen (vgl. Abschnitt «Empa Abrasionstests»). Die Anlage kann auch mit künstlicher Beregnung der Belagsoberfläche betrieben werden. Dies kann sich in jenen Fällen als zweckmässig erweisen, wo die Wirkung von Wasser auf das Verhalten des Strassenbelages untersucht werden soll.

Der MLS10 ist ca. 11 m lang, 3 m hoch und 2,5 m breit. Er hat ein Gewicht von ca. 34 t und kann auf einem Spezialtieflader zur Prüfstelle transportiert werden. Einmal dort angekommen, kann der MLS10 selbstständig mit einem Zusatzmotor auf eigenen Transporträdern im Schritttempo von einer Prüfstelle zur anderen manövriert werden. Dieses Fahrsystem erlaubt auch das selbstständige Beladen des Tiefladers über eine maximal 10 % geneigte Rampe. Für periodische Messungen und Inspektionen der Belagsoberfläche lässt sich die Anlage mittels der hydraulisch beweglichen Arme für die Transporträder um ca. 80 cm anheben.

Teststrecken

Im Folgenden wird eine kurze Übersicht über verschiedene in der Schweiz untersuchte Teststrecken vermittelt.

Zürcher Oberlandautobahn A53 bei Hinwil

Erste Tests wurden im Zeitraum von August bis November 2007 auf der Zürcher Oberlandautobahn A53 durchgeführt, wo im Hinblick auf die spätere geplante Linienführung im Bereich Betzholz/Hinwil ein kurzes unbefahrenes 20 Jahre altes Fortsetzungsstück zur Verfügung stand, welches hauptsächlich als Deponie von Schnee aus der Schneeräumung im Winter genutzt wurde. Das Strassenstück besass denselben halbstarren Aufbau aus Zementstabilisierung und Asphaltbeton wie die unter Verkehr stehende Originalausführung der Oberlandautobahn, die nach etwa 10 Jahren hinsichtlich Deckschicht erneuert werden musste. Der Aufbau bestand aus 40 mm Asphaltbeton-Deckschicht auf 80 bis 100 mm Asphaltbeton Binderschicht und zwei ca. 180 mm dicken zementstabilisierten Tragschichten. Die Strecke wies ein Quergefälle von 3 % auf und war durch zahlreiche klimabedingte Risse charakterisiert. Insgesamt wurde 1 Million (= 1000 k) unidirektionaler Überrollungen (Ürlg.) aufgebracht. Auf ein Spurdriften wurde verzichtet, um einen möglichst hohen Beschleunigungsgrad der künstlichen Verkehrseinwirkung zu erzielen. Es wurden verschiedene Sensoren stationär eingebaut und periodische Messungen mit verschiedenen anderen Verfahren durchgeführt. Erwähnt seien hier namentlich:

■ Spurbildung mittels Profilometermessung
■ Statische und dynamische Deflektion mit dem ETH-DELTA Gerät, einem neuen am ETH-IGT entwickelten elektronischen Messsystem (Rabaiotti 2008).

■ Seismischer dynamischer Modul mit dem Portable Seismic Pavement Analyzer PSPA (Hugo 2008).
■ Georadar GPR (Hugenschmidt 2008).
■ Ausbildung von Oberflächenrissen durch visuelle Inspektion.
■ Vertikalbeschleunigung in den Belagsschichten (Arraigada et al. 2009,2).
■ Vertikalverformung in den Belagsschichten mit magnetostriktivem Sensor (Raab et al. 2005).

Einzelheiten über die einzelnen Messverfahren sowie die im konkreten Fall angewendeten detaillierten Auswertungen sind in der oben erwähnten Literatur und im entsprechenden Schlussbericht enthalten (Arraigada et al. 2009). Die Untersuchungen ergaben eine kontinuierliche rasch einsetzende Spurbildung, die etwa nach 50 k Ürlg. bereits einen Drittel jener nach 1000 k Ürlg. erreichte und, der Querneigung der Strasse entsprechend, in den beiden Rollspuren der Doppelbereifung etwas unterschiedlich war. Gemäss kontinuierlicher Messungen mit den Beschleunigungs- und Magnetostriktiv-Sensoren nahmen die Vertikalverformungen unter Last trotz klimatisch bedingt sinkender Belagstemperaturen nach 400 k bis 600 k Ürlg. sukzessive zu, was auf eine einsetzende Schädigung hindeutete (siehe Markierungspfeile in Abb. 2). Tatsächlich
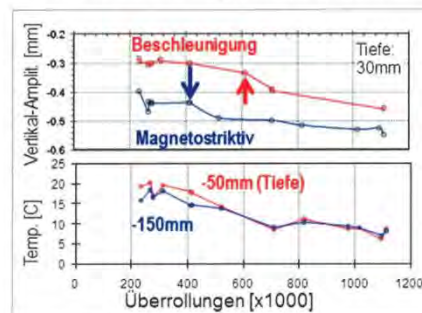
2: Amplituden der Vertikaldeflektionen beim Überrollen mit Beschleunigungssensoren und magnetostriktiver Relativmessung inklusive Belagstemperatur in verschiedenen Tiefen; die Pfeile bezeichnen den mutmasslichen Beginn massgeblicher Schädigung.

2: Amplitudes des déflexions verticales mesurées pendant le passage de rouleaux compacteurs au moyen de capteurs d'accélération et selon une technologie magnétorestrictive, température du revêtement à différentes profondeurs comprise; les flèches indiquent le début probable d'un endommagement manifeste.

lieferten die Untersuchungen mit GPR nach etwa 600 k Ürlg. Anzeichen für horizontale Anomalien in 4,5 cm Tiefe (dunkle Zonen in Abb. 3), also etwa auf dem Niveau des Übergangs von Deckschicht zur Binderschicht, die sich bis zu 1000 k Ürlg. noch verstärkten und sich nach der forensischen Entnahme von Belagsriegeln als Lagentrennung erwiesen.

Die Messungen mit dem ETH-DELTA Gerät liessen nach 1000 k Ürlg. deutlich kanalisierte Einsenkungsmulden erkennen, was auf einen Funktionsverlust der zementstabilisierten Tragschichten hindeutete (Abb. 4). Entsprechend erwies sich die Zementstabilisierung bei der Riegelentnahme als nahezu pulverisiert, konnte sie doch leicht mit einem Schraubendreher von Hand durchstossen werden. Dass die beschleunigte Verkehrslastwirkung des MLS10 nicht nur eine bleibende Verformung in den Asphaltschich-

3: Lagetrennung (LT) und Risszone im entnommenen Riegel nach 1000 k Überrollungen (links unten); GPR-Landkarte in 4,5 cm Tiefe nach 600 k und 1000 k Überrollungen (rechts unten).

3: Changement d'état (CE) et zone de dislocation dans le prélèvement après 1 million de passages des rouleaux compacteurs (en bas à gauche); imagerie géoradar à 4,5 cm de profondeur après 600 000/1 million de passages (en bas à droite).

4: ETH-DELTA Gerät mit gemessenen Deflektionsmulden nach 0 und 1000 k Überrollungen.

4: Appareil ETH-DELTA avec mesure des bassins de déflexion après 0 et 1 million de passages des rouleaux compacteurs.
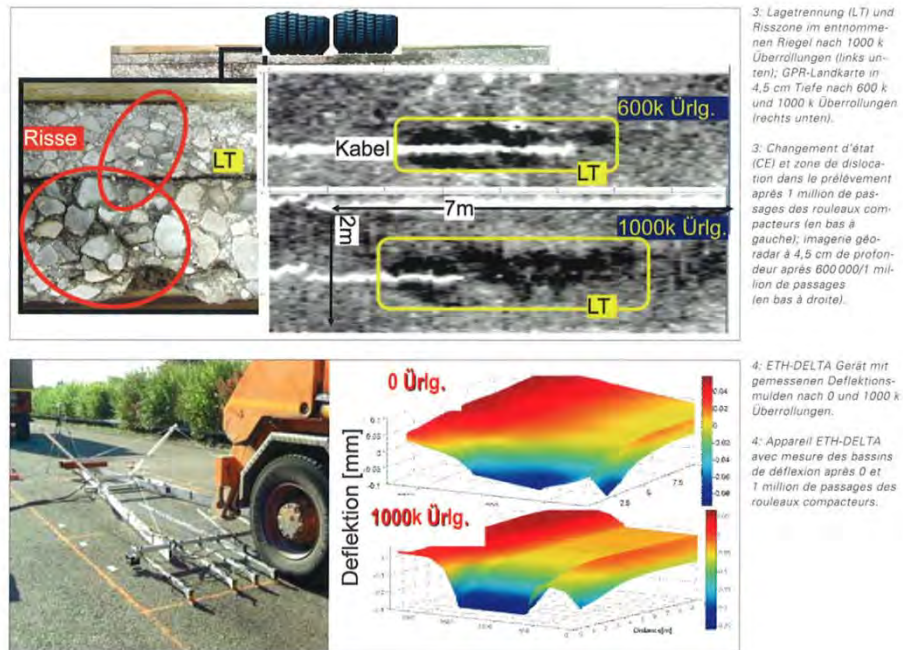
ten, sondern vor allem auch ein Durchstanzen des Asphalts verursachte, wurde durch die an den entnommenen Riegeln festgestellte Schubrissbildung an den Flanken der Rollspuren bestätigt.

Aufgrund der Verkehrszählungen dürfte die während der letzten 20 Betriebsjahre auf der Oberlandautobahn aufgetretene Verkehrsbelastung bei etwa 5,5 bis 6,5 Millionen Einheitsachslasten à 81,6 kN liegen; dies unter der Annahme eines Lastwagenanteils von 6,3 % und einer jährlichen Zuwachsrate von 4,45 %. Die vor 10 Jahren erneuerte Deckschicht wies in der befahrenen Normalspur starke Risse auf. Dies deutet darauf hin, dass eine Verkehrsbelastung in der erwähnten Grössenordnung tatsächlich einen Grenzwert für die Tragfähigkeit der Strecke darstellt. In den MLS10-Versuchen mit einer Halbachsenlast von 65 kN (entsprechend einer Achslast von 130 kN) war daher mit einer strukturellen Schädigung nach ca. 750 k Ürlg. zu rechnen, eine Grössenordnung, die sich in den Tests bestätigte.

Empa Abrasionstests
Im Rahmen des Forschungsprojektes APART (Abriebspartikel des Strassenverkehrs) über nicht auspuffbedingte PM10-Emissionen wurden im Auftrag des Bundesamtes für Strassen ASTRA und des Bundesamtes für Umwelt BAFU neben Feinstaubemissionen unter Normalverkehr auch solche infolge MLS10 gemessen (Gehrig et al. 2010); dies nicht zuletzt, um den Anteil der Feinstpartikel infolge Strassenabrieb und Staubaufwirbelung trotz chemischer Ähnlichkeit jeweils quantitativ zuordnen zu können. Die

Messungen erfolgten auf einem oberflächlich leicht vorbeanspruchten AC11 Belag auf dem Empa-Gelände. Ermittelt wurden die Partikel der Fraktion 0,5 bis 20 µm mit einem aerodynamischen Partikelgrössenanalysator (TSI APS Modell 3321). Gleichzeitig wurde die Verdünnung eines genau dosierten Tracer Gases SF6 (Schwefelhexafluorid) bestimmt, welches zur rechnerischen Berücksichtigung der Strömungsverhältnisse im MLS10 während des Überrollvorganges diente. Abbildung 5 zeigt die Partikelkonzentration in der Aussenluft und während des MLS10-
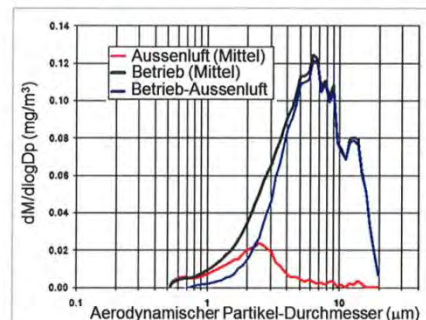
5: Typische Partikelgrössenverteilung bei AC11 während des MLS10-Betriebes.

5: Distribution granulométrique type du AC11 pendant l'utilisation du MLS10

Betriebes in Funktion der Partikelgrösse. Da sich die Aufwirbelung im vorliegenden Fall als vernachlässigbare Grösse erwies, stellt die Differenz der beiden Messungen den Abrieb dar. Verglichen mit der Verteilung der Partikelgrösse in der Aussenluft ist die Verteilung der Abriebspartikel deutlich in Richtung der gröberen Partikel verschoben.

Anschluss an die neue Zürcher Westumfahrung A20
Zur Untersuchung des Belagskonzeptes der A4 im Anschluss an die neue Westumfahrung A20 von Zürich wurden von November 2008 bis September 2009 mit dem MLS10 auf separatem Gelände drei entsprechende Testfelder mit unterschiedlich vollständigem Belagsaufbau untersucht. Die Schichtfolge des Vollaufbaus von unten nach oben umfasste zwei hydraulisch stabilisierte Schichten von insgesamt 480 mm Dicke, eine SAMI-Schicht, eine 80-mm-Tragschicht AC T 22 H, eine 80-mm-Binderschicht AC B 22 H und eine 30-mm-Deckschicht aus Rauasphalt AC MR 8. Auf dem Feld 4 mit dem Vollaufbau wurden insgesamt 740 k Ürlg. durchgeführt. Bei Feld 3 ohne Deckschicht wurden 427 k Ürlg. aufgebracht, während Feld 1 nur noch die Tragschicht umfasste und mit 439 k Ürlg. belastet wurde. Erneut wurden Spurbildung, statische Deflektionsmulde mit ETH-DELTA Gerät, seismischer Modul mit PSPA, Lagentrennung mit GPR und die Deflektionen über Dehnungssensoren erfasst. Zudem wurden in verschiedenen Tiefen die Längs- und Querdehnungen über Dehnmess-Sensoren (DMS) ermittelt und durch das Institut für Strassen- und Eisenbahnwesen (ISE) des Karlsruher Instituts für Technologie (KIT) an drei Messkampagnen Tragfähigkeitsmessungen mit dem Falling Weight Deflectometer (FWD) durchgeführt (Karcher et al. 2010).
Die Ergebnisse zeigen, dass der Belag verglichen mit der Strecke bei Hinwil extrem steif und tragfähig ist. Die Längsdehnungen im Bereich von 10 bis 70 µm/m, die bei sommerlichen Temperaturen zwischen dem 21. Juli und 19. August 2008 im deckschichtlosen Feld 3 unmittelbar unter der Rollspur in einer Tiefe von 8 cm (d. h. auf der Tragschichtoberfläche) ermittelt wurden, lassen in Funktion der Überrollungen mit einer Halbachslast von 65 kN unabhängig von den Belagstemperaturen keinen Deh-
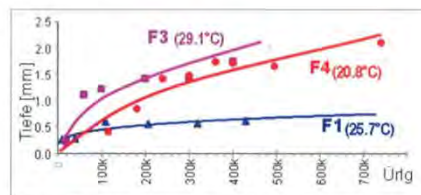
7: Zunahme der maximalen Spurbildung in den Testfeldern F1, F3, F4. Ebenfalls angegeben ist die mittlere Prüftemperatur.

7: Augmentation de la formation maximale de stries dans les zones de test F1, F3 et F4. La température moyenne de test est également indiquée.

nungszuwachs erkennen (Abb. 6). Im Feld 4 wurde auch nach 740 k Ürlg. für den vorliegenden Aufbau eine praktisch unverändert hohe Stabilität festgestellt. Durch die FWD-Messungen konnte ebenfalls keine Verringerung der Tragfähigkeit infolge der MLS10-Beanspruchung festgestellt werden.
Der in der Abbildung 7 angegebenen Spurbildungsentwicklung in den drei Testfeldern bei mittleren Temperaturen von 20,8 bis 29,1 °C ist zu entnehmen, dass die bleibenden Deformationen vor allem den Asphaltschichten zuzuordnen sind und nicht, wie im Falle der Strecke bei Hinwil, dem Versagen der Stabilisierungsschichten. Entsprechend ist die Spurbildung bei Feld F1 mit nur alleiniger Tragschicht deutlich geringer als bei den Feldern F3 und F4 mit Binderschicht und Vollaufbau; dies, obwohl die mittlere Temperatur bei Feld F1 sogar etwas höher war als während der Prüfung des Vollaufbaus. Es bleibt jedoch festzustellen, dass die Spurrinnentiefe mit lediglich 2 mm am Ende des Versuchsprogrammes, trotz Prüfung während der Sommermonate, als sehr gering einzustufen ist. Somit kann gefolgert werden, dass die gewählte Dimensionierung erfolgreich war und der Belag eine gute Qualität aufweist.

Rastplatz der A1 bei Suhr und neue Staffeleggstrasse
Die Steifigkeit der aktuell in der Schweiz für Hochleistungsstrassen angewendeten Belagskonzepte bestätigte sich auch in den beiden jüngsten Einsätzen des MLS10 auf einem Fahrstreifen im Bereich des Rastplatzes der A1 (Bern–Zürich) bei Suhr sowie auf der neuen Staffeleggstrasse, die Teil der neuen Nordumfahrung der Kantonshauptstadt Aarau bildet. Die Schichtenfolge der neuen Staffeleggstrasse umfasst 40 mm Deckschicht SMA11, 45 mm Binderschicht AC B16S, 65 mm Tragschicht ACT 22 H auf 100 mm Kaltmischfundation KMF22. Verglichen mit den Messungen auf dem Belag der Zürcher Westumfahrung wurden auf dem Rastplatz Suhr nach 405 k Ürlg. mit etwa 3 mm etwa doppelt so tiefe Spurrinnen festgestellt. Trotzdem darf der Belag generell noch als recht steif bezeichnet werden. Die Rückfederungs-Dehnungsamplituden an der Oberfläche in Längsrichtung und damit der Steifigkeitsverlust nahmen während des Versuchs bei einer Referenztemperatur von 20 °C um 16 % bzw. um 10 µε zu (Abb. 8). Im Falle der Staffeleggstrasse erwies sich das relativ grosse Längs- und Quergefälle von 6 % bzw. 5,5 % als kritisch für die Versuchsdurchführung, weil die Laufschienen des MLS10 ungleichmässig belastet werden und die Gefahr der einseitigen Abnutzung besteht. Um diese Problematik zu lösen, wurde der MLS10 in Fallrichtung, d.h. mit einem leichten Winkel zur Richtung
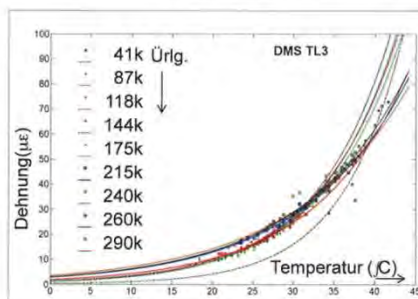
6: Längsdehnungen in Testfeld 3 unter der Rollstrecke in 8 cm Tiefe in Abhängigkeit der Belagstemperaturen bei zunehmender Anzahl Überrollungen.

6: Lien entre les élongations observées dans la zone de test 3 à 8 cm de profondeur sous la surface de compaction et la température du revêtement, en fonction du nombre de passages des rouleaux compacteurs.
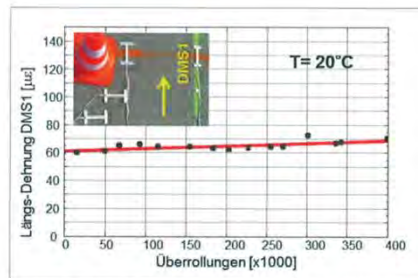
8: Längsdehnungen in Abhängigkeit der Überrollungen (Referenztemperatur 20 °C).

8: Elongations en fonction du nombre de passages des rouleaux compacteurs (température de référence: 20 °C).

des Strassenverkehrs, positioniert. Die festgestellten Änderungen der Belagseigenschaften waren auch in diesem Falle relativ gering. Wie aus Abbildung 9 ersichtlich, wurden mit ETH-DELTA Messungen gewisse Unterschiede im Deflektionsverhalten festgestellt. Generell konnte aber auch dieser moderne Belag im Vergleich zur Strecke in Hinwil als bedeutend tragfähiger eingestuft werden.

Vielversprechende Aussichten

Die bisherigen Erfahrungen mit dem MLS10 bestätigen, dass die beschleunigte Verkehrslastsimulation im 1:1-Massstab ein wichtiges Forschungs- und Validierungsinstrument darstellt, das allgemein noch zu wenig eingesetzt wird, um die Übertragung von Laborergebnissen und Modellen auf das tatsächliche Verhalten unter Verkehr wissenschaftlich zu begleiten und dadurch dem Risiko von technischen Fehlentwicklungen entgegenzuwirken.
Die mobile von der Empa betriebene zukunftsweisende MLS10-Anlage hat sich in Kombination mit geeigneter Sensorik und Messverfahren als vielversprechendes, praktisches Hilfsmittel zur Erfassung der mechanischen Leistungsfähigkeit von real eingebauten Asphaltbelägen erwiesen, dessen Einsatzbereich dank der hohen Mobilität nachgewiesenermassen nicht nur auf die Schweiz be-

schränkt ist. Der MLS10 zeichnet sich somit durch folgende klare Vorteile aus:
■ Kompakte Grösse; daher vergleichsweise gut transportierbar, auch bei engen Kurvenradien (z. B. wie Kreisel) und engem Lichtraumprofil; zudem auf engem Raum im Selbstfahrmodus übersichtlich manövrierbar.
■ Unidirektionale Überrollrichtung; d. h. keine realitätsfremde Hin- und Herüberrollung.
■ Hohe Anzahl realistischer Halbachslasten in relativ kurzer Zeit möglich; daher ist die Prüfzeit und das Staurisiko in Feldversuchen minimal.
■ Mit 22 km/h Überrollgeschwindigkeit erlaubt der MLS10 bei vertretbarem Zeitaufwand Ermüdungsprüfungen unter realistischen dynamischen Lasten, sodass das Risiko von Fehlschlüssen durch Überhöhung der Achslasten zwecks Reduktion der Anzahl Überrollungen entfällt.

Nach den bisherigen Erfahrungen mit bald 10 Millionen Überrollungen beträgt die durchschnittliche Leistungsfähigkeit bei normalem 8,5-Stunden-Betrieb etwa 40 000 unidirektionale Überrollungen pro Tag mit einer Halbachs-Last von 65 kN. Allerdings darf nicht vergessen werden, dass der von der Empa betriebene MLS10 noch ein Prototyp ist, der im gegenwärtigen Zustand einen relativ aufwendigen Unterhalt durch gut geschultes Personal erfordert und im Rahmen seiner Weiterentwicklung einem kontinuierlichen konstruktiven und betrieblichen Optimierungsprozess unterworfen ist.
Die bisherigen Anwendungen des MLS10 in der Schweiz dürfen als vielversprechend bezeichnet werden, da wichtige – wenn auch noch nicht abschliessende – Hinweise über die Einsatzmöglichkeiten der beschleunigten Verkehrslastsimulation zur grossmassstäblichen Beurteilung der Leistungsfähigkeit realer Strecken gewonnen werden konnten. Namentlich konnte bei den Tests auf der A53 bei Hinwil nach ca. 0,4 bis 0,6 Mio. Überrollungen mit E130 (Einheitsachslasten von 130 kN) Versagen infolge Lagentrennung und Durchstanzen der Zementstabilisierung festgestellt werden. Dies entspricht etwa dem reellen Versagen nach ca. 0,74 Mio. E130, die in der vierzigjährigen Betriebsperiode zwischen 1967 und 2007 aufgebracht wurden.
Als unerwartete positive Erkenntnis zu werten ist das im Rahmen von Partikelgrössenuntersuchungen gefundene Resultat, dass der MLS10 trotz der passiv angetriebenen Lasträder zu Partikelabriebsmessungen herangezogen
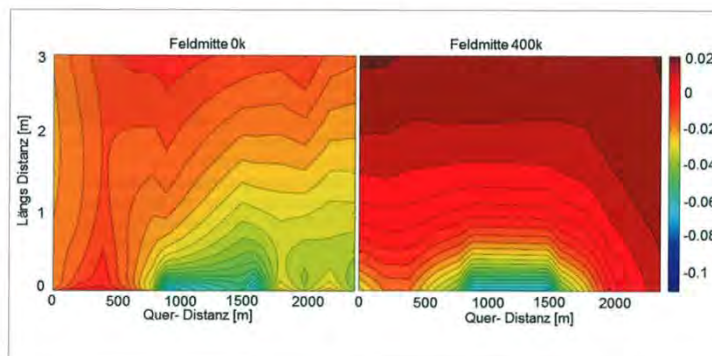
9: Veränderung der ETH-DELTA Deflektions-Isohypsen auf der Staffeleggstrasse nach 0 k und 400 k Ürlg.

9: Modification des isohypses de déflexion ETH-DELTA dans la Staffeleggstrasse après 0 et 400 000 passages des rouleaux compacteurs.

werden kann, insbesondere auch zur Unterscheidung von Strassenabrieb und Staubaufwirbelung.

Hinsichtlich moderner schweizerischer Belagskonzepte ist zu erwähnen, dass sich gegenüber der Strecke bei Hinwil die moderne Belagsstruktur der A4 im Anschluss an die neue Zürcher Westumfahrung A20 als extrem steif und tragfähig erwiesen hat. Auch nach 0,8 Mio. Überrollungen des Vollaufbaus waren keine deutlichen Veränderungen im Verhalten feststellbar und die Spurbildung betrug lediglich 2 mm. Somit konnte gefolgert werden, dass die gewählte Dimensionierung erfolgreich war und der Belag eine gute Qualität aufweist. Dass mit den gegenwärtigen modernen Belagskonzepten in der Schweiz eine hohe Tragfähigkeit erreicht werden kann, wurde aber auch in den MLS10-Tests im Bereich des Rastplatzes der A1 (Bern–Zürich) bei Suhr sowie der Nordumfahrung Aarau auf der neuen Staffeleggstrasse deutlich. Die festgestellten Änderungen der Belagseigenschaften infolge 0,4 Mio. Ürlg. waren auch in diesen Fällen relativ gering. Die Versuche auf der neuen Staffeleggstrasse bestätigten, dass ein Einsatz des MLS10 bei Gefällen von mehr als 3 % aus maschinentechnischen Gründen problematisch ist.

Bis heute ergab sich noch keine Gelegenheit, mit dem MLS10 einen modernen schweizerischen Autobahnbelag bis zum vollständigen Versagen zu beanspruchen und durch Kombination der erwähnten Messverfahren die Veränderung der mechanischen Leistungsfähigkeit solcher Belagsstrukturen zu erfassen und zu beurteilen. Auch war es noch nicht möglich, Restfestigkeiten von Belägen vor und nach der Erneuerung zu bestimmen, um Hinweise über die Dimensionierung von Belagsverstärkungen zu erhalten. Dies wird neben der mechanischen Validierung neuer Belagskonzepte sicherlich Gegenstand künftiger Einsätze des MLS10 sein. ■

Literatur

Arraigada, M., A., Hugenschmidt, J., Partl, M. N., Caprez, M., Rabaiotti, C. (2009): Pilotstudie zur Evaluation einer mobilen Grossversuchsanlage für beschleunigte Verkehrslastsimulation auf Strassenbelägen. Eidgenössisches Departement für Umwelt, Verkehr, Energie und Kommunikation, Bundesamt für Strassen. Forschungsauftrag ASTRA 2004/018, Bericht Nr. 1261.

Arraigada, M., Partl, M. N., Angelone, S. M., Martinez, F (2009,2): Evaluation of Accelerometers to Determine Pavement Deflections under traffic Loads. Material and Structures, 42, 6, Springer Verlag, 779–790.

Gehrig, R., Zeyer, K., Bukowiecki, N., Lienemann, P., Poulikakos, L. D., Furger, M., Buchmann, B. (2010): Mobile Load Simulators – a tool to distinguish between the emissions due to abrasion and resuspension of PM10 from road surfaces. Atmospheric Environment, 44, 38 Elsevier Verlag, 4937–4943.

Hugenschmidt, J. (2008): Georadar zur zerstörungsfreien Prüfung von Verkehrsbauwerken. «strasse und verkehr», Nr. 1-2. Verlag Vereinigung Schweizerischer Strassen- und Verkehrsfachleute, 26–35.

Hugenschmidt, J. (2010): Geophysics and non-destructive testing for transport infrastructure, with emphasis on ground penetrating radar. Doktorarbeit, Diss ETH Nr. 19225.

Hugo, F., de Vos, E., Tayob, H., Kannemeyer, L., Partl, M. N. (2008): Innovative Applications of the MLS10 for Developing Pavement Design Systems. Proceedings of 3rd International Conference on Accelerated Pavement Testing, APT 2008, Madrid.

Karcher, C., Partl, M. N., Plachkova, P., Arraigada, M., Umminger, M. (2010): Untersuchung der Veränderung der strukturellen Substanz von Asphaltkonstruktionen. Strasse und Autobahn, 61, 9, Kirschbaum Verlag, 631–637.

Raab, C., Partl, M. N., Anderegg, P., Brönnimann, R. (2005): A LTPP Study with a new Device for Vertical Deformation Measurements. Int. Journal of Pavement Engineering, 6, 3, Taylor and Francis Verlag, 211–216.

Rabaiotti, C., Partl, M. N., Caprez, M. (2008): APT device evaluation for road research in Switzerland: test campaign on a Swiss Highway with the MLS10. Proceedings of 3rd Int. Conf. on Accelerated Pavement Testing, APT08, Madrid.

Abbreviations

Abbreviation	Definition
MLS10	Mobile Load Simulator
APT	Accelerated Pavement Testing
Empa	Eidgenössische Materialprüfungs- und Forschungsanstalt (Swiss Federal Laboratories for Materials Science and Technology)
ETH	Eidgenössische Technische Hochschule Zürich (Swiss Institute of Technology)
FWD	Falling Weight Deflectometer
LIM	Linear Induction Motor
SAMI	Stress Absorbing Membrane Interlayer
IGT	Institute for Geotechnical Engineering
DAQ	Data Acquisition System
KIT	Karlsruhe Institute of Technology
ASTRA	Bundesamt für Strassen (Federal Roads Office)
UVEK	Eidgenössisches Departement für Umwelt, Verkehr, Energie und Kommunikation
DATEC	Dipartimento federale dell'ambiente, dei trasporti, dell'energia e delle comunicazioni
DETEC	Département fédéral de l'environnement, des transports, de l'énergie et de la communication
FEM	Finite Element Method
GPR	Ground Penetrating Radar
LPDS	Layer-Parallel Direct Shear
MMLS3	Model Mobile Load Simulator
PSPA	Portable Seismic Pavement Analyzer
SN	Structural Number
VSS	Schweizerischer Verband der Strassen- und Verkehrsfachleute (Swiss Association of Road and Transportation Experts)
DMS	Dehnungsmessstreifen (Strain gauge)

Bibliography

[1] Arraigada M., Kalogeropoulos A., Hugenschmidt J., Partl M. N. Caprez M., Rabaiotti C. (2009): Pilotstudie zur Evaluation einer mobilen Grossversuchsanlage für beschleunigte Verkehrslastsimulation auf Strassenbelägen, Eidgenössisches Departement für Umwelt, Verkehr, Energie und Kommunikation, Bundesamt für Strassen. Forschungsauftrag 2004/018, Bericht Nr 1261

[2] Pugliessi., A., Partl, M.N., Martinez, F., Arraigada, M., Angelone, S. (2011): Utilización de simuladores móviles de carga MMLS3 y MLS10 para el estudio de Pavimentos, Proceedings of 36th CPA Conference, Buenos Aires, 30 Nov-3 Dec, 18pages (http://www.cpasfalto.org/36reunion/Trabajos%20XXXVI%20Reunion%20del%20Asfalto.pdf)

[3] Karcher, C., Partl, M.N., Plachkova, P., Arraigada, M., Umminger. M.(2011): Untersuchungen von Veränderungen der strukturellen Substanz von Asphaltkonstruktionen. Strasse und Autobahn 63/1, p 5…11

[4] VSS, 1997. Schweizer Norm (SN) 640324a: Dimensionierung Strassenaufbaus, Unterbau und Oberbau. Schweizerischer Verband der Strassen- und Verkehrsfachleute (VSS)

[5] VSS, 2008. Schweizer Norm (SN) 640430b: Walzasphalt - Konzeption, Ausführung und Anforderungen an die eingebauten Schichten. Schweizerischer Verband der Strassen- und Verkehrsfachleute (VSS)

[6] VSS, 2008. Schweizer Norm (SN) 640431-1b-NA: Asphaltmischgut – Mischgutanforderungen – Teil 1 :Asphaltbeton. Schweizerischer Verband der Strassen- und Verkehrsfachleute (VSS)

[7] VSS, 1998. Schweizer Norm (SN) 670317b: Böden - Plattendruckversuch E_V und M_E. Schweizerischer Verband der Strassen- und Verkehrsfachleute (VSS)

[8] Poulikakos, L.D., Heutschi, K., Muff, R., Arraigada, M., Soltic, P., Anderegg, P., Partl, M.N., Jordi, P. (2010): Footprint II-Long term pavement performance and environnemental monitoring on A1. Eidgenössisches Departement für Umwelt, Verkehr, Energie und Kommunikation, Bundesamt für Strassen. ASTRA 2005/009, Report Nr 1288

[9] Poulikakos,L. D., Arraigada, M., Morgan,G.C.J., Heutschi,K. , Anderegg,P., Partl, M. N., Soltic, P. (2008): In Situ Measurements of the Environmental Footprint of Freight Vehicles in Switzerland. Transportation Research Part D: Transport and Environment 13, pp 274…282

[10] Nazarian, S., Yuan, D., Tandon, V., Arellano, M. (2002): Quality Management of Flexible Pavement Layers with Seismic Methods. Res. Rep 1735-3F, Univ. of Texas at El Paso

[11] Mallick, R.B., Das, A., Nazarian, S. (2005): Fast Nondestructive Field Test Method to Determine Stiffness of Subsurface Layer in This Surface Hot-Mix Asphalt Pavement. Transp. Res. Record Vol 1905, pp 82..89

[12] Celaya, M. Nazarian, S. (2006): Seismic Testing to Determine Quality of Hot-Mix Asphalt. Paper 06-2654 ,CD-Rom Proceedings of 85th Annual TRB Meeting, Washington DC

[13] Arraigada, M., Partl, M. N., Angelone, S. M. (2007): Determination of Road Deflections from Traffic Induced Accelerations. International Journal of Road Materials and Pavement Design, JRMPD, Hermes Science Publications, Vol 8/3, pp 399...421

[14] Arraigada, M., Partl, M.N., Angelone, S.M., Martinez, F. (2008): Evaluation of Accelerometers to Determine Pavement Deflections under traffic Loads. Material and Structures, Online version DOI 10.1617/s11527-008-9423-5

[15] Bohn, A., Ullidtz, P., Stubstad, R., Sørensen, A. (1972): Danish Experiments with the French Falling Weight Deflectometer. Proc. 3rd International Conference on Structural Design of Asphalt Pavements, Univ. of Michigan, Ann Arbor, 1:1119–1128

[16] Beckedahl, H., Hürtgen, H., Straube, E., Horz, H-W. (1996): Begleitende Forschung zur Einführung des Falling Weight Deflectometer (FWD) in der Bundesrepublik Deutschland. Bonn-Bad Godesberg : Bundesministerium für Verkehr, Abteilung Strassenbau. (Forschung Strassenbau und Strassenverkehrstechnik ; Heft 733)

[17] Rabaiotti,C. Partl, M. N., Caprez, M. (2008): APT device evaluation for road research in Switzerland: test campaign on a Swiss Highway with the MLS10. Proceedings of 3rd Int. Conf. on Accelerated Pavement Testing, APT08, Madrid October, 2008

[18] Umminger, M.(2010): Veränderungen in der strukturellen Substanz von Asphaltkonstruktionen bei Beanspruchung mit dem Mobile Load Simulator. Diplomarbeit Karlsruher Institut für Technologie, Institut für Straßen- und Eisenbahnwesen.

[19] Hildebrand, G. (2002): Verification of Flexible Pavement Response from a Field Test. Danish Road Institute. Report 121. ISBN 87-91177-07-3

[20] Elsefi, M., Al-Quadi, I., Yoo, P. J. (2006): Viscoelastic Modeling and Field Validation of Flexible Pavements J. Eng. Mech.132 (2) pp.172…178

[21] CEN, 2004. European Standard EN 12697-26: Bituminous mixtures - Test methods for hot mix asphalt – Part 26: Stiffness. Ref. No. EN 12697-26:2004

[22] VSS, 2006. Schweizer Norm (SN) 670641: Bituminöses Mischgut. Bestimmung des Schichtenverbunds (nach Leutner) . Schweizerischer Verband der Strassen- und Verkehrsfachleute (VSS)

[23] Hugo, F., Arraigada, M.; Shu-ming, L.; Zefeng, T., Kim, R.Y.(2012): International case studies in support of successful applications of accelerated pavement testing in pavement engineering. Jones, Harvey, Mateos & Al-Qadi (Eds.) Taylor & Francis Group, London, ISBN 978-0-415-62138-0

[24] Raab, C., Partl, M.N. (2008): Investigation on Long-Term Interlayer Bonding of Asphalt Pavements. Baltic Journal of Road and Bridge Engineering. Vol 3 No 2, p65…70

[25] VSS, 2011. Schweizer Norm (SN) 640420: Dimensionierung des Strassenaufbaus-Äquivalente Verkehrslast. Schweizerischer Verband der Strassen- und Verkehrsfachleute (VSS)

[26] VSS, 2003. Schweizer Norm (SN) 640925b: Erhaltungsmanagement der Fahrbahnen (EMF). Anleitung zur visuellen Zustandserhebung und Indexbewertung mit dem Schadenkatalog. Schweizerischer Verband der Strassen- und Verkehrsfachleute (VSS)

Project close-out

Schweizerische Eidgenossenschaft
Confédération suisse
Confederazione Svizzera
Confederaziun svizra

Eidgenössisches Departement für
Umwelt, Verkehr, Energie und Kommunikation UVEK
Bundesamt für Strassen ASTRA

FORSCHUNG IM STRASSENWESEN DES UVEK
Formular Nr. 3: Projektabschluss

erstellt / geändert am: 30.12.12

Grunddaten

Projekt-Nr.: ASTRA 2007/011; ASTRA 2010/005;

Projekttitel: Praxiskalibrierung der neuen mobilen Grossversuchsanlage MLS10 für beschleunigte Verkehrslastsimulation auf Strassenbelägen in der Schweiz

Enddatum: Juli 2012

Texte

Zusammenfassung der Projektresultate:

The experience gathered in the three testing sites confirm that the MLS10, which accelerates the traffic loading of a pavement with full scale rolling loads, is an important tool to validate the construction of pavement and /or confirm the bearing capacity and remaining life of old pavements.
This work confirmed that the MLS10, in combination with the right type of sensors and pavement evaluation techniques, is a promising tool for the evaluation of the mechanical service capability of real pavements. The MLS10 demonstrated that it can be deployed in many places thanks to its design, which showed high flexibility and mobility. The device is characterized by the following clear advantages:
• Compact size in comparison with other similar machines. It is relatively easy to transport in one move on the site.
• Unidirectional loading direction, similar to real traffic.
• High amount of realistic load applications in a relatively short period of time
• With a speed of 22km/h, the load is the most realistic one compared to other machines.
For short periods of time, during a normal working day of about 8.5 hours the machine allows to apply up to 40'000 load cycles, although this performance reduces if the tests requires a high total amount of load cycles (e.g. stiff pavements) because of maintenance requirements and the possible risk of unexpected breakdowns of this prototype machine, which may occur in spite of the continuous improvements of performance achieved so far.
The tests in Filderen revealed that the new structure of the A1 highway and the other weaker versions of this pavement have high stiffness and bearing capacity and require a considerable amount of time and effort in order to see changes in the response due to load induced distress. This confirms that the actual Swiss dimensioning of the pavement and its construction allows to achieve good mechanical quality. The same conclusions can be drawn for the old pavement in Rastplatz Suhr and the new pavement in Neue Staffeleggstrasse.

Schweizerische Eidgenossenschaft
Confédération suisse
Confederazione Svizzera
Confederaziun svizra

Eidgenössisches Departement für
Umwelt, Verkehr, Energie und Kommunikation UVEK
Bundesamt für Strassen ASTRA

Zielerreichung:

The objectives of the project have been reached. It was possible to correlate and calibrate the destructive effect of the MLS10 loadings to different selected pavement types. In addition, it was possible to evaluate the performance of the MLS10 itself by means of assessing the required human and technical resources needed to conduct APT tests. Furthermore the goal of establishing and formalizing data handling, cleansing, processing and storage has been achieved. Last but not least, it was possible to improve the functioning of the MLS10 and to evaluate on a long term routine basis how the machine can be operated in an efficient way.

Folgerungen und Empfehlungen:

For next uses of the MLS10 it is recommended to test weaker pavements in order to reach the bearing capacity limit within a reasonable period of time and therefore to learn what are the most common distress mechanisms present for this types of constructions. It is also recommended to increase the data basis to different types of pavements and extend the range of application of this tool, e.g. by investigating also new pavement types, such as energy saving and/or recycling pavements.

Publikationen:

- Arraigada M., Partl M.N., Pugliessi A. (2012): Initial Tests Results from the new MLS10 Mobile Load Simulator in Switzerland. Proceedings of the 4th international Conference on Accelerated Pavement Testing, Davis, CA, USA, 19-21 September 2012
- Hugo F., Arraigada M., Shu-ming L., Zefeng T., Kim R.Y. (2012): International case studies in support of successful applications of accelerated pavement testing in pavement engineering. Proceedings of the 4th international Conference on Accelerated Pavement Testing, Davis, CA, USA, 19-21 September 2012
- Partl M.N., Arraigada M. (2011): Der neue Mobile Load Simulator (MLS10). Strasse und Autobahn, 62. Jahrgang April 2011, 252-257
- Partl M.N., Arraigada M. (2011): Beschleunigte Verkehrslastsimulation mit dem Mobile Load Simulator MLS10. Strasse und Verkehr, Nr. 3 / März 2011, 32-38

Der Projektleiter/die Projektleiterin:

Name: Partl   Vorname: Manfred

Amt, Firma, Institut: Empa Dübendorf, Abteilung Strassenbau und Abdichtungen

Unterschrift des Projektleiters/der Projektleiterin:

Schweizerische Eidgenossenschaft
Confédération suisse
Confederazione Svizzera
Confederaziun svizra

Eidgenössisches Departement für
Umwelt, Verkehr, Energie und Kommunikation UVEK
Bundesamt für Strassen ASTRA

FORSCHUNG IM STRASSENWESEN DES UVEK

Formular Nr. 3: Projektabschluss

Beurteilung der Begleitkommission:

Beurteilung:

Die Ziele sind wie folgt umschrieben:
The project focuses on the performance oriented calibration and valida-tion of the recently purchased Full Scale Mobile Load Simulator MLS10 for APT in Switzerland.
• Correlate the destructive effect of the MLS10 loading to different types of pavements designed and constructed using Swiss norms and under the influence of local weather conditions. « calibration" is then used to account for the correlation between the numbers of load applications necessary to cause a certain distress.
• Learn to operate the MLS10 and assess the required resources needed to conduct APT tests. Provide invaluable practical experience to improve the organization of resources.
• Evaluate the MLS10 itself, detect operational shortcomings and technical defects, improving the performance of the machine.
• Propose and evaluate testing procedures as well as instrumentation and software to collect research data. Establish and formalize the data handling

Diese Ziele wurden erreicht. Die Kalibration wurde erheblich aufwendiger, als zu erwarten war. Anstatt eines Testplatzes wurde um die Qualität der Ergebnisse sicherzustellen auf deren drei ausweitet. Ein wesentlicher Umstand war die extrem hohe Standfestigkeit der getesteten Beläge. Als Folge der Verwendung einer Anlage im Prototypstadium, was im Interesse einer innovativen Forschung steht, kamen Erschwernisse technischer Art dazu. Die MLS10 Technologie erwies sich als effizientes Mittel zur Verkehrslastsimulation.

Umsetzung:

Nach Abschluss der Kalibration ist die MLS10 für Forschung und Testzwecke einsetzbar. Die Untersuchungen zeigten, dass diese moderne Anlage die lange bewirtschaftete Rundlaufanlage der ETH (welche viele Grundlagen zur CH-Strassenbemessung geliefert hat) sehr gut zu ersetzen vermag und dessen Zeitraffer bei weitem übertrifft, sodass die Untersuchungsdauer für Forschungsarbeiten und Oberbautests massiv kürzer wird.
Verschiedene Anschlussforschungen mit der MLS10 sind am Laufen oder gar bereits abgeschlossen.
Die Ergebnisse der Forschung wurden in nationalen und internationalen Publikationen dargelegt und an internationale Fachanlässen vorgestellt. Die Zusammenarbeit mit interessierten Fachstellen, vor allem in Deutschland und Österreich ermöglicht Synergien und verläuft vielversprechend.
Der Zugang für Forschungsstellen zum Einsatz der MLS10 sollte erleichtert werden. Dazu unternimmt der zur Begleitung der MLS10 Forschung gegründete Nutzerbeirat ASTRA/EMPA einen Vorstoss.

weitergehender Forschungsbedarf:

Es besteht ein Programm mit Einsatzmöglichkeiten zu ganz unterschiedlich gelagerten Fragen und verschiedenen Strassenbelägen. Das Anwendungsfeld ist sehr breit und vielfältig und überschreitet das Thema der Belagsforschung.

Einfluss auf Normenwerk:

Der Einsatz der MLS10 kann mit technischen/ökonomischen Ergebnissen die dringende Gesamtüberarbeitung der Dimensionierungsnormen des Strassenoberbaus erleichtern und neue Baustoffentwicklungen hinsichtlich deren Performance unter realitätsnaher Verkehrbeanspruchungen fördern.

Der Präsident/die Präsidentin der Begleitkommission:

Name: Gantenbein   Vorname: Andreas

Amt, Firma, Institut: -

Unterschrift des Präsidenten/der Präsidentin der Begleitkommission:

Digital unterschrieben von Andreas Gantenbein
DN: cn=Andreas Gantenbein, o, ou,
email=kapellplatz@bluewin.ch, c=CH
Datum: 2013.01.08 14:25:05 +01'00'

Forschung im Strassenwesen des UVEK: Formular 3   Seite 3 / 3

List of reports in road research

Report-Nr.	Project Nr.	Title	Date
1356	SVI 2007/014	Kooperation an Bahnhöfen und Haltestellen *Coopération dans les gares et arrêts* *Coopération at railway stations and stops*	2011
1362	SVI 2004/012	Aktivitätenorientierte Analyse des Neuverkehrs Activity oriented analysis of induced travel demand Analyse orientée aux acitivtés du trafic induit	2012
1361	SVI 2004/043	Innovative Ansätze der Parkraukmbewirtschaftung Approches innovantes de la gestion du stationnement Innovative approaches to parking management	2012
1357	SVI 2007/007	Unaufmerksamkeit und Ablenkung: Was macht der Mensch am Steuer? Driver Inattention and Distraction as Cause of Accident: How do Drivers Behave in Cars? L'inattention et la distraction: comment se comportent les gens au volant?	2012
1360	VSS 2010/203	Akustische Führung im Strassentunnel Acoustical guidance in road tunnels Guidage acoustique dans les tunnels routiers	2012
1365	SVI 2004/014	Neue Erkenntnisse zum Mobilitätsverhalten dank Data Mining? De nouvelles découvertes sur le comportement de mobilité par Data Mining? New findings on the mobility behavior through Data Mining?	2011
1359	SVI 2004/003	Wissens- und technologientransfer im Verkehrsbereich Know-how and technology transfer in the transport sector Transfert de savoir et de technologies dans le domaine des transports	2012
1363	VSS 2007/905	Verkehrsprognosen mit Online -Daten Pronostics de trafic avec des données en temps réel Traffic forecast with real-time data	2011
1367	VSS 2005/801	Grundlagen betreffend Projektierung, Bau und Nachhaltigkeit von Anschlussgleisen Principes de bases concernant la conception, la construction et la durabilité de voies de raccorde-ment Basic Principles on the Design, Construction and Sustainability of Sidings	2011
1370	VSS 2008/404	Dauerhaftigkeit von Betongranulat aus Betongranulat	2011
1373	VSS 2008/204	Vereinheitlichung der Tunnelbeleuchtung	2012
1369	VSS 2003/204	Rétention et traitement des eaux de chaussée	2012

Report-Nr.	Project Nr.	Title	Date
648	AGB 2005/023 + AGB 2006/003	Validierung der AAR-Prüfungen für Neubau und Instandsetzung	2011
1371	ASTRA 2008/017	Potenzial von Fahrgemeinschaften *Potentiel du covoiturage* *Potential of Car Pooling*	2011
1374	FGU 2004/003	Entwicklung eines zerstörungsfreien Prüfverfahrens für Schwiessnähte von KDB *Dévelopment d'une méthode d'éssais non-déstructif pour des soudures de membranes polymères d'étanchéité* *Development of a nondestructive test method for welded seams of polymeric sealing membranes*	2012
1375	VSS 2008/304	Dynamische Signalisierungen auf Hauptverkehrsstrassen *Signalisations dynamiques sur des routes principales* *Dynamic signalling at primary distributors*	2012
1376	ASTRA 2011/008_004	Erfahrungen im Schweizer Betonbrückenbau *Expériences dans la construction de ponts en Suisse* *Experiences in Swiss Bridge Construction*	2012
1379	VSS 2010/206_OBF	Harmonisierung der Abläufe und Benutzeroberflächen bei Tunnel-Prozessleitsystemen *Harmonisation of procedures and user interface in Tunnel-Process Control Systems* *Harmonisation des processus et des interfaces utilisateurs dans les systèmes de supervision de tunnels*	2012
1380	ASTRA 2007/009	Wirkungsweise und Potential von kombinierter Mobilität *Mode of action and potential of combined mobility* *Mode d'action et le potentiel de la mobilité combinée*	2012
1381	SVI 2004/055	Nutzen von Reisezeiteinsparungen im Personenverkehr *Bénéfices liés à une réduction des temps de parcours du trafic voyageur* *Benefits of travel time savings in passenger traffic*	2012
1383	FGU 2008/005	Einfluss der Grundwasserströmung auf das Quellverhalten des Gipskeupers im Chienbergtunnel *Influence de l'écoulement souterrain sur le gonflement du Keuper gypseux dans le Tunnel du Chienberg* *Influence of groundwater flow on the swelling of the Gipskeuper formation in the Chienberg tunnel*	2012
1386	VSS 2006/204	Schallreflexionen an Kunstbauten im Strassenbereich *Réflexions du trafic routier aux ouvrages d'art* *Noise reflections on structures in the street*	2012
1387	VSS 2010/205_OBF	Ablage der Prozessdaten bei Tunnel-Prozessleitsystemen *Data storage in tunnel process control systems* *Enregistrement ds données de systèmes de supervision de tunnels*	2012

Report-Nr.	Project Nr.	Title	Date
649	AGB 2008/012	Anforderungen an den Karbonatisierungswiderstand von Betonen *Exigences par rapport à la résistance à la carbonatationdes bétons* *Requirements for the carbonation resistance of concrete mixes*	2012
650	AGB 2005/010	Korrosionsbeständigkeit von nichtrostenden Betonstählen *Résistance à la corrosion des aciers d'armature inoxydables* *Use of stainless steels in concrete structures*	2012